A TIDAL STUDY OF GREAT BAY, NEW HAMPSHIRE

BY

SEAN ORLANDO DENNEY

Bachelors of Science in Geomatics, University of Florida, 2009

THESIS

Submitted to the University of New Hampshire

in Partial Fulfillment of

the Requirements for the Degree of

Master of Science

in

Ocean Engineering with an Ocean Mapping Option

May, 2012

UMI Number: 1518013

UMI®

Dissertation Publishing

ProQuest®

This thesis has been examined and approved.
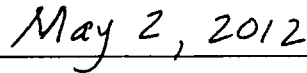
_____
Thesis Director, Andrew A. Armstrong, Captain, NOAA (Ret.)
Affiliate Professor of Ocean Engineering and
Marine Sciences and Earth Sciences

_____
Semme J. Dijkstra, Ph.D.,
Lecturer of Ocean Engineering

_____
James D. Irish, Ph.D.,
Research Professor of Ocean Engineering

_____
May 2, 2012
Date

DEDICATION

To my mother, Anita Orlando, whose love of the sea has forever changed my life.

Guard, Newcastle Station for the use of their facilities in aide of this project.

FOREWORD

The field of surveying, in all areas of study, comprises a vast amount of technical terminology. Even practitioners with many decades in the art do not have a complete grasp of it all. For the sake of reaching a broader audience as well as providing a quick reference to the already adept, a list of acronyms, a list of symbols, and a glossary have been incorporated into this thesis. Most terms that are *italicized* are given definitions in the glossary.

Likewise, the analysis of time series in the spatial (*i.e.* time) and spectral (*i.e.* frequency) domains is of import to tidal research. General techniques, which are applicable to this study, have been appended, including descriptions of source code algorithms used in the data processing.

In the discussion of historic observations, it is necessary to "follow in the footsteps of the original surveyor." In order to do this, different units of measure and different surveying techniques must be taken into account. The use of "feet," unless otherwise noted, is always in U.S. Survey Foot (1 foot = 1200/3937 meter).

TABLE OF CONTENTS

LIST OF TABLES

LIST OF FIGURES

xix

LIST OF ACRONYMS

ASCII	American Standard Code for Information Interchange
BM	Benchmark
CCOM	Center for Coastal and Ocean Mapping
CA	California
CI	Confidence Interval
CO-OPS	Center for Operational Oceanographic Products and Services
CORS	Continuously Operating Reference Station(s)
CSDL	Coast Survey Development Laboratory
C-T	Conductivity – Temperature
C-T-P	Conductivity – Temperature – Pressure
DHQ	Mean Diurnal High Water Inequality
DLQ	Mean Diurnal Low Water Inequality
DTL	Diurnal Tide Level
EDT	Eastern Daylight Time
EST	Eastern Standard Time
FAA	Federal Aviation Administration
FFT	Fast Fourier Transform
GMT	Greenwich Mean Time
GOES	Geostationary Operational Environmental Satellite
GPS	Global Positioning System
GRS80	Geodetic Reference System 1980
Gt	Great Tropic Range
H	High
HH	Higher-High
HSTP	Hydrographic Systems and Technology Program
HWI	High Water Lunitidal Interval
I/O	Input/ Output
JEL	Jackson Estuarine Laboratory

JHC	Joint Hydrographic Center
L	Low
LL	Lower-Low
LWI	Low Water Lunitidal Interval
ME	Maine
MHHW	Mean Higher-High Water
MHW	Mean High Water
MLLW	Mean Lower-Low Water
MLW	Mean Low Water
Mn	Mean Range of Tide
MSL	Mean Sea Level
MTL	Mean Tide Level
MWWL	MicroWave Water Level
N	North
NAD83	North American Datum of 1983
NAVD88	North American Vertical Datum of 1988
NCDC	National Climate Data Center
NGS	National Geodetic Survey
NH	New Hampshire
NOAA	National Oceanic and Atmospheric Administration
NOS	National Ocean Service
OCS	Office of Coast Survey
OPUS	Online Positioning User Service
PPK	Post-Processed Kinematic
RNC	Raster Navigational Chart
RTK	Real-Time Kinematic
R/V	Research Vessel
RMSE	Root Mean Square Error
SNR	Signal-to-Noise Ratio
TBM	Tidal Benchmark
TBYT	Tide-by-Tide

TCARI	Tidal Constituent and Residual Interpolation
TX	Texas
UNH	University of New Hampshire
USAF	United States Air Force
USCG	United States Coast Guard
USC&GS	United States Coast and Geodetic Survey
W	West
WGS84	World Geodetic System 1984
WL	Water Level

LIST OF SYMBOLS

°		degrees (*e.g.* of arc, of phase)
°C		degrees Celsius
cpd		cycles per day
cph		cycles per hour
dbar		decibars
Δ	(Delta)	finite difference
η	(eta)	sea surface elevation
f_n		frequency at the *n*-th index
ft		feet
g		gravity
g_{Lat}		gravity based upon latitude
GHz		GigaHertz
$\bar{\gamma}^2$	(gamma)	smoothed squared coherency spectrum
$\hat{G}^2$		power
h		reference elevation
hrs		hours
kPa		kiloPascals
m		meters
μ	(mu)	geometric mean
n		specific sample point
{n}		sample point count
N		total number of sample points
P_{atm}		atmospheric pressure
P_{H_2O}		water pressure
psia		pounds per square inch absolute
psid		pounds per square inch differential

psig		pounds per square inch gauge
PSU		practical salinity units
$\bar{\phi}$	(phi)	smoothed phase spectrum
ρ_{atm}	(rho)	atmospheric density
ρ_{H_2O}	(rho)	water density
s		seconds
S/m		Siemens per meter
$\bar{\bar{S}}$		smoothed, one-sided spectral density

ABSTRACT

A TIDAL STUDY OF GREAT BAY, NEW HAMPSHIRE

By

Sean Orlando Denney

University of New Hampshire, May, 2012

Since 1913, a number of short-term studies have failed to provide comprehensive tidal observations within the Great Bay (Bay). The purpose of this study was to make widespread observations of the tides in and to implement a tidal prediction model of the Bay.

With the use of four different tide gauges, calibration against a control gauge was necessary to determine systematic bias. After comparative analysis, each experiment gauge was found to be statistically equivalent to the control gauge.

Water level observations were taken at four strategic tide stations in the Bay. The tidal constituents and datums at each station were then derived. Using the NOAA TCARI prediction method, a tide prediction model of the Great Bay was implemented.

Verification of the model was made using water level measurements from three spatially and temporally strategic tide stations. The model was found to be statistically significant for tidal predictions within the Bay.

I. INTRODUCTION

One of the many *estuaries* that intersect the North Atlantic coastline, the Great Bay of New Hampshire (the Bay) has been the subject of numerous surveys and research studies (Fig. 1.0.1). One subject area that has eluded a successful result is that of a tidal prediction model representing the Bay. There is a need for more accurate tidal predictions within the Great Bay for navigation, recreational boating, environmental research, etc. The purpose of this study is to provide an accurate and comprehensive tidal prediction model for the Bay. In this study four tide gauges of different types were used to determine the tidal harmonics and *datums* at strategic locations in and around the Bay. From that information a tide prediction model was implemented and then verified using data collected *a posteriori*.

The tides in the Great Bay are driven by the tides in the Gulf of Maine, which in turn are driven by the tides in the North Atlantic Ocean. Additionally, the morphology of and frictional forces within the Bay have an impact on the observed tides (See §2.2). To the present day, the National Oceanic and Atmospheric Administration (NOAA) Center for Operational Oceanographic Products and Services (CO-OPS) tidal prediction estimates for the Squamscott River Railroad Bridge utilize Portland, ME as the primary station, Fort Point, NH as the secondary station, and no tertiary station (Fig. 1.0.1). (CO-OPS, 2010)

However, with limited comprehensive tidal observations in the Great Bay, quantifying

1
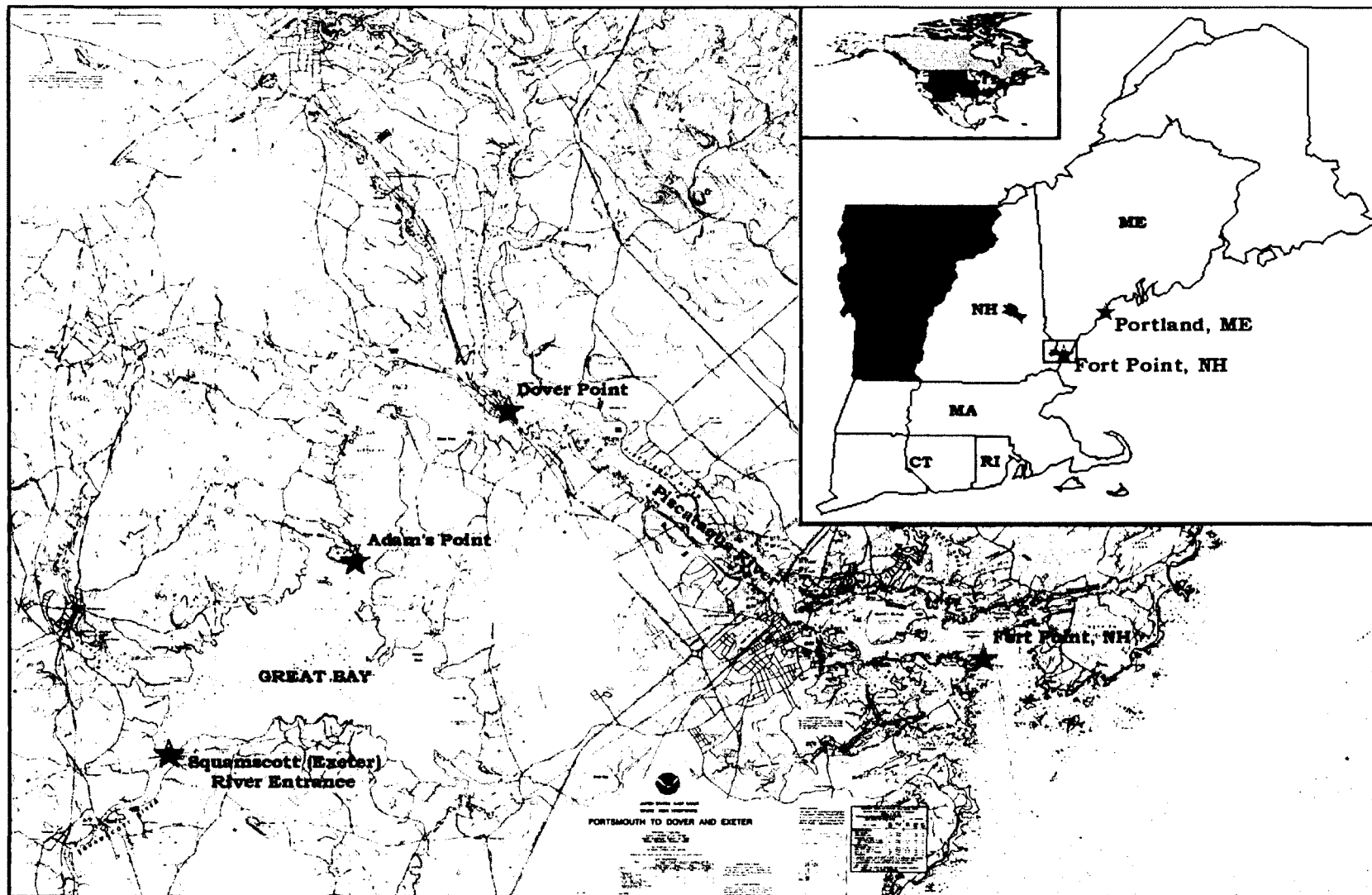
Figure 1.0.1: Points of interest related to the current study of Great Bay, Piscataqua River Estuary, New Hampshire. (Modified from OCS, 2005; 2011)

the *harmonic constituents* that make up the tides is difficult and modeling the tides from such sources is ineffective. A concise discussion of these historical tidal observations pertaining to as well as attempts at modeling the tides within the Bay is presented.

1.1 Historic Data. The United States Coast and Geodetic Survey (USC&GS) conducted the first official survey of the Great Bay in 1913. The tidal control work was performed relative to a tide staff located on a dock north of the former railroad bridge at Dover Point, NH (Fig. 1.0.1). *Mean Low Water* (MLW) and *Mean Range of Tide* (Mn) were computed from 41 high- and 42 low-water daytime observations. (Hoskinson and Le Lacheur, 1929) While the tide staff has long since been lost, and hence any comparison of vertical datums meaningless, the computed Mn (6.4 feet) can be useful for historic contrast. Additional observations that are relevant to the overall tidal characteristic of the Great Bay are further noted in the descriptive report submitted by the chief of party, R.P. Strough. For the area of the Great Bay— Fox Point to the Exeter River (now known as the Squamscott River),— Strough noted that "at low tide the mud flats in Great Bay extend nearly a mile from shore and are covered with eel grass." (Strough, 1913, p. 6)

In 1922, the USC&GS started a series of comprehensive tide and current surveys for the *important waterways* in the United States. The growth in commerce, defense, and scientific and engineering work since the end of World War I had created a need for "complete and up-to-date tide and current information." (Hoskinson and Le Lacheur, 1929, p. ii) One such important waterway was the Piscataqua River, owing to the location of one of the United States Navy's most important submarine bases on the

Atlantic Coast. In 1926, a comprehensive tide and current survey was conducted at ten locations, from Portsmouth Harbor to points upriver on the Piscataqua, Exeter, Cocheco, and Bellamy Rivers. Two such locations, *Station H: Dover Point* and *Station J: Exeter River Entrance*, are of historical interest to the study of tides in the Great Bay (Fig. 1.0.1).

At *Station H: Dover Point*, the tidal observations recorded in the 1913 hydrographic survey were recomputed against the long-term tide station at Portland, ME. Further, in 1926 an automatic tide gauge was affixed to the center pier of the former railroad bridge. The automatic tide gauge recorded tides continuously for six days. Through comparison against the long-term station at Portland, ME, the six-day record was then reduced to mean values. The Mn computed for both Dover Point tide records— 6.34 feet and 6.39 feet, respectively— and computation of the *lunitidal intervals for high water* (HWI)— 12.59 hours and 12.88 hours, respectively— and *low water* (LWI)— 6.34 hours and 6.75 hours, respectively— provide useful information for historical comparison. Lunitidal intervals are a useful measure of the time difference of high tide (or low tide) between tide stations, provided that the HWI (or LWI) are referenced to a particular meridian of *longitude* for both stations.

Each of the lunitidal intervals at *Station H* was referenced to the meridian of the Portland, ME tide station (70°14.8' W Longitude); conversion to the Greenwich meridian requires the subtraction of 7.32 hours from the HWI value— 5.27 hours Greenwich Mean Time

4

(GMT) and 5.56 hours GMT, respectively— and the addition of 4.68 hours to the LWI

values— 11.02 hours GMT and 11.43 hours, respectively.

Looking at the Mean Range of Tide, by comparison to the original computation previously discussed, the 1913 tide staff had apparently lost 0.06 feet (0.018 m). It is important to realize, however, that the recomputed value is in reference to the long-term tide station at Portland, ME, whereas the previous computation was referenced to itself. For comparison of the lunitidal intervals HWI and LWI for both tide records, a fair discrepancy seems to exist. As noted by Hoskinson and Le Lacheur (1929, p. 26), "fresh-water discharge would have a considerable effect on the tidal action, and it is, therefore, quite probable that the difference in the time relations [of the duration of fall being considerably longer than the duration of rise] are due to this cause." Further, they note the difference between the 1913 and 1926 records as likely due to the seasonal variation— mid-summer and early-fall, respectively— in fresh-water discharge. Mid-summer run-off volume is generally small in comparison to early summer for the Piscataqua River estuary. (Hoskinson and Le Lacheur, 1929)

At *Station J: Exeter River Entrance*, an automatic tide gauge was affixed to the draw span of the Boston and Maine Railroad bridge across the Exeter River (now known as the Squamscott River). While this draw span bridge has since been replaced by a fixed truss bridge, *benchmarks* (BM) and *tidal benchmarks* (TBM) had been set on the railroad bridge's granite abutments. The Mn (6.90 feet), HWI (13.69 hours ref Portland, ME or 6.37 hours GMT) and LWI (7.64 hours ref Portland, ME or 12.32 hours GMT) were

5

computed for this tide station, having been reduced by comparison to the long-term gauge at Portland, ME. Again, the difference between the 1913 and 1926 surveys show variation in the lunitidal intervals caused by changes in the seasonal variations in fresh-water discharge. (Hoskinson and Le Lacheur, 1929)

On March 6, 1953 the USC&GS had called for a "modern hydrographic survey of the coastal regions of New Hampshire and Northern Massachusetts." (Reed, 1955, p. 1) Between 1953 and 1954, a hydrographic survey was conducted for the Great Bay and Squamscott River. An automatic tide gauge affixed to the railroad bridge spanning the Squamscott River performed tidal control for that portion of the survey in the Great Bay (Fig. 1.0.1). The Mean Range of Tide was noted to be 6.9 feet while Mean Low Water was computed to be -9.7 feet below benchmark *B.M.1 (1926)*.

Additional observations that are relevant to the overall tidal characteristic of the Great Bay are further noted in the descriptive report submitted by the chief of party, C.R. Reed. The soundings observed during both the surveys of 1913 (H-3525) and 1953/4 (H-8093) were corrected for MLW at the previously discussed tide stations, respectively. Copies of the smooth sheets for these surveys are attached in Appendix A: Historic Data. In comparing these two smooth sheets, Reed noted "considerable change in shallow channels throughout Great Bay. Information from local fishermen reveals that eel grass holding channels left the Bay about ten years ago and the channels have filled in." (Reed, 1955, p. 2) It was further noted, "present depths along the ... natural channel through Great Bay are generally from 1 to 3 ft. less than prior depths." (Reed, 1955, p. 14) It is

additionally noted that the 1913 hydrographic survey was reduced to MLW using tidal observations at the Dover Point station rather than at the Squamscott River station.

In 1975 a cooperative research program between the University of New Hampshire (UNH) Sea Grant program and the NOAA's National Ocean Service (NOS) was realized to "measure currents and sea level in the Great Bay Estuarine System, New Hampshire." (Swenson *et. al.*, 1977, p. v) Tidal measurements were conducted by UNH and NOS at several locations in the estuary. Within Great Bay, two locations were chosen: *Station UNH* at the Jackson Estuarine Laboratory (JEL) at Adam's Point and *Station T-19* at the Boston and Maine Railroad bridge spanning the Squamscott River (Fig. 1.0.1). Two tidal *time series* records were made at *Station UNH* with 62- and 15-day record lengths, respectively, with half-hour *sample intervals*. At *Station T-19*, a 30-day tidal time series was recorded with 6-minute sample intervals using an automated tide gauge. (Swenson *et. al.*, 1977)

As evidenced by the results of the previous surveys and research studies conducted over the past century, discrepancies in tidal observations have occurred. The discrepancies relate, both directly and indirectly, to changes in the morphology of the estuary as well as to advancements in tide observing technology. With the disappearance of eelgrass, the alteration and loss of channels may have directly changed the tides in the Bay. Likewise, moving from manual methods of tidal observation to automatic tide recorders meant an increase in both precision and accuracy.

7

1.2 Modeling Efforts. In 1981, the seminal work by Swift and Brown (1983), using the data collected by the previously discussed UNH/ NOS collaboration, modeled the tidal energies as they propagated through an estuarine system. A tidal analysis was performed during the study with remarks related to the Great Bay, in particular:

> In the Great Bay estuary the M_2 constituent of the tide is clearly dominant exhibiting sealevel ... amplitudes an order of magnitude greater than the two other significant semi-diurnal constituents N_2 and S_2. (Swift and Brown, 1983, p. 304)

Further, a *harmonic analysis* conducted on the time series records from *Station UNH* and *Station T-19* are presented in Table 1.2.1. As previously noted, the M_2 constituent is the dominant tidal frequency in the Great Bay. Unfortunately, R. Swift and W. Brown made a crucial error in the phase computations. In converting local phase of tide to Greenwich meridian, rather than use the four species of tide [1, 2, 4, 6], only species [2] was used. The result of this mistake is that only the semidiurnal tidal constituents (M_2, S_2 and N_2 in Table 1.2.1) show the proper phase of tide. Corrected phase arguments, utilizing Equation 1.2.1, where G is Greenwich *epoch*, κ is local epoch, p is species number, and L is longitude are shown in Table 1.2.2. (Schureman, 1958)

Names	Frequency (cph)	Station UNH		Station T-19	
		Amplitude (m ± 0.04m)	Phase (° ± 2°)	Amplitude (m ± 0.04m)	Phase (° ± 2°)
M2	0.080511400	0.87	171	0.92	176
S2	0.083333330	0.13	221	0.10	225
N2	0.078999250	0.19	124	0.18	153
K1	0.041780750	0.11	301	0.11	324
M4	0.161022800	0.03	300	0.03	107
O1	0.038730650	0.10	287	0.10	306
M6	0.241534200	0.02	191	0.04	248

Table 1.2.1: Results, as published, of tidal harmonic analysis from the 1975 Great Bay Estuarine Field Program (Modified from Swift and Brown, 1983)

8

Names	Frequency (cph)	Station UNH		Station T-19	
		Amplitude (m ± 0.04m)	Phase (° ± 2°)	Amplitude (m ± 0.04m)	Phase (° ± 2°)
M2	0.080511400	0.87	171	0.92	176
S2	0.083333330	0.13	221	0.10	225
N2	0.078999250	0.19	124	0.18	153
K1	0.041780750	0.11	231	0.11	253
M4	0.161022800	0.03	216	0.03	235
O1	0.038730650	0.10	81	0.10	249
M6	0.241534200	0.02	115	0.04	171

Table 1.2.2: Corrected results of tidal harmonic analysis from the 1975 Great Bay Estuarine Field Program. Phase arguments in red are corrected compared to Table 1.2.1 (Modified from Swift and Brown, 1983)

$$G = \kappa + p \cdot L \qquad\qquad Eq. 1.2.1$$

Utilizing the same tidal observations from the 1975 Great Bay Estuarine Field Program, Ip et. al. (1998) attempted to model the tidal regime in the Bay using a finite element model. This model was designed to simulate the flooding and dewatering of shallow estuaries, based solely upon the amplitude of the M_2 constituent as computed by Swift and Brown (1983). Ertürk et. al. (2002) attempted to reproduce this model with a numerical approach. This numerical model was based upon both the amplitude and phase of the M_2, M_4, and M_6 tidal constituents as computed by Swift and Brown (1983). While the idea behind the model was sound, the application to Great Bay resulted in large discrepancies when looking at the amplitude and phase of the M_2 harmonic constituent. (Ertürk et. al., 2002) The most likely cause of the discrepancies are the nonlinearities of the estuarine system that were not taken into account in the model.

Using the same tidal observations from the 1975 Great Bay Estuarine Field Program, McLaughlin et. al. (2002) attempted to solve for the discrepancies that arose in the finite element model created by Ip et. al. (1998) and the numerical model created by Ertürk et. al. (2002). A numerical model was developed using dynamic physics for deep-water

areas and kinematic physics for shallower areas. The result of this model was a much smaller residual in the amplitude and phase of the M_2 harmonic constituent for those stations within the Bay. Unfortunately, the amplitudes and phases of the N_2 and S_2 harmonic constituents still had large residuals. (McLaughlin *et. al.*, 2002)

One key point of these modeling efforts is their commonly dependent nature. All three modeling attempts utilize select data from Swift and Brown (1983) and then utilize the same tidal data in their comparative analyses. In other words there is no independent corroboration of the tides in the Bay; internal consistency is analyzed, but there is a lack of groundtruthing, which allows for a high probability that bias, error or *blunders* in the data go unnoticed.

From both the historic accounts of tidal observations as well as the modeling efforts, it is clear that the Great Bay is a highly dynamic environment. This dynamism is primarily related to those factors involving shallow-water tides (*e.g.* water depth, morphology, and friction) as well as non-tidal factors (*e.g.* weather forcing).

II. SHALLOW-WATER TIDE THEORY

In order to discuss the problem and objectives of the study, an understanding of tides is imperative. However, for the sake of brevity, the discussion of tides will be limited to the understanding of tides as they relate to shallow-water environments, namely estuaries.[1] Thus, an assumption is made as to a basic understanding of Isaac Newton's Law of Universal Gravitation and of tide generating and tractive forces (Hawking, 2000), of the Equilibrium Theory of Tides conceived by Newton and advanced by Daniel Bernoulli, Leonhard Euler, and Colin Maclaurin (Cartwright, 1999), of the Dynamical Theory of Tides developed by Pierre Simon, the Marquis de Laplace, and refined by George B. Airy (Simon, 1829; Cartwright, 1999), and of tidal friction investigated by Airy and George H. Darwin (Airy, 1847; Darwin, 1898).

2.1 Harmonic Analysis. Since the middle of the nineteenth century, any reduction of tides has relied upon the harmonic analysis approach. With advancements in mathematics it is now possible to perform analysis on periodic data series by approximation. Daniel Bernoulli, in 1753, made the first reference to a method of expressing the periodic oscillations of a vibrating string as a trigonometric series. It would not be until Jean Baptiste Joseph Fourier, in 1807, that the harmonic method of analysis would be refined enough to express such a periodic data set in terms of a definite integral. (Harris, 1898) It was Fourier's researches in to heat flow that led to the general

---

[1] For an indepth look at tidal history and theory, numerous compilations have been written on the subject, including Darwin (1898), Harris (1898), Cartwright (1999), and Parker (2007).

11

discovery of the *Fourier series* and the *Fourier transform*. (Fourier, 1878) Further

mathematical advancements related to the harmonic analysis of tides include the

Legendre differential equation and *Legendre Polynomial* by Adrien-Marie Legendre

(1785), and the *least-squares method* by Laplace (1820).

Sir William Thomson (Lord Kelvin), in 1867, performed the first harmonic analysis of

the tides using *Fourier's Theorem* (Fourier series) and Laplace's least-squares method.

Borrowing the concept of *astres fictifs* from Laplace, Thomson treated the moon not as a

single mass revolving in its oblique, elliptic orbit around the earth, but as multiple

satellites with simplified orbits and motions about the earth's equatorial plane. In doing

so, each faux moon contributes different harmonic constituents to the tide at a given

location on earth. (Thomson and Tait, 1888)

Thomson, after much investigation into the simple harmonic motion of these faux

satellites and the knowledge of celestial motions and perturbations of the earth, moon and

sun, was able to infer the existence of numerous diurnal, semidiurnal and ter-diurnal

tides, as well as quarter-, sixth- and eighth-diurnal shallow-water tides. The term *tide* in

this context is interchangeable with the faux satellite as previously discussed. Thomson

labeled each tide with a distinguishing letter or letters, most notably $S, R, T, P, K, M, L,$

$N, O, J, Q, \lambda, \nu, \mu$ (or $2MS$), $2SM, MS, 3MS$ and $3SM$. Applying the least-squares method

to a number of observed tidal records, William Thomson, with the aide of Edward

Roberts, was able to analytically deduce the diurnal, semidiurnal, ter-diurnal, and

shallow-water tidal amplitude and phase for these numerous inferred tides. (Thomson and Roberts, 1872)

Following Thomson, George H. Darwin focused considerable work on the harmonic analysis method— primarily in the study of the earth's elasticity through the study of the tides. Darwin abandoned Thomson's previous treatment of *astres fictifs* in the method of harmonic analysis of the tides, instead focusing on the use of spherical trigonometry to solve for the moon's (and sun's) tide-generating potential. Aside from redefining the method of harmonic analysis of tides, Darwin's major contribution was to incorporate both the "obliquity of the lunar orbit to the equator," I in Figure 2.1.1, and the "eccentricity of the moon's orbit" in the solution. (Darwin, 1883, p. 54) Darwin, unfortunately, retained the naming convention used by Thomson, however with one slight modification. A numerical subscript corresponding to the nth-diurnal tide was added to identify tides with multiple cycles per day (*i.e.* Thomson's *M for diurnal tides* and *M for semidiurnal tides*, etc. corresponds to Darwin's M_1 and M_2, etc., respectively).

The next individual to contribute greatly to the understanding and analysis of tides was Arthur T. Doodson. In analyzing the residuals between observed and predicted tides from the harmonic analysis and reduction method as devised by Darwin, Doodson noticed that there were a number of potential tidal constituents that were left unresolved. Since Darwin's work in 1883, advancements in lunar theory, especially those of Ernest W. Brown (1896), allowed Doodson to increase the accuracy to which tidal constituents were computed. Likewise, the use of Legendre's Polynomial in the solution to tidal

13
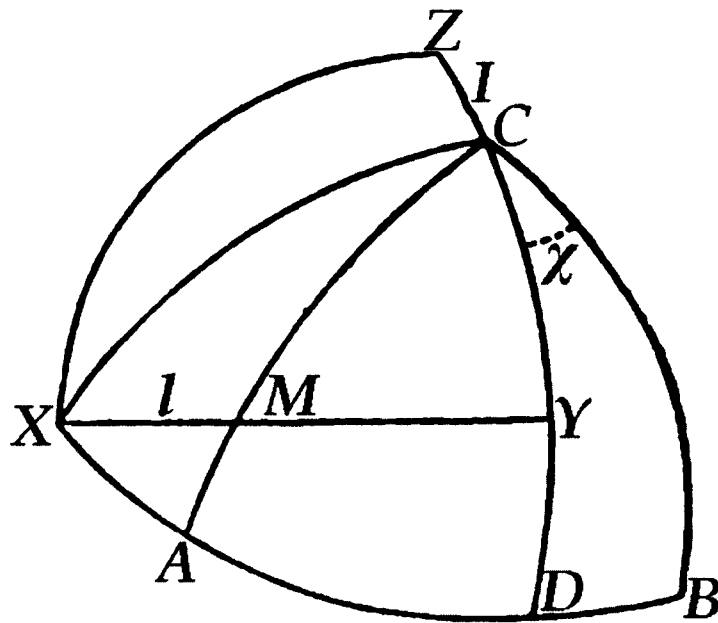
Figure 2.1.1: Reproduction of G.H. Darwin's illustration for spherical coordinates of the moon's motions in reference to axes fixed on the earth. A, B, and C represent the axes of the earth, with C representing the north pole, and AB representing the equator; X, Y, and Z represent the axes corresponding to the plane of the moon's orbit. XY; M is the projection of the moon in its orbit; I represents the obliquity of the lunar orbit to the equator, AB; l represents the moon's longitude in its orbit as measured from X; and χ represents the angle AX and BCY. (Darwin, 1883)

potential allowed Doodson to increase the accuracy to which the tidal harmonics could be determined. Another modification in Doodson's method of harmonic analysis over Darwin's was to reference the coordinate system not to the lunar orbit, XY (Fig. 2.1.1) and ΥM (Fig. 2.1.2), but instead to the ecliptic, ΥL (Fig. 2.1.2), where Υ represents the *first point of Aries*. (Doodson, 1921) Using these methods Doodson was able to resolve 399 harmonic constituents. (Doodson, 1921; 1924; 1928)

Independent of Thomson, Darwin and Doodson, William Ferrel (1874; 1878), Rollin Harris (1898) and Paul Schureman (1924; 1958) of the United States Coast and Geodetic Survey (known as the United States Coast Survey prior to 1878) developed a similar tidal harmonic analysis and prediction method. While both methods are built upon the work

14

of Laplace and both utilize Fourier's Theorem, Ferrel also incorporated the theories of

George Biddell Airy (to be discussed further in §2.2) into the harmonic analysis.
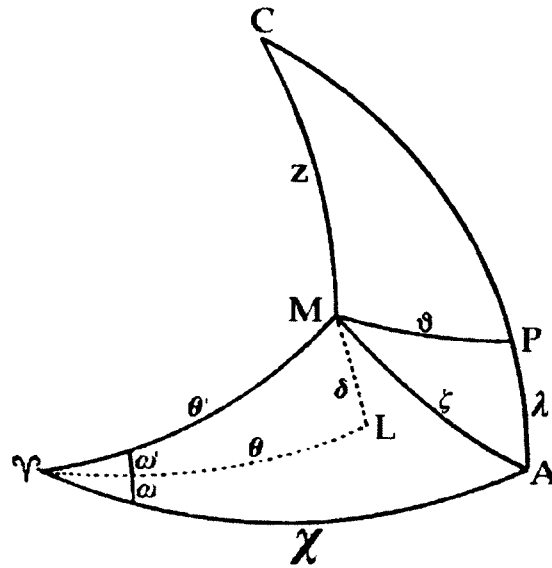
Figure 2.1.2: Reproduction of A.T. Doodson's illustration of the different orbital reference planes. In the illustration ♈ represents the first point of Aries (or vernal equinox), M represents the moon, C represents the celestial north pole, P represents an arbitrary location on the celestial sphere, and A represents the intersection of the meridian of P with the celestial equator, λ. (Doodson, 1921)

2.2 Tides in Estuaries. While the method of harmonic analysis of the tides was being

developed and refined, research into the phenomena that produce shallow-water tides was

unfolding. Shallow-water tides are those tides that are affected by the depth of water,

frictional forces caused by terrigenous sediments, and the shape of the water body in

which the tides occur. Examples of shallow-water environments include, but are not

limited to, *bays* and estuaries.

Through the investigations of fluid motion by Joseph Louis Lagrange, in a shallow canal

of infinite length whose cross-section is rectangular, the velocity of a wave (or

progression of the phase of tide) whose wavelength is much greater than the depth of

water was shown to be expressed as the square-root of the product of gravity, g, and water depth, α, independent of the wavelength of the tide (Eq. 2.2.1). (Lagrange, 1869; Cartwright, 1999)

$$\text{wave velocity} = \sqrt{g\alpha} \qquad\qquad \text{Eq. 2.2.1}$$

Expanding upon Lagrange's work, George Biddell Airy's primary focus was to generalize the wave motion in order to study the tides in the real world. Having derived both the equation of continuity and the equation of equal pressure, and assuming the motion of the waves to be oscillatory, Airy first investigated whether both equations hold for waves within a canal of equal breadth and variable depth. He concluded that the equation of equal pressure must hold everywhere, however the equation of continuity must cease and the tide wave must become discontinuous (or "broken"). (Airy, 1847, p. 289; Harris, 1898)

The next issue that Airy took up was the study of the motion of a very long wave in a canal. His deductions led him to showing how, as a wave progresses in a canal farther from the sea, the front slope of the wave becomes shorter and steeper while the rear slope becomes longer and gentler (Figure 2.2.1). (Airy, 1847)

In the same analysis, Airy also shows that the duration of the fall of tide above its mean state will exceed the duration of the rise of tide for this same long wave. As most estuaries and rivers leading to the sea have a non-tidal current running toward the sea,
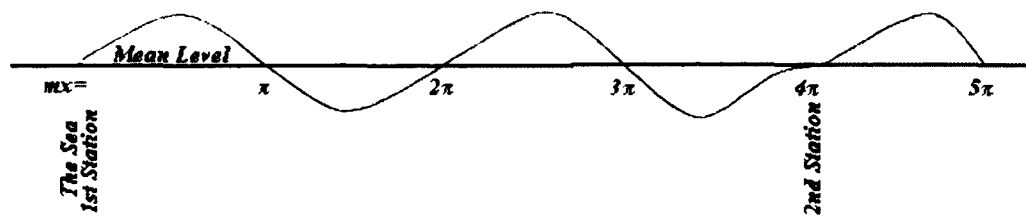
Figure 2.2.1: Reproduction of G.B. Airy's figure captioned "*Theoretical form of a tide-wave in a shallow river to second approximation*" which demonstrates the progression of a "very long wave, as the tide wave in a canal whose depth is so small that the range of elevation and depression of the surface bears a considerable proportion to the whole depth." (Airy, 1847)

Airy's solution to this problem shows that the duration of fall is not just longer, but much longer than the duration of rise as compared to the case with no such seaward current. Further investigations by Airy include canals of variable breadth and length. As a canal becomes narrower in breadth or shallower in depth, the slack before either ebb or flood will occur earlier than if the canal had not contracted or shoaled.

Taking into account the force of friction, Airy concludes that the "greatest tide follows the greatest [tidal] force" in a time proportional to the coefficient of friction. (Airy, 1847, p. 333) Likewise, due to the force of friction, both the vertical and horizontal motions of the fluid particles will diminish the further upstream they are from the sea. As well, the flow ceases prior to the water surface returning to mean elevation causing the tide to turn earlier than in the case of no friction. (Airy, 1847; Harris, 1898)

2.3 Shallow-water Tide Generation. With an understanding of the primary forces affecting shallow-water tides, a discussion of shallow-water tidal harmonic constituents can commence. Arthur T. Doodson and Harold D. Warburg, in the *Admiralty Manual of*

17

Tides (1941), provides a simple illustration of the relationship between the tides in the open ocean and the shallow-water tides as they progress in an estuary upstream.

Referring to Figure 2.3.1,

> *Suppose ... the curve* (a) *represents the profile of a progressive wave entering a channel from deep water. Such a wave will be represented by a simple harmonic curve in which the time interval from low water to high water is equal to that from high water to low water.* (Doodson and Warburg, 1941, p. 62)
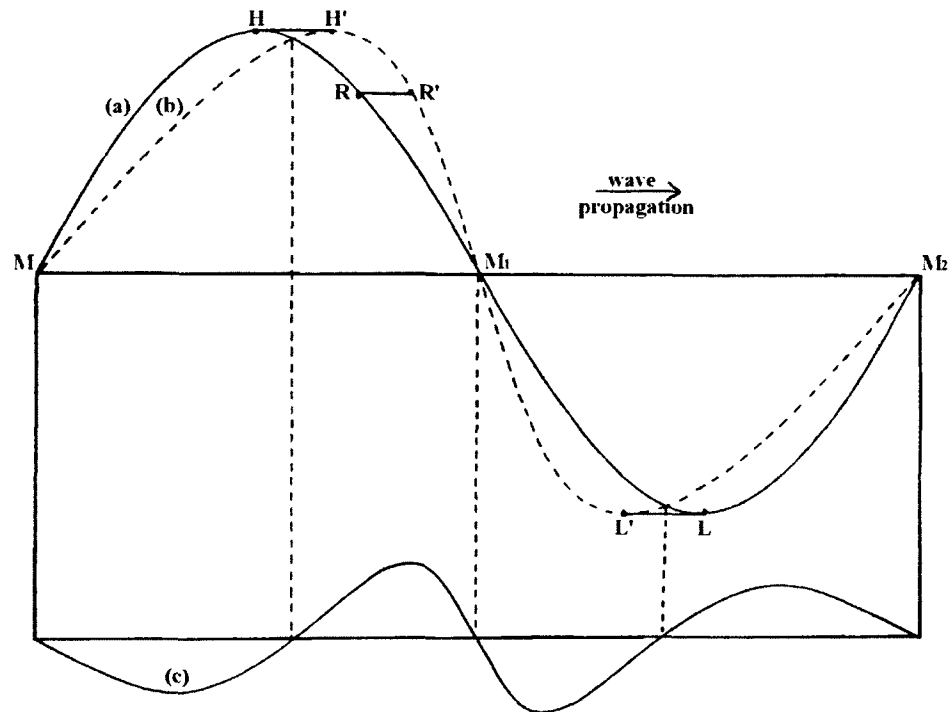
Figure 2.3.1: Reproduction of A.T. Doodson's figure captioned "Deduction of quarter-diurnal tide from change of shape of progressive wave" which demonstrates the harmonic analysis of shallow-water tides. (Doodson and Warburg, 1941)

As discussed previously in section 2.2,

It is shown ... that the effect of travelling along an infinitely long channel in shallow water is to change the shape of the wave so that high water is accelerated and low water is retarded ... (Doodson and Warburg, 1941, p. 62)

As the simple harmonic tide represented by (a) progresses up the estuary a certain distance, the curve (b) is depicted, thus

Suppose that after a certain lapse of time t *the profile is again drawn on the same diagram as the original profile, so that the points* M *at the mean level* [(Fig. 2.3.1)] *are made to coincide. Then the high water* H *will appear to have moved to* H' *and the low water* L *will have appeared to have moved to* L'. ... (Doodson and Warburg, 1941, p. 62)

Remarking upon the apparent change from curve (a) to curve (b), Doodson and Warburg notes

Hence the distance RR' *through which* R *will appear to have moved will be proportional to the elevation at* R, *and therefore* RR'/HH' *will be equal to the ratio of the elevations at* R *and* H.

Now let the elevations for (a) *be subtracted from those of* (b), *and let the result be given in* (c). *It is at once apparent that the latter curve has two complete oscillations for one of the original curve* (a). *... If* (a) *represents a tidal oscillation with a period of 12 hours, then* (c) *will represent an oscillation with a period of six hours.* (Doodson and Warburg, 1941, p. 63)

Finally, at a time and distance from the mouth of the estuary, a shallow-water tide, curve *(c)*, is generated from the pure harmonic tide, curve *(a)*, and the actual tide, curve *(b)*.

... it may be readily seen that the curve (c) *is not a pure harmonic curve, for the distances between the points of zero level are not equal. For the further examination of this curve let it be transferred to* [Figure 2.3.2], *where it is still called* (c), *and let curve* (d) *be a simple sine curve whose amplitude is the average high water height of curve* (c). (Doodson and Warburg, 1941, p. 63)
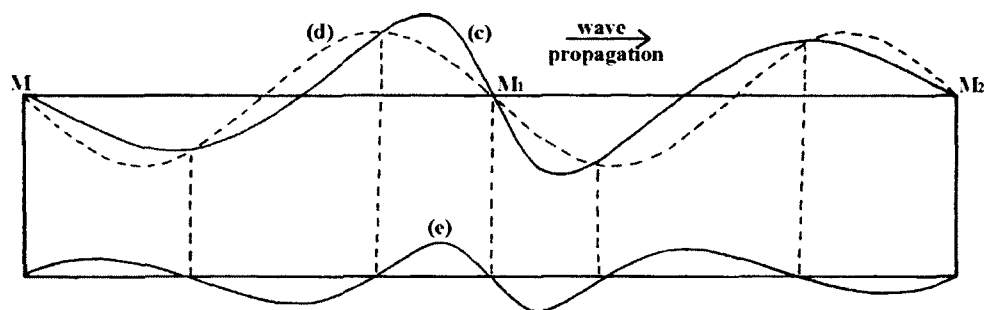
Figure 2.3.2: Reproduction of A.T. Doodson's figure captioned "*Deduction of higher species of shallow-water tides from change of shape of progressive wave*" which further demonstrates the harmonic analysis of shallow-water tides. (Doodson and Warburg, 1941)

As before with curves *(a)*, *(b)* and *(c)*, curve *(e)* is a shallow-water tide generated from the difference between the pure harmonic tide, curve *(d)*, and the previous shallow-water tide, curve *(c)*. If the original curve *(a)* entering the mouth of the estuary were a semi-diurnal tide, then curve *(c)* represents a quarter-diurnal tide and curve *(e)* represents a sixth-diurnal tide.

Doodson and Warburg concludes the analysis of shallow-water tide generation

Hence we conclude that any tide upon the earth may be expected to contain terrestrially generated tide, so that with a semidiurnal primary the secondary tides so generated will be of the quarter-diurnal, sixth-diurnal, and higher species of tides, while if the primary is a diurnal tide it will generate semidiurnal, third-diurnal, and higher species of tides. (Doodson and Warburg, 1941, p. 63)

From this illustration, it can be seen that an iterative process is involved in deducing the shallow-water harmonic constituents. As an example, if the primary tide entering an estuary is composed simply of the semi-diurnal lunar tide, M_2, and the semi-diurnal solar tide, S_2, then the following derivation of shallow-water tides is as follows

> *Let the elevation* [of a point above the mean level, y,] *be composed of two terms* M_2 *and* S_2 *and let these be denoted by* $A \cdot \cos a$ *and* $B \cdot \cos b$ *respectively. Then ...*
>
> $$y = A \cdot \cos a + B \cdot \cos b$$
> $$y^2 = A^2 \cdot \cos^2 a + B^2 \cdot \cos^2 b + 2AB \cdot \cos a \cos b$$
>
> [In order to maintain an oscillatory function, the squares must be taken out of the trigonometric terms.] *This can be written*
>
> $$y^2 = \tfrac{1}{2} A^2 \cdot \cos 2a + \tfrac{1}{2} B^2 \cdot \cos 2b + AB \cos(a+b) + AB \cos(a-b) + C$$
>
> *From two harmonic terms in* y *we get four harmonic terms in* y^2. *From* [Cartwright and Edden (1973)] *take*
>
> $$A = 0.90809 \; for \; M_2 \; and \; B = 0.42248 \; for \; S_2$$
>
> *then we get constituents as* [noted in Table 2.3.1]. (Doodson and Warburg, 1941, p. 67)

Repeating the steps used to generate the quarter-diurnal tides from the semi-diurnal tides, the sixth-diurnal and higher species of tides can be derived (Table 2.3.1). It will be noted that perturbations in the primary tides— M_2 and S_2 in the example— will arise in the higher species of shallow-water tide. Using this method of analysis for shallow-water tides, hundreds of tidal constituents can be derived. (Doodson, 1921; 1924; 1928)

The main contribution of shallow-water tides is to cause the steepening of the rise of tide and the hastening of the time of high water— or flattening of the fall of tide and the

lengthening of the time of low water. This effect is due to the factors that affect shallow-water environments.

Tidal Harmonic Const.	Cartwright Potential Coefficient	Argument	Elevation
M_2	$A = 0.90809$	a	$y_{M_2} = A\cos a$
S_2	$B = 0.42248$	b	$y_{S_2} = B\cos b$
$M_2 + S_2$			$y = y_{M_2} + y_{S_2} = A\cos a + B\cos b$
$(M_2 + S_2)^2$			$y^2 = \frac{1}{2}A^2\cos 2a + \frac{1}{2}B^2\cos 2b + AB\cos(a+b) - AB\cos(a-b) + C$
M_4	$\frac{1}{2}A^2$	$2a$	
MS_4	AB	$a+b$	
S_4	$\frac{1}{2}B^2$	$2b$	
MSf	AB	$a-b$	
$(M_2 + S_2)^3$			$y^3 = \frac{1}{4}A^3(\cos 3a + \cos a) + \frac{1}{4}AB^2\left[\cos(2b+a) + \cos(2b-a)\right] + \frac{1}{2}A^2B\left[\cos b + \cos(2a+b)\right]$ $+ \frac{1}{4}A^2B\left[\cos(2a+b) + \cos(2a-b)\right] + \frac{1}{4}B^3(\cos 3b + \cos b) + \frac{1}{2}AB^2\left[\cos(a+2b) + \cos a\right] + C$
M_6	$\frac{1}{4}A^3$	$3a$	
$2MS_6$	$\frac{3}{4}A^2B$	$2a+b$	
$2SM_6$	$\frac{3}{4}AB^2$	$2b+a$	
S_6	$\frac{1}{4}B^3$	$3b$	
M_2	$\frac{1}{4}A^3 + \frac{1}{2}AB^2$	a	
S_2	$\frac{1}{2}A^2B + \frac{1}{4}B^3$	b	
$2MS_2$	$\frac{1}{4}A^2B$	$2a-b$	
$2SM_2$	$\frac{1}{4}AB^2$	$2b-a$	
...	...	...	...
$(M_2 + S_2)^n$			$y^n = y^{n-1}\cdot y$

Table 2.3.1: Generation of shallow-water tidal harmonic constituents from the M_2 (semidiurnal lunar) and S_2 (semidiurnal solar) tidal harmonic constituents. (Doodson and Warburg, 1941; Parker, 2007)

2.4 Meteorological Tides. George H. Darwin, in a series of lectures given in 1897, coined the term *meteorological tides*. Meteorological tides are "any regular alternation of sea-level" due to "regularly, periodic winds," "variation of atmospheric pressure," and "the melting of the snows ... and the annual variability in rainfall and evaporation." (Darwin, 1898, p. 2-3)

While many of the periodic meteorological elements require extremely long records to account for them, the variation in atmospheric pressure can be corrected for when observing the tides. Daniel Bernoulli, while most famous for his contributions to the equilibrium theory of tides, had focused much attention to the phenomena of hydrodynamics. From Bernoulli's equation for hydrostatic pressure (Eq. 2.4.1) it is possible to derive the time-varying equation for sea-surface elevation corrected for atmospheric pressure and water density (Eq. 2.4.2).

$$p = \int_{-h}^{\infty} \rho g \, dz \qquad \qquad \text{Eq. 2.4.1}$$

$$p_{H_2O}(t) = \int_{\eta}^{\infty} \rho_{atm}(z,t) g \, dz + \int_{0}^{\eta} \rho_0(t) g \, dz + \int_{-h}^{0} \overline{\rho}_{H_2O}(t) g \, dz + \int_{-h}^{0} \rho'_{H_2O}(t) g \, dz$$

$$= p_{atm}(t) + \rho_0(t) g \eta(t) + \overline{\rho}_{H_2O}(t) g h + \text{constant}$$

$$p_{H_2O}(t) - p_{atm}(t) \approx \rho_{H_2O}(t) g \eta(t)$$

$$\eta(t) \approx \frac{p_{H_2O}(t) - p_{atm}(t)}{\rho_{H_2O}(t) g_{Lat}} \qquad \qquad \text{Eq. 2.4.2}$$

In the derivation of Equation 2.4.2, the assumption is made that the fluid is both incompressible and inviscid. The integral terms, from right to left, represent: (1) the time-varying atmospheric pressure, (2) the time-varying surface density elevation, (3) hydrostatic depth, and (4) the perturbation due to depth-varying density. Sea surface elevation is relative to the depth of water at which water pressure and density are measured. Gravity is computed as a function of *latitude* using the *International Gravity Formula of 1980* (Moritz, 1980).

III. PHASE 1: CALIBRATION

With the large range of tidal sensors used in this experiment, determining the accuracy to which each tide gauge is capable of observing the tides is a necessity. The requirements for selecting a testing protocol included a control tide gauge, geographic proximity, and existing infrastructure to support additional tide gauges.

3.1 Tide Gauges. During the initial planning stage of the project, the availability of resources, namely tide gauges, was a major concern. Further, each tide gauge is made up of a number of sensors, the combination of which are used to determine water level. For each sensor included in one or more tide gauges mentioned in the study, a brief discussion of its functions is presented in Appendix B: Tide Sensors. Along with the discussion of each sensor and tide gauge, Table 3.1.1 and Table 3.1.2 summarize the numerous sensors and tide gauges, respectively, used in the study.

Sensor Name	Sensor Model	Sensor Measurements
NCDC *Atmospheric Pressure Sensor [Coastal Environmental Systems, (Druck)]*	*RPT410F-8999*	Barometric Pressure (mbar)
Onset HOBO logger	U20-001-02	Temperature (°C), Pressure (kPa)
Paroscientific Digiquartz Intelligent Transmitter	6000-30G	Gauge Pressure (psig)
SeaBird MicroCAT C-T Recorder	SBE 37-SM	Temperature (°C), Conductivity (S/m)
SeaBird SeaCAT C-T-P Recorder	SBE 16plus	Temperature (°C), Conductivity (S/m), Pressure (psia)
Aquatrak	3000 Series	Differential Time-of-flight (s)
WaterLog Gas Purge Bubbler	H-355-30-PM	Head Pressure (psia)
WaterLog Radar Water Level Sensor	H-3611	Averaged time-of-flight (s)

Table 3.1.1: Tide sensor names, models, and measurements.

For those gauges that are governed by Equation 2.4.2— the Onset HOBOlogger, the SeaBird SeaCAT, and the WaterLog Bubbler,— measurement of water pressure, atmospheric pressure, and water density are required. Water density is often computed indirectly through measurement of temperature, conductivity, and pressure (although pressure is often a constant for shallow-water environments).

Tide Gauge Name	Tide Gauge Primary Components
NOAA Aquatrak	Aquatrak Absolute Liquid Level Sensor, Model 3000 Series; Sutron Aquatrak Controller; Sutron SatLink 2 Logger/ Transmitter.
Onset HOBOlogger	NCDC Atmospheric Pressure Sensor; Onset HOBO logger, Model U20-001-02; SeaBird MicroCAT C-T Recorder, Model SBE 37-SM.
SeaBird SeaCAT	NCDC Atmospheric Pressure Sensor; SeaBird SeaCAT C-T-P Recorder, Model SBE 16plus.
WaterLog Bubbler	NCDC Atmospheric Pressure Sensor; Paroscientific Digiquartz Intelligent Transmitter, Model 6000-30G; SeaBird MicroCAT C-T Recorder, Model SBE 37-SM; Sutron 9210 XLite, Model 9210-0000-2A; Trimble Bullet III GPS Antenna; WaterLog Gas Purge Bubbler, Model H-355-30-PM; Wilkerson Manual Desiccant Dryer, Model X03-02-Q03.
WaterLog MWWL	Sutron 8080 Xpert, Model 8080-0000-2B; Trimble Receiver/ Antenna GPS, Model GPS 17x HVS; WaterLog Radar Water Level Sensor, Model H-3611.

Table 3.1.2: Tide gauge names and primary components.

The NOAA Aquatrak is, currently, the principal sensor of the NOAA CO-OPS for use at long-term control and secondary tide stations. The NOAA Aquatrak consists, primarily, of the Aquatrak sensor (See Appendix B: Tide Sensors), a Sutron Aquatrak microcontroller, and a Geostationary Operational Environmental Satellite (GOES) transmitter. Within the microcontroller, a patented ratiometric method is used to calculate the distance between the sensor and the sea surface height based upon differential time-of-flight. The method also involves compensation for temperature variations in the gauge. (Aquatrak, 2006) Vertical referencing the air-gap distance— the

distance between the sensor reference and the water surface— to a water level datum is accomplished via *leveling* to vertical benchmarks or GPS measurement.

The Onset HOBOlogger is a pressure-based gauge consisting of the Onset HOBO logger and the SeaBird MicroCAT C-T Recorder sensors. While the Onset HOBO logger sensor measures water temperature and water pressure, it does not record any information related to water conductivity or atmospheric pressure (Eq. 2.4.2). Water density is computed from temperature and conductivity measured by the SeaBird MicroCAT sensor. Atmospheric pressure is obtained from the NOAA National Climate Data Center (NCDC) database record for the nearby weather station at Pease International Tradeport, Portsmouth, NH. The Coastal Environmental Systems FMQ19's three Druck RPT410F barometric sensors provide the atmospheric pressure data recorded in the NCDC database (See Appendix B: Tide Sensors). From this point forward, this sensor will be referred to as the "NCDC atmospheric pressure sensor" or the "NCDC weather station." Vertical referencing of the water level for this gauge is made to an orifice on the Onset HOBO logger sensor.

The SeaBird SeaCAT tide gauge consists of the SeaBird SeaCAT C-T-P Recorder (See Appendix B: Tide Sensors). As this gauge is pressure based, the computation of sea surface elevation is governed by Equation 2.4.2. Water density is computed from temperature, conductivity, and pressure measured by the SeaBird SeaCAT sensor. Atmospheric pressure record is obtained from the NOAA NCDC weather station at Pease International Tradeport, Portsmouth, NH. Vertical referencing of the water level at this

gauge is made to the strain pressure gauge orifice on the SeaBird SeaCAT C-T-P Recorder sensor.

The WaterLog Bubbler tide gauge is comprised of the WaterLog Gas Purge Bubbler, the Paroscientific Digiquartz Intelligent Transmitter, a Sutron XLite data logger, a Trimble Bullet III GPS Antenna, and a Wilkerson Desiccant Dryer (See Appendix B: Tide Sensors). A pressure-based gauge, the WaterLog Bubbler records the differential pressure (psid) between the gauge pressure measured by the Digiquartz sensor and the head pressure measured by the WaterLog Gas Purge Bubbler sensor ($p_{H_2O} - p_{atm}$ in Eq. 2.4.2). In order to account for moisture and salt in the air, all air used in the tide gauge is passed through the Wilkerson Desiccant Dryer. In order to comply with Equation 2.4.2, water density is computed from temperature and conductivity measured by the SeaBird MicroCAT sensor. While this gauge measures differential pressure, the numerator in Equation 2.4.2, a localized atmospheric pressure record is obtained from the NOAA NCDC weather station at Pease International Tradeport, Portsmouth, NH for use in the analysis of pressure measurements. Time synchronization is achieved via the attached Trimble Bullet III GPS antenna. Vertical referencing for the water level at this gauge is made to a submerged brass orifice.

The WaterLog MWWL tide gauge is made up of the WaterLog Radar Water Level Sensor, a Trimble GPS17x HVS receiver/ antenna, and a Sutron Xpert data logger (See Appendix B: Tide Sensors). The Sutron Xpert records air-gap distance as computed by the WaterLog Radar Water Level Sensor from the measured time-of-flight information.

Time synchronization is attained via the attached Trimble GPS receiver/ antenna unit. Vertical referencing for water level is achieved via leveling to nearby vertical benchmarks, reference measurements taken on the tide gauge, and a fixed-range test conducted on the tide gauge.

3.2 Methods. The United States Coast Guard (USCG) boathouse at Fort Point, NH was selected for the calibration site. The pre-existence of a NOAA secondary tide gauge (Aquatrak), the proximity to the study area, and the USCG boathouse infrastructure meant this location met all the requirements previously listed (Fig. 3.2.1; Table 3.2.1). Each tide gauge in the study was placed near the control gauge (Fig. 3.2.2a-c).

Figure 3.2.1: Phase 1 tide gauge location. (OCS, 2005; 2011)

ID	Location Name	Gauge Name	Latitude (N)	Longitude (W)
1	Fort Point, Newcastle, NH	NOAA Aquatrak	43.07166667°	70.71166667°

Table 3.2.1: Phase 1 tide gauge identification, location, name, latitude and longitude.

A second-order, *three-wire level* loop was run between nearby, pre-existing vertical benchmarks, following the prescribed procedures outlined by Paul R. Wolf. (Wolf and

Brinker, 1994) The purpose of this level run was to relate the water level observations from the experiment gauges to the control gauge. As some of the benchmarks in the area have deteriorated or have been lost, finding two that were stable and checked to known elevations took some time. The field notes for the numerous level runs in this area can be found in Appendix C: Field Notes. Misclosure for the final level run was 0.000 m.

Figure 3.2.2a-c: Tide gauge calibration deployment at Fort Point, NH; a. NOAA Aquatrak, b. WaterLog MWWL, c. WaterLog Bubbler. Not shown: Onset HOBOlogger, SeaBird MicroCAT, and SeaBird SeaCAT (See Appendix B: Tide Sensors for additional imagery).

Each sensor was set to a sample interval that was both memory-efficient and allowed for a simple averaging to match the control gauge's six-minute sample interval. An ideal record length of thirty or thirty-one days was planned for, however this was not always possible due to project time constraints (Table 3.2.2). Data from the control gauge was downloaded from the NOAA CO-OPS Tides and Currents database for the concurrent time period for each gauge.

Tide Gauge or Sensor Name	Sample Interval	Record Length
Onset HOBOlogger	360 seconds	53 days, 12 hours, 00 minutes
SeaBird MicroCAT	120 seconds	20 days, 22 hours, 54 minutes
SeaBird SeaCAT	60 seconds	09 days, 20 hours, 18 minutes
WaterLog Bubbler	360 seconds	20 days, 22 hours, 54 minutes
WaterLog MWWL	1 second	34 days, 13 hours, 00 minutes

Table 3.2.2: Tidal instrumentation sample interval and record length.

The WaterLog Bubbler was coupled with the SeaBird MicroCAT during calibration. The unknown water density in Equation 2.4.2 was then determinable. Similarly, the Onset HOBOlogger was coupled to the SeaBird SeaCAT for the same reason.

3.3 Data Processing. Subsequent to each phase of data collection, the computation of water level, tidal constituents, datums, and other statistics were necessary. The sheer volume of information and the disjointed raw data sets suggested automating this process. Devising a common data format was one of the first concerns. A large portion of time during the study was dedicated to this process of automation. See Appendix D: Data Processing for more detailed information on general data processing techniques and algorithms.

In order to analyze and compare time series, the time records must exist on the same time reference. In the case of the Onset HOBOlogger, time is referenced to the local time zone— Eastern Daylight Time (EDT) for Phase 1,— while the remaining sensors are referenced to GMT. An offset of +4 hours was applied to reference the time series to GMT. Furthermore, due to human error, the date encoded in the SeaBird MicroCAT was off by forty-four days. Another offset was applied to correct for this blunder.

As three of the tide gauges are based on water pressure, an atmospheric pressure time series was needed to either fill this unknown in Equation 2.4.2 or for further analysis of pressure measurements. The NCDC atmospheric pressure record was used for this purpose. However, when control of the sensor was changed from the United States Air Force (USAF) to the Federal Aviation Administration (FAA) on March 01, 2011, the sample time switched from on-the-hour to a more erratic schedule. A linear interpolation was applied to gain an on-the-hour time series. Further linear interpolation was used to attain a time series with a six-minute sample interval. While a cubic spline interpolation is preferable, the low variance in the atmospheric pressure (See §3.4) allows for a linear interpolation in this case.

Duplicates and gaps were dealt with and block-averaging was applied to all time series (Table 3.3.1-4). Following these steps, all time series are both continuous and have on-the-six-minute sample intervals.

Time Series	Raw Data Size	Duplicates	Gaps (Longest Gap)	Processed Size, N
Onset HOBOlogger	12841	0	0 (0)	12841
NCDC Weather Station	1287	0	0 (0)	12841
NOAA Aquatrak at Fort Point, NH	12841	0	0 (0)	12841

Table 3.3.1: Duplicates and gaps in the time series referenced to calibration of the Onset HOBOlogger.

Time Series	Raw Data Size	Duplicates	Gaps (Longest Gap)	Processed Size, N
SeaBird SeaCAT	14186	0	0 (0)	2364
NCDC Weather Station	246	0	0 (0)	2364
NOAA Aquatrak at Fort Point, NH	2364	0	0 (0)	2364

Table 3.3.2: Duplicates and gaps in the time series referenced to calibration of the SeaBird SeaCAT.

Time Series	Raw Data Size	Duplicates	Gaps (Longest Gap)	Processed Size, N
WaterLog Bubbler	5030	0	0 (0)	5030
SeaBird MicroCAT	15078	0	1 (1)	5030
NCDC Weather Station	502	0	0 (0)	5030
NOAA Aquatrak at Fort Point, NH	5030	0	0 (0)	5030

Table 3.3.3: Duplicates and gaps in the time series referenced to calibration of the WaterLog Bubbler.

Time Series	Raw Data Size	Duplicates	Gaps (Longest Gap)	Processed Size, N
WaterLog MWWL	2955461	10	76 (63)	8291
NOAA Aquatrak at Fort Point, NH	8291	0	10 (10)	8291

Table 3.3.4: Duplicates and gaps in the time series referenced to calibration of the WaterLog MWWL.

Computation of water level for the pressure-based tide gauges occurred next. Due to human error, the SeaBird SeaCAT record did not coincide with the Onset HOBOlogger. The effect of this blunder is an unknown water density for the calibration of the Onset HOBOlogger. Fortunately, while the salinity at the calibration site did fluctuate, the mean value over time was relatively stable (Fig. 3.3.1). The mean salinity value (26.8023 PSU) was then used to compute water density during calibration of the Onset HOBOlogger. Using the maximum standard deviation (±1.7976 PSU) of the salinity, the root mean square error (RMSE) value (±0.004 m) for water level was computed. The RMSE is an estimation of the accuracy of an assumed value. While an error is inherent in the use of the mean salinity value, the computed RMSE value is much lower than the error value of the Onset HOBOlogger sensor (±0.015m). (Onset, 2011) Therefore, the use of the mean salinity value in this case is valid.

Prior to vertically referencing the time series, a fixed-range reference was computed for the WaterLog MWWL (Table 3.3.5). With such a small standard deviation the mean value was chosen for the fixed-range reference. Reference elevations were then applied

to all the tide gauge time series to equate the water levels to that of the control gauge (*e.g.* NAVD88). From this referenced data, a comparison between each tide gauge and the control gauge was made and any systematic bias was deduced for use in later data processing and analysis.

3.4 Analysis. The primary focus of the calibration phase of the project was to determine any systematic bias in the experiment gauges with respect to a control gauge. Both *time domain* analysis and *spectral domain* analysis were performed on the processed data. The first aspect of time domain analysis performed was to look at the sample means of each time series and the maximum, mean and standard deviation of the residuals for both the computed water level observations as well as the t_tide generated water levels from the experiment gauges versus the water level observations from the control gauge (Table 3.4.1-8). (Pawlowicz *et. al.*, 2002) t_tide is a tidal analysis library for MathWorks MATLAB (See Appendix D: Data Processing). At the same time, the computed water level and t_tide generated water level records were plotted (Fig. 3.4.1-8). The result of these analyses shows that there are no aberrations in the tidal signals that would preclude determining systematic calibration values.

Phase I: Calibration
Onset HOBOlogger
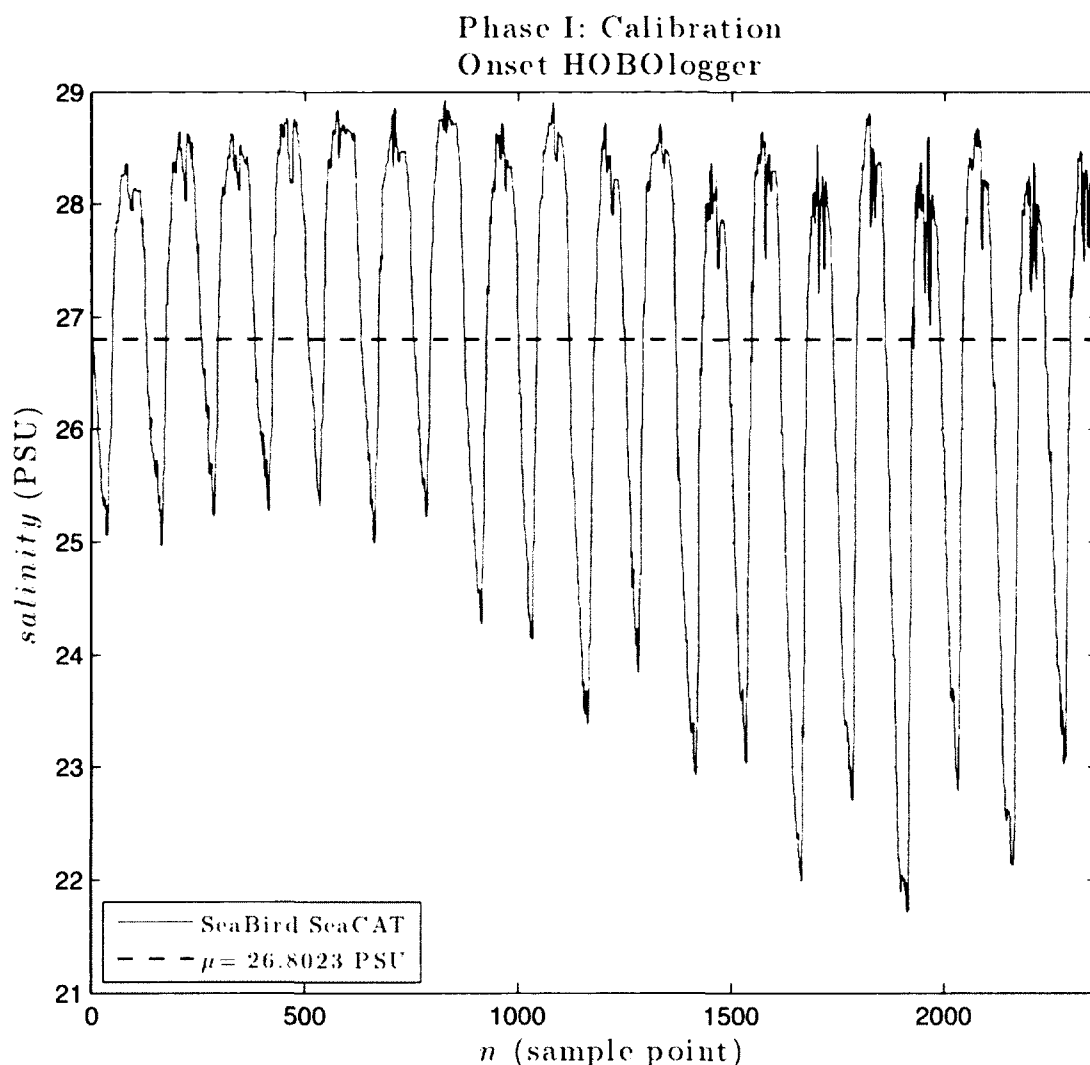
Figure 3.3.1: Salinity at the calibration site from observations of the SeaBird SeaCAT. Note that the salinity fluctuates with the tide, however the maximum and mean values are rather stable over a neap-spring tidal cycle.

N	Mean (m)	Median (m)	Mode (m) {n}	Std. Dev. (m)
1800	0.8743	0.8740	0.8740 {1046}	±0.000014

Table 3.3.5: Fixed-range test results for the WaterLog MWWL air-gap reference.

Time Series	Computed Water Level from Observations			
	μ (m)	Maximum Residual (m)	Residual Mean (m)	Residual Std. Dev. (m)
NOAA Aquatrak	−0.0033	--	--	--
Onset HOBOlogger	−0.0305	0.2030	0.0272	± 0.0134

Table 3.4.1: Maximum, mean, and standard deviation for the computed water level residuals for the Onset HOBOlogger referenced to the NOAA Aquatrak. Sample mean for both time series are given.

Time Series	Computed Water Level from Observations			
	μ (m)	Maximum Residual (m)	Residual Mean (m)	Residual Std. Dev. (m)
NOAA Aquatrak	0.0892	--	--	--
SeaBird SeaCAT	-0.0024	0.1180	0.0916	± 0.0087

Table 3.4.2: Maximum, mean, and standard deviation for the computed water level residuals for the SeaBird SeaCAT referenced to the NOAA Aquatrak. Sample mean for both time series are given.

Time Series	Computed Water Level from Observations			
	μ (m)	Maximum Residual (m)	Residual Mean (m)	Residual Std. Dev. (m)
NOAA Aquatrak	0.0116	--	--	--
WaterLog Bubbler	0.0068	0.0290	0.0047	± 0.0070

Table 3.4.3: Maximum, mean, and standard deviation for the computed water level residuals for the WaterLog Bubbler referenced to the NOAA Aquatrak. Sample mean for both time series are given.

Time Series	Computed Water Level from Observations			
	μ (m)	Maximum Residual (m)	Residual Mean (m)	Residual Std. Dev. (m)
NOAA Aquatrak	-0.0140	--	--	--
WaterLog MWWL	-0.0061	-0.3150	-0.0031	±0.0098

Table 3.4.4: Maximum, mean, and standard deviation for the computed water level residuals for the WaterLog MWWL referenced to the NOAA Aquatrak. Sample mean for both time series are given.

Time Series	t_tide Generated Water Level			
	μ (m)	Maximum Residual (m)	Residual Mean (m)	Residual Std. Dev. (m)
NOAA Aquatrak	0.0014	--	--	--
Onset HOBOlogger	0.0014	-0.0272	-0.0000	± 0.0091

Table 3.4.5: Maximum, mean, and standard deviation for the t_tide generated water level residuals for the Onset HOBOlogger referenced to the NOAA Aquatrak. Sample mean for both time series are given.

Time Series	t_tide Generated Water Level			
	μ (m)	Maximum Residual (m)	Residual Mean (m)	Residual Std. Dev. (m)
NOAA Aquatrak	-0.0005	--	--	--
SeaBird SeaCAT	-0.0005	0.0141	0.0000	± 0.0070

Table 3.4.6: Maximum, mean, and standard deviation for the t_tide generated water level residuals for the SeaBird SeaCAT referenced to the NOAA Aquatrak. Sample mean for both time series are given.

Time Series	t_tide Generated Water Level			
	μ (m)	Maximum Residual (m)	Residual Mean (m)	Residual Std. Dev. (m)
NOAA Aquatrak	-0.0077	--	--	--
WaterLog Bubbler	-0.0077	0.0151	0.0000	± 0.0054

Table 3.4.7: Maximum, mean, and standard deviation for the t_tide generated water level residuals for the WaterLog Bubbler referenced to the NOAA Aquatrak. Sample mean for both time series are given.

Time Series	t_tide Generated Water Level			
	μ (m)	Maximum Residual (m)	Residual Mean (m)	Residual Std. Dev. (m)
NOAA Aquatrak	-0.0068	--	--	--
WaterLog MWWL	-0.0069	-0.0160	0.0001	± 0.0066

Table 3.4.8: Maximum, mean, and standard deviation for the t_tide generated water level residuals for the WaterLog MWWL referenced to the NOAA Aquatrak. Sample mean for both time series are given.

The next step in the analysis was to plot the atmospheric versus water pressure for the pressure-based tide gauges to determine whether any tidal forcing by the atmospheric pressure had occurred (Fig. 3.4.9-11). Visual inspection of the atmospheric tide signal shows low variation; therefore the corrections to the pressure records were merely in magnitude only.

The last time domain analysis technique performed was a look at the linear regression between the experiment gauges and the control gauge (Fig. 3.4.12). Regression coefficients were then determined using the MATLAB™ polynomial curve fitting function polyfit (Table 3.4.9). These regression coefficients form the basis for the systematic bias correction to the experiment gauges in this study. Equations composed of these coefficients make the regression completely linear, or in other words there is no statistically significant difference in the tides observed between the control and experiment gauges.

Name	$p_n x$	p_{n+1} (m)
Onset HOBOlogger	0.99798050	-4.7594143e-5
SeaBird SeaCAT	0.99175154	3.0668759e-5
WaterLog Bubbler	0.99866352	-9.8566434e-5
WaterLog MWWL	0.99447603	-7.0457188e-6

Table 3.4.9: Computed tide gauge regression coefficients.

The first analysis technique performed in the spectral domain was to look at a comparison of the resolved tidal harmonics between the experiment gauges and the control gauge (Table 3.4.4-7). For those gauges that are pressure-based, the tidal harmonics resolved from the atmospheric pressure time series are also provided. The full report generated by t_tide for each time series is presented in Appendix E: t_tide Reports. Simultaneously, the *power spectrum* of each time series was plotted (Fig. 3.4.13-23). The power spectra plots show clear signals at the resolved tide constituents, most prominently for the nth order harmonics of the semidiurnal lunar tide, M_2. The result of these analyses confirms that the tidal signals and tidal constituents show no aberrations.

The last spectral domain analysis performed was to compute and plot the smoothed spectral densities, smoothed squared *coherency spectrum*, and smoothed *phase spectrum*. These cross-spectral analyses were computed and plotted for comparison between the control gauge and each experiment gauge (Fig. 3.4.24-27). For each of the experiment gauges the coherence at each of the resolved tidal constituents was very strong with respect to the control gauge. Still coherent, but much less so, was the background noise between the gauges. This is to be expected as both gauges are in close proximity recording the same tidal signals. Likewise, the tidal signals from the control and experiment gauges are in phase for both the resolved tidal constituents as well as much of the background noise. The result of this analysis shows very strong correlations between the control and experiment gauges, both in magnitude and phase for the tidal frequencies.

The computed maximum residual (-0.0272 m) and the mean residual (-0.0000 m ± 0.0091

m) for the tidal signal comparison of the Onset HOBOlogger were less than the

maximum (± 0.03 m) and mean error (±0.015 m) estimates for the sensor as determined

by the manufacturer (Onset, 2011). The computed maximum residual (0.0141 m) for the

tidal signal comparison of the SeaBird SeaCAT was less than the maximum (± 0.104 m)

estimate for the sensor as determined by the manufacturer (SeaBird, 2010). Similarly, the

maximum residuals (0.0151 m and -0.0160 m, respectively) and the mean residuals

(0.0000 m ± 0.0054 m and 0.0001 m ± 0.0066 m, respectively) for the tidal signal

comparisons of the WaterLog Bubbler and WaterLog MWWL were less than the error

budgets given by NOAA for primary water level stations (CO-OPS, 2008; 2011).

Furthermore, the regression analysis for all experiment gauges resulted in a strong

correlation to the control gauge.

It is interesting to note the difference in computed water level from observations (tide

gauges) that use stilling wells versus those that do not. While the NOAA Aquatrak and

Onset HOBOlogger use stilling wells, the remaining tide gauges do not. The stilling well

acts as a mechanical low-pass filter, however the tidal signal deduced by t_tide is not

much affected by its use or disuse.

In the spectral domain, residuals in amplitude and phase for all experiment gauges were

statistically equivalent to the control gauge. From the cross-spectral analysis, the time

series are strongly coherent and in phase. From the analysis of the calibration data in

both the time domain and spectral domain, each of the experimental gauges is statistically

accurate relative to the control gauge.

Phase I: Calibration
Onset HOBOlogger

Aquatrak — — — HOBOlogger ———— Residual
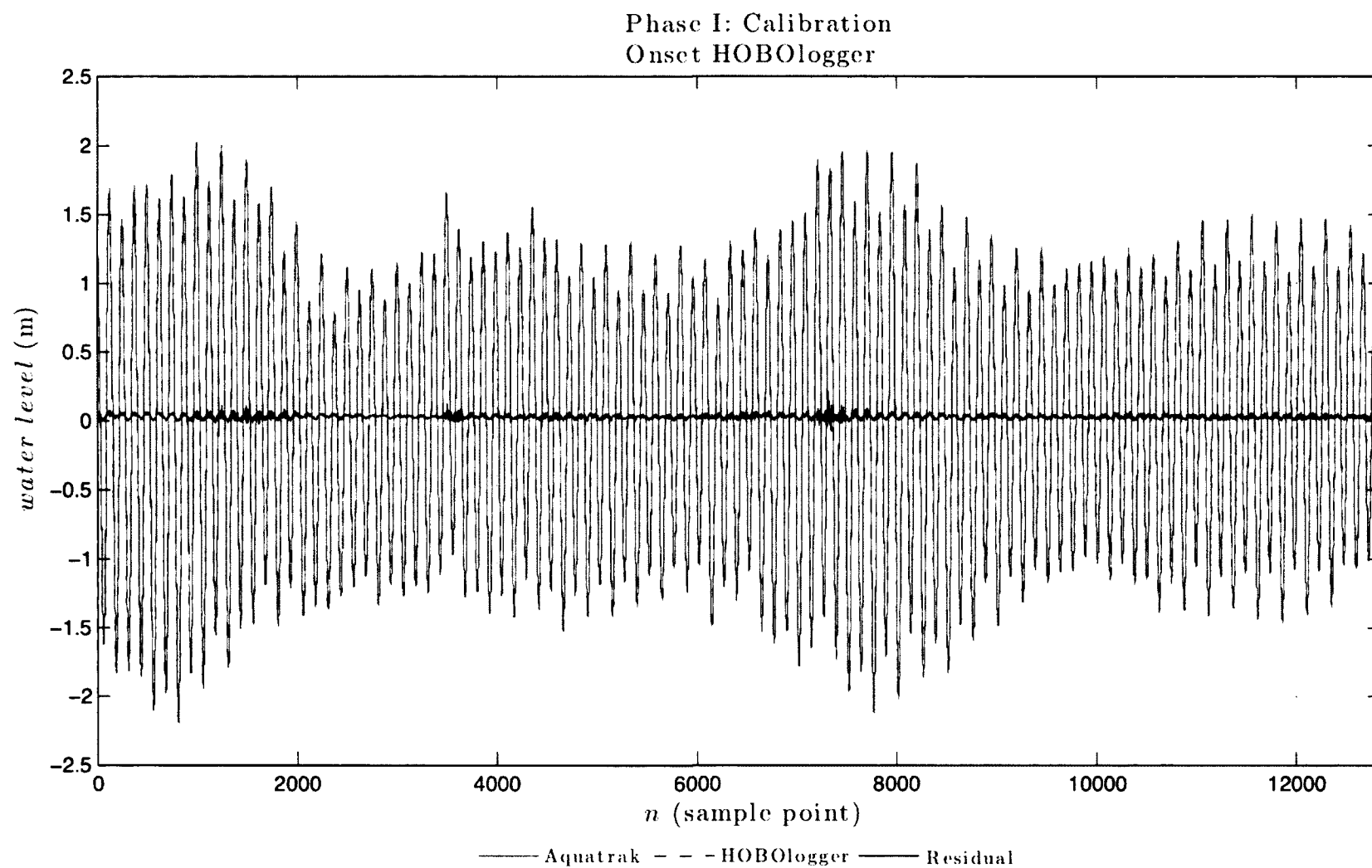
Figure 3.4.1: Water level from the control gauge (NOAA Aquatrak) v. computed water level from Onset HOBOlogger observations and computed residual. N=12841. Note the residual water level fluctuates with the tidal cycle; some noise is apparent, especially during spring tides.
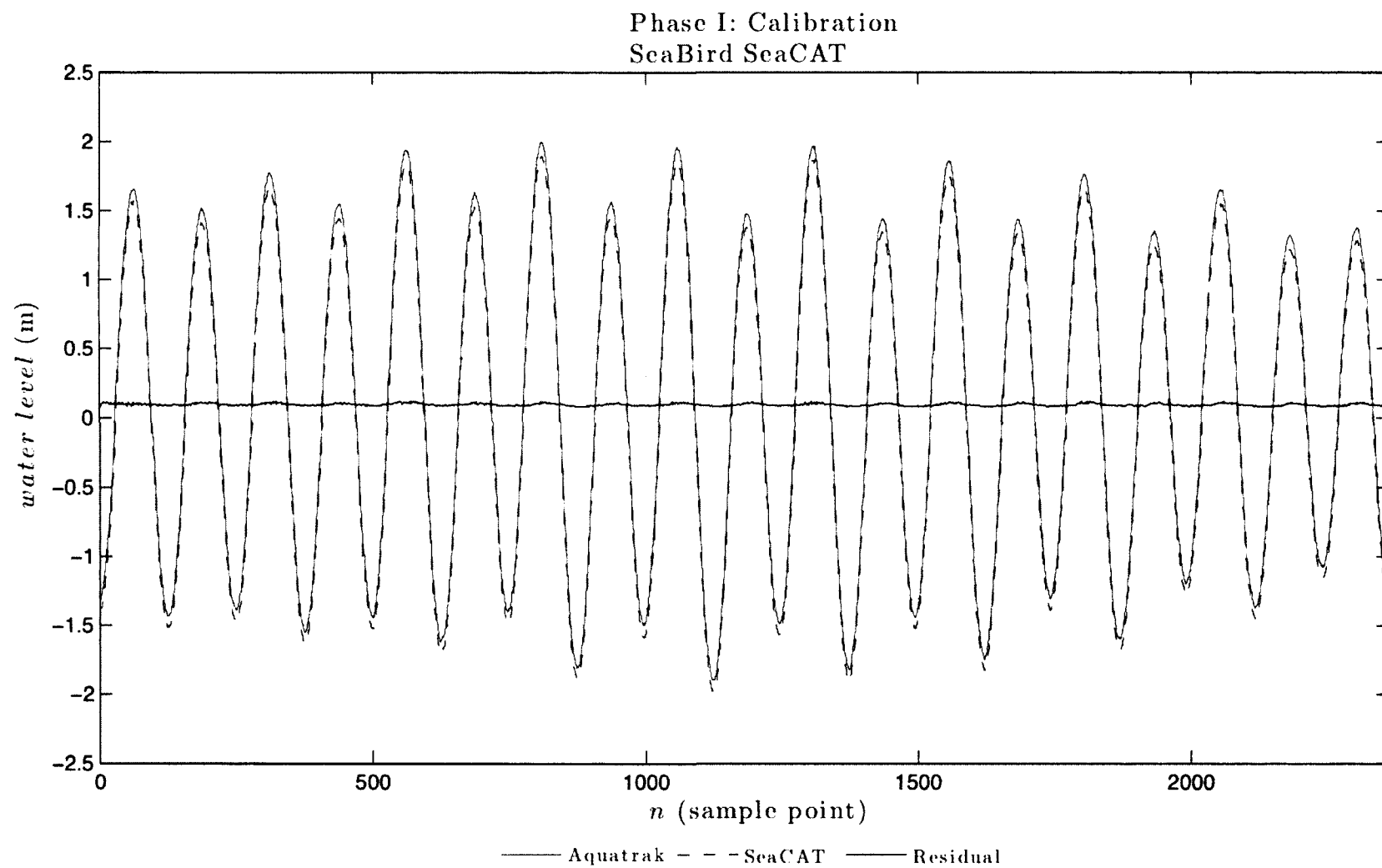
Figure 3.4.2: Water level from the control gauge (NOAA Aquatrak) v. computed water level from SeaBird SeaCAT observations and computed residual. N=2364. Note the residual water level fluctuates with the tidal cycle; an offset is apparent, most likely due to a blunder in vertical referencing.

Phase I: Calibration
WaterLog Bubbler

Aquatrak — — — Bubbler ——— Residual
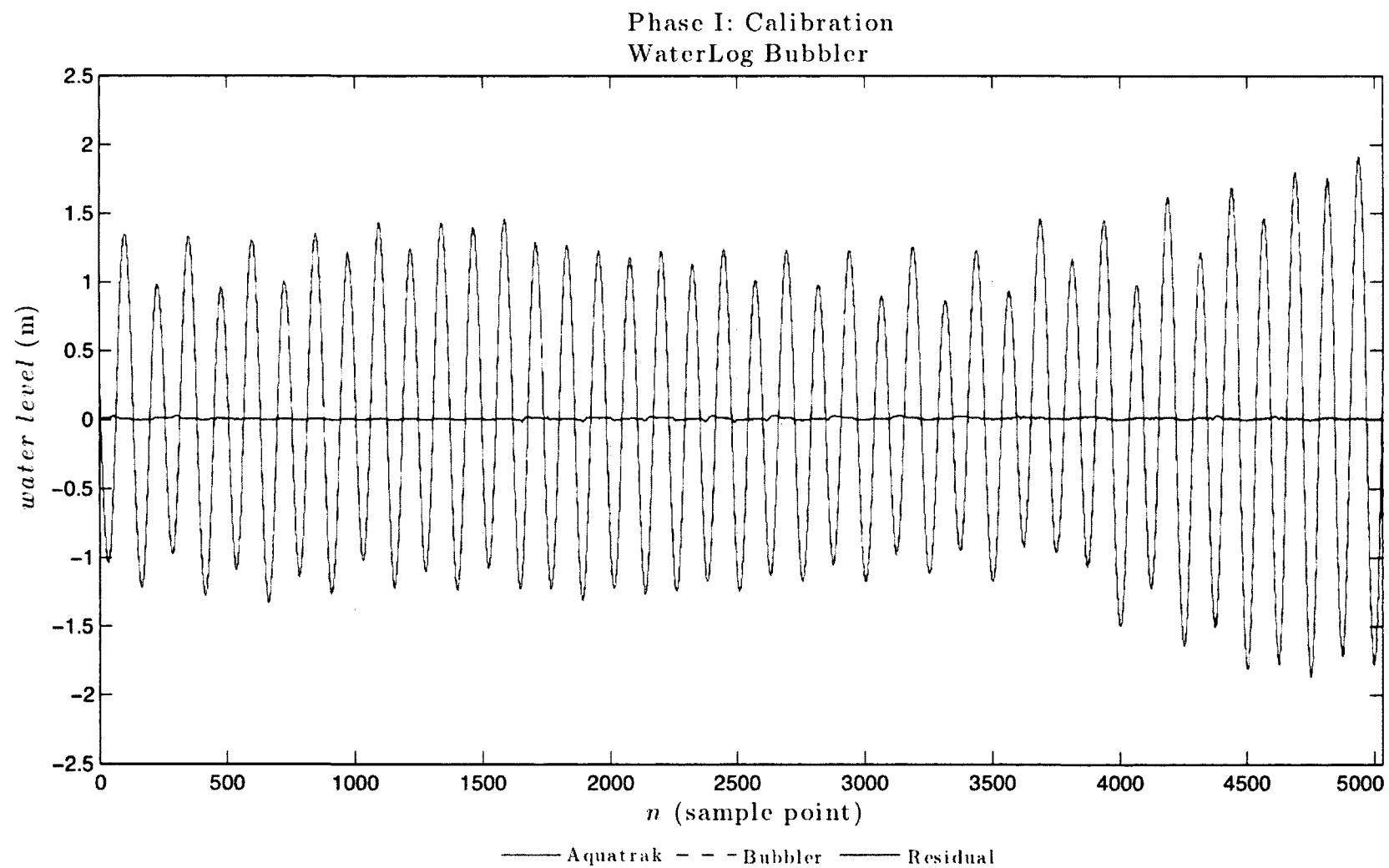
Figure 3.4.3: Water level from the control gauge (NOAA Aquatrak) v. computed water level from WaterLog Bubbler observations and computed residual. N=5030. Note the residual water level fluctuates with the tidal cycle; some noise is apparent.

Phase I: Calibration
WaterLog MWWL

Aquatrak − − −MWWL ———— Residual
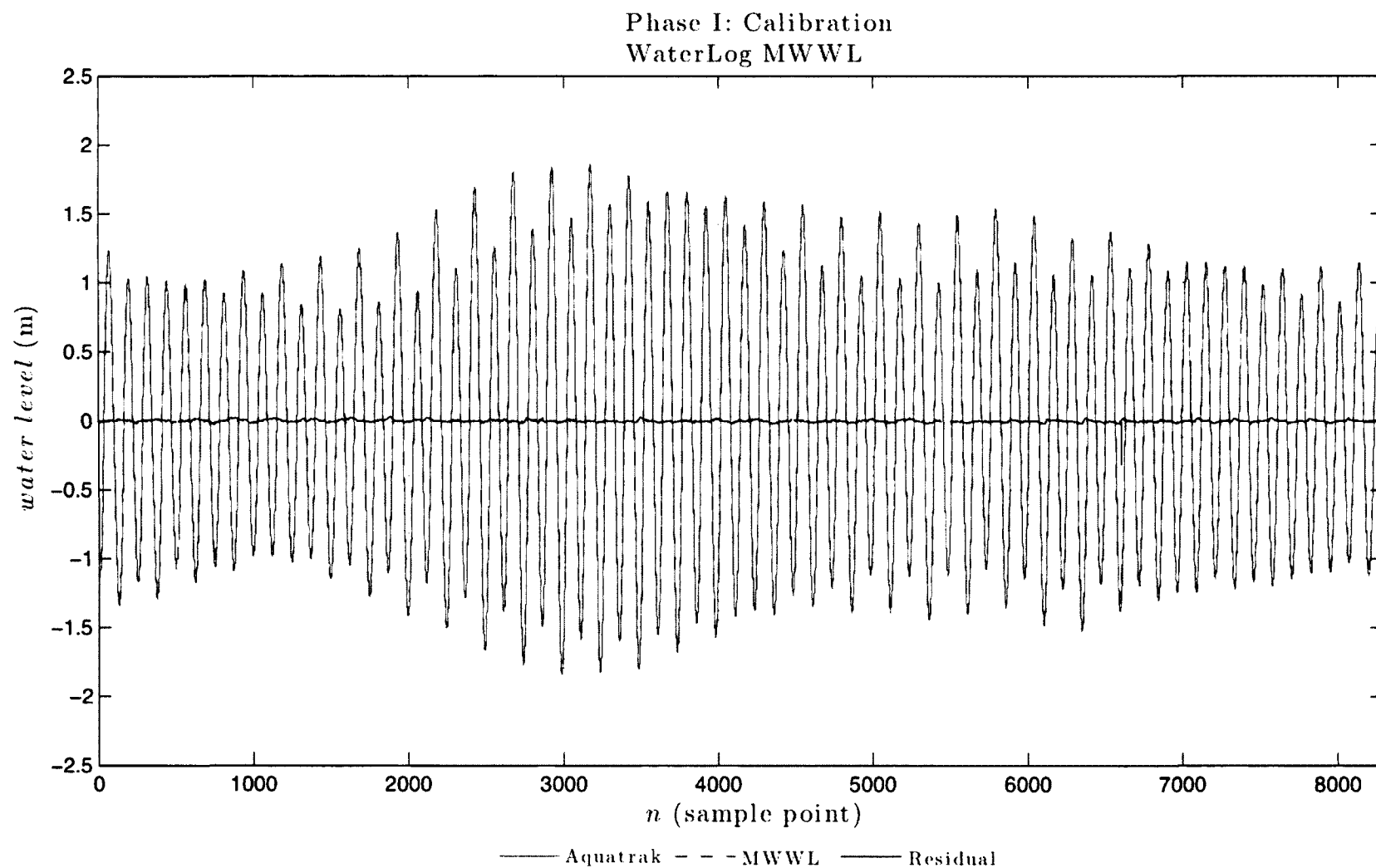
Figure 3.4.4: Water level from the control gauge (NOAA Aquatrak) v. computed water level from WaterLog MWWL observations and computed residual. N=8291. Note the residual water level fluctuates with the tidal cycle; a gap in data, some noise, and one large spike are apparent.

43

Phase I: Calibration
Onset HOBOlogger

———— t_tide (Aquatrak)— — —t_tide (HOBOlogger)———— Residual
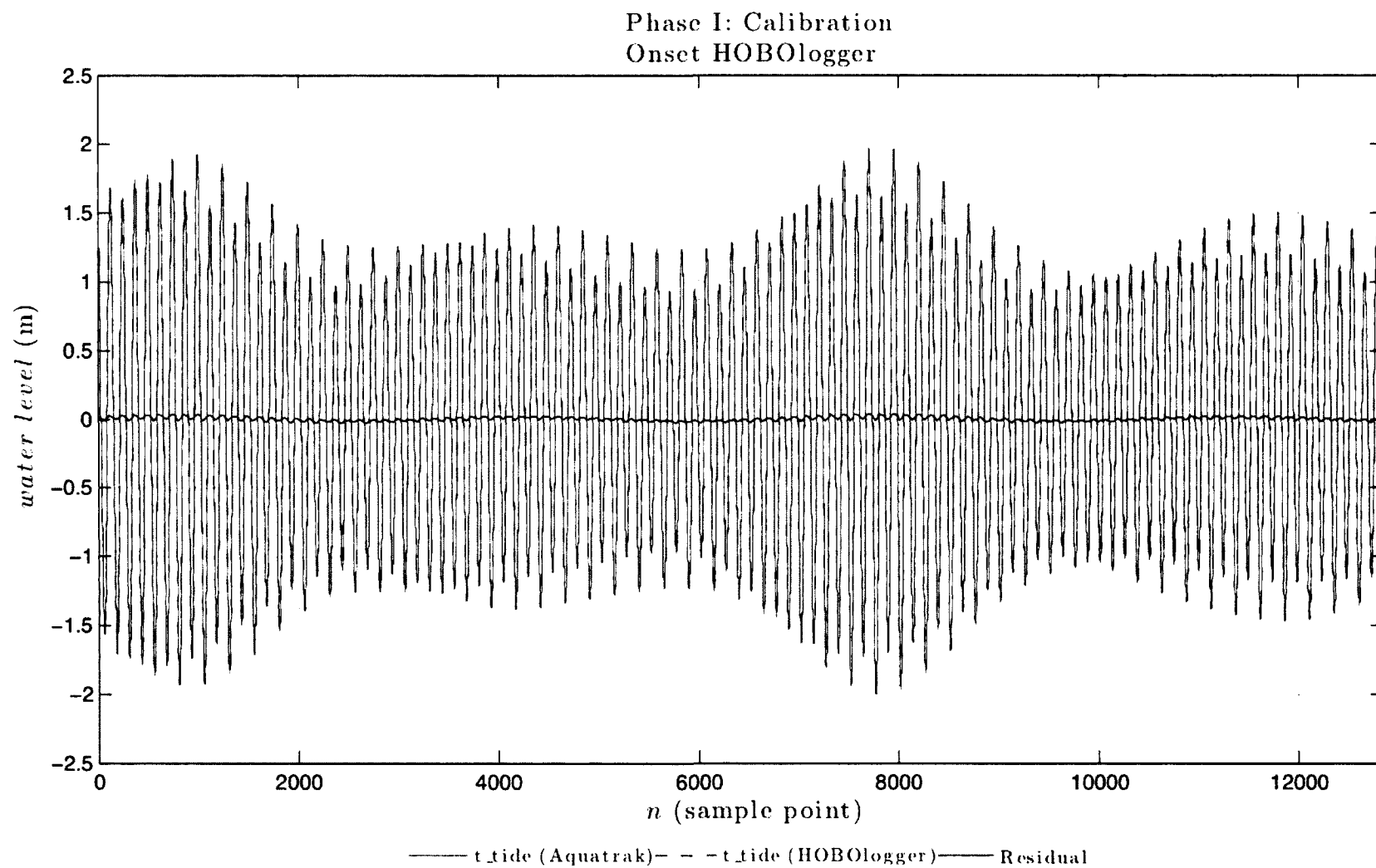
Figure 3.4.5: t_tide generated water level from the control gauge (NOAA Aquatrak) v. t_tide generated water level from Onset HOBOlogger observations and computed residual. N=12841. Note the residual tide signal still fluctuates with the tidal cycle; noise eliminated compared to Figure 3.4.1.

Phase I: Calibration
SeaBird SeaCAT

——— t_tide (Aquatrak)— − −t_tide (SeaCAT) ——— Residual
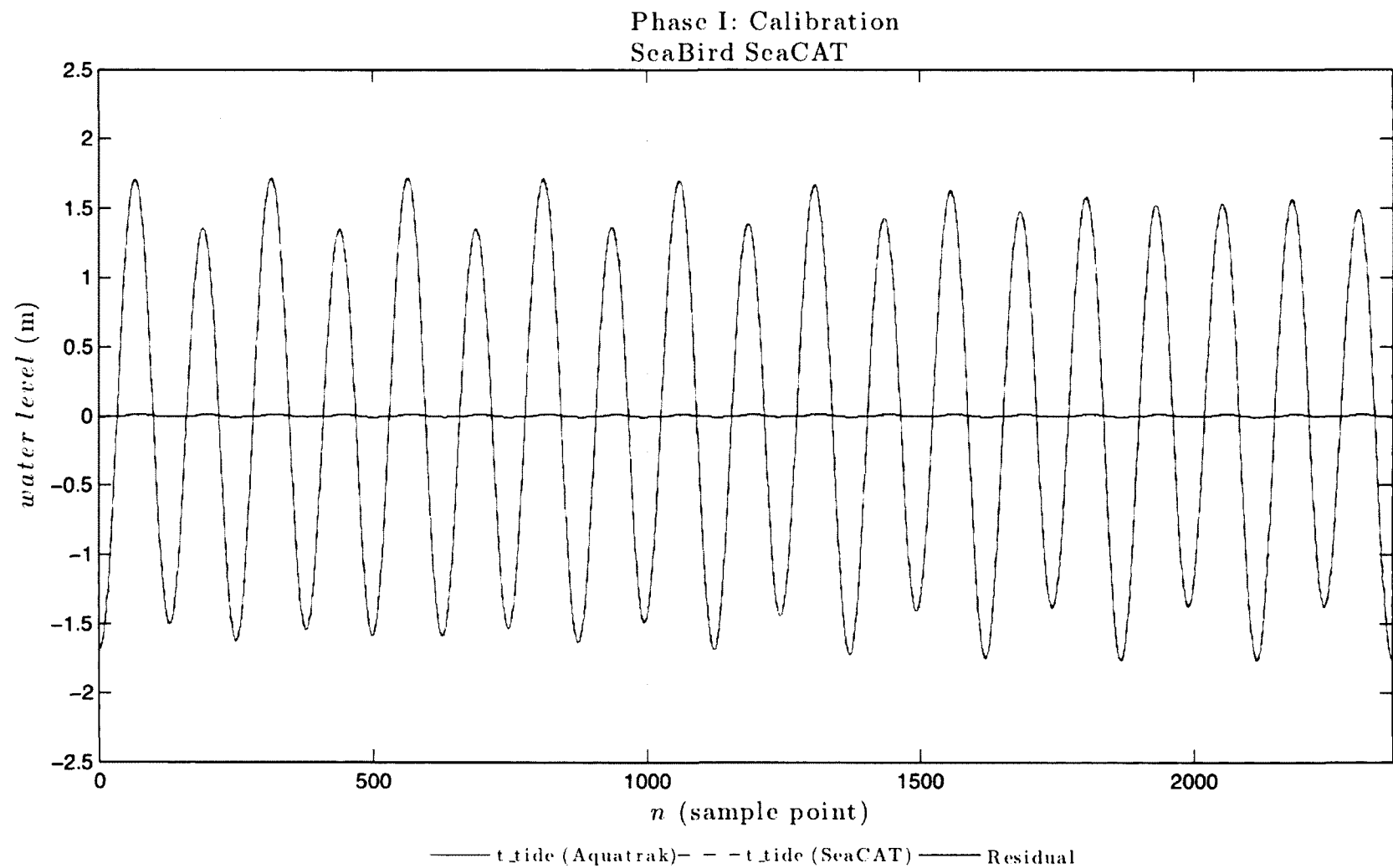
Figure 3.4.6: t_tide generated water level from the control gauge (NOAA Aquatrak) v. t_tide generated water level from SeaBird SeaCAT observations and computed residual. N=2364. Note the residual tide signal still fluctuates with the tidal cycle; vertical offset issue nullified compared to Figure 3.4.2.

Phase I: Calibration
WaterLog Bubbler

t_tide (Aquatrak)— — —t_tide (Bubbler) ———— Residual
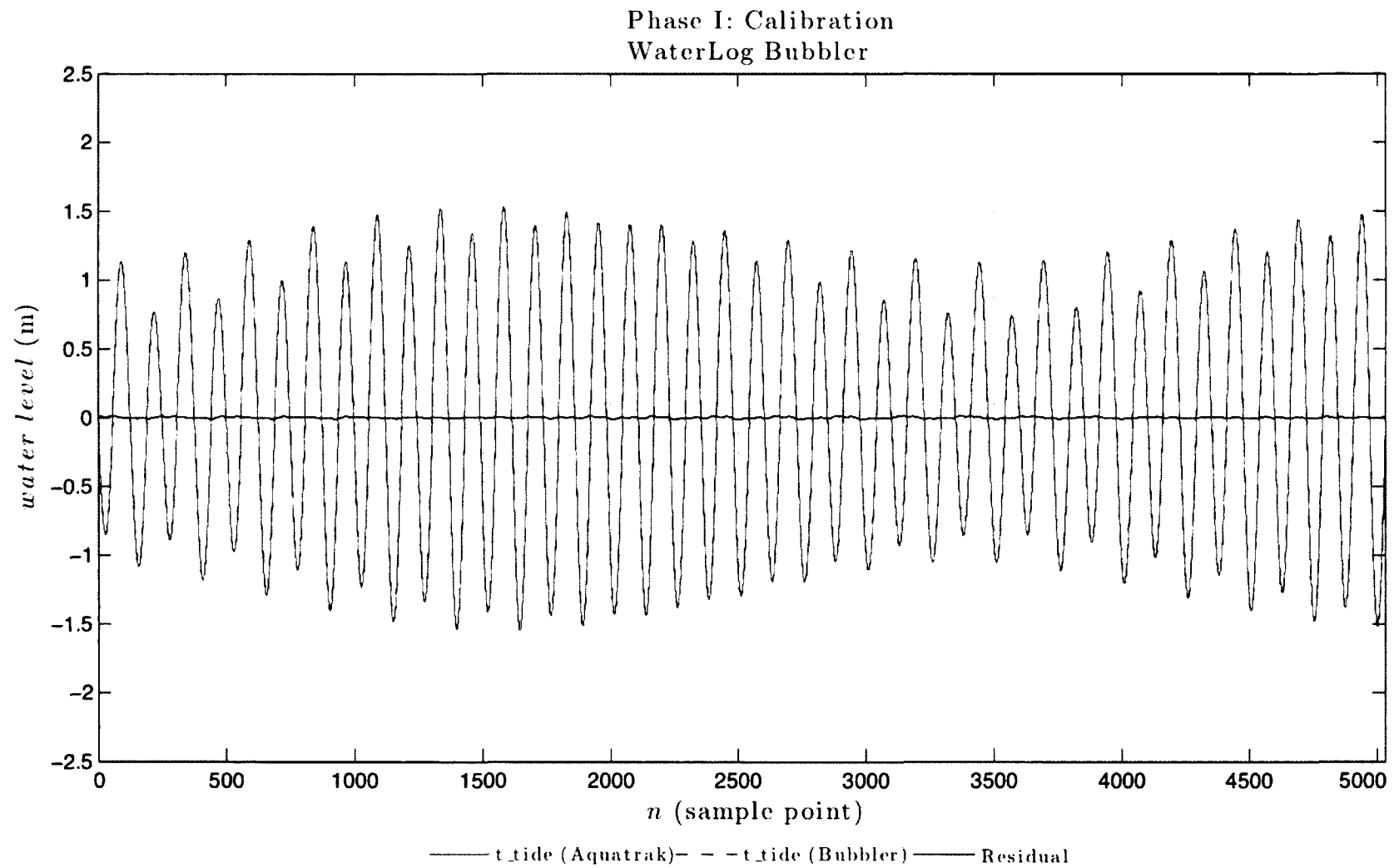
Figure 3.4.7: t_tide generated water level from the control gauge (NOAA Aquatrak) v. t_tide generated water level from WaterLog Bubbler observations and computed residual. N=5030. Note the residual tide signal still fluctuates with the tidal cycle; noise eliminated compared to Figure 3.4.3.

Phase I: Calibration
WaterLog MWWL
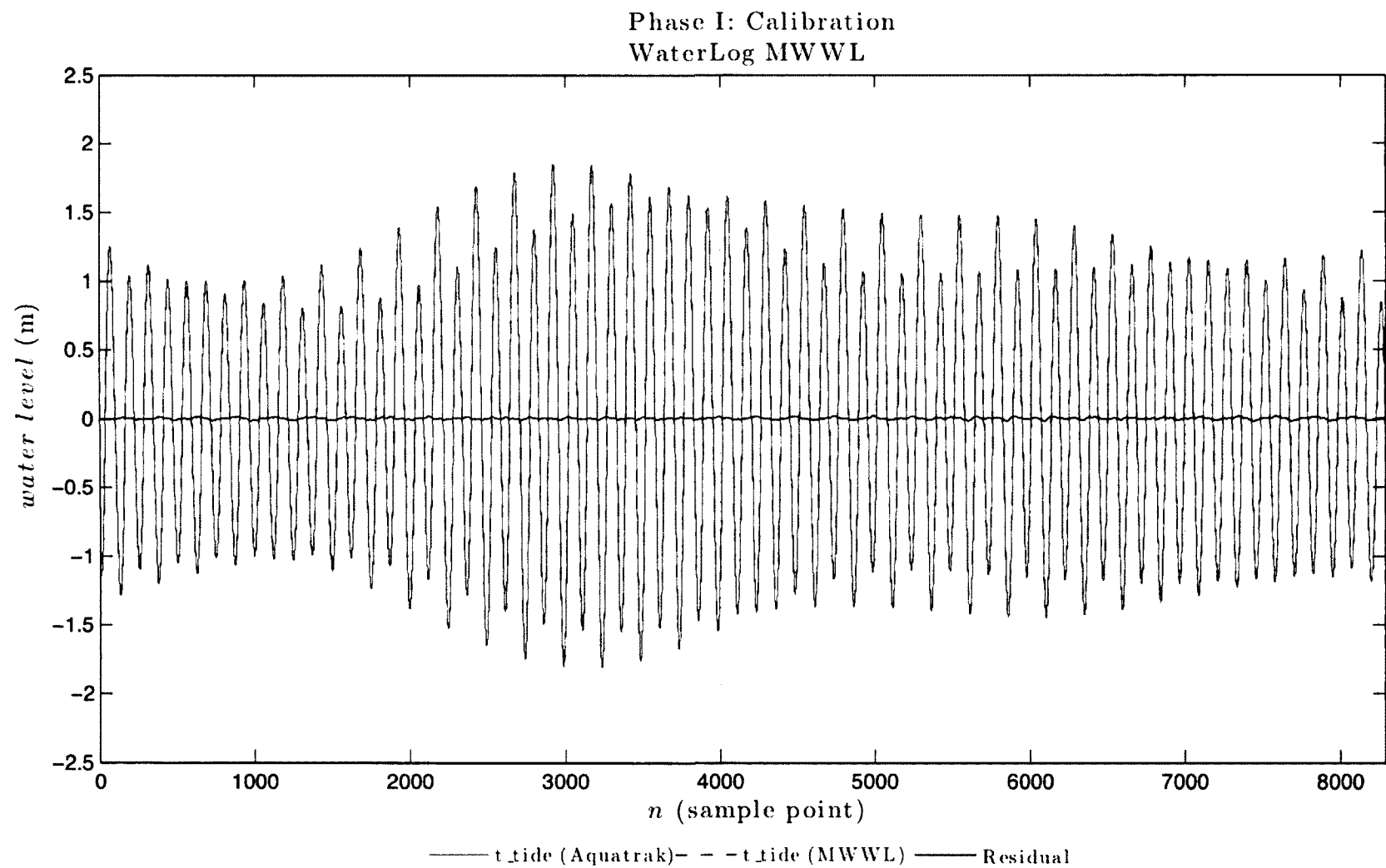
Figure 3.4.8: t_tide generated water level from the control gauge (NOAA Aquatrak) v. t_tide generated water level from WaterLog MWWL observations and computed residual. N=8291. Note the residual tide signal still fluctuates with the tidal cycle; the gap filled and noise eliminated compared to Figure 3.4.4.

Phase I: Calibration
Onset HOBOlogger

Atmospheric ——— Water ——— Residual
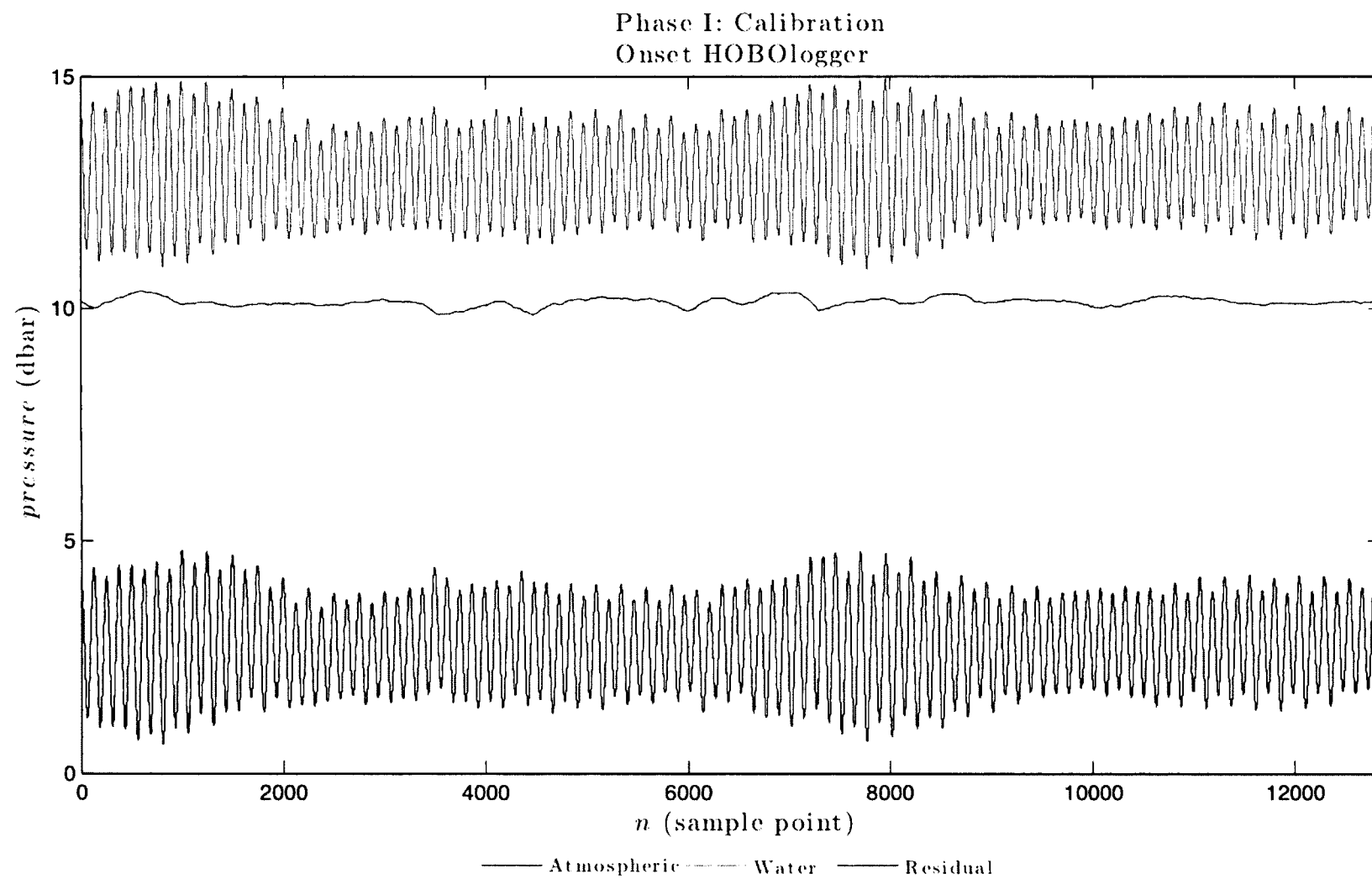
Figure 3.4.9: Observed atmospheric v. water pressure from the Onset HOBOlogger and computed residual. N=12841. Focus is on atmospheric pressure affect on water level. No aberrations are apparent in the residual (differential) pressure in comparison to the water pressure.

Phase I: Calibration
SeaBird SeaCAT
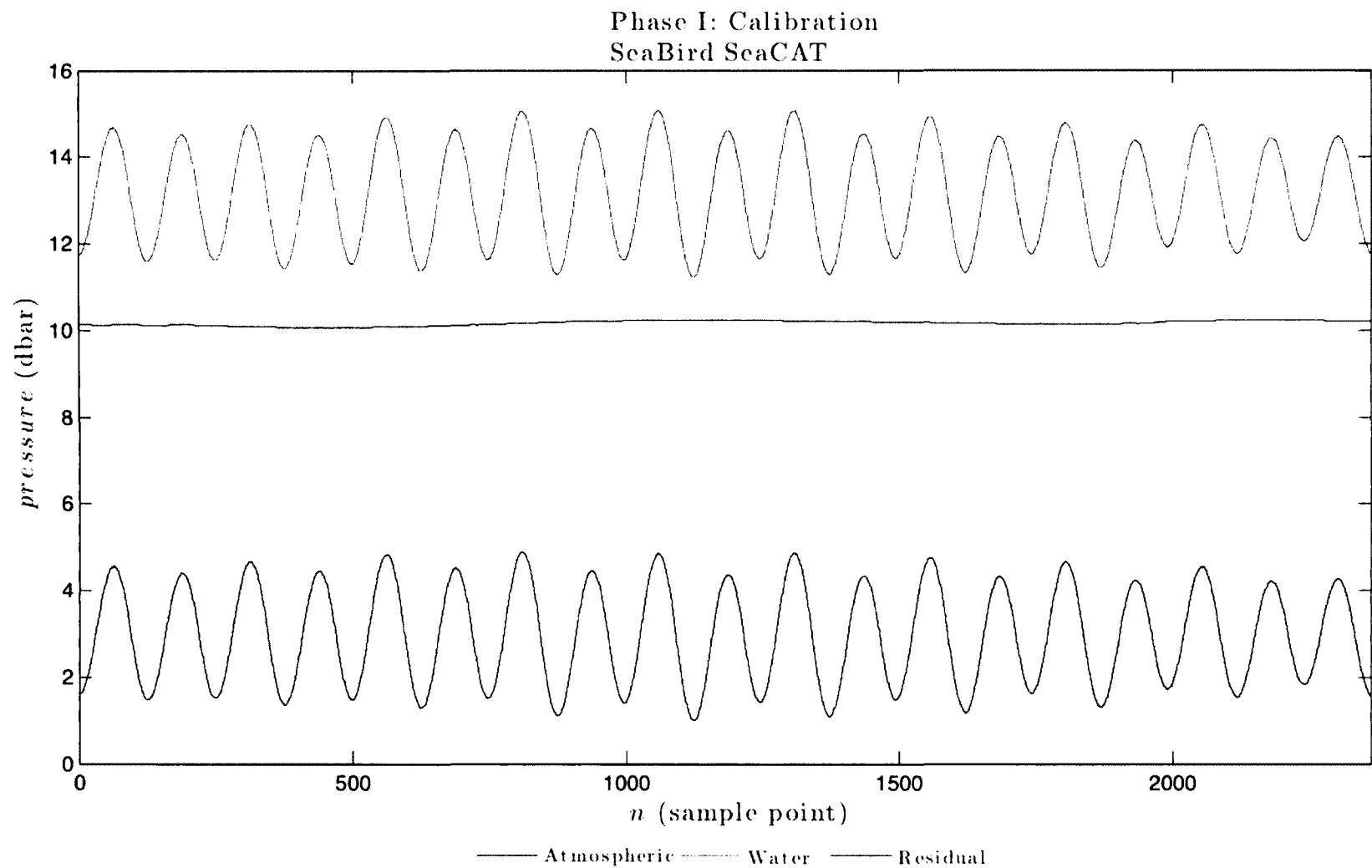
Figure 3.4.10: Observed atmospheric v. water pressure from the SeaBird SeaCAT and computed residual. N=2364. Focus is on atmospheric pressure affect on water level. No aberrations are apparent in the residual (differential) pressure in comparison to the water pressure.

Phase I: Calibration
WaterLog Bubbler
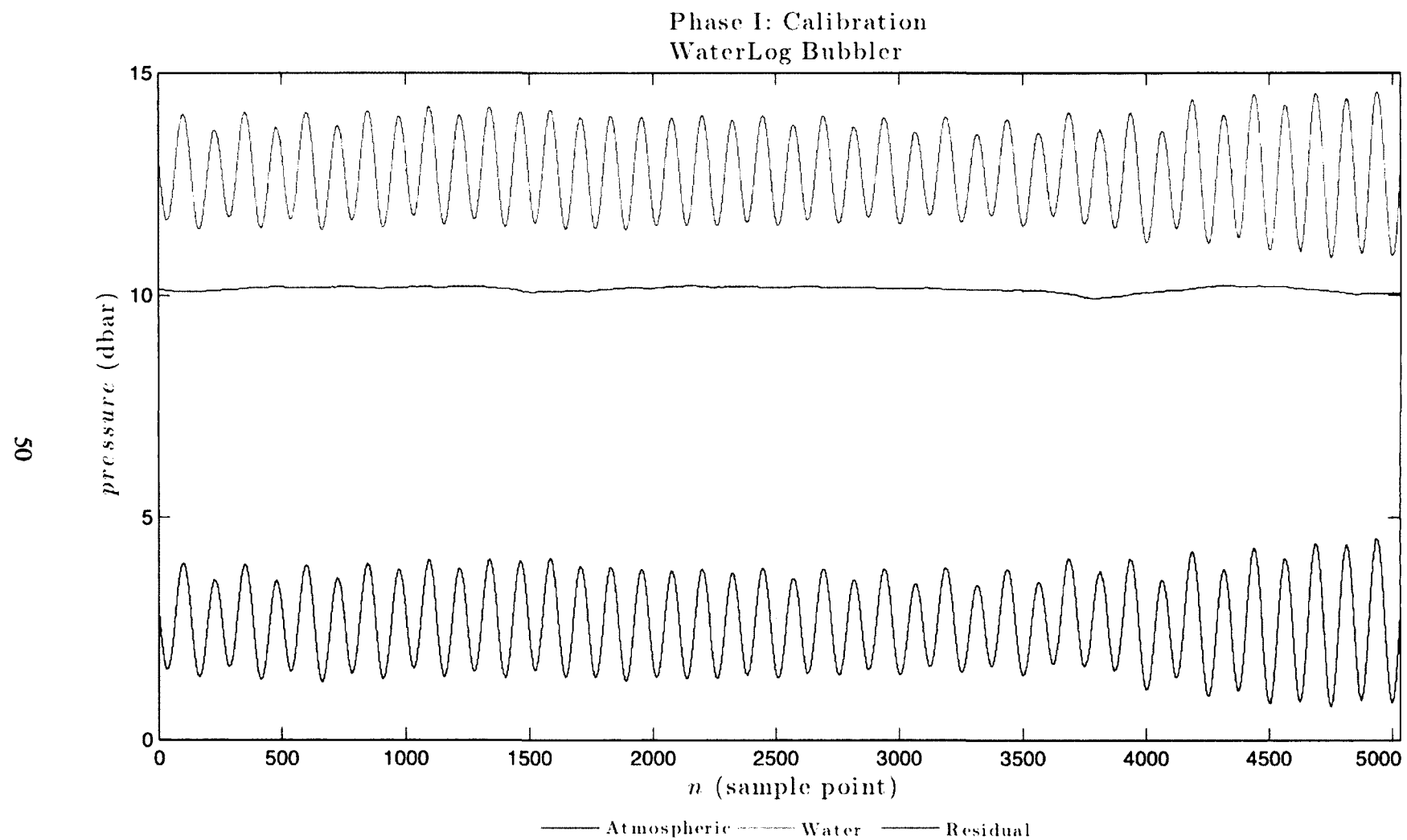
Figure 3.4.11: Observed atmospheric v. water pressure from the WaterLog Bubbler and computed residual. N=5030. Focus is on atmospheric pressure affect on water level. No aberrations are apparent in the water pressure in comparison to the residual (differential) pressure.

Phase I: Calibration

a. Onset HOBOlogger

Onset HOBOlogger: *water level* (meters)

NOAA Aquatrak: *water level* (meters)

b. SeaBird SeaCAT

SeaBird SeaCAT: *water level* (meters)

NOAA Aquatrak: *water level* (meters)

c. WaterLog Bubbler

WaterLog Bubbler: *water level* (meters)

NOAA Aquatrak: *water level* (meters)

d. WaterLog MWWL

WaterLog MWWL: *water level* (meters)

NOAA Aquatrak: *water level* (meters)
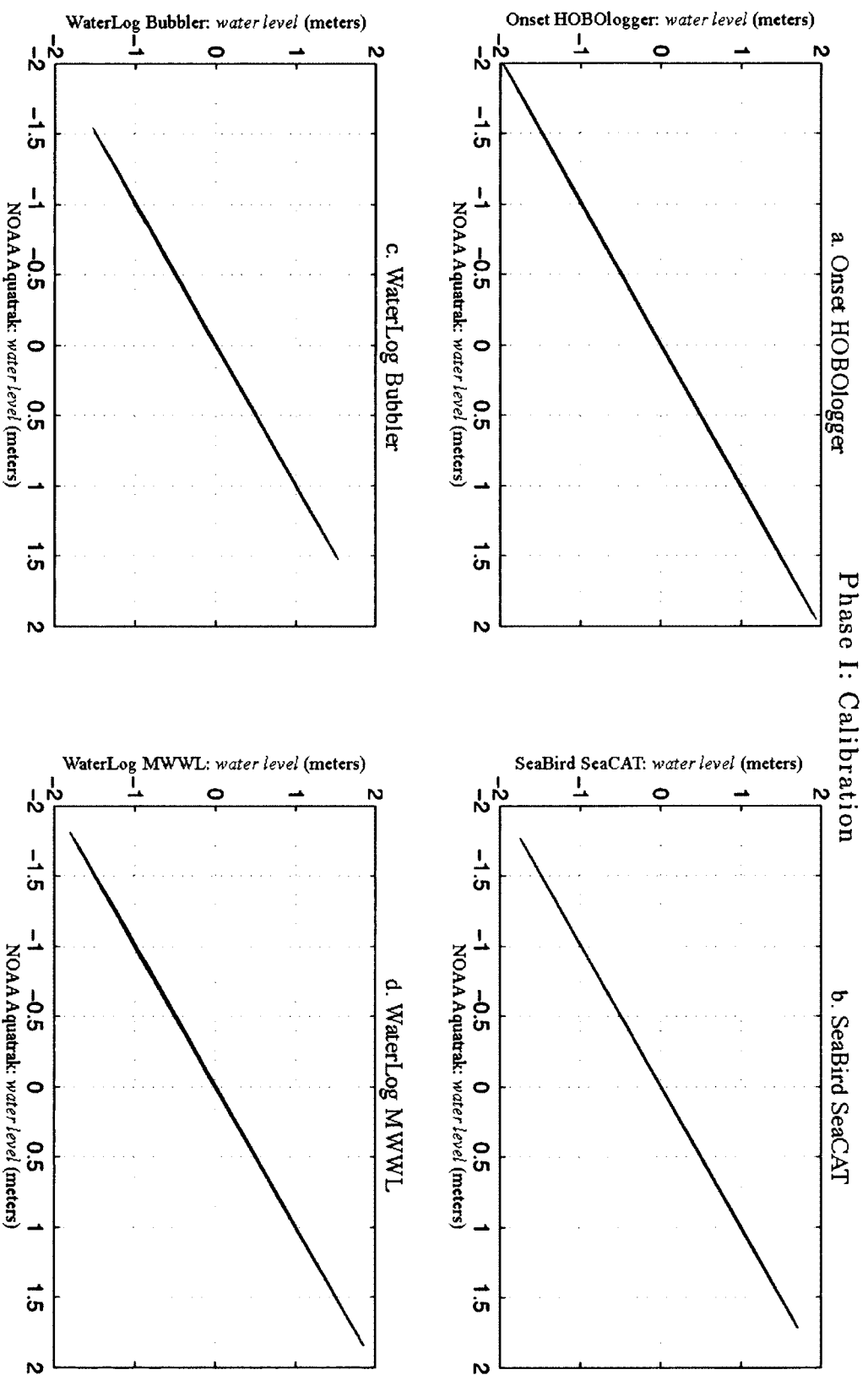
Figure 3.4.12a-d: Tide gauge water level regression referenced to the control tide gauge (NOAA Aquatrak): a. Onset HOBOlogger (N=12841), b. SeaBird SeaCAT (N=2364), c. WaterLog Bubbler (N=5030), d. WaterLog MWWL (N=8291). Subjective analysis shows a linear fit for each experiment tide gauge.

Names	Frequency (cpd)	NOAA Aquatrak		Onset HOBOlogger		Residuals		NCDC Atmospheric Pressure	
		Amplitude (m)	Phase (°)	Amplitude (m)	Phase (°)	Amplitude (m)	Phase (°)	Amplitude (m)	Phase (°)
ALP1	0.825517676							0.0027	339.24
2Q1	0.856952412	0.0137	186.58	0.0132	187.88	-0.0004	1.29	0.0027	40.55
Q1	0.893244060	0.0245	155.02	0.0247	153.99	0.0002	-1.03		
O1	0.929535707	0.1219	188.05	0.1213	187.43	-0.0006	-0.61	0.0032	271.15
NO1	0.966446262	0.0157	225.96	0.0156	226.00	-0.0001	0.04	0.0029	58.48
K1	1.002737909	0.1083	188.23	0.1101	188.35	0.0018	0.12	0.0050	252.22
OO1	1.075940112	0.0124	246.63	0.0124	248.29	0.0000	1.65		
UPS1	1.112231759	0.0096	303.22	0.0096	300.09	0.0000	-3.14		
EPS2	1.828255585							0.0006	106.93
MU2	1.864547232	0.0465	68.03	0.0453	68.03	-0.0013	0.01	0.0007	116.01
N2	1.895981969	0.3510	67.54	0.3469	67.66	-0.0041	0.12		
M2	1.932273616	1.2908	104.85	1.2804	104.86	-0.0104	0.02		
L2	1.968565263	0.0971	145.18	0.0987	145.22	0.0017	0.04		
S2	2.000000000	0.2272	135.60	0.2243	135.53	-0.0030	-0.06	0.0061	65.31
MO3	2.861809323	0.0066	231.65	0.0062	236.30	-0.0004	4.65		
M3	2.898410424	0.0038	153.90	0.0035	147.52	-0.0004	-6.38	0.0003	277.06
MK3	2.935011525	0.0029	249.70	0.0028	229.37	-0.0001	-20.33		
SK3	3.002737909			0.0019	207.70				
MN4	3.828255585	0.0078	306.06	0.0073	302.18	-0.0005	-3.88	0.0003	85.34
M4	3.864547232	0.0183	335.35	0.0177	334.32	-0.0007	-1.03		
SN4	3.895981969							0.0004	109.95
MS4	3.932273616	0.0074	5.73	0.0071	359.47	-0.0003	-6.27	0.0002	136.16
S4	4.000000000	0.0015	102.76					0.0005	8.47
2MK5	4.867285141	0.0009	108.94	0.0010	104.29	0.0001	-4.65		
2SK5	5.002737909	0.0025	99.14	0.0024	98.71	-0.0001	-0.43	0.0003	216.63
2MN6	5.760529201	0.0051	98.66	0.0052	96.40	0.0001	-2.26	0.0002	177.00
M6	5.796820848	0.0065	139.72	0.0061	137.24	-0.0003	-2.48		
2MS6	5.864547232	0.0046	178.09	0.0043	178.01	-0.0003	-0.08	0.0002	11.09
3MK7	6.799558758	0.0010	290.18	0.0012	289.70	0.0003	-0.49	0.0002	42.71
M8	7.729094464	0.0021	251.11	0.0022	258.02	0.0000	6.91		

Table 3.4.10: t_tide resolved tidal harmonic constituents and residuals with a signal-to-noise ratio (SNR) greater than 2.0 in reference to calibration of the Onset HOBOlogger.

Names	Frequency (cpd)	NOAA Aquatrak		SeaBird SeaCAT		Residuals		NCDC Atmospheric Pressure	
		Amplitude (m)	Phase (°)	Amplitude (m)	Phase (°)	Amplitude (m)	Phase (°)	Amplitude (m)	Phase (°)
K1	1.002737909	0.2025	181.52	0.2012	181.40	-0.0013	-0.12		
M2	1.932273616	1.5604	109.17	1.5518	109.03	-0.0086	-0.14		
M3	2.898410424	0.0164	13.54	0.0163	12.46	-0.0002	-1.08	0.0009	295.77
M4	3.864547232	0.0224	347.23	0.0216	353.49	-0.0008	6.25	0.0009	107.54
2MK5	4.867285141	0.0053	91.51	0.0049	96.44	-0.0004	4.93	0.0003	113.65
2SK5	5.002737909	0.0043	121.57	0.0038	120.52	-0.0004	-1.05	0.0004	355.21
M6	5.796820848	0.0134	140.21	0.0141	142.14	0.0007	1.93	0.0003	354.14
3MK7	6.799558758	0.0024	347.13	0.0022	346.84	-0.0001	-0.29	0.0003	51.91
M8	7.729094464	0.0037	309.14	0.0038	307.94	0.0001	-1.20	0.0003	308.11

Table 3.4.11: t_tide resolved tidal harmonic constituents and residuals with a signal-to-noise ratio (SNR) greater than 2.0 in reference to calibration of the SeaBird SeaCAT.

Names	Frequency (cpd)	NOAA Aquatrak		WaterLog Bubbler		Residuals		NCDC Atmospheric Pressure	
		Amplitude (m)	Phase (°)	Amplitude (m)	Phase (°)	Amplitude (m)	Phase (°)	Amplitude (m)	Phase (°)
O1	0.929535707	0.1032	174.16	0.1003	174.57	-0.0029	0.41	0.0032	153.03
K1	1.002737909	0.1143	224.23	0.1128	226.70	-0.0015	2.47	0.0050	83.74
M2	1.932273616	1.2124	101.84	1.2107	101.89	-0.0017	0.05	0.0010	65.03
S2	2.000000000	0.2742	144.49	0.2717	144.49	-0.0025	0.00	0.0053	75.34
M3	2.898410424	0.0050	166.72	0.0053	178.29	0.0003	11.58	0.0006	119.61
SK3	3.002737909	0.0055	230.67	0.0051	242.45	-0.0004	11.78		
M4	3.864547232	0.0168	318.85	0.0161	320.56	-0.0007	1.70	0.0004	114.29
MS4	3.932273616	0.0137	5.49	0.0128	1.70	-0.0008	-3.79	0.0005	135.40
S4	4.000000000	0.0029	152.26					0.0003	124.14
2MK5	4.867285141	0.0026	125.53	0.0026	130.78	0.0000	5.24	0.0005	213.51
2SK5	5.002737909	0.0019	255.64	0.0015	253.41	-0.0004	-2.23	0.0006	299.22
M6	5.796820848	0.0047	129.92	0.0052	130.93	0.0005	1.02	0.0004	128.33
2MS6	5.864547232	0.0059	194.09	0.0061	195.21	0.0002	1.12	0.0004	158.83
2SM6	5.932273616	0.0027	4.00	0.0028	355.44	0.0001	-8.56	0.0004	192.55
3MK7	6.799558758	0.0027	60.43	0.0026	56.32	0.0000	-4.11	0.0002	220.09
M8	7.729094464	0.0013	268.63	0.0012	272.51	-0.0001	3.89	0.0003	136.04

Table 3.4.12: t_tide resolved tidal harmonic constituents and residuals with a signal-to-noise ratio (SNR) greater than 2.0 in reference to calibration of the WaterLog Bubbler.

53

Names	Frequency (cpd)	NOAA Aquatrak		WaterLog MWWL		Residuals	
		Amplitude (m)	Phase (°)	Amplitude (m)	Phase (°)	Amplitude (m)	Phase (°)
ALP1	0.825517676	0.0055	296.50	0.0055	303.25	0.0000	6.74
2Q1	0.856952412	0.0046	258.39	0.0058	254.19	0.0012	-4.20
Q1	0.893244060	0.0165	170.27	0.0165	169.24	0.0000	-1.03
O1	0.929535707	0.1134	185.09	0.1103	185.37	-0.0031	0.28
NO1	0.966446262	0.0146	202.80	0.0144	204.27	-0.0002	1.47
K1	1.002737909	0.1647	214.18	0.1665	216.25	0.0018	2.08
J1	1.039029557	0.0074	196.91	0.0078	191.75	0.0004	-5.16
OO1	1.075940112	0.0031	229.20	0.0034	234.76	0.0003	5.56
UPS1	1.112231759	0.0037	321.05	0.0036	322.41	-0.0001	1.36
EPS2	1.828255585	0.0025	346.22				
MU2	1.864547232	0.0268	350.73	0.0267	348.78	-0.0001	-1.96
N2	1.895981969	0.3155	84.69	0.3158	84.85	0.0003	0.16
M2	1.932273616	1.2968	107.29	1.2951	107.38	-0.0018	0.09
L2	1.968565263	0.0956	147.21	0.0948	147.74	-0.0008	0.54
S2	2.000000000	0.1639	159.71	0.1628	160.05	-0.0012	0.35
ETA2	2.041767466	0.0079	298.41	0.0080	299.24	0.0001	0.83
MO3	2.861809323	0.0057	200.84	0.0062	211.76	0.0005	10.91
M3	2.898410424	0.0031	145.73	0.0037	145.65	0.0006	-0.09
MK3	2.935011525	0.0047	278.11	0.0064	272.60	0.0017	-5.50
SK3	3.002737909			0.0018	268.78		
MN4	3.828255585	0.0092	321.09	0.0087	324.85	-0.0005	3.75
M4	3.864547232	0.0208	329.02	0.0201	331.32	-0.0007	2.30
SN4	3.895981969	0.0029	243.54	0.0023	241.41	-0.0006	-2.13
MS4	3.932273616	0.0066	31.34	0.0063	26.42	-0.0003	-4.92
S4	4.000000000	0.0020	137.49	0.0009	137.40	-0.0011	-0.08
2MK5	4.867285141	0.0022	112.08	0.0016	118.20	-0.0005	6.12
2SK5	5.002737909	0.0021	155.37	0.0017	161.68	-0.0004	6.32
2MN6	5.760529201	0.0041	140.40	0.0037	133.01	-0.0004	-7.40
M6	5.796820848	0.0078	141.73	0.0071	142.89	-0.0007	1.15
2MS6	5.864547232	0.0027	209.87	0.0027	214.81	0.0001	4.94
3MK7	6.799558758	0.0008	14.87	0.0006	340.55	-0.0002	-34.32
M8	7.729094464	0.0018	324.08	0.0018	332.04	0.0000	7.96

Table 3.4.13: t_tide resolved tidal harmonic constituents and residuals with a signal-to-noise ratio (SNR) greater than 2.0 in reference to calibration of the WaterLog MWWL.

Phase I: Calibration
NOAA Aquatrak ref Onset HOBOlogger
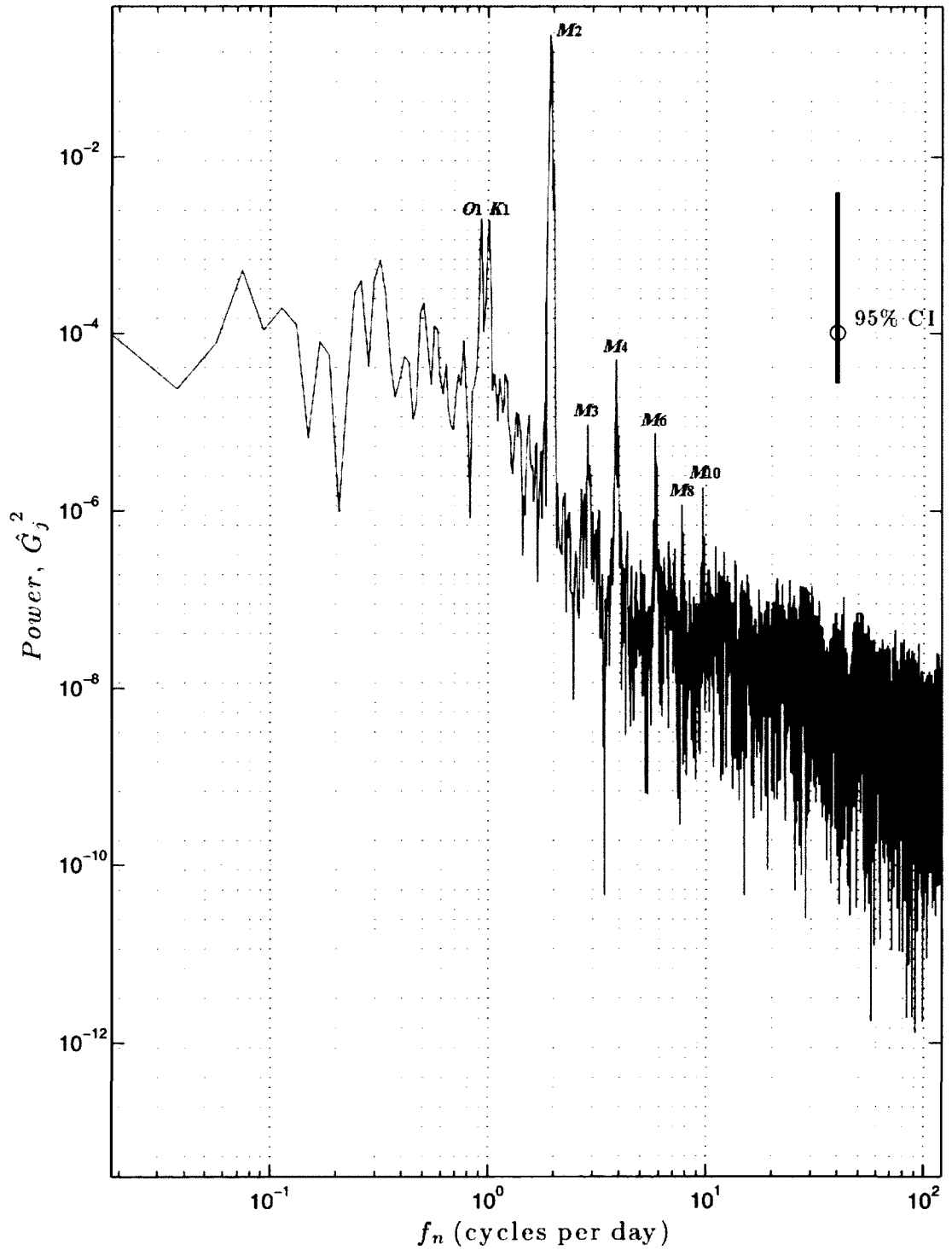
Figure 3.4.13: Water level power spectrum from the control gauge (NOAA Aquatrak) in reference to the Onset HOBOlogger (Fig. 4.4.14). Hanning window, N=12841. Observable n-th order harmonics of the primary lunar tide, M, and the diurnal constituents, O_1 and K_1, are labeled.

Phase I: Calibration
Onset HOBOlogger
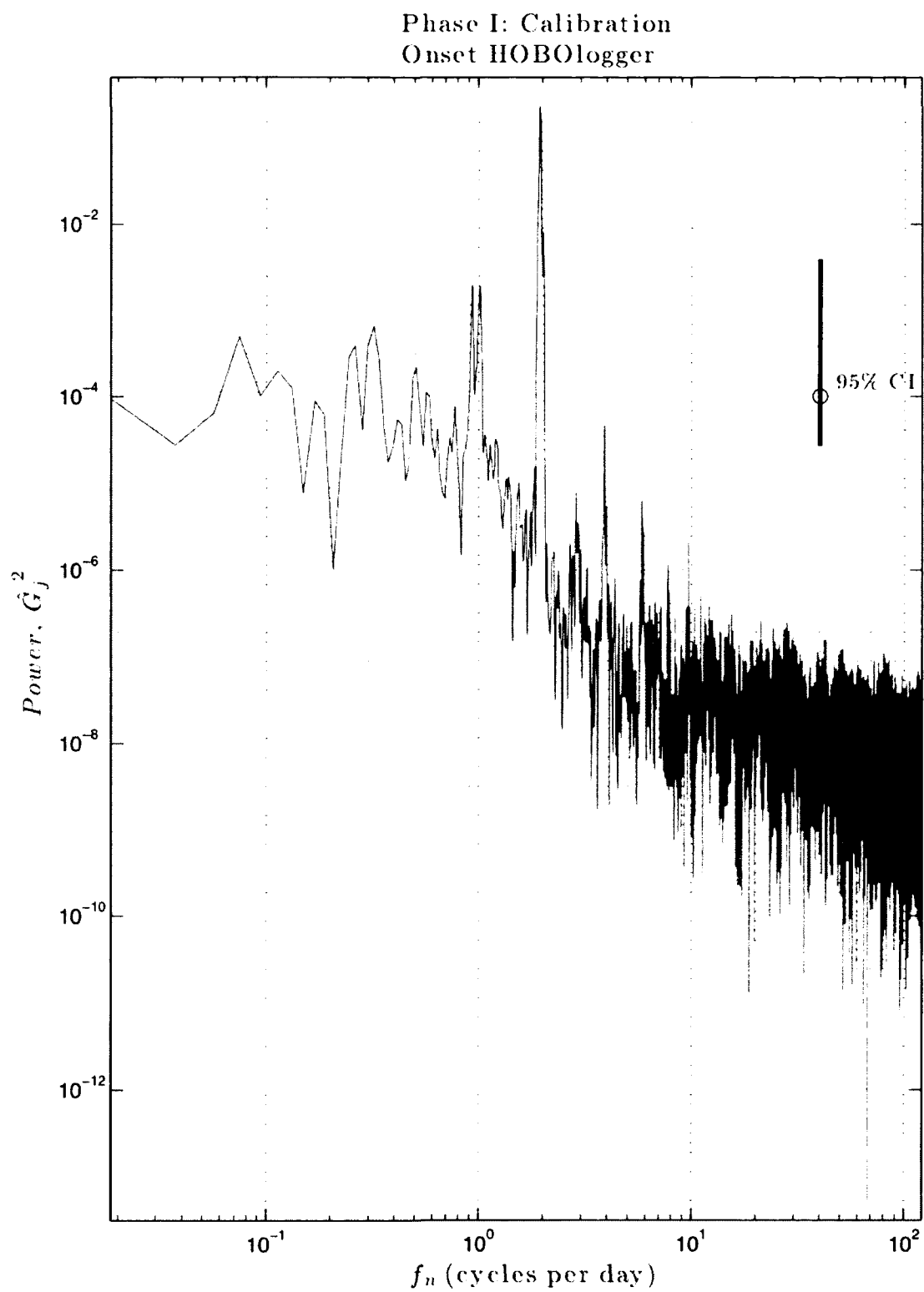
Figure 3.4.14: Water level power spectrum from the Onset HOBOlogger. Hanning window, N=12841. See Figure 3.4.13 for labels of the observable n-th order harmonics of the primary lunar tide, M.

Phase I: Calibration
NOAA Aquatrak ref SeaBird SeaCAT
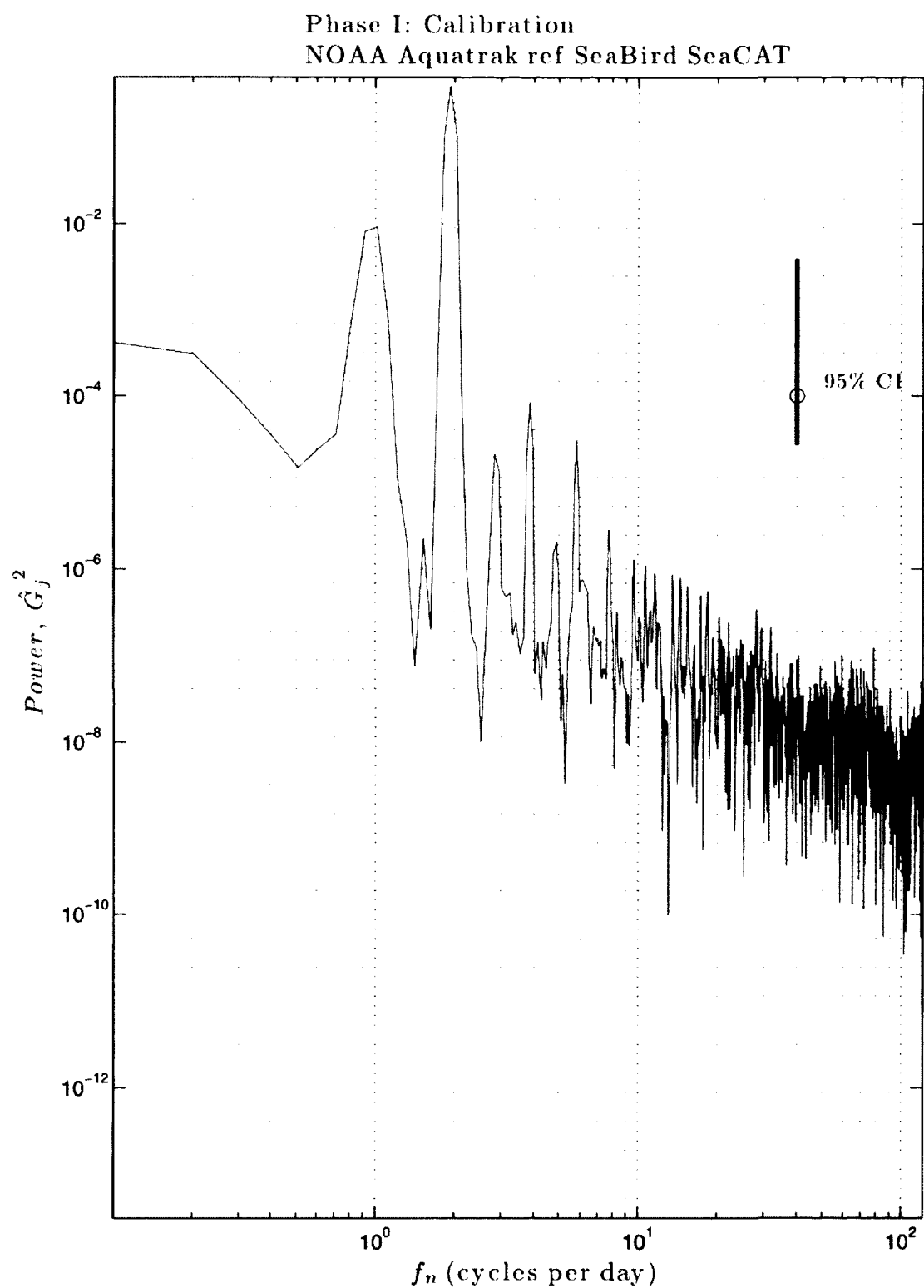
Figure 3.4.15: Water level power spectrum from the control gauge (NOAA Aquatrak) in reference to the SeaBird SeaCAT (Fig. 3.4.16). Hanning window, N=2363. See Figure 3.4.13 for labels of the observable n-th order harmonics of the primary lunar tide, M.

Phase I: Calibration
SeaBird SeaCAT
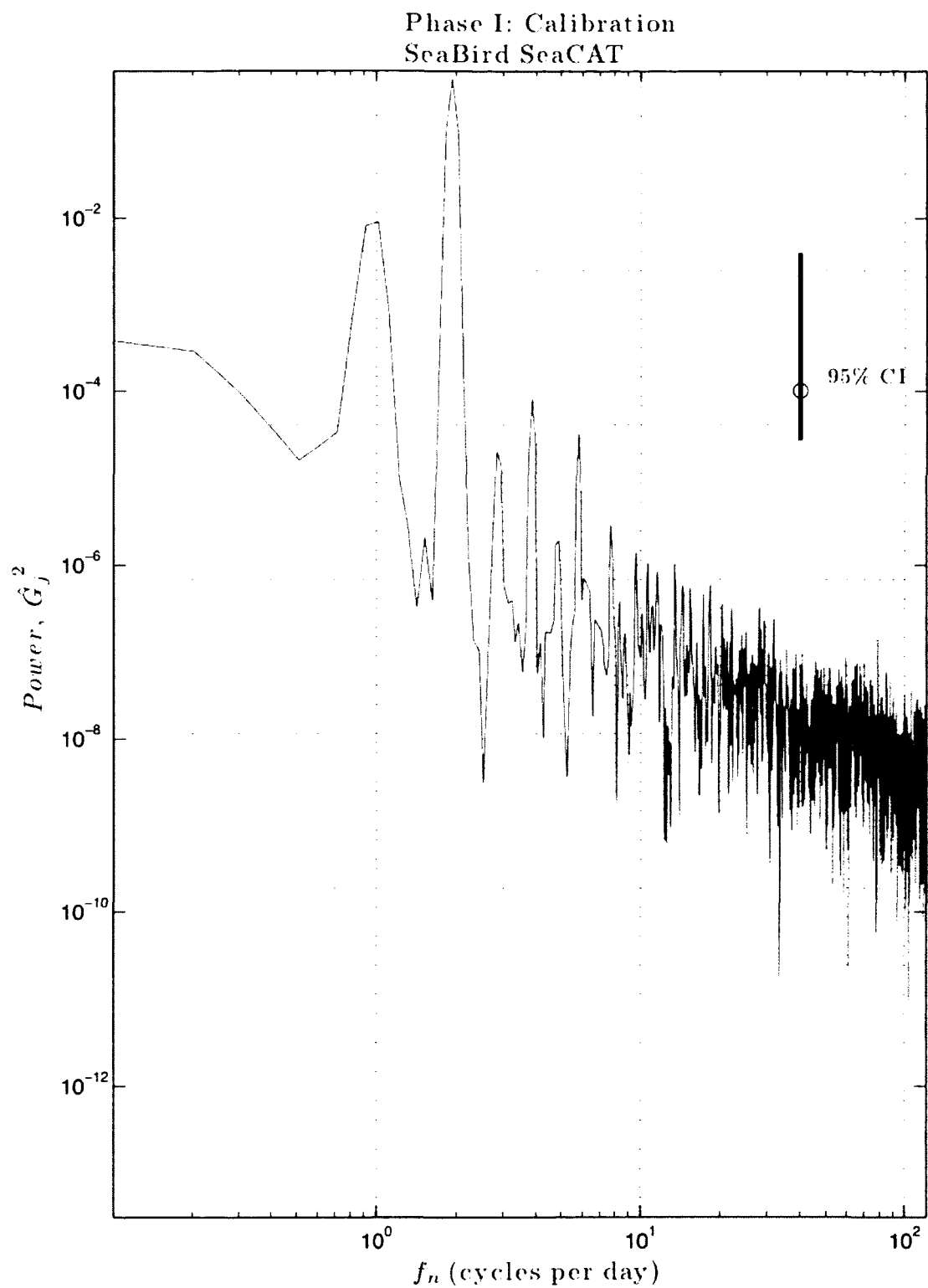
Figure 3.4.16: Water level power spectrum from the SeaBird SeaCAT. Hanning window, N=2363. See Figure 3.4.13 for labels of the observable n-th order harmonics of the primary lunar tide, M.

Phase I: Calibration
NOAA Aquatrak ref WaterLog Bubbler
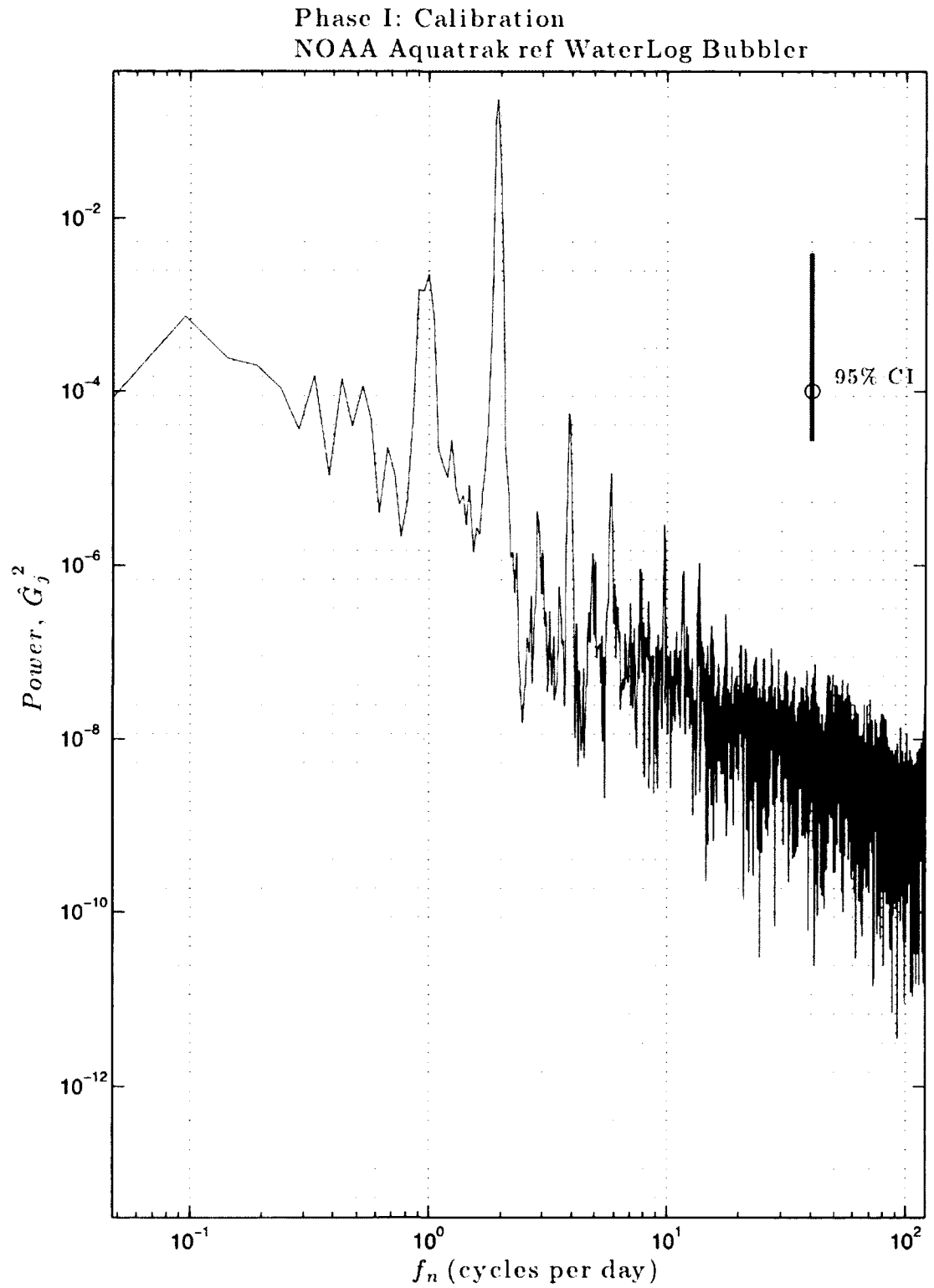
Figure 3.4.17: Water-level power spectrum from the control gauge (NOAA Aquatrak) in reference to the WaterLog Bubbler (Fig. 3.4.18). Hanning window, N=5029. See Figure 3.4.13 for labels of the observable n-th order harmonics of the primary lunar tide, M.

Phase I: Calibration
WaterLog Bubbler
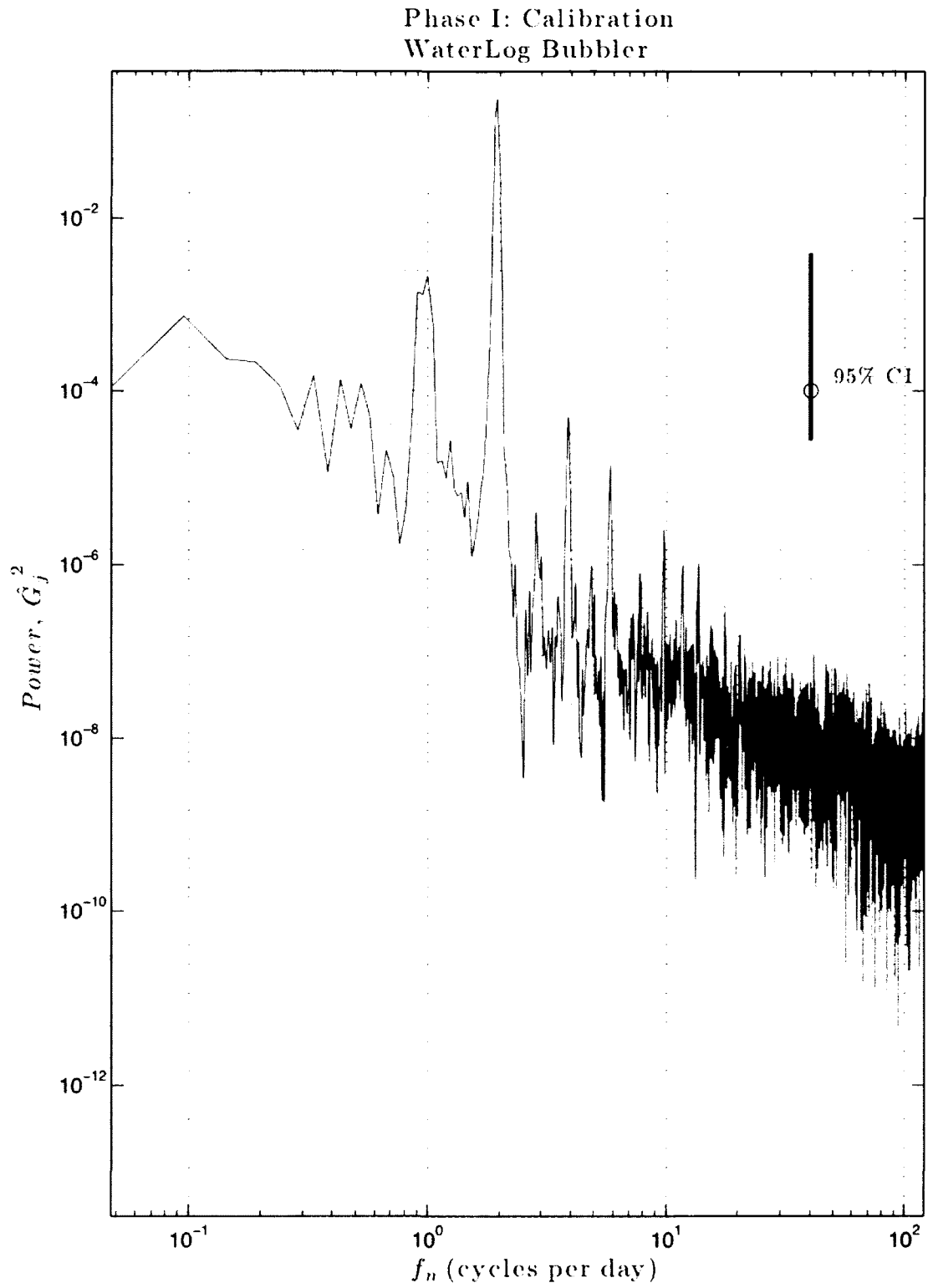
Figure 3.4.18: Water level power spectrum from the WaterLog Bubbler. Hanning window, N=5029. See Figure 3.4.13 for labels of the observable n-th order harmonics of the primary lunar tide, M.

Phase I: Calibration
NOAA Aquatrak ref WaterLog MWWL
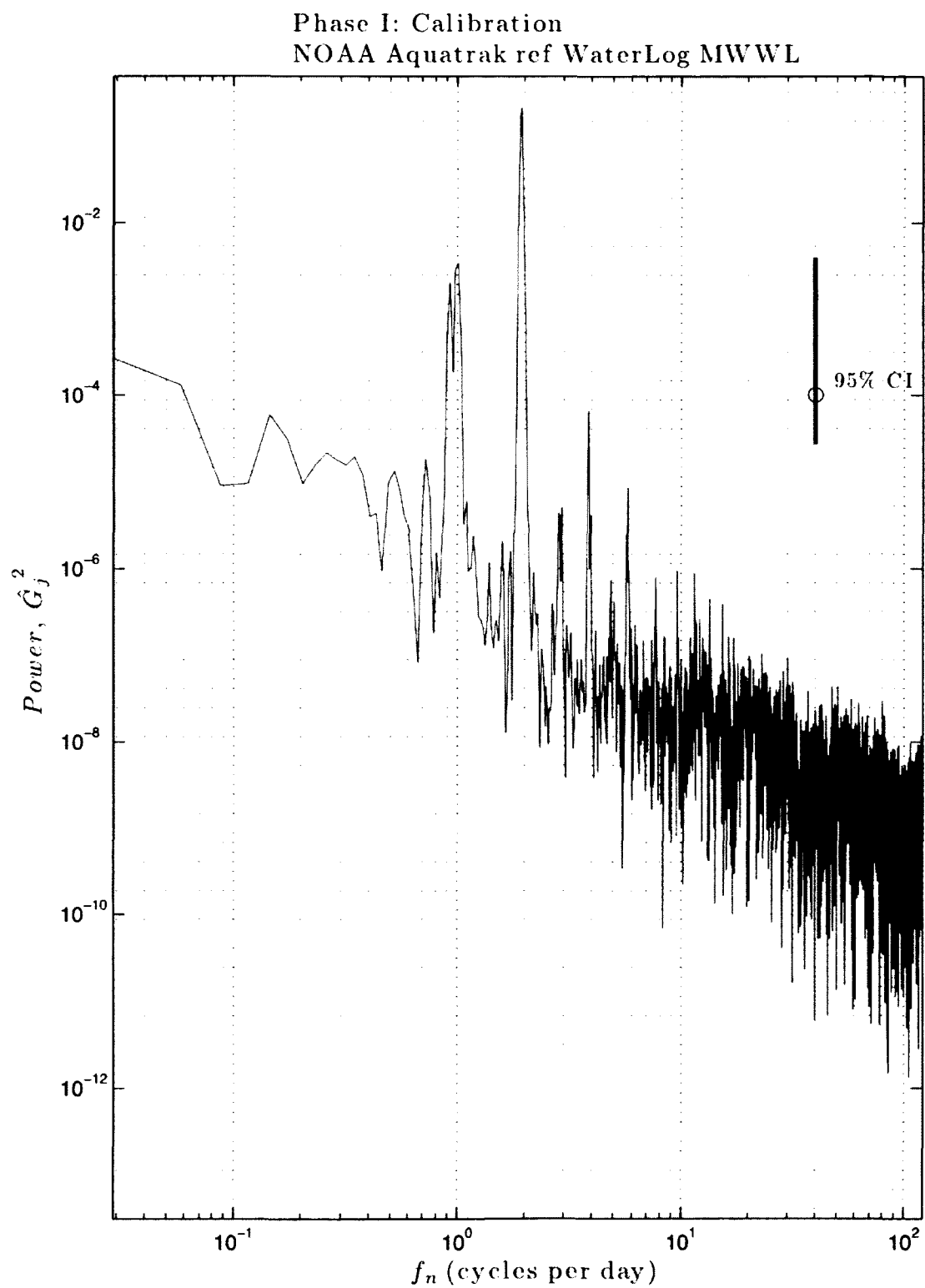
Figure 3.4.19: Water level power spectrum from the control gauge (NOAA Aquatrak) in reference to the WaterLog MWWL (Fig. 3.4.20). Hanning window, N=8291. See Figure 3.4.13 for labels of the observable n-th order harmonics of the primary lunar tide, M.

Phase I: Calibration
WaterLog MWWL

Figure 3.4.20: Water level power spectrum from the WaterLog MWWL. Hanning window, N=8291. See Figure 3.4.13 for labels of the observable n-th order harmonics of the primary lunar tide, M.

Phase I: Calibration
NCDC ref Onset HOBOlogger

Figure 3.4.21: Atmospheric pressure power spectrum in reference to the Onset HOBOlogger (Fig. 3.4.14). Hanning window, N=12841. See Figure 3.4.13 for labels of the observable n-th order harmonics of the primary lunar tide, M.

63

Phase I: Calibration
NCDC ref SeaBird SeaCAT
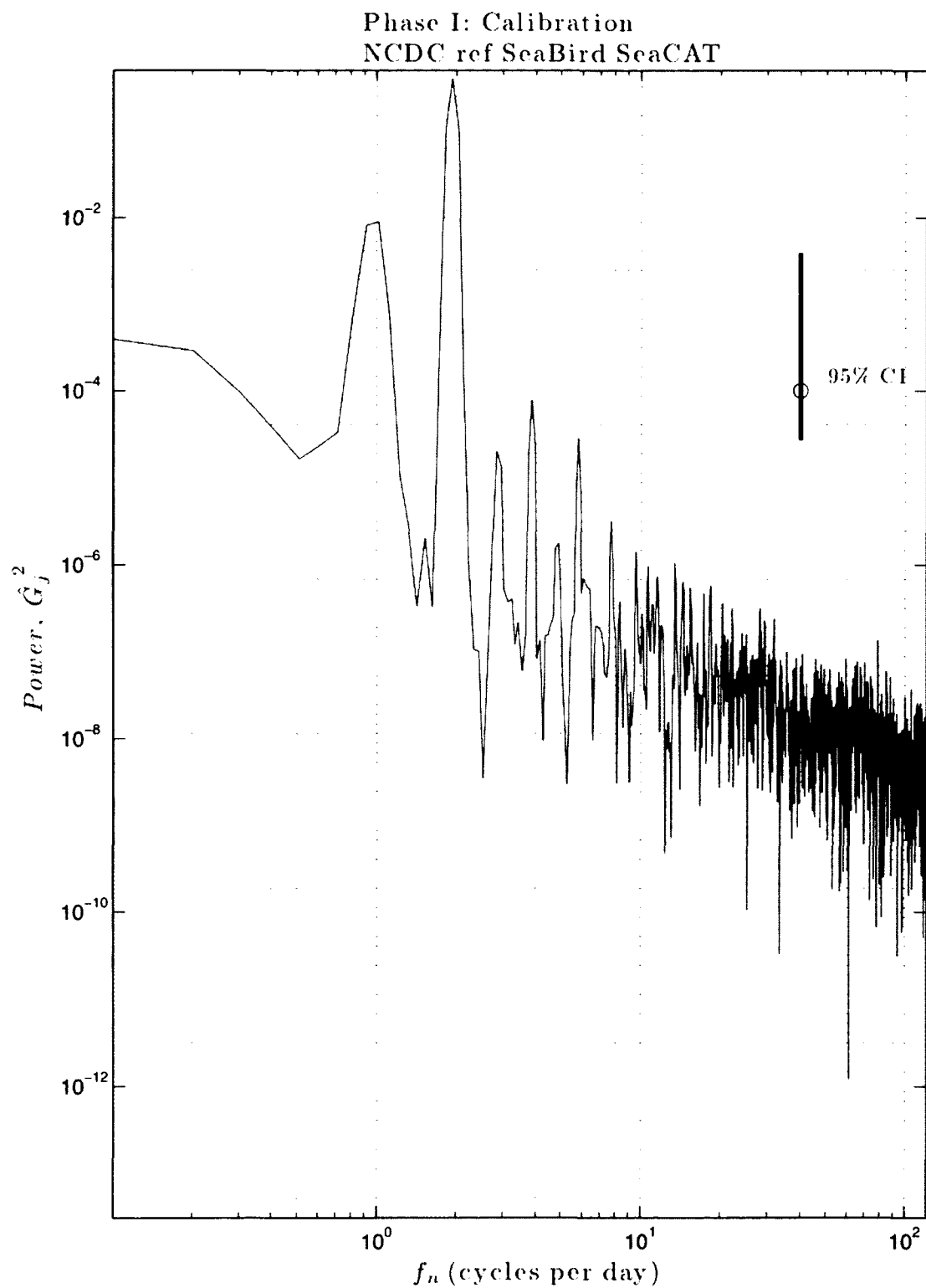
Figure 3.4.22: Atmospheric pressure power spectrum in reference to the SeaBird SeaCAT (Fig. 3.4.16). Hanning window, N=2363. See Figure 3.4.13 for labels of the observable n-th order harmonics of the primary lunar tide, M.

Phase I: Calibration
NCDC ref WaterLog Bubbler
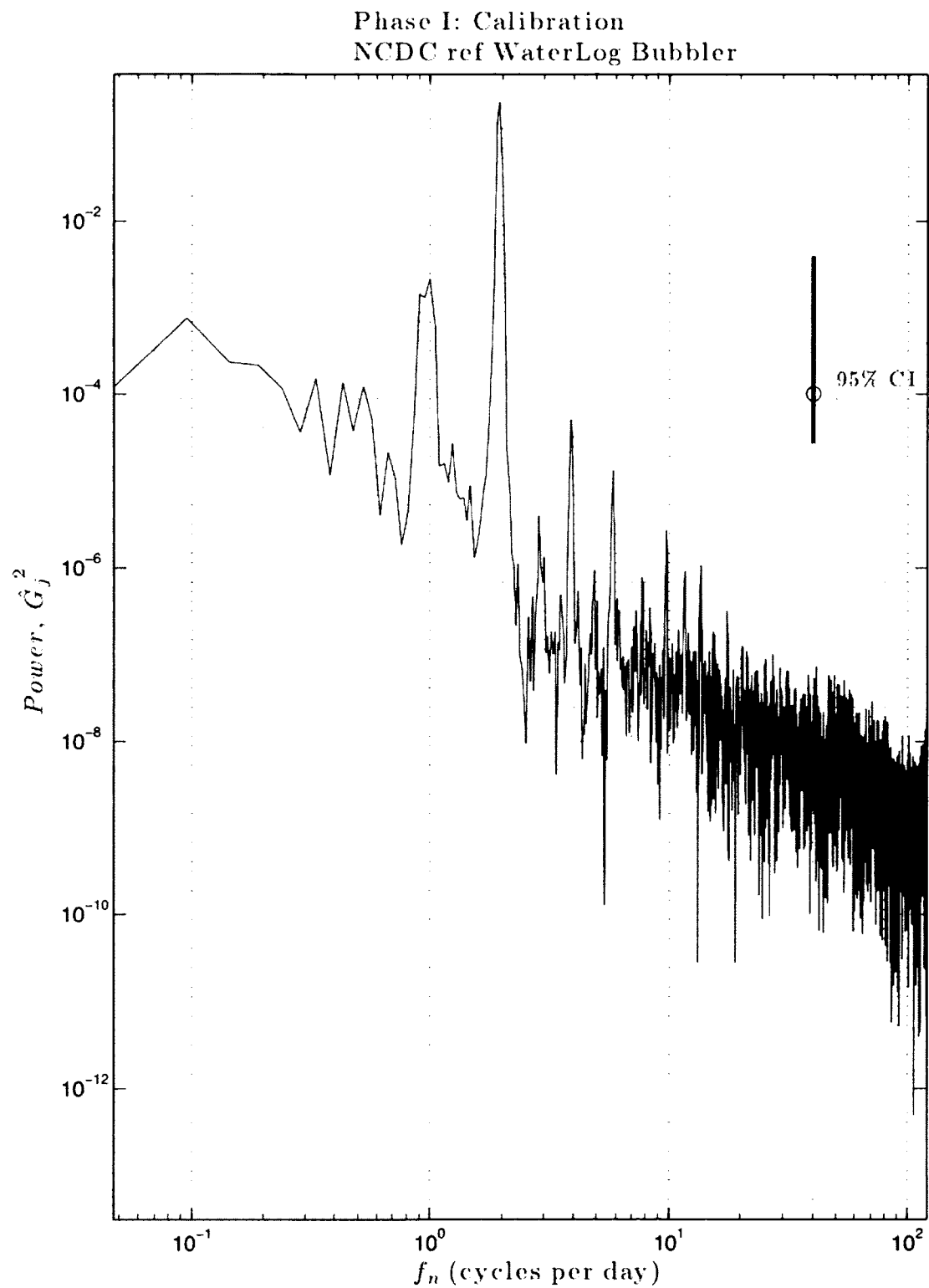
Figure 3.4.23: Atmospheric pressure power spectrum in reference to the WaterLog Bubbler (Fig. 3.4.18). Hanning window, N=5029. See Figure 3.4.13 for labels of the observable n-th order harmonics of the primary lunar tide, M.

Phase I: Calibration
Fort Point, Newcastle, NH
Smoothed Spectral Density

Smoothed Squared Coherency Spectrum

Smoothed Phase Spectrum
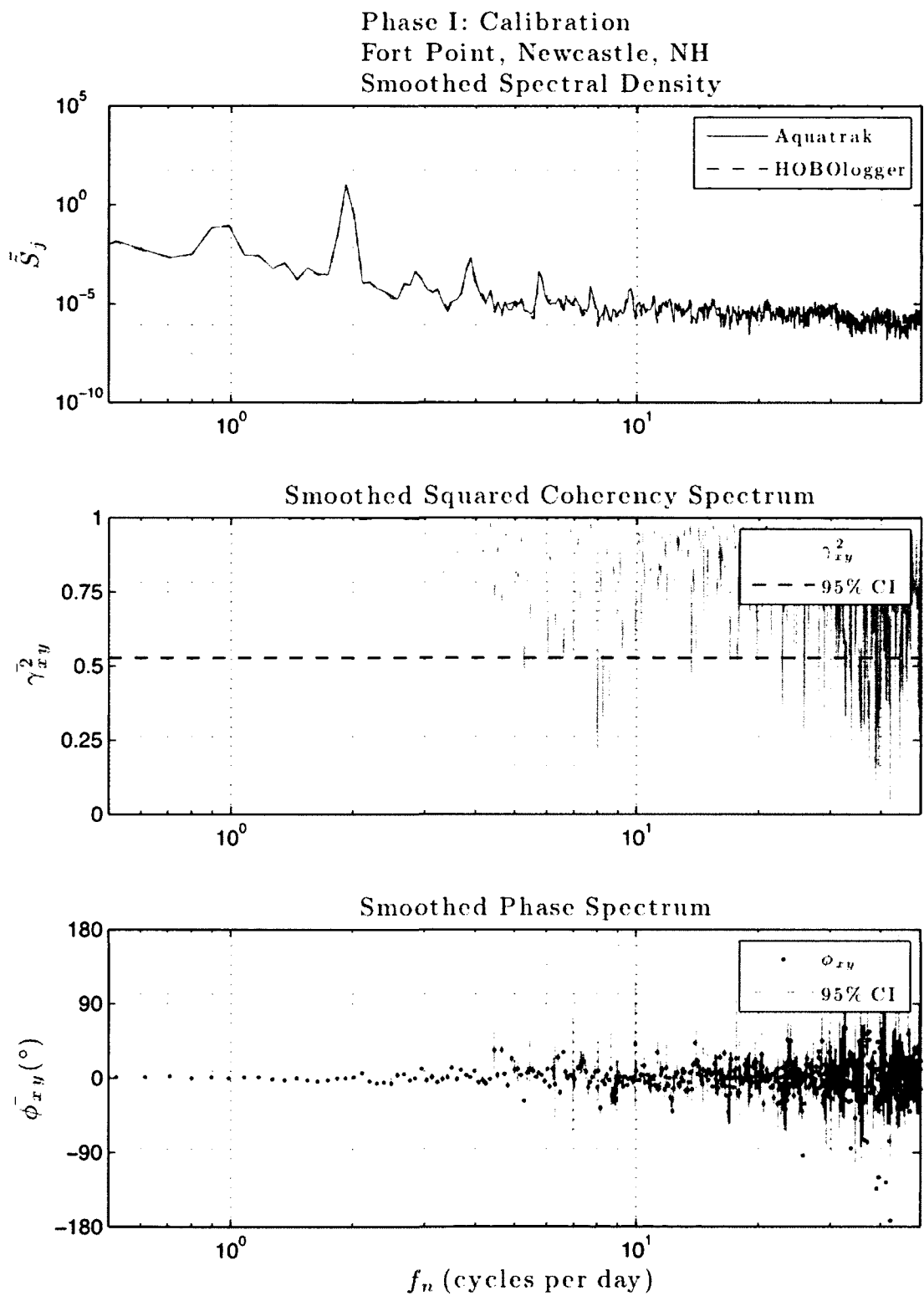
Figure 3.4.24: Smoothed spectral density, smoothed squared coherency spectrum, and smoothed phase spectrum for water level from the control gauge (NOAA Aquatrak) v. computed water level observations from the Onset HOBOlogger. Band-averaged, DOF = 10, N=12841.

Phase I: Calibration
Fort Point, Newcastle, NH
Smoothed Spectral Density

Smoothed Squared Coherency Spectrum

Smoothed Phase Spectrum
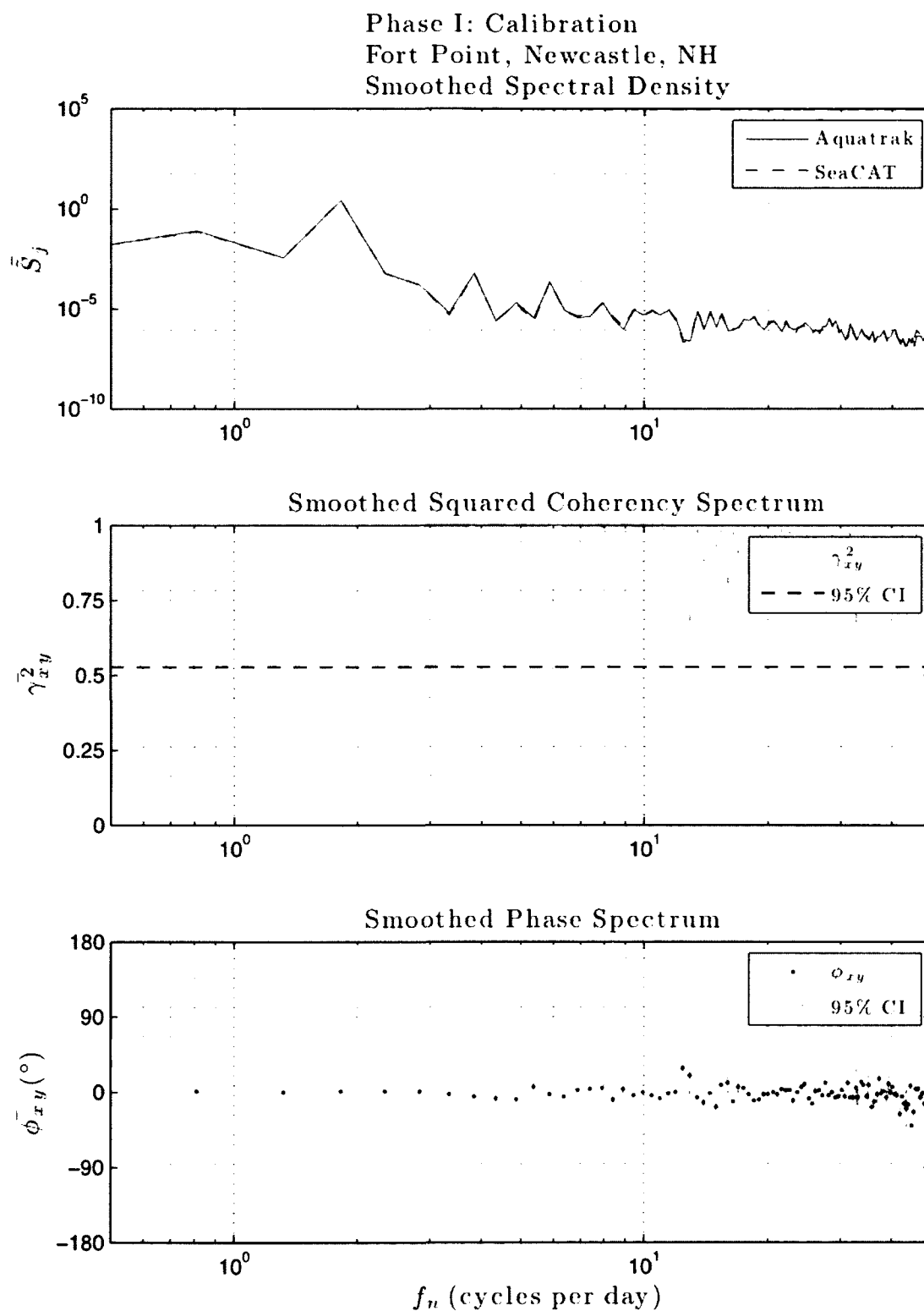
Figure 3.4.25: Smoothed spectral density, smoothed squared coherency spectrum, and smoothed phase spectrum for water level from the control gauge (NOAA Aquatrak) v. computed water level observations from the SeaBird SeaCAT. Band-averaged, DOF = 10, N=2364.

67

Phase I: Calibration
Fort Point, Newcastle, NH
Smoothed Spectral Density
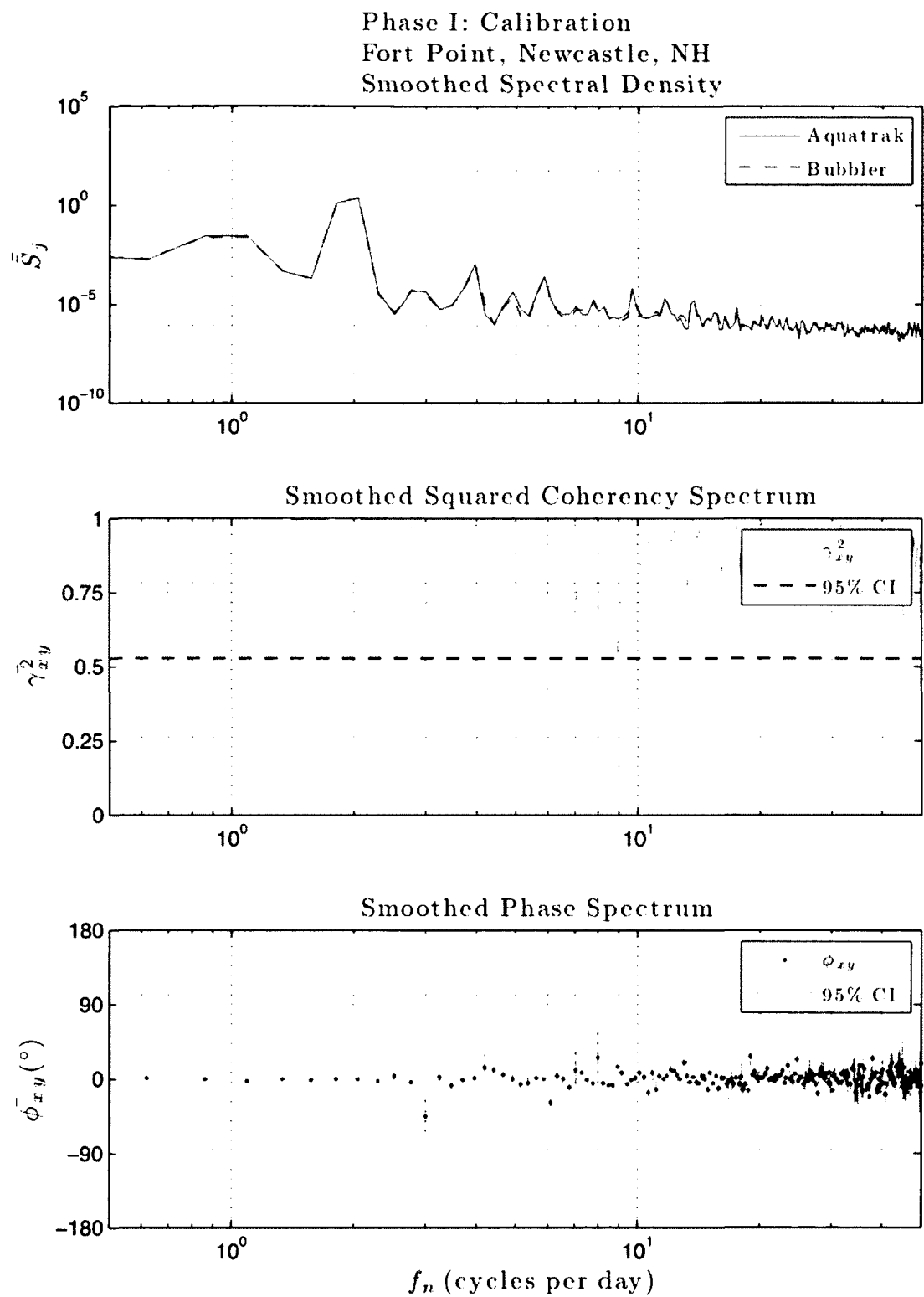
Figure 3.4.26: Smoothed spectral density, smoothed squared coherency spectrum, and smoothed phase spectrum for water level from the control gauge (NOAA Aquatrak) v. computed water level observations from the WaterLog Bubbler. Band-averaged, DOF = 10, N=5030.

Phase I: Calibration
Fort Point, Newcastle, NH
Smoothed Spectral Density

Smoothed Squared Coherency Spectrum

Smoothed Phase Spectrum

f_n (cycles per day)
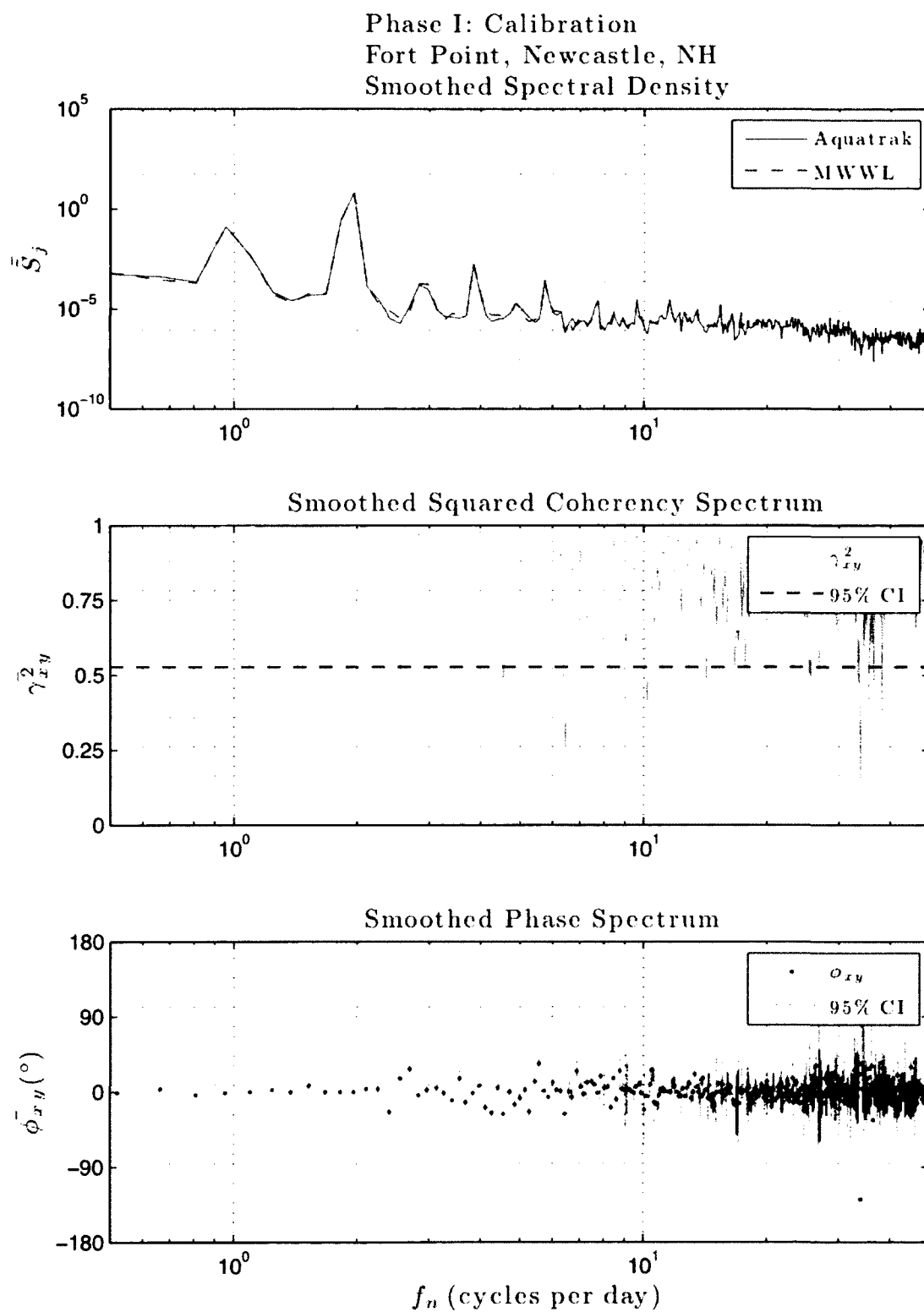
Figure 3.4.27: Smoothed spectral density, smoothed squared coherency spectrum, and smoothed phase spectrum for water level from the control gauge (NOAA Aquatrak) v. computed water level observations from the WaterLog MWWL. Band-averaged, DOF = 10, N=8291.

IV. PHASE 2: STUDY AREA

With the experiment tide gauges calibrated and systematic bias computed for each, collection of tide data within the Great Bay could begin. A combination of site availability, pre-existing infrastructure, and geographical importance were among the many components that weighed on where to collect tide data from within the Bay.

4.1 Methods. When selecting sites based upon geographic importance, numerous locations were selected (Adam's Point, Nannie Island, Lamprey River, etc.). With only a limited number of tide gauges, it was important to strategically place them in order to cover the Bay.

Each tide gauge has infrastructure requirements that must be met. The Onset HOBOlogger requires a stilling well and an immobile, freestanding structure to mount the stilling-well to. The SeaBird SeaCAT must be affixed to some subsurface structure to eliminate motion, both vertically and laterally, during data collection. The WaterLog Bubbler requires an immobile, freestanding structure for both above-water and sub-surface components. The WaterLog MWWL requires an immobile, freestanding structure where water permanently inundates the site. The infrastructure requirements of each tide gauge were then cross-referenced to the list of geographic locations.

The last crucial factor in selecting site locations for the tide gauges was availability, whether from private landowners or public institutions. The locations of all Phase 2 data

70

collection sources in relation to the calibration site are listed in Table 4.1.1 and are depicted in Figure 4.1.1.

ID	Location Name	Gauge Name	Latitude (N)	Longitude (W)
2	Shankhassic, Great Bay, NH	Onset HOBOlogger	43.08246980°	70.88430316°
3	Winnicut River, Great Bay, NH	SeaBird SeaCAT	43.04957120°	70.84480492°
4	Adam's Point, Great Bay, NH	SeaBird MicroCAT; WaterLog Bubbler	43.09212219°	70.86468119°
5	Squamscott River, Great Bay, NH	WaterLog MWWL	43.05264471°	70.91224518°

Table 4.1.1: Phase 2 tide gauge identification, location, name, latitude and longitude.
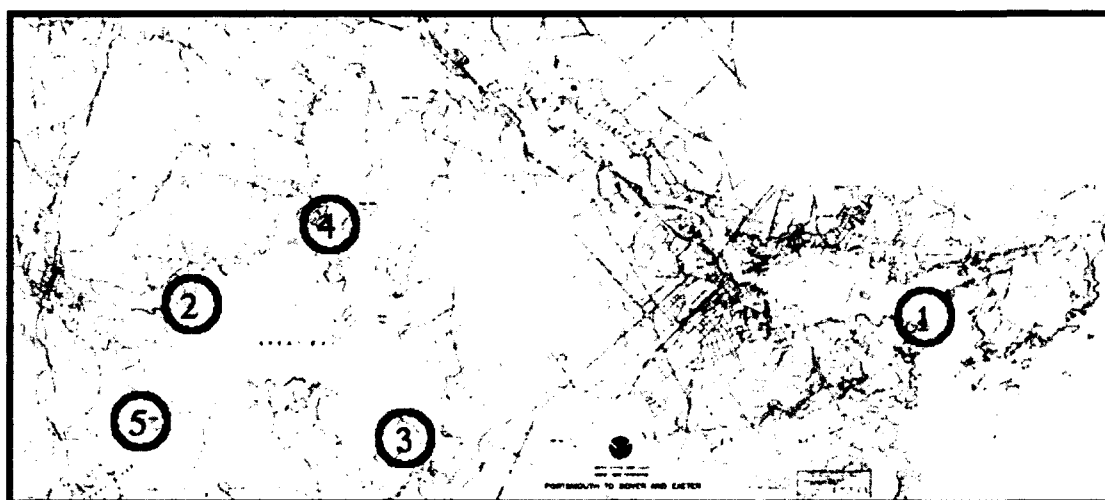
Figure 4.1.1: Phase 2 tide gauge locations. Current areas of study are highlighted in red, while previous areas of interest are muted in grey. (OCS, 2005; 2011)

The WaterLog Bubbler was placed at the UNH Jackson Estuarine Laboratory (JEL) pier at Adam's Point (Fig. 4.1.2). Its geographic location at the interface between Great Bay and Squamscott River was the primary factor in choosing this site. Security, ease of access, and the pre-existence of an immobile pier with shore-power were the factors in choosing the WaterLog Bubbler.

Figure 4.1.2: WaterLog Bubbler installation at Adam's Point, Great Bay, NH.

The WaterLog MWWL was placed at the Boston and Maine Railroad trestle spanning the Squamscott River (Fig. 4.1.3). Its geographic location at the interface between the Great Bay and Squamscott River was the primary factor in choosing this site. The pre-existence of an immobile bridge was the primary factor in choosing the WaterLog MWWL.

Near Shankhassic, the Onset HOBOlogger was placed in a stilling well affixed to a steel pipe that was jetted into the mud-bottom of the Great Bay. The sensor was placed well below the observed water level near low tide. Geographic location between Adam's Point and Squamscott River was the primary factor in choosing this location. The lack of

security and pre-existing infrastructure were the main reasons for choosing the Onset HOBOlogger.

Figure 4.1.3: WaterLog MWWL installation at Squamscott River, Great Bay, NH.

In the mouth of the Winnicut River, The SeaBird SeaCAT was placed on a mount affixed to a steel pipe that was jetted into the mud-bottom. The mount was then placed at the sediment-water interface for maximum clearance of the water column above. Geographic location across the Bay from the Shankhassic site was the primary factor in choosing this location. The lack of pre-existing infrastructure and accessibility were the main reasons for choosing the SeaBird SeaCAT.

As in Phase 1, each sensor was set to a sample interval that was both memory-efficient and allowed for a simple averaging to match NOAA's standard six-minute sample

interval. An ideal record length of thirty or thirty-one days was planned for, although longer records would be invaluable (Table 4.1.2).

Tide Gauge or Sensor Name	Location ID	Sample Interval	Record Length
Onset HOBOlogger	2	360 seconds	44 days, 14 hours, 30 minutes
SeaBird MicroCAT	4	120 seconds	102 days, 00 hours, 00 minutes
SeaBird SeaCAT	3	60 seconds	57 days, 00 hours, 00 minutes
WaterLog Bubbler	4	360 seconds	102 days, 00 hours, 00 minutes
WaterLog MWWL	5	1 second	57 days, 17 hours, 18 minutes

Table 4.1.2: Tidal instrumentation, location ID, sample interval and record length.

As in Phase 1, the WaterLog Bubbler was coupled with the SeaBird MicroCAT when placed at Adam's Point, Great Bay, NH. This was done in order to provide water density in Equation 2.4.2 when solving for water level.

For each tide station, a static GPS session was run on either a nearby benchmark or directly atop a reference mark on the tide gauge. The data collected from each session was processed using the rapid-static option of the NOAA National Geodetic Survey (NGS) Online Positioning User Service (OPUS) (Table 4.1.3). Latitude, longitude, and *ellipsoidal height* information were referenced to the North American Datum of 1983 (NAD83) reference frame (CORS96/ Epoch: 2002), while *orthometric height* was referenced to the North American Vertical Datum of 1988 (NAVD88) using the Geoid09 *geoid* model. This position was then referenced to the tide gauge through either (or both) three-wire leveling or tape measurement techniques. Leveling and tape reference field notes can be found in Appendix C: Field Notes. Full OPUS GPS positioning reports can be found in Appendix F: OPUS Reports.

The use of the NAD83 reference frame, as opposed to the World Geodetic System 1984

(WGS84) reference frame, is for both convenience of comparison to and incorporation of

data from agencies of the United States, chiefly the NOAA in regards to the current

study. The horizontal control datum of the United States is the North American Datum of

1983 (NAD83) utilizing the Geodetic Reference System 1980 (GRS80) *ellipsoid*. The

NAD83 reference frame is readjusted on a periodic basis by the NOAA NGS.

Position	Shankhassic, Great Bay,NH	Winnicut River, Great Bay,NH	Adam's Point, Great Bay,NH	Squamscott River, Great Bay,NH
Latitude (N)	43.08246980	43.04957120	43.09212219	43.05264471
Longitude (W)	70.88430316	70.84480492	70.86468119	70.91224518
Ellipsoid Height (m)	-28.187	-28.477	-28.357	-24.628
Orthometric Height (m)	-1.409	-1.718	-1.601	2.199

Table 4.1.3: Measured latitude, longitude, ellipsoidal and orthometric height for Phase 2 stations. Latitude, longitude and ellipsoidal height referenced to the North American Datum of 1983 (NAD83) reference frame (CORS96/ Epoch: 2002). Orthometric height referenced to the North American Vertical Datum of 1988 (NAVD88) using Geoid09.

4.2 Data Processing. Recall that subsequent to each phase of data collection, the

computation of water level, tidal constituents, datums, and other statistics are necessary.

See Appendix D: Data Processing for more detailed information on general data

processing techniques and algorithms.

Again, in order to analyze time series, the time records must exist on the same time

reference. In the case of the Onset HOBOlogger at Shankhassic, time is referenced to the

local time— Eastern Standard Time (EST) for Phase 2,— while the remaining sensors are

referenced to GMT. An offset of +5 hours was applied to reference the time series to

GMT. Moreover, while the previous blunder in the SeaBird MicroCAT was detected, in

order to maintain a continuous time record throughout, the blunder was left in place and

an offset of four-four days was applied to the time series. Furthermore, while the

SeaBird MicroCAT at Adam's Point recorded with a two-minute sampling rate, the time

series was offset from an on-the-two-minute sample interval. A linear interpolation was

used to correct for this offset. For the SeaBird SeaCAT at Winnicut River, a one-second

truncation of the time series was applied to realize an on-the-six-minute sample interval

(*e.g.* 14:06:00 GMT v. 14:06:01 GMT).

For the Onset HOBOlogger, while water pressure and temperature were recorded, no

conductivity or salinity information was available, thus water density could not be

computed (Eq. 2.4.2). In order to determine the most suitable source for conductivity

information, the temperature records from the SeaBird SeaCAT at Winnicut River and

the SeaBird MicroCAT at Adam's Point were compared to that from the Onset

HOBOlogger at Shankhassic (Fig. 4.2.1-2). A simple analysis was conducted on the

temperature data (Table 4.2.1). While the temperature analysis favors the SeaBird

SeaCAT at Winnicut River temperature record, further analysis of the conductivity

records from the SeaBird SeaCAT at Winnicut River and the SeaBird MicroCAT at

Adam's Point points out one glaring downside (Fig. 4.2.2). The fluctuating freshwater

input from the Winnicut River that appears in the SeaBird SeaCAT conductivity record is

troublesome when extrapolating information to another geographic location. The

conductivity record of the SeaBird MicroCAT at Adam's Point was more consistent and

the temperature record was still close to that of the Onset HOBOlogger. Thusly, the

conductivity information from the SeaBird MicroCAT was used to compute water

density for the Onset HOBOlogger. Applying the maximum standard deviation (±0.2394

S/m) of the conductivity, the RMSE for water level (±0.004m) was computed. While an error is inherent in the use of the spatially disparate conductivity measurements, the computed RMSE value is much lower than the error value of the Onset HOBOlogger sensor (±0.015m). (Onset, 2011) Therefore, the use of the conductivity measurements from the SeaBird SeaCAT at Adam's Point is valid in this case.

For the three gauges that are pressure-based, the NCDC atmospheric pressure record was used to either fill in the unknown in Equation 2.4.2 or for further analysis of the pressure measurements. The same problem of erratic sample interval was observed in the on-the-hour pressure record. A linear interpolation was applied to attain an on-the-hour time series. Further linear interpolation was used to achieve a time series with a six-minute sample interval. While a cubic spline interpolation is preferable, the low variance in the atmospheric pressure (See §4.3) allows for a linear interpolation in this case. Duplicates and gaps were solved for and block-averaging was applied to all time series (Table 4.2.2-5). At this point, all time series are both continuous and have six-minute sample intervals.

Phase II: Study Area
Temperature Comparison

Shankhassic ——— Adam's Point   Winnicut River
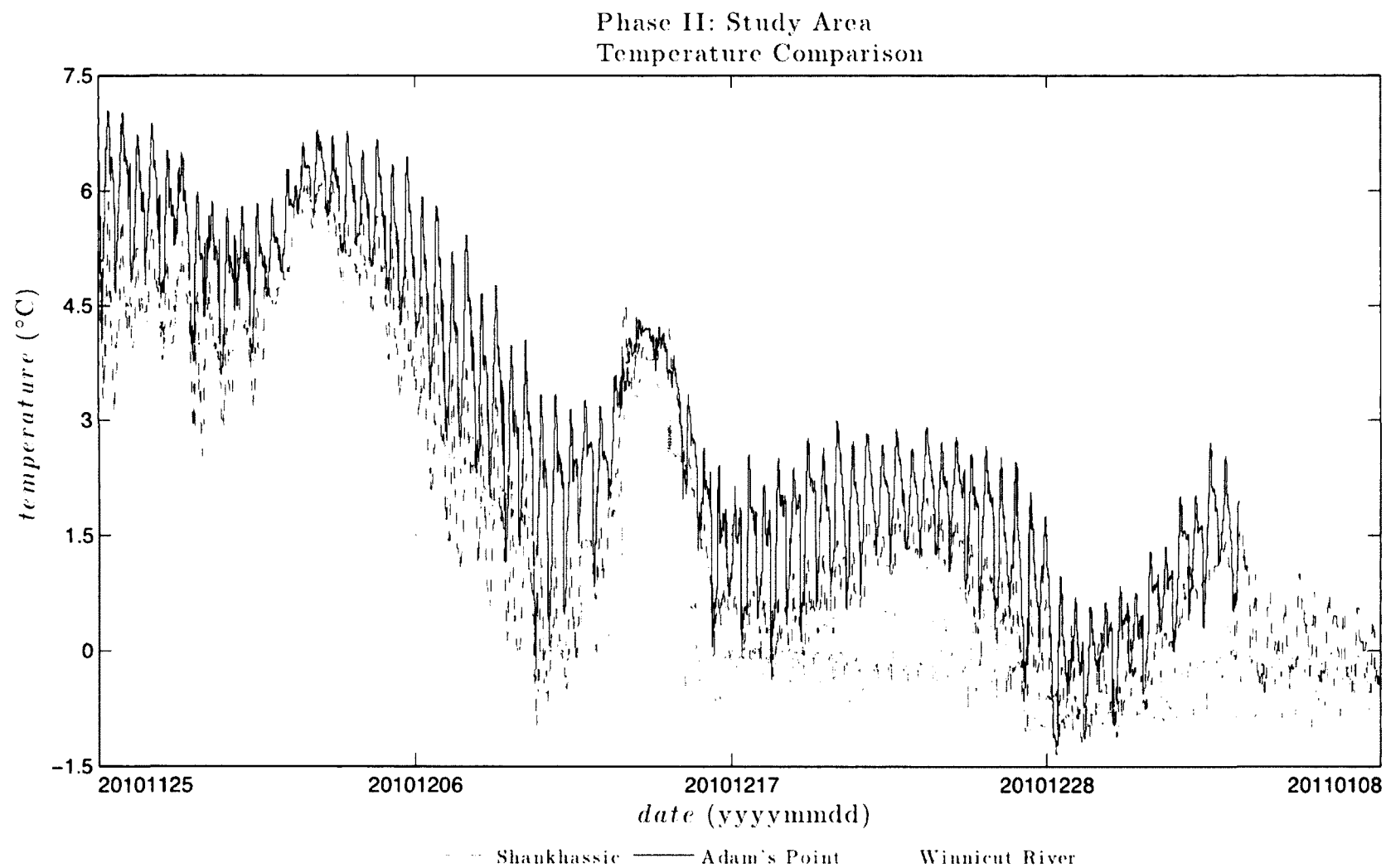
Figure 4.2.1: Conductivity extrapolation at Shankhassic, Great Bay, NH through temperature comparison at Adam's Point and Winnicut River, Great Bay, NH.

Phase II: Study Area
Temperature Differential: Shankhassic v.
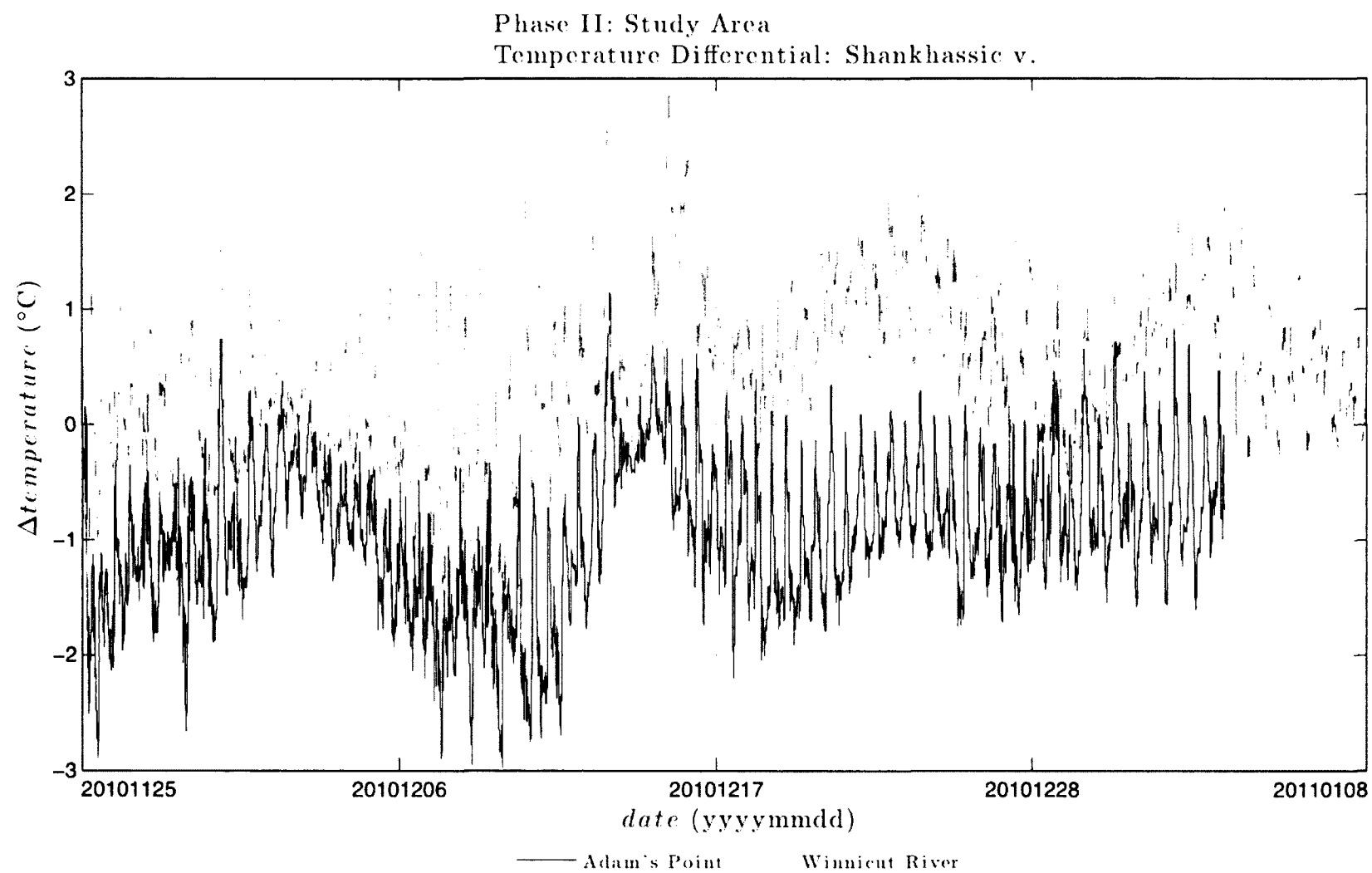
Figure 4.2.2: Conductivity extrapolation at Shankhassic, Great Bay, NH through residual temperature at Adam's Point and Winnicut River, Great Bay, NH.

79

Phase II: Study Area
Conductivity Comparison
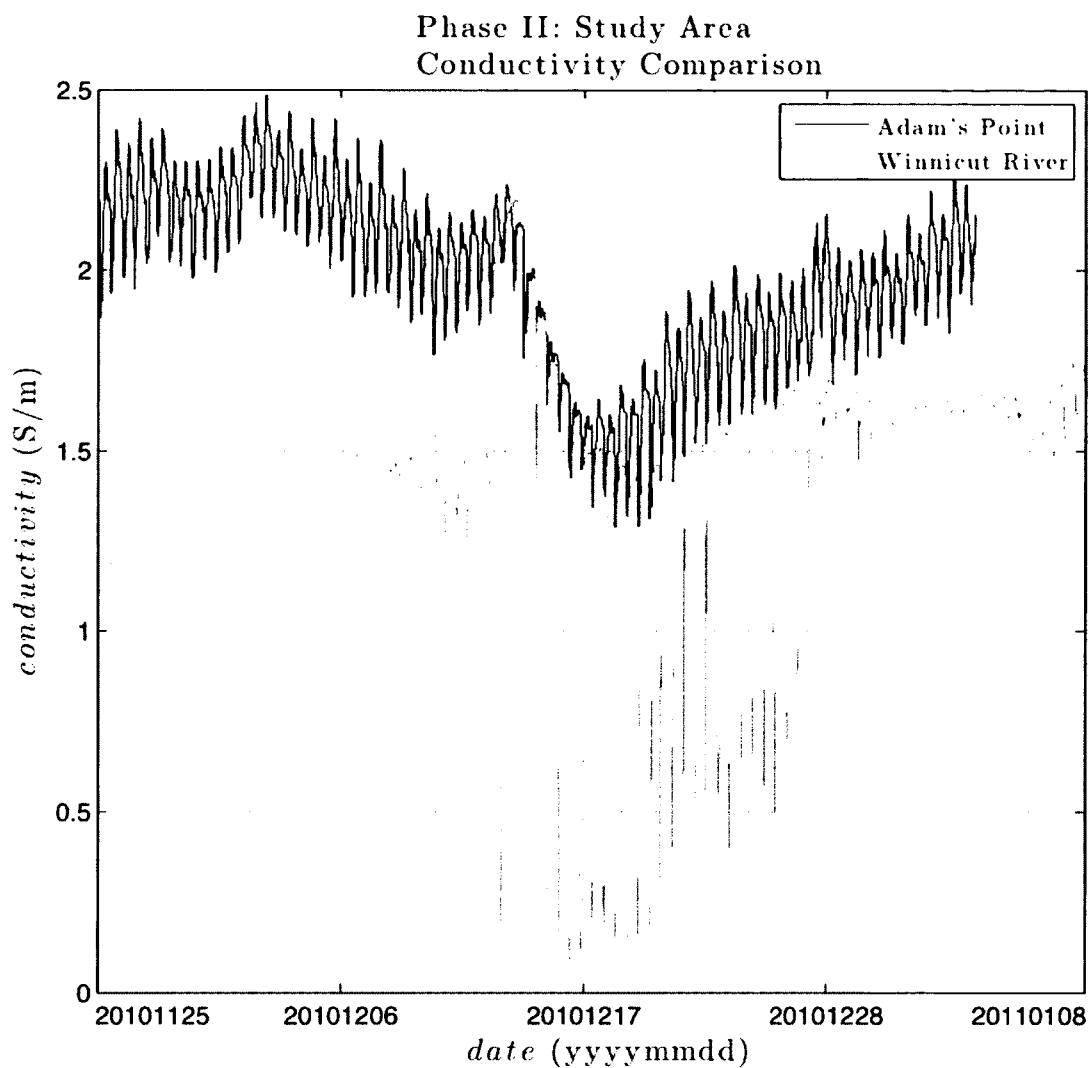
Figure 4.2.3: Conductivity at Adam's Point and Winnicut River, Great Bay, NH. Note the influence of the freshwater discharge from the Winnicut River on the salinity, fluctuating with the tidal cycle.

Sensor Name	Mean Temperature (°C)	Mean Residual Temperature (°C)
Onset HOBOlogger ref SeaBird MicroCAT	2.0397	N/A
SeaBird MicroCAT	2.9603	-0.9206
Onset HOBOlogger ref SeaBird SeaCAT	1.8309	N/A
SeaBird SeaCAT	1.3852	0.4456

Table 4.2.1: Conductivity extrapolation at Shankhassic, Great Bay, NH through temperature and temperature residual comparison at Adam's Point and Winnicut River, Great Bay, NH.

Time Series	Raw Data Size	Duplicates	Gaps (Longest Gap)	Processed Size, N
Onset HOBOlogger	10706	0	0 (0)	10706
SeaBird MicroCAT	32121	1	0 (0)	10706
NCDC Weather Station	1072	0	0 (0)	10706
NOAA Aquatrak at Portland, ME	177	0	0 (0)	177

Table 4.2.2: Duplicates and gaps in the time series referenced to Shankhassic, Great Bay, NH.

Time Series	Raw Data Size	Duplicates	Gaps (Longest Gap)	Processed Size, N
SeaBird SeaCAT	82085	0	0 (0)	13681
NCDC Weather Station	1369	0	0 (0)	13681
NOAA Aquatrak at Portland, ME	225	0	0 (0)	225

Table 4.2.3: Duplicates and gaps in the time series referenced to Winnicut River, Great Bay, NH.

Time Series	Raw Data Size	Duplicates	Gaps (Longest Gap)	Processed Size, N
WaterLog Bubbler	24481	0	0 (0)	24481
SeaBird MicroCAT	73361	3	25 (11)	24481
NCDC Weather Station	2446	0	0 (0)	24481
NOAA Aquatrak at Portland, ME	399	0	0 (0)	399

Table 4.2.4: Duplicates and gaps in the time series referenced to Adam's Point, Great Bay, NH.

Time Series	Raw Data Size	Duplicates	Gaps (Longest Gap)	Processed Size, N
WaterLog MWWL	4986723	29	0 (0)	13854
NOAA Aquatrak at Portland, ME	311	0	0 (0)	311

Table 4.2.5: Duplicates and gaps in the time series referenced to Squamscott River, Great Bay, NH.

With the relevant data compiled, computation of water level for the pressure-based tide gauges occurred next. Using the same fixed-range test values for the WaterLog MWWL and both ellipsoidal and orthometric elevations for each gauge measured, the computed water level observations were referenced to both the ellipsoid and geoid. From these referenced data, an analysis can be performed that will eventually lead to the creation of a tidal prediction model for the Great Bay.

4.3 Analysis. The objective of the study phase of the project was to determine those harmonic constituents responsible for the tides at numerous, strategic points in the Great Bay. For Phase 2, while visualizations are presented in the time domain, analysis of the processed data was performed only in the spectral domain. The computed water levels from observation as well as the t_tide generated water levels are presented in Figures 4.3.1-8. For those locations that use pressure-based tide gauges, the atmospheric versus water pressure comparisons are presented in Figures 4.3.9-11. A subjective look at these figures shows that there are no distortions in the tidal signals that would preclude modeling tides from these tide stations.

The first of two spectral domain analysis techniques performed was to look at the resolved harmonic constituents for each time series (Table 4.3.1-4). For those locations that use pressure-based tide gauges, the tidal harmonics resolved from the atmospheric pressure time series are also provided. The full report generated by t_tide for each time series is presented in Appendix E: t_tide Reports. Concurrently, at each location the power spectra of each time series were plotted (Fig. 4.3.12-22). In comparing those relevant power spectra from Phase 1 of the study (Fig. 3.4.14, 3.4.16, 3.4.18, and 3.4.20) to those of Phase 2 of the study (Fig. 4.3.12-15), respectively, it is quite evident that higher frequency, shallow-water tides are occurring in the Great Bay which are not occurring at Fort Point. In respect to the harmonics of the semidiurnal lunar tide, M_2, much greater harmonics are evident in the Bay ($n \geq 12$) as compared to Fort Point ($n \leq 8$). From a look at the atmospheric pressure analysis, while the atmospheric tides are resolved, they are two orders of magnitude less than the water tides, thus their effect

is negligible. The result of these analyses shows, once more, that there was nothing unexpected in the harmonic constituents or the power spectra.

While no direct statistical comparisons were made between tidal stations in this phase, visual inspection of the time domain analysis shows a similar range of water level measurement. This is to be expected within an area such as the Great Bay. Similarly, for the computed water level time series, each station shows, to some extent, the effect of the Nor'easter that occurred December 26, 2010. While not significant in and of itself, it does show the ability of t_tide to resolve the tidal signal despite any significant storm surge events. The conclusion of this limited analysis is that the primary objective of obtaining representative tidal time series and harmonic constituents has been achieved.
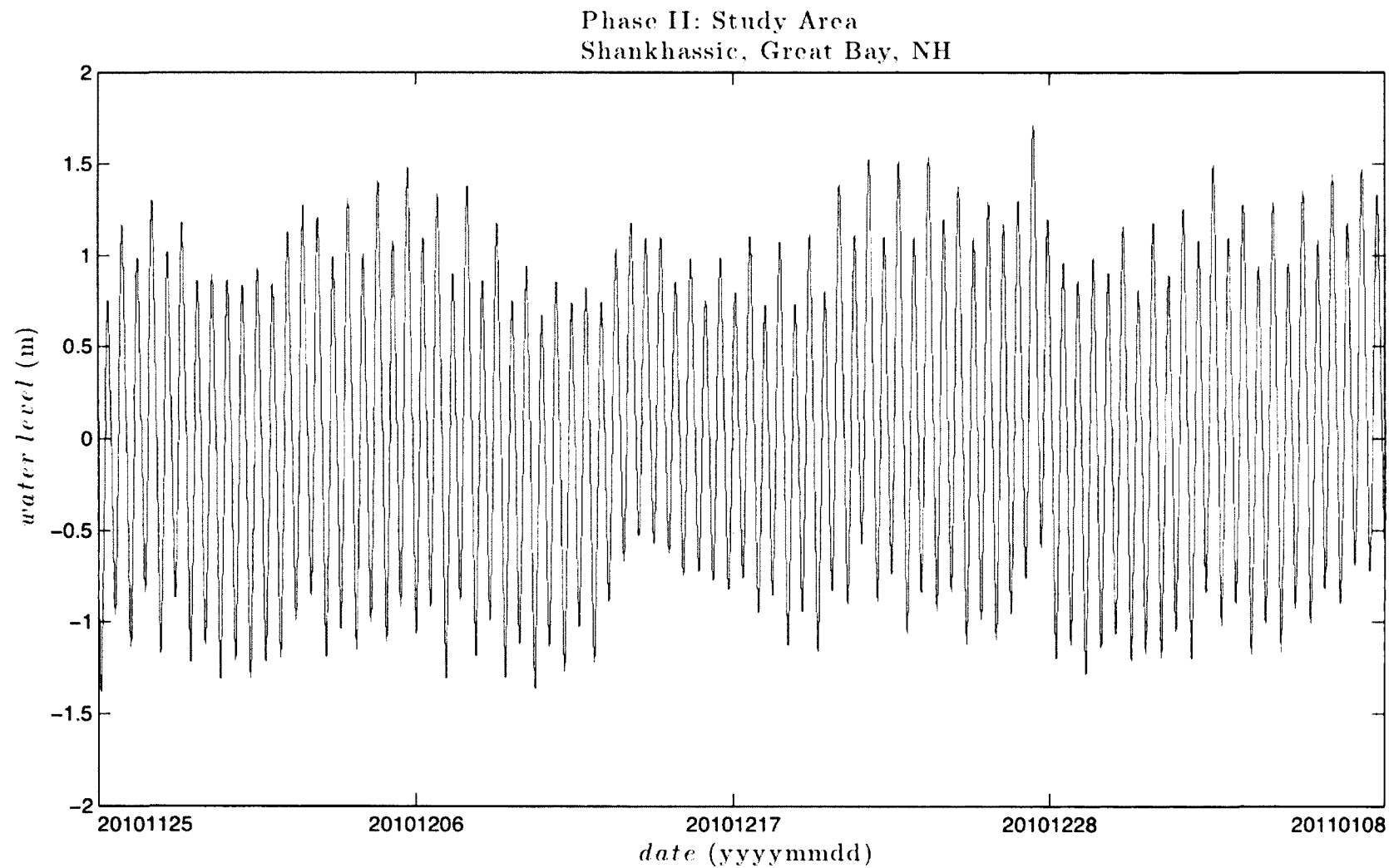
Figure 4.3.1: Computed water level at Shankhassic, Great Bay, NH using observations from the Onset HOBOlogger. N=10706. Note the non-linear affect on the tides compared to those of Phase 1 (Fig. 3.4.1-4); the Nor'easter event of 20101226 is apparent in the water level record.

Phase II: Study Area
Winnicut River, Great Bay, NH
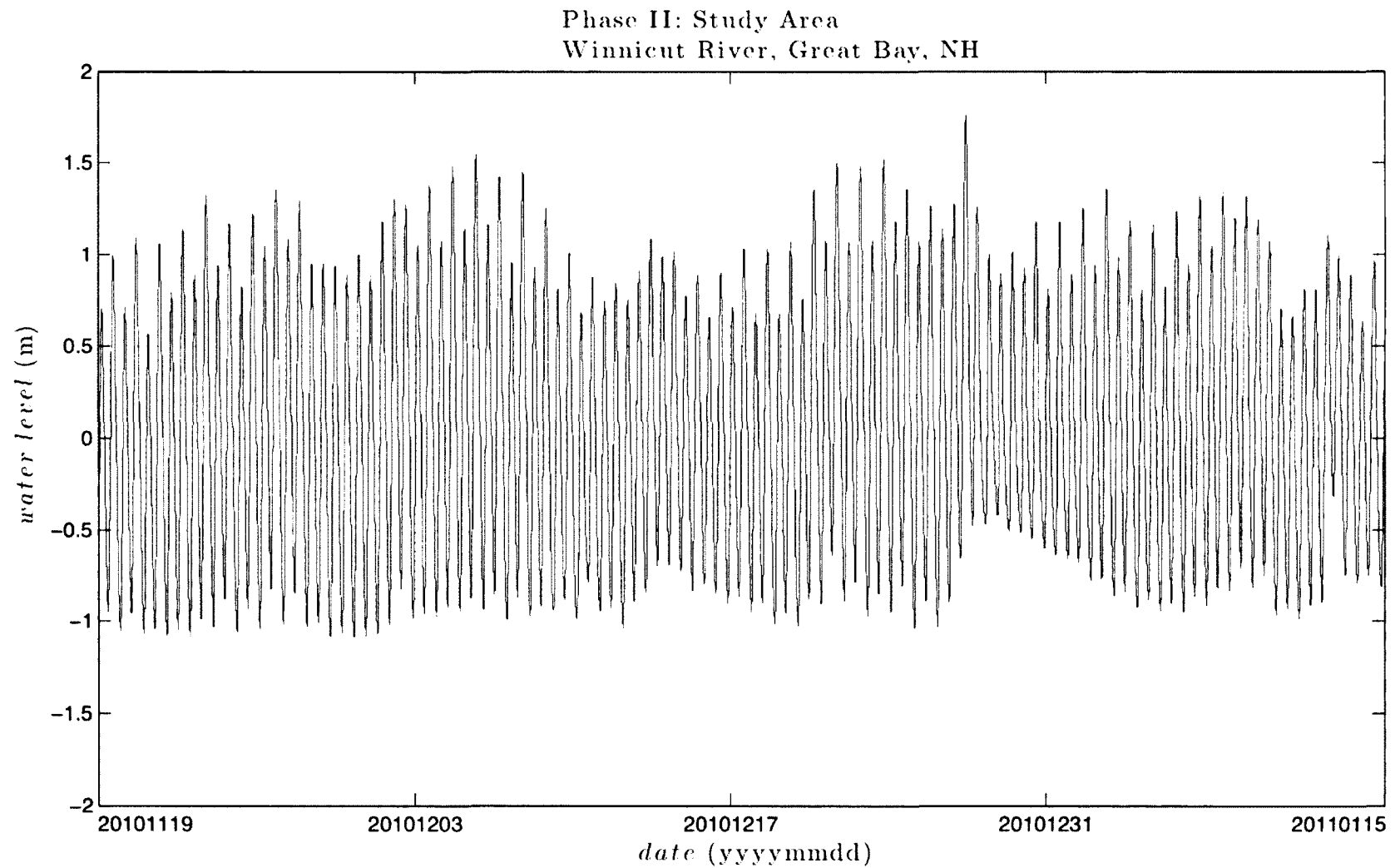
Figure 4.3.2: Computed water level at Winnicut River, Great Bay, NH using observations from the SeaBird SeaCAT. N=13681. Note the non-linear affect on the tides compared to those of Phase 1 (Fig. 3.4.1-4); the Nor'easter event of 20101226 and ice formation in mid-January is apparent in the water level record.
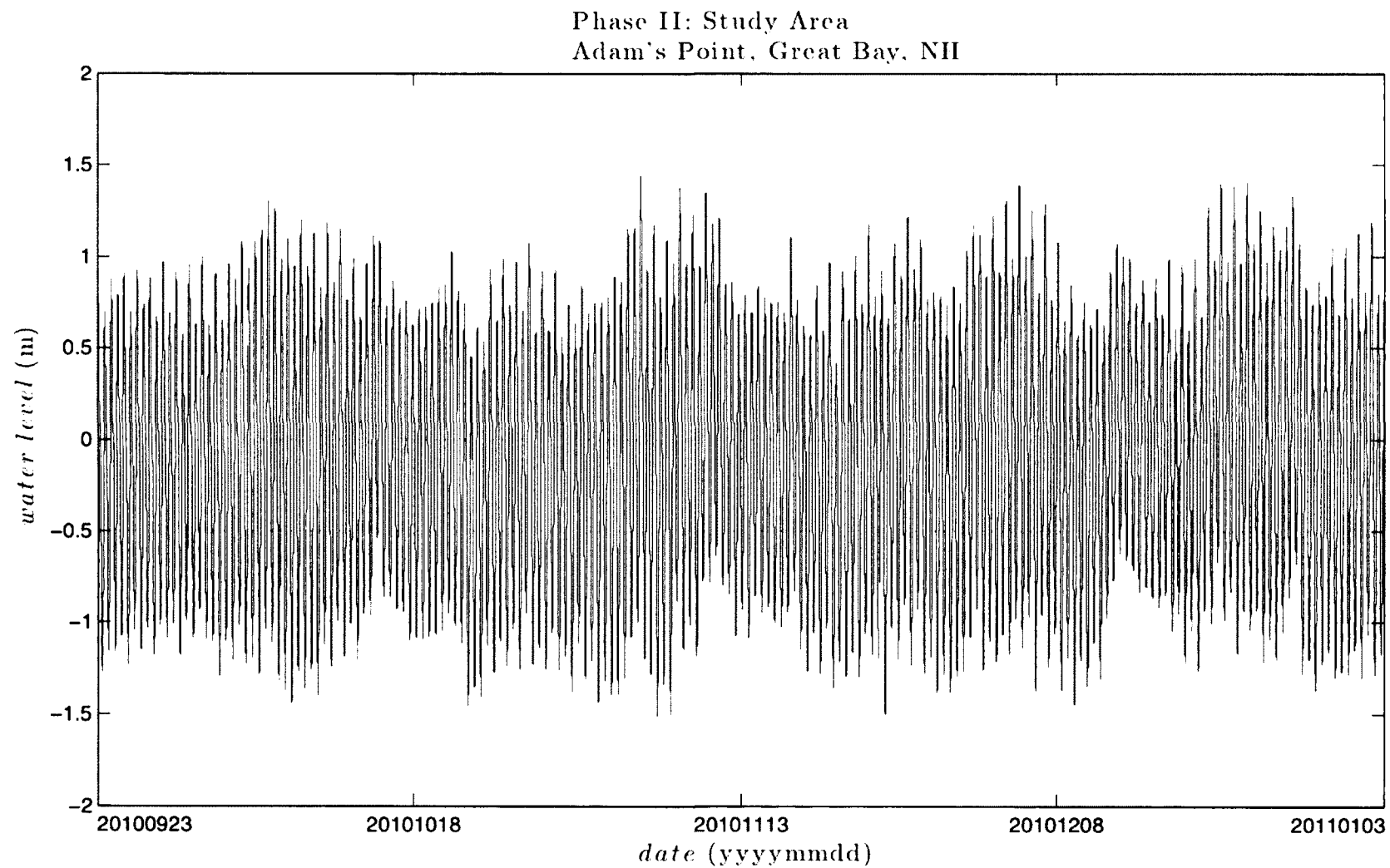
Figure 4.3.3: Computed water level at Adam's Point, Great Bay, NH using observations from the WaterLog Bubbler. N=24481. Note the non-linear affect on the tides compared to those of Phase 1 (Fig. 3.4.1-4); the Nor'easter event of 20101226 is apparent in the water level record.

Phase II: Study Area
Squamscott River, Great Bay, NH
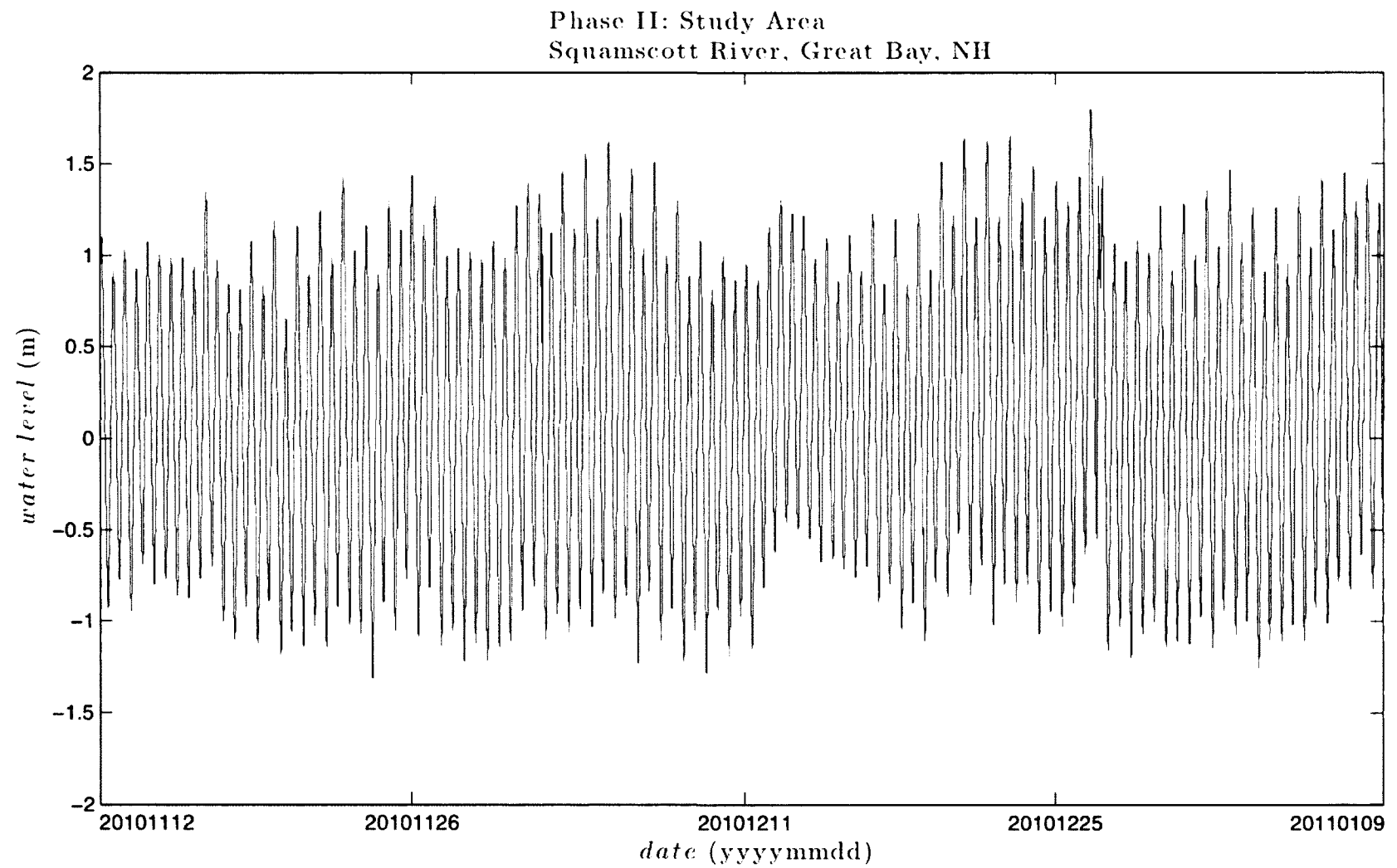
Figure 4.3.4: Computed water level at Squamscott River, Great Bay, NH using observations from the WaterLog MWWL. N=13854. Note the non-linear affect on the tides compared to those of Phase I (Fig. 3.4.1-4); the Nor'easter event of 20101226 is apparent in the water level record.

Phase II: Study Area
Shankhassic, Great Bay, NH
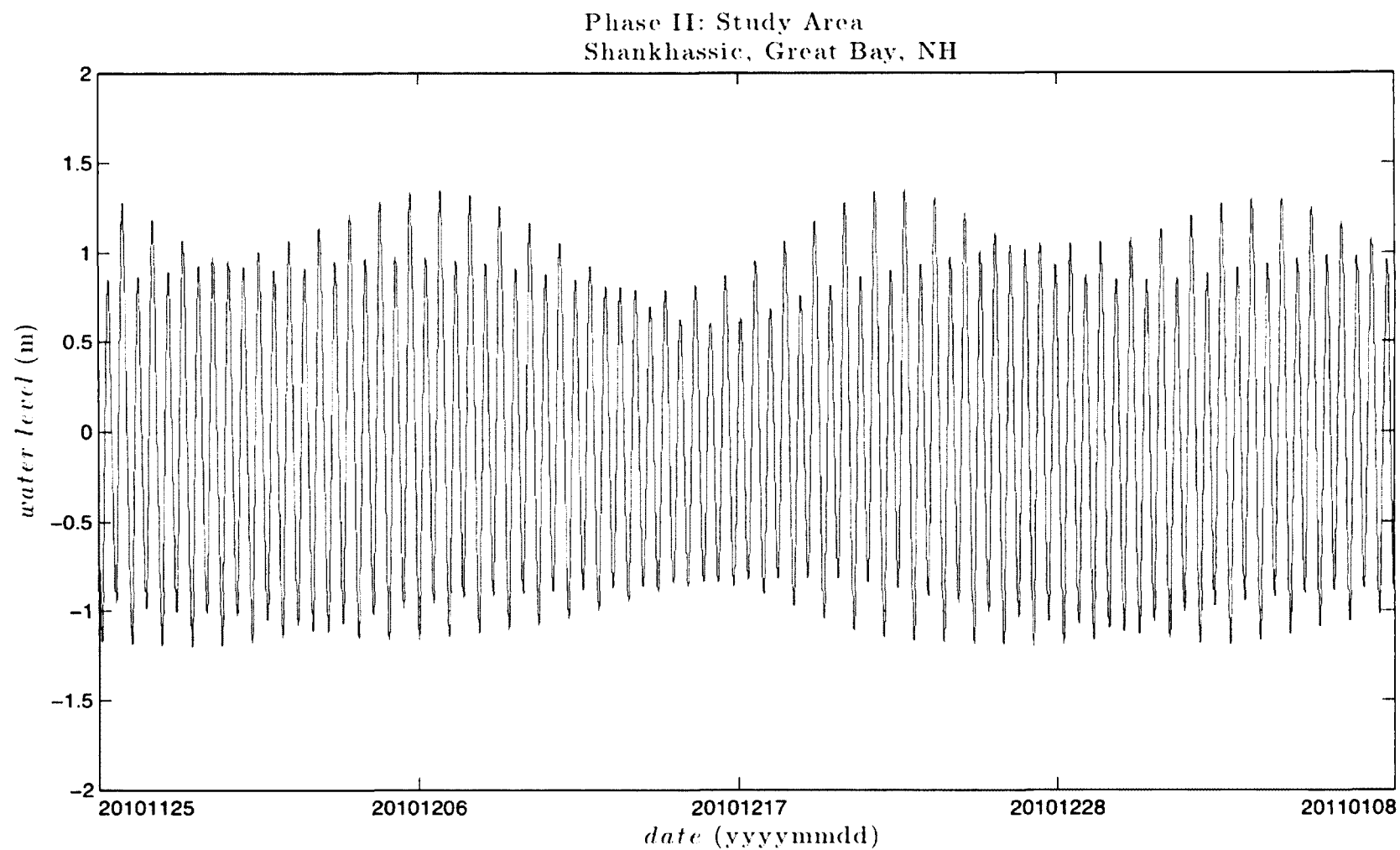
Figure 4.3.5: t_tide generated water level at Shankhassic, Great Bay, NH using computed water level observations from the Onset HOBOlogger. N=10706. Note the non-linear affect on the tides compared to those of Phase 1 (Fig. 3.4.5-8); no aberrations are apparent in the tide signal compared to Figure 4.3.1.

Phase II: Study Area
Winnicut River, Great Bay, NH
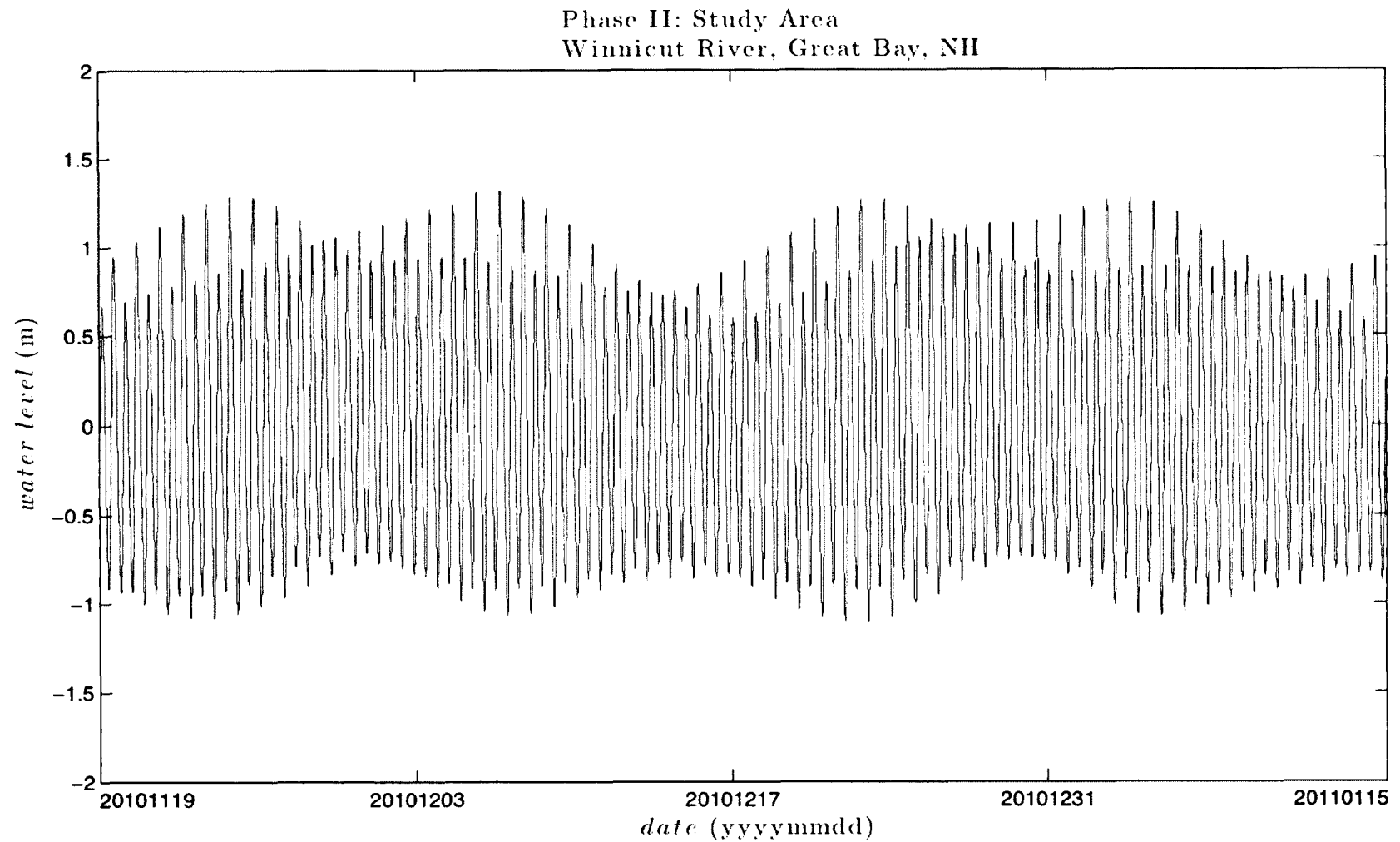
Figure 4.3.6: t_tide generated water level at Winnicut River, Great Bay, NH using computed water level observations from the SeaBird SeaCAT. N=13681. Note the non-linear affect on the tides compared to those of Phase 1 (Fig. 3.4.5-8); no aberrations are apparent in the tide signal compared to Figure 4.3.2.

Phase II: Study Area
Adam's Point, Great Bay, NH
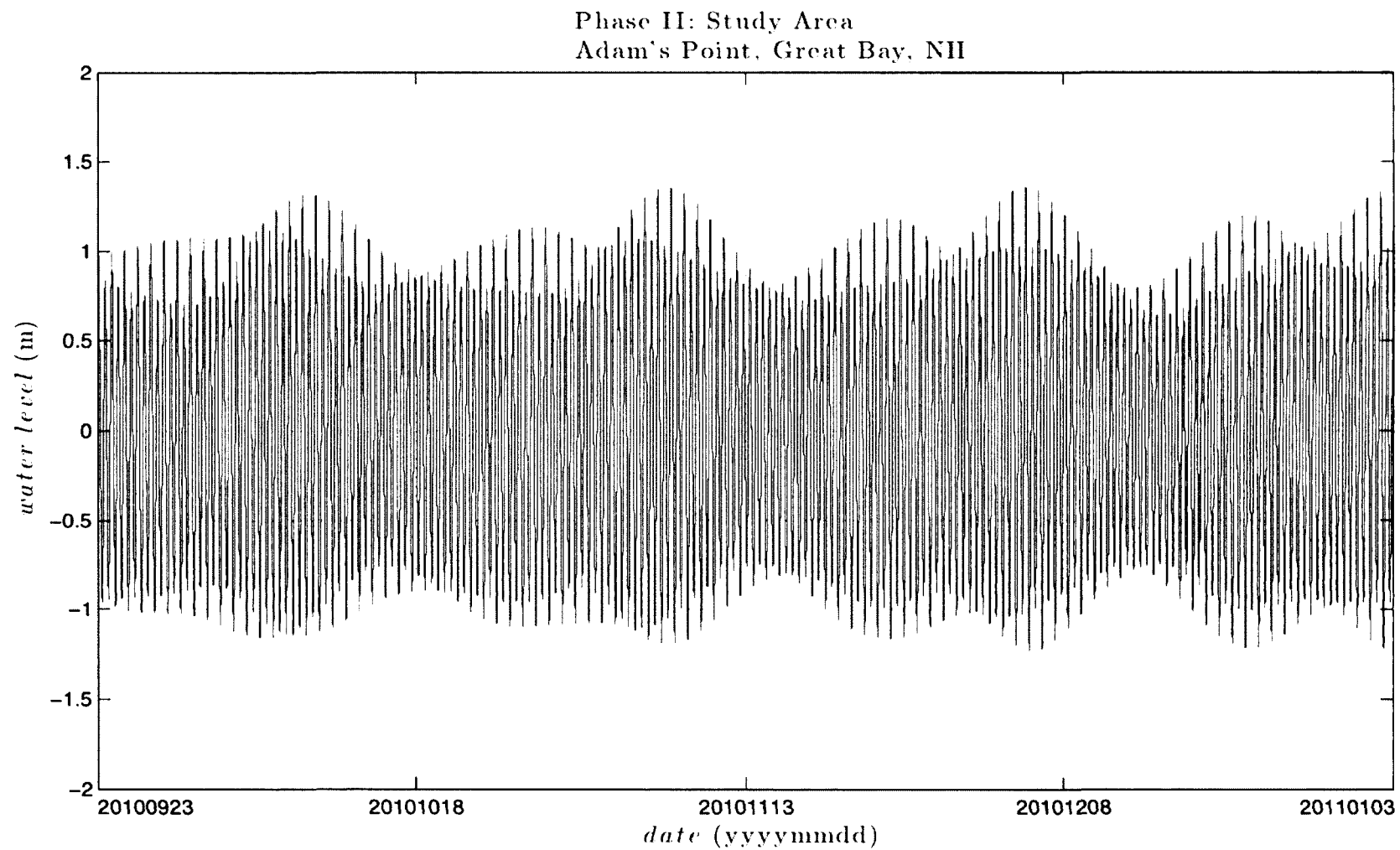
Figure 4.3.7: t_tide generated water level at Adam's Point, Great Bay, NH using computed water level observations from the WaterLog Bubbler. N=24481. Note the non-linear affect on the tides compared to those of Phase 1 (Fig. 3.4.5-8); no aberrations are apparent in the tide signal compared to Figure 4.3.3.
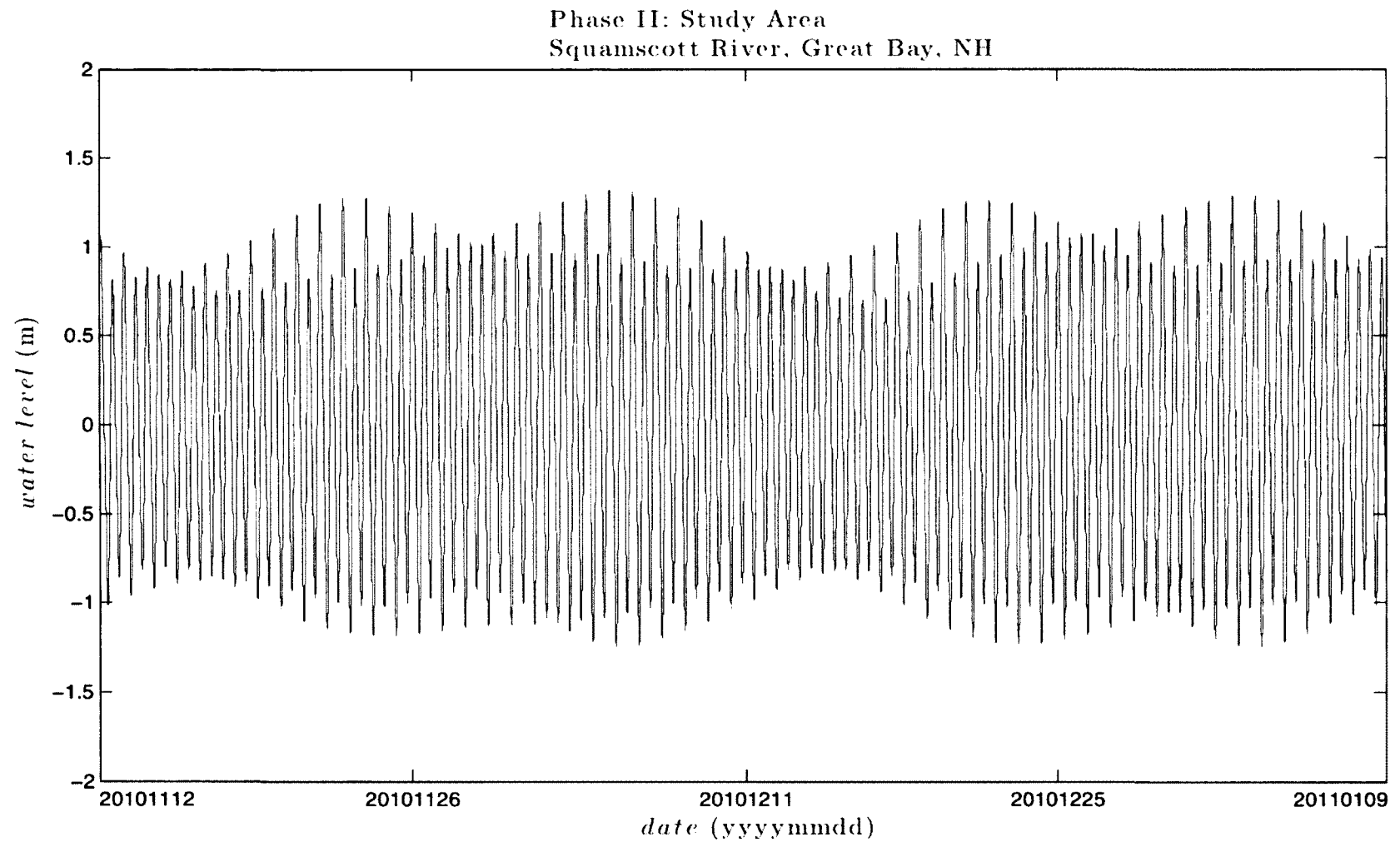
Phase II: Study Area
Squamscott River, Great Bay, NH

Figure 4.3.8. t_tide generated water level at Squamscott River, Great Bay, NH using computed water level observations from the WaterLog MWWL. N=13854. Note the non-linear affect on the tides compared to those of Phase 1 (Fig. 3.4.5-8); no aberrations are apparent in the tide signal compared to Figure 4.3.4.

Phase II: Study Area
Shankhassic, Great Bay, NH
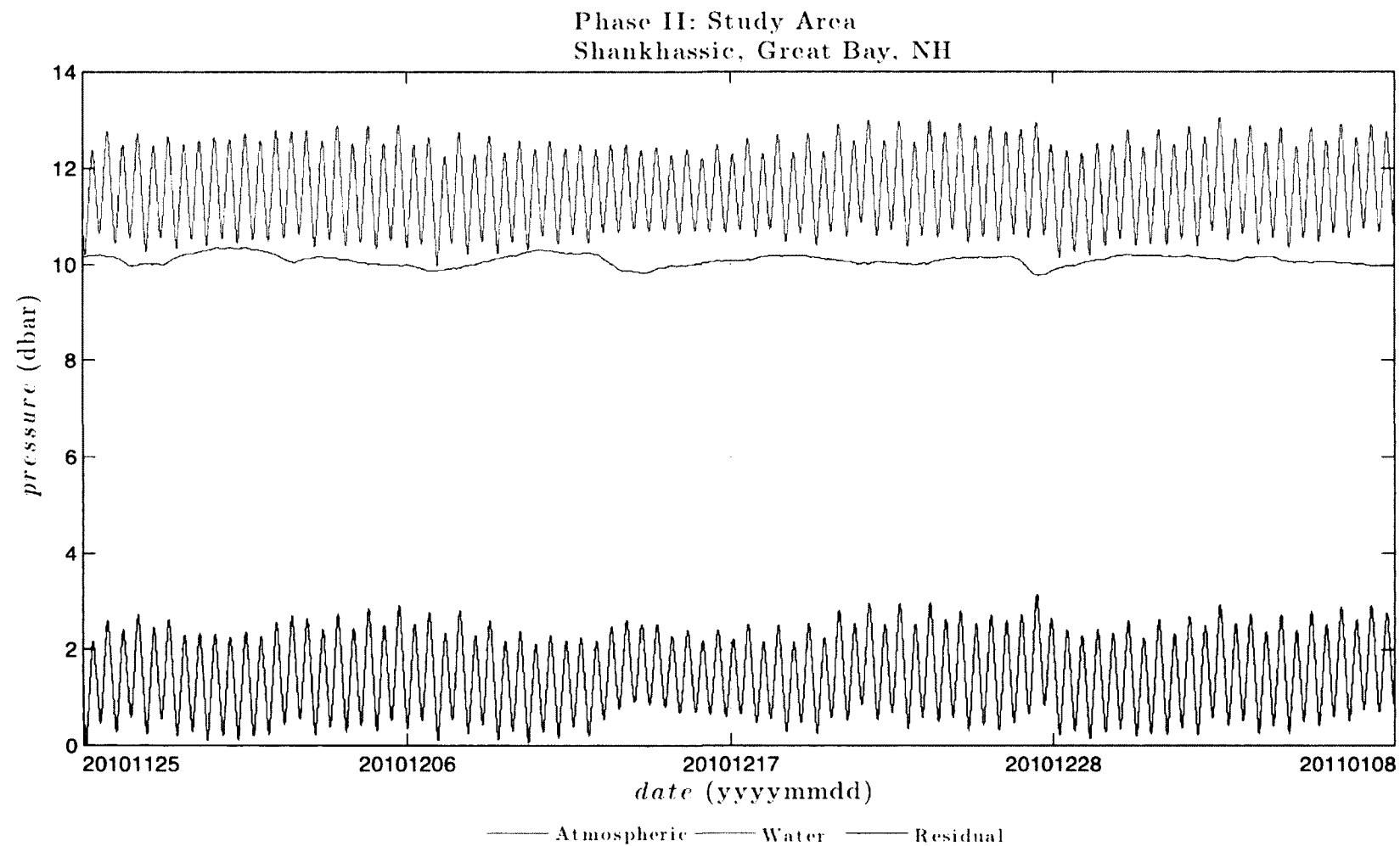
Figure 4.3.9: Observed atmospheric v. water pressure and computed residual at Shankhassic, Great Bay, NH using observations from the Onset HOBOlogger. N=10706. Focus is on atmospheric pressure affect on water level. The Nor'easter event of 20101226 is apparent in each pressure record; no other aberrations are apparent in the residual (differential) pressure in comparison to the water pressure.

Phase II: Study Area
Winnicut River, Great Bay, NH

Atmospheric ——— Water ——— Residual
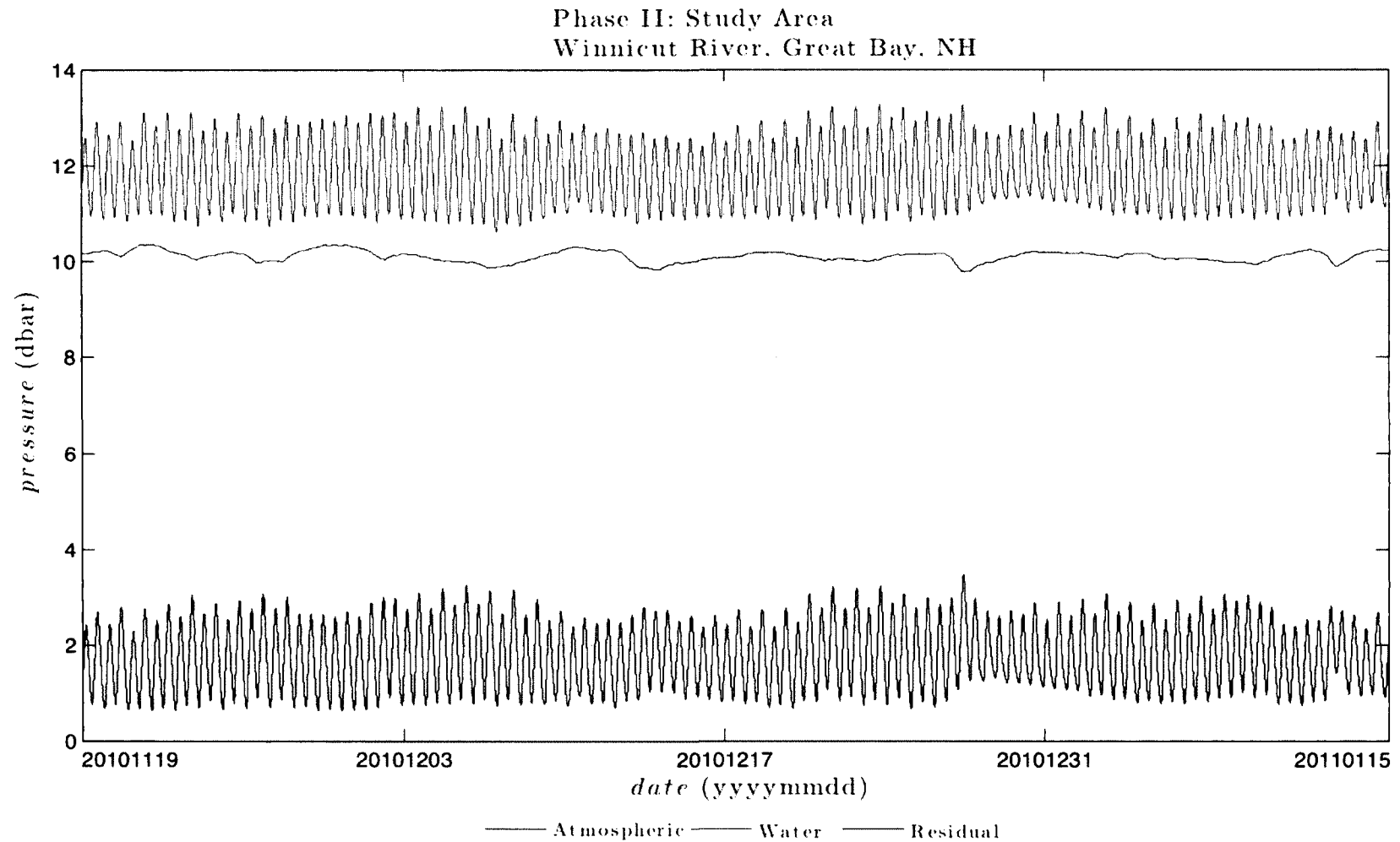
Figure 4.3.10: Observed atmospheric v. water pressure and computed residual at Winnicut River, Great Bay, NH using observations from the SeaBird SeaCAT. N=13681. Focus is on atmospheric pressure affect on water level. The Nor'easter event of 20101226 is apparent in each pressure record; no other aberrations are apparent in the residual (differential) pressure in comparison to the water pressure.

Phase II: Study Area
Adam's Point, Great Bay, NH
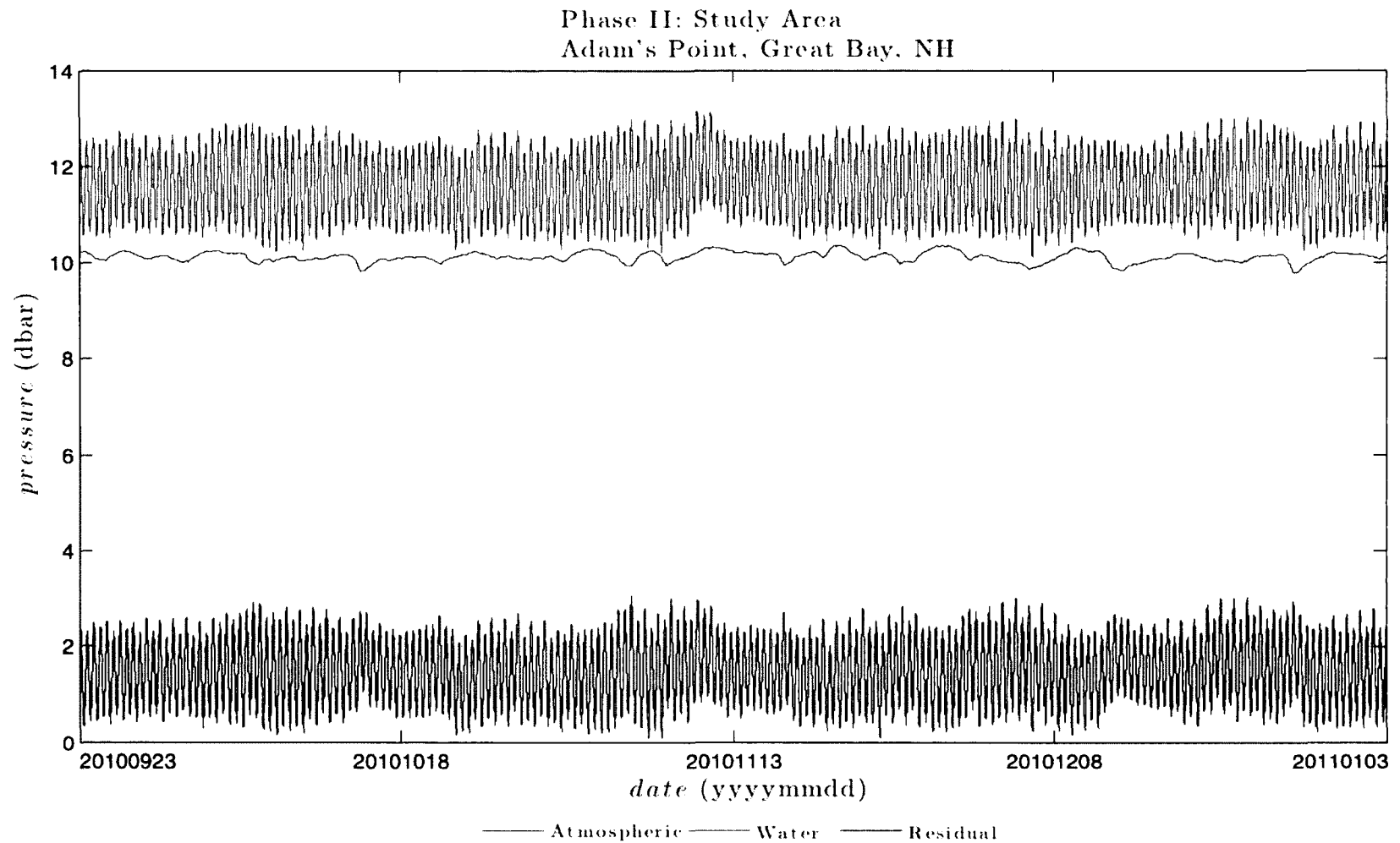
Figure 4.3.11: Observed atmospheric v. water pressure and computed residual at Adam's Point, Great Bay, NH using observations from the WaterLog Bubbler. N=24481. Focus is on atmospheric pressure affect on water level. The Nor'easter event of 20101226 is apparent in each pressure record; no other aberrations are apparent in the water pressure in comparison to the residual (differential) pressure.

94

Names	Frequency (cpd)	Shankhassic, Great Bay, NH Water Level		NCDC Atmospheric Pressure	
		Amplitude (m)	Phase (°)	Amplitude (m)	Phase (°)
ALP1	0.825517676	0.0096	211.39	0.0049	13.83
2Q1	0.856952412	0.0144	350.94	0.0026	86.66
Q1	0.893244060	0.0099	208.10	0.0025	298.17
O1	0.929535707	0.0943	230.33	0.0024	14.69
NO1	0.966446262	0.0147	288.58	0.0024	114.12
K1	1.002737909	0.1426	242.04		
J1	1.039029557	0.0080	154.11	0.0017	34.57
OO1	1.075940112	0.0087	143.68	0.0022	321.97
EPS2	1.828255585	0.0138	233.87	0.0004	359.08
MU2	1.864547232	0.0383	279.41	0.0008	324.45
N2	1.895981969	0.1470	145.56		
M2	1.932273616	0.9353	168.50	0.0010	43.58
L2	1.968565263	0.0768	183.75	0.0010	101.90
S2	2.000000000	0.0907	218.12	0.0052	40.24
ETA2	2.041767466	0.0070	259.93		
MO3	2.861809323	0.0182	271.11	0.0004	274.13
M3	2.898410424	0.0080	202.69	0.0004	312.24
MK3	2.935011525	0.0144	287.63	0.0003	331.80
SK3	3.002737909	0.0023	307.97	0.0022	316.38
MN4	3.828255585	0.0051	184.81	0.0003	264.02
M4	3.864547232	0.0167	236.86	0.0003	357.75
SN4	3.895981969	0.0025	272.15	0.0004	16.57
MS4	3.932273616	0.0051	282.94	0.0003	258.25
S4	4.000000000			0.0011	161.88
2MK5	4.867285141	0.0125	214.47	0.0003	217.73
2SK5	5.002737909			0.0004	100.35
2MN6	5.760529201	0.0204	113.98		
M6	5.796820848	0.0404	146.06	0.0002	170.47
2MS6	5.864547232	0.0116	202.68		
3MK7	6.799558758	0.0053	272.43	0.0001	221.57
M8	7.729094464	0.0043	177.12	0.0001	32.11

Table 4.3.1: t_tide resolved tidal harmonic constituents with a signal-to-noise ratio (SNR) greater than 2.0 in reference to Shankhassic, Great Bay, NH.

Names	Frequency (cpd)	Winnicut River, Great Bay, NH Water Level		NCDC Atmospheric Pressure	
		Amplitude (m)	Phase (°)	Amplitude (m)	Phase (°)
Q1	0.893244060	0.0108	211.84	0.0029	292.26
O1	0.929535707	0.0858	234.93		
NO1	0.966446262	0.0087	255.52		
K1	1.002737909	0.1373	250.88	0.0027	126.21
J1	1.039029557	0.0133	133.50		
OO1	1.075940112	0.0060	157.02		
UPS1	1.112231759	0.0077	186.11		
MU2	1.864547232	0.0256	275.75		
N2	1.895981969	0.1366	160.28		
M2	1.932273616	0.8836	171.58	0.0006	62.14
L2	1.968565263	0.1084	186.68	0.0006	144.11
S2	2.000000000	0.1064	218.09	0.0051	34.77
ETA2	2.041767466			0.0004	25.12
MO3	2.861809323	0.0213	293.90		
M3	2.898410424	0.0138	221.78	0.0002	239.12
MK3	2.935011525	0.0285	334.62		
SK3	3.002737909			0.0025	307.90
MN4	3.828255585	0.0360	267.87	0.0003	245.34
M4	3.864547232	0.0664	292.92		
SN4	3.895981969	0.0163	209.15		
MS4	3.932273616	0.0103	302.76	0.0004	292.82
S4	4.000000000			0.0011	167.51
2MK5	4.867285141			0.0004	181.89
2MN6	5.760529201	0.0036	197.56		
M6	5.796820848	0.0209	166.10		
2MS6	5.864547232	0.0074	259.37		
3MK7	6.799558758	0.0056	334.97	0.0001	279.17
M8	7.729094464	0.0092	266.38	0.0001	12.07

Table 4.3.2: t_tide resolved tidal harmonic constituents with a signal-to-noise ratio (SNR) greater than 2.0 in reference to Winnicut River, Great Bay, NH.

Names	Frequency (cpd)	Adam's Point, Great Bay, NH Water Level		NCDC Atmospheric Pressure	
		Amplitude (m)	Phase (°)	Amplitude (m)	Phase (°)
2Q1	0.856952412			0.0020	57.33
Q1	0.893244060	0.0102	201.39	0.0019	246.31
O1	0.929535707	0.0846	224.76		
NO1	0.966446262	0.0105	277.54		
K1	1.002737909	0.1182	236.79	0.0033	77.59
J1	1.039029557	0.0085	294.88		
UPS1	1.112231759	0.0056	141.68		
EPS2	1.828255585	0.0125	226.28	0.0007	355.77
MU2	1.864547232	0.0389	269.69		
N2	1.895981969	0.1714	131.58		
M2	1.932273616	0.9199	165.82	0.0006	68.00
L2	1.968565263	0.1007	196.92		
S2	2.000000000	0.1039	199.25	0.0049	50.74
ETA2	2.041767466			0.0004	18.01
MO3	2.861809323	0.0128	270.14		
M3	2.898410424	0.0058	188.46		
MK3	2.935011525	0.0117	278.67		
SK3	3.002737909	0.0020	339.72	0.0017	284.95
MN4	3.828255585	0.0045	202.74		
M4	3.864547232	0.0087	263.03		
SN4	3.895981969	0.0017	297.80	0.0001	49.95
MS4	3.932273616	0.0022	284.59	0.0002	270.61
S4	4.000000000	0.0011	212.99	0.0005	169.40
2MK5	4.867285141	0.0107	185.68	0.0002	137.63
2SK5	5.002737909			0.0002	85.99
2MN6	5.760529201	0.0204	97.60	0.0001	255.27
M6	5.796820848	0.0372	136.82	0.0001	76.08
2MS6	5.864547232	0.0127	164.21	0.0001	45.48
2SM6	5.932273616			0.0001	29.59
3MK7	6.799558758	0.0031	213.25	0.0001	236.87
M8	7.729094464	0.0021	130.87	0.0001	169.00

Table 4.3.3: t_tide resolved tidal harmonic constituents with a signal-to-noise ratio (SNR) greater than 2.0 in reference to Adam's Point, Great Bay, NH.

Names	Frequency (cpd)	Squamscott River, Great Bay, NH Water Level	
		Amplitude (m)	Phase (°)
2Q1	0.856952412	0.0079	51.01
Q1	0.893244060	0.0065	146.08
O1	0.929535707	0.0879	233.05
NO1	0.966446262	0.0152	276.54
K1	1.002737909	0.1407	246.63
EPS2	1.828255585	0.0159	222.04
MU2	1.864547232	0.0437	293.78
N2	1.895981969	0.1459	145.13
M2	1.932273616	0.9482	172.08
L2	1.968565263	0.0911	196.93
S2	2.000000000	0.0965	213.10
MO3	2.861809323	0.0190	272.37
M3	2.898410424	0.0110	218.07
MK3	2.935011525	0.0241	307.45
SK3	3.002737909	0.0026	71.02
MN4	3.828255585	0.0108	218.46
M4	3.864547232	0.0369	253.88
SN4	3.895981969	0.0065	258.64
MS4	3.932273616	0.0114	285.44
S4	4.000000000	0.0038	35.25
2MK5	4.867285141	0.0088	250.35
2SK5	5.002737909	0.0024	327.68
2MN6	5.760529201	0.0198	126.50
M6	5.796820848	0.0485	162.78
2MS6	5.864547232	0.0118	215.36
3MK7	6.799558758	0.0060	299.94
M8	7.729094464	0.0066	206.31

Table 4.3.4: t_tide resolved tidal harmonic constituents with a signal-to-noise ratio (SNR) greater than 2.0 in reference to Squamscott River, Great Bay, NH.

Phase II: Study Area
Shankhassic, Great Bay, NH
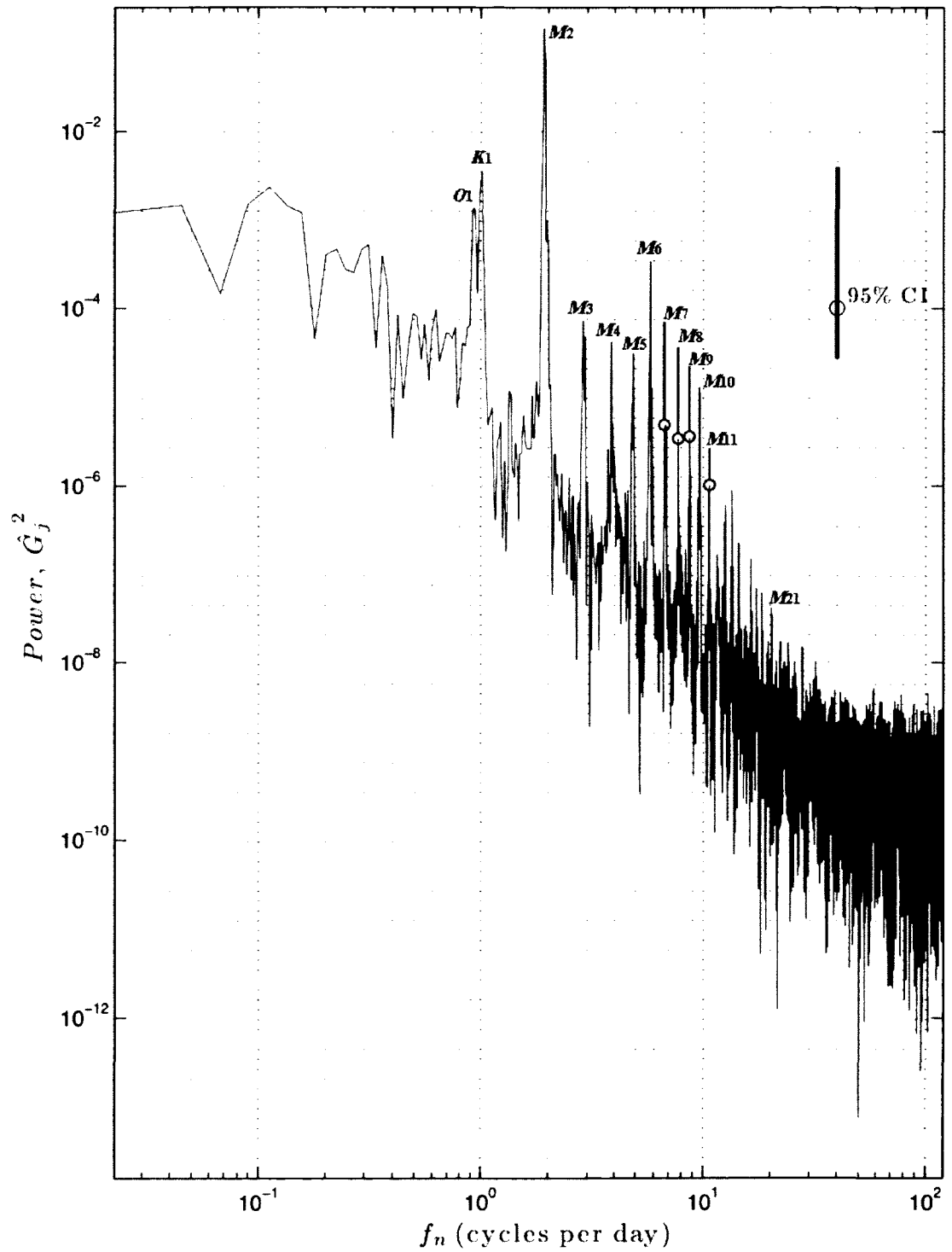
Figure 4.3.12: Water level power spectrum at Shankhassic, Great Bay, NH using observations from the Onset HOBOlogger. Hanning window, $N=10705$. Observable n-th order harmonics of the primary lunar tide, M, and the diurnal constituents, O_1 and K_1, are labeled.

Phase II: Study Area
Winnicut River, Great Bay, NH
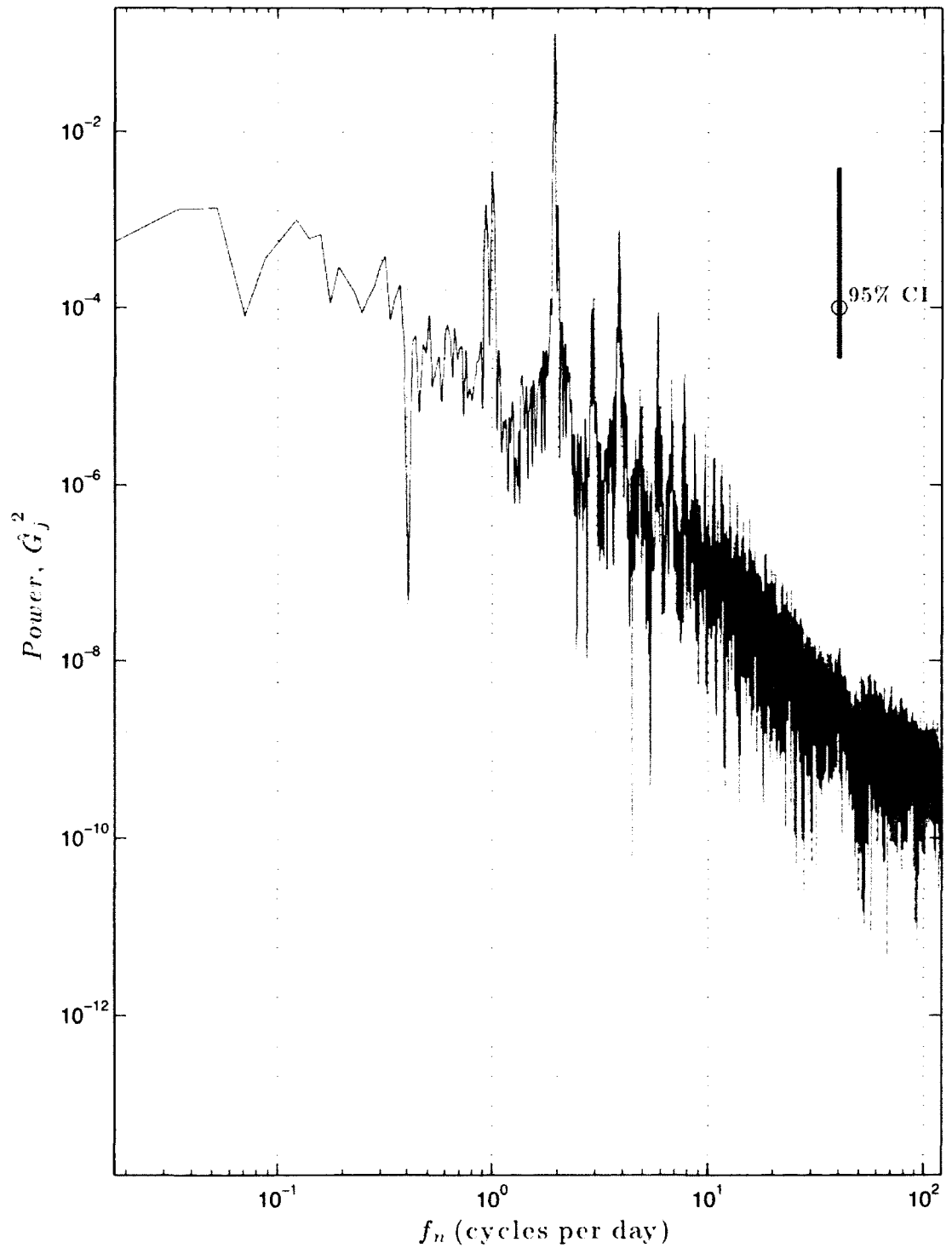
Figure 4.3.13: Water level power spectrum at Winnicut River, Great Bay, NH using observations from the SeaBird SeaCAT. Hanning window, N=13681. See Figure 4.3.12 for labels of the observable n-th order harmonics of the primary lunar tide, M.

Phase II: Calibration
Adam's Point, Great Bay, NH
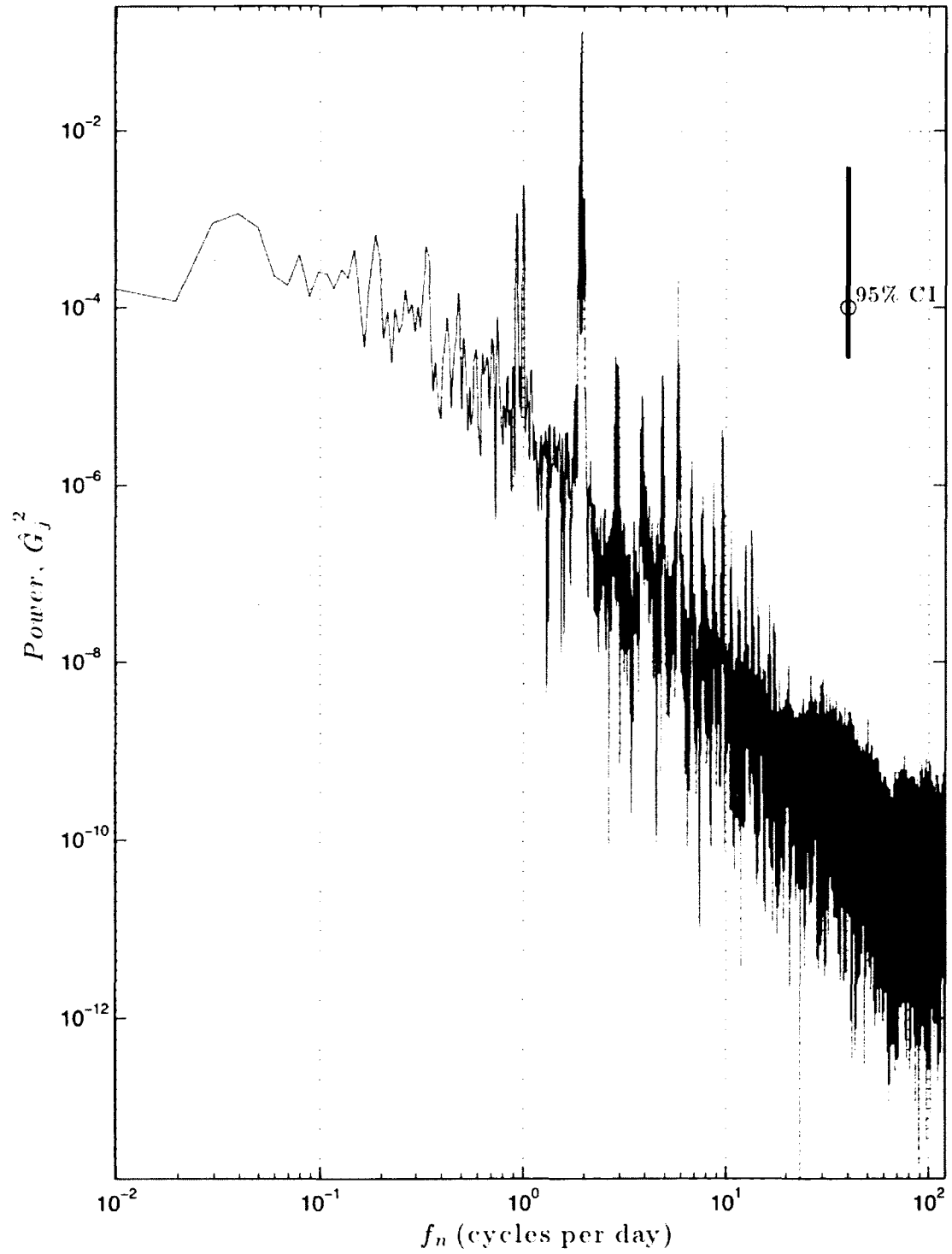
Figure 4.3.14: Water level power spectrum at Adam's Point, Great Bay, NH using observations from the WaterLog Bubbler. Hanning window, N=24481. See Figure 4.3.12 for labels of the observable n-th order harmonics of the primary lunar tide, M.

Phase II: Study Area
Squamscott River, Great Bay, NH
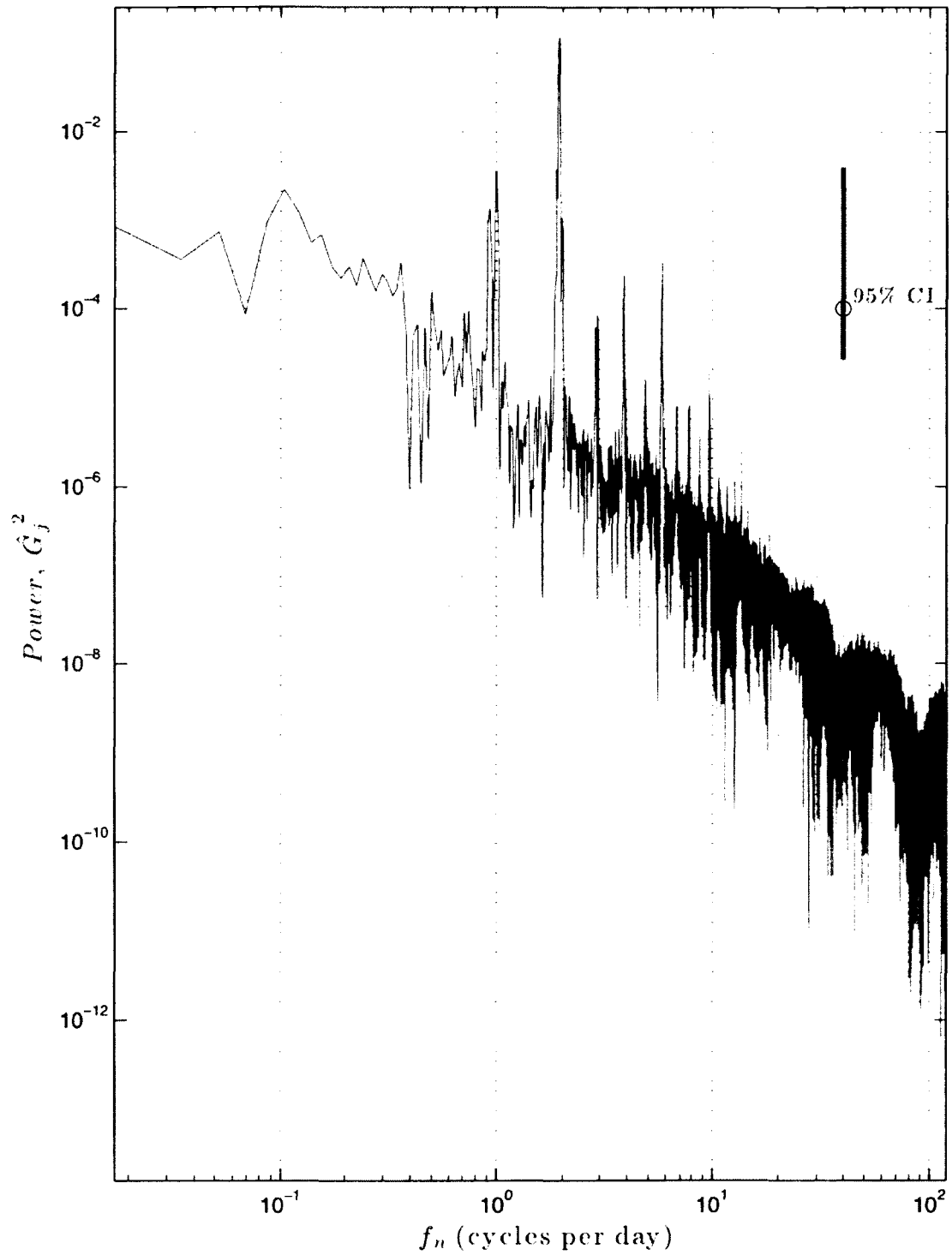
Figure 4.3.15: Water level power spectrum at Squamscott River, Great Bay, NH using observations from the WaterLog MWWL. Hanning window, N=13853. See Figure 4.3.12 for labels of the observable n-th order harmonics of the primary lunar tide, M.
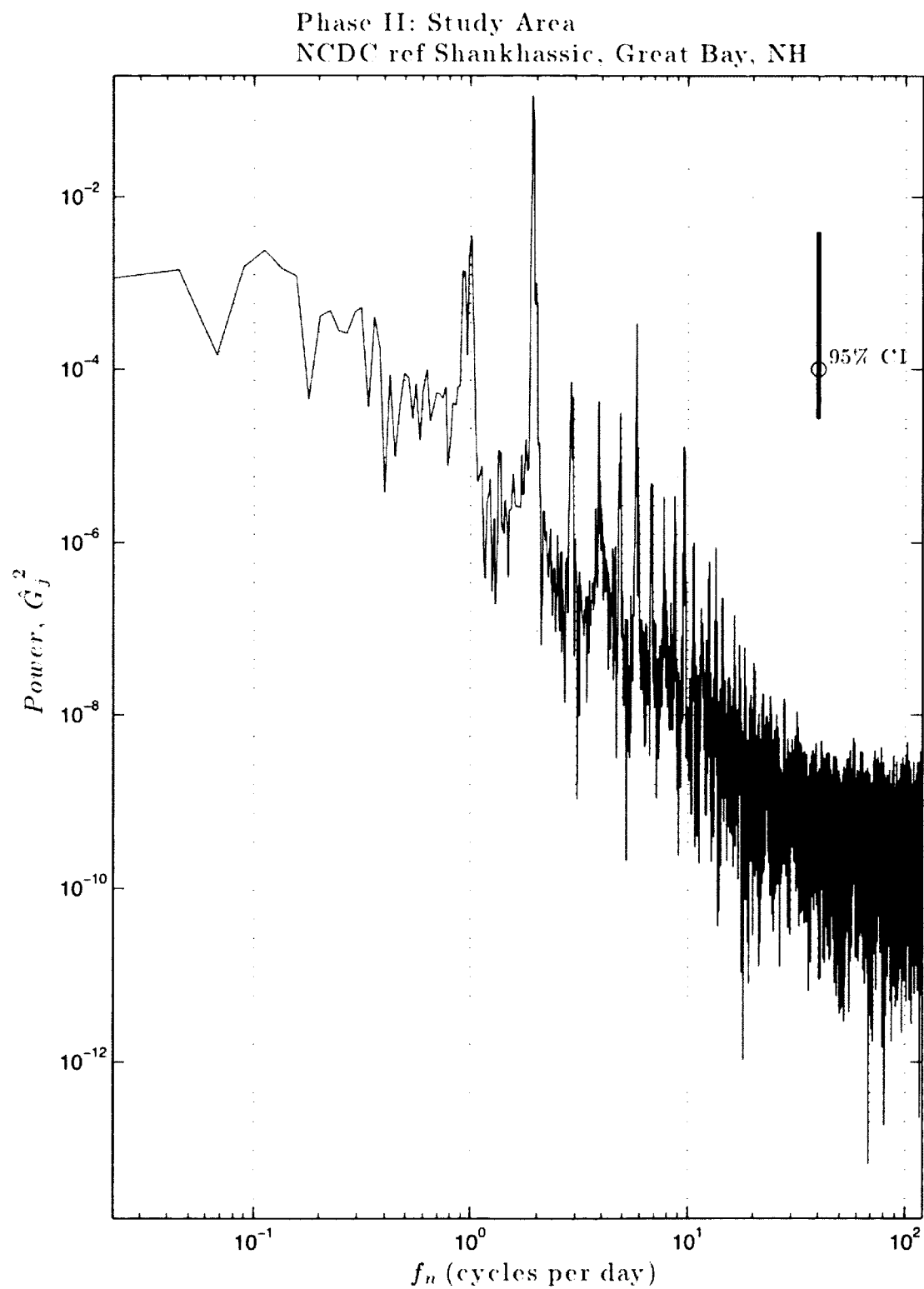
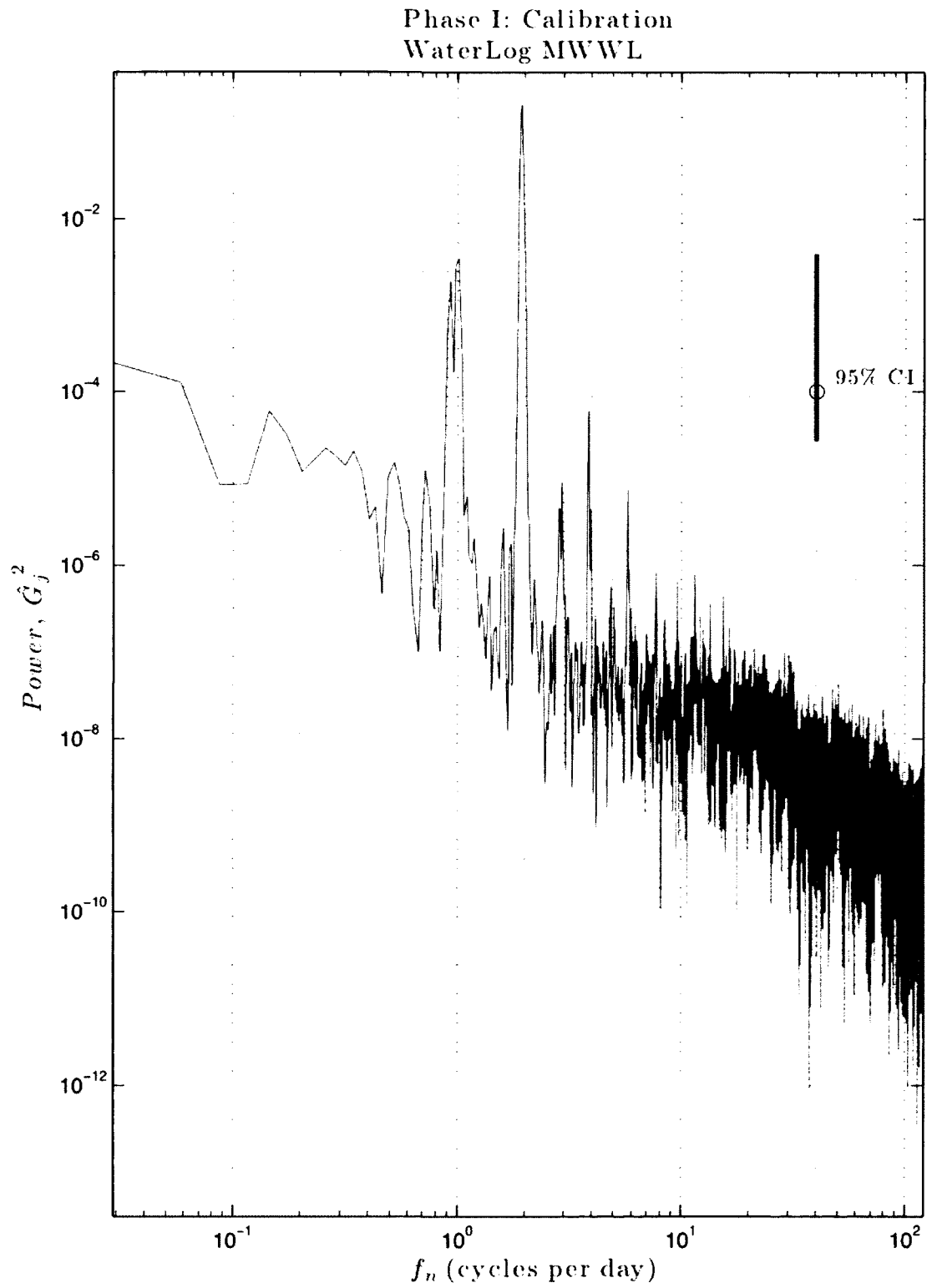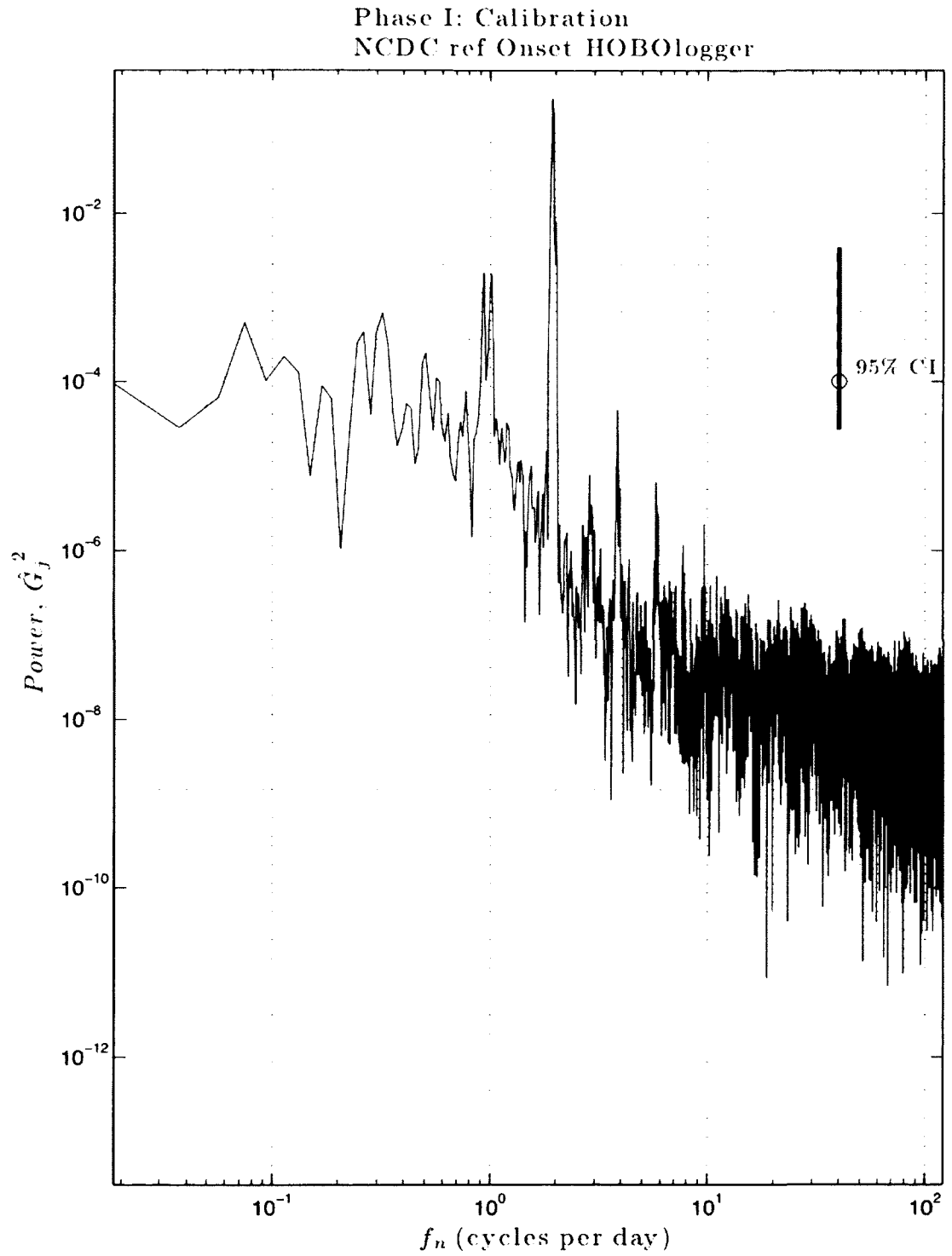Figure 4.3.16: Atmospheric pressure power spectrum at Shankhassic, Great Bay, NH. Hanning window, N=10705. See Figure 4.3.12 for labels of the observable n-th order harmonics of the primary lunar tide, M.

Phase II: Study Area
NCDC ref Winnicut River, Great Bay, NH
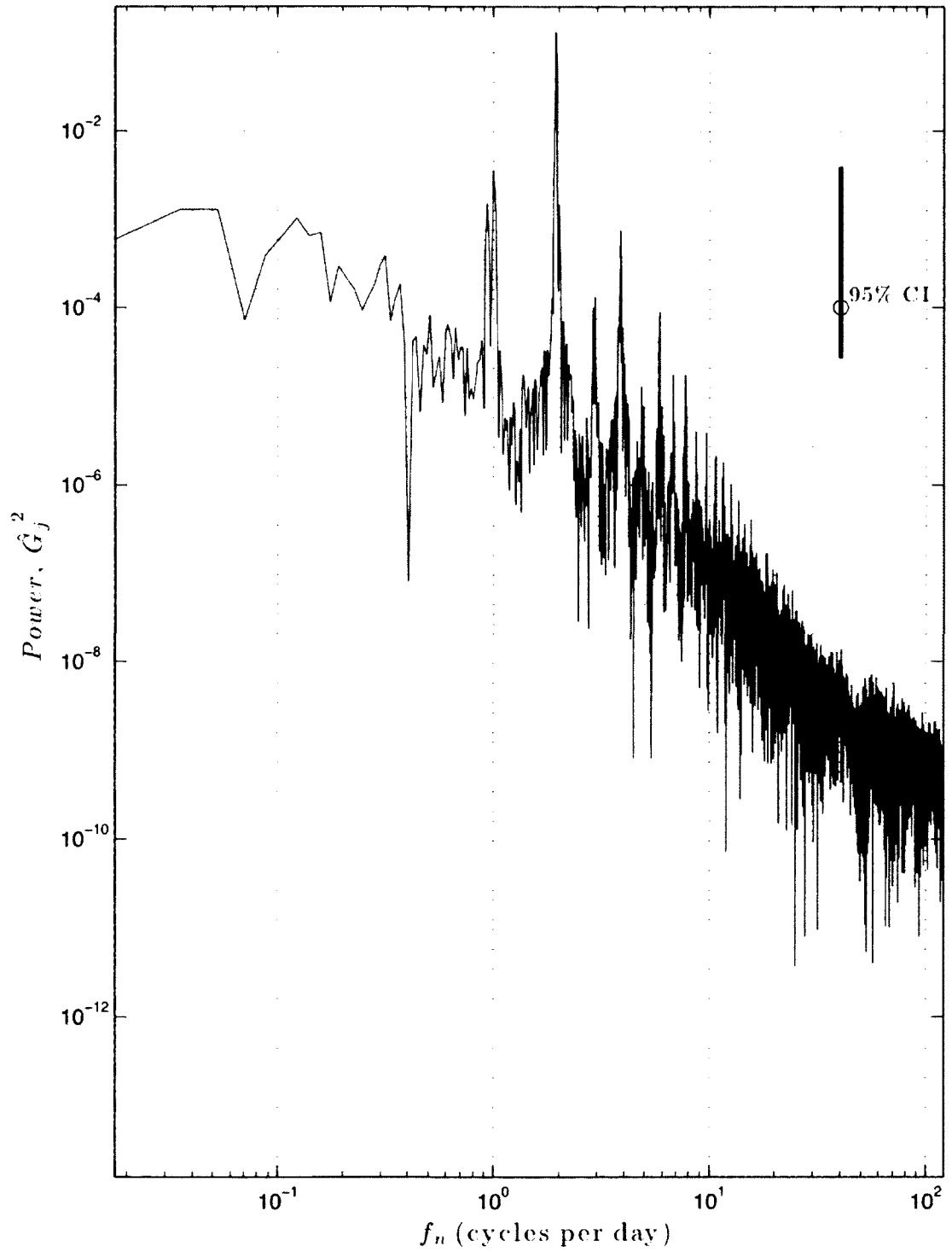
Figure 4.3.17: Atmospheric pressure power spectrum at Winnicut River, Great Bay, NH. Hanning window, N=13681. See Figure 4.3.12 for labels of the observable n-th order harmonics of the primary lunar tide, M.

Phase II: Study Area
NCDC ref Adam's Point, Great Bay, NH
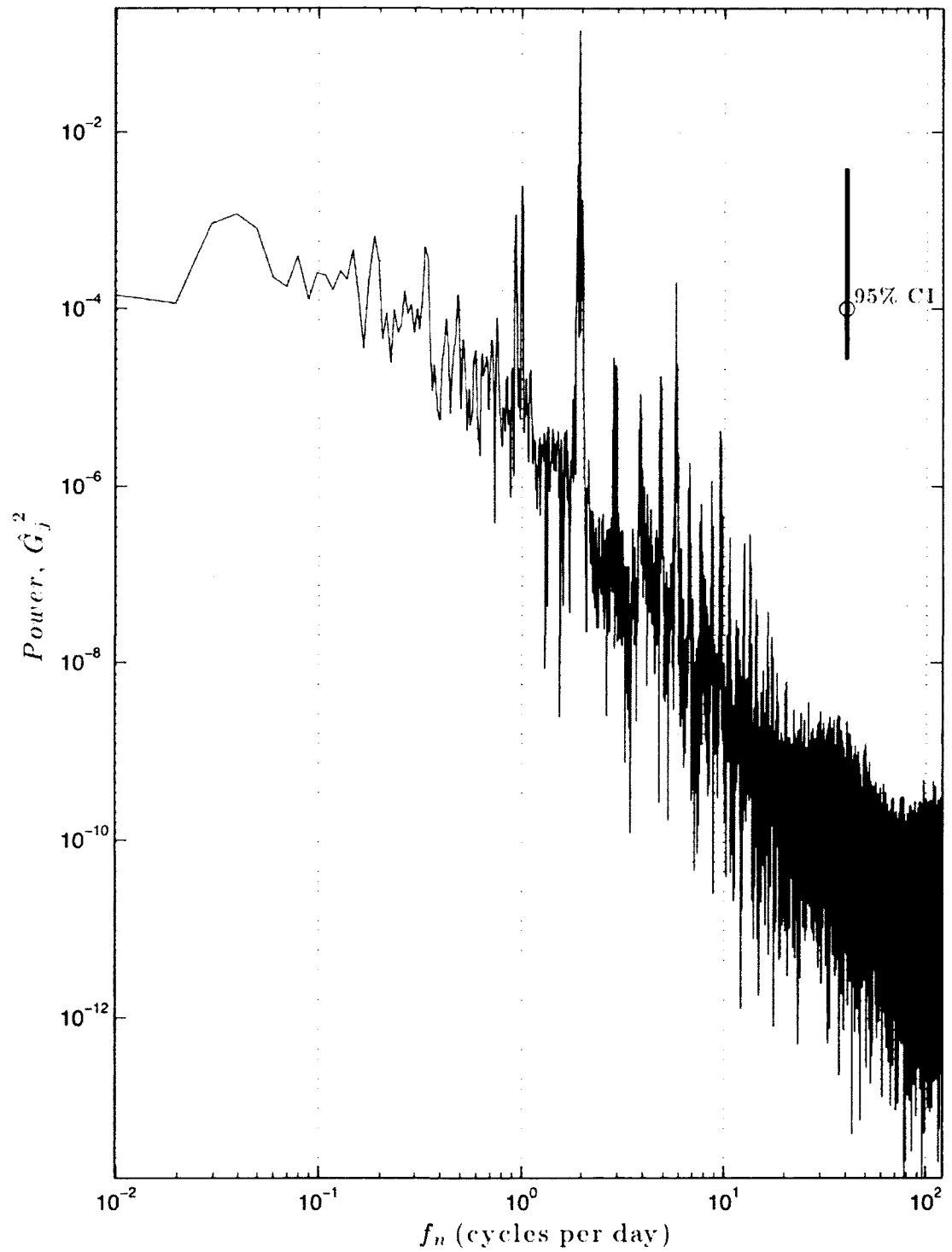
Figure 4.3.18: Atmospheric pressure power spectrum at Adam's Point, Great Bay, NH. Hanning window, N=24481 See Figure 4.3.12 for labels of the observable n-th order harmonics of the primary lunar tide, M.

105

V. PHASE 3: MODEL IMPLEMENTATION

With reasonable water level time series and the harmonic constituents resolved at each study location in the Great Bay, the development of a tidal prediction model could commence. The Tidal Constituents and Residual Interpolation (TCARI) modeling method was chosen to generate the prediction model for the project. Primary references for TCARI— both theoretical and implemented— include Hess *et. al.* (2004) as well as personal communications with Barry Gallagher of the NOAA Hydrographic Systems Technology Program (HSTP) (See Appendix G: Personal Communiqués).

The TCARI method is a numerical model that uses a mesh generator to generate a non-uniform, triangular grid over an area. Solving for Laplace's tidal equations over the mesh grid, weighting functions are computed using a finite element solver. These weighting functions are then used to spatially interpolate harmonic constituents, water level residuals, and datum offsets from multiple tide stations across the model area. The result is a continuous tidal solution surface. (Cisternelli *et. al.*, 2008)

5.1 Methods. Prior to creating a tide prediction model, further data processing and analysis was needed. The first objective was to determine the tidal datums at each subordinate location (or station) in the study area. Toward that end, the *tide-by-tide* (TBYT), *modified range ratio method for semidiurnal tides* was used (CO-OPS, 2003). The first step in this method is to obtain a verified high-low water level data series from, preferably, a nearby primary control gauge. This verified high-low water level data

106

series forms the basis for the computation of tidal datums, tidal ranges and lunitidal intervals for each of the subordinate stations.

The next step in the TBYT, modified range ratio method is, for each subordinate station water level record, to determine the times and amplitudes of higher-high (HH), high (H), low (L) and lower-low (LL) tide for each daily tidal cycle. For the TBYT comparison to work properly, the order of high-low designations must be identical between the control and subordinate high-low water level data. For this reason, any deviation in the subordinate water level designations is overridden by the verified high-low water level information from the primary control gauge.

The last step in the TBYT comparison is the calculation of the tidal datums, tidal ranges, and lunitidal intervals at each subordinate station. Tidal datums computed in the TBYT, modified range ratio for semidiurnal tides comparison include the *mean higher-high water* (MHHW), *mean high water* (MHW), *mean tide level* (MTL), *diurnal tide level* (DTL), *mean sea level* (MSL), mean low water (MLW), and *mean lower-low water* (MLLW). Tidal ranges computed include the *great tropic range* (Gt), the mean range (Mn), and both the *mean diurnal high water* (DHQ) and *low water* (DLQ) *inequality* differences. Lastly, the Greenwich mean high water lunitidal interval (HWI) and the Greenwich mean low water lunitidal interval (LWI) are computed. As the water level time series at each subordinate station is less than a full 19-year *Metonic cycle*, the computed tidal datums, tidal ranges and lunitidal intervals are termed "the equivalent 19-year values." (CO-OPS, 2003)

107

The TCARI method of model generation is divided into two components: 1. grid generation, including weighting function calculations; and 2. tide model solution. (Hess *et. al.*, 2004) The requirements of grid generation, in reference to the area to be gridded, are:

    i. a boundary *shapefile* representing the *shoreline*;

    ii. the selection of at least two tide stations that will act as model control locations;

    iii. the latitude, longitude, and ellipsoidal elevations of the tidal stations;

    iv. the tidal datums for each tide station; and

    v. the resolved tidal constituents for each tide station.

The tide model solution requirements are:

    i. the TCARI *.tc grid file from the previous step; and

    ii. water level time series referenced to MLLW for each model control station.

<u>5.2 Data Processing</u>. Recall that subsequent to each phase of data collection, the computation of water level, tidal constituents, datums, and other statistics are necessary. See Appendix D: Data Processing for more detailed information on general data processing techniques and algorithms.

Forming the basis for the TBYT, modified range ratio method is the verified high-low water level data from the NOAA primary tide station at Portland, ME. There are two reasons for using the verified data from Portland, ME as opposed to Fort Point, NH. The first reason is that, at the time of data collection, the gauge at Portland, ME was a primary control gauge whereas the gauge at Fort Point, NH was a secondary gauge. The second,

and more important, reason is that, for the period of data collection in Phase 2, the verified high-low water level data record at Fort Point, NH has gaps. These gaps would make a tide-by-tide comparison difficult, if not impossible. The tidal datums, tidal ranges, and lunitidal intervals were likewise obtained from the station at Portland, ME. For comparisons sake, the verified high-low water level data and the tidal datums were referenced to NAVD88.

The next step was to reanalyze the orthometric-referenced water level time series for each study location (or subordinate station) in Phase 2 using t_tide. The date and time of higher-high (HH), high (H), low (L), and lower-low (LL) tide for each daily tidal cycle was then determined using the t_tide generated water level time series. From this date and time information, the HH, H, L and LL water levels were then obtained from the computed water level time series. Deviations between the subordinate station water level designations were then overridden by the verified high-low water level information from the primary gauge at Portland, ME as per the requirements of the TBYT method. (CO-OPS, 2003)

With the verified high-low water level data and associated tidal datums, tidal ranges and lunitidal intervals and subordinate high-low water level data processed for each tide station in Phase 2, the tide-by-tide modified range ratio for semidiurnal tides commenced. The results are presented in Table 5.2.1.

		Shankhassic, Great Bay,NH	Winnicut River, Great Bay,NH	Adam's Point, Great Bay,NH	Squamscott River, Great Bay,NH
Datum:	MHHW (m)	1.012	1.016	0.868	1.119
	MHW (m)	0.899	0.895	0.753	1.005
	MTL (m)	0.072	0.143	-0.083	0.134
	DTL (m)	0.047	0.096	-0.106	0.106
	MSL (m)	0.043	0.012	-0.112	0.071
	MLW (m)	-1.113	-0.987	-1.242	-1.080
	MLLW (m)	-1.176	-1.013	-1.311	-1.141
Range of Tide:	Gt (m)	2.300	2.066	2.212	2.304
	Mn (m)	2.083	1.889	2.012	2.094
	DHQ (m)	0.112	0.121	0.114	0.114
	DLQ (m)	0.063	0.026	0.070	0.062
Lunitidal Interval:	HWI (hrs)	5.85	5.87	5.79	5.90
	LWI (hrs)	12.15	12.55	12.03	12.34

Table 5.2.1: Computed equivalent 19-year tidal datums and ranges, and lunitidal intervals. Datums referenced to the North American Vertical Datum of 1988 (NAVD88); Lunitidal intervals referenced to Greenwich Mean Time (GMT).

For comparison sake to historic data, the mean range of tide (Mn) at Squamscott River—

6.9 feet (2.103 meters) for both the 1926 and 1953/4 USC&GS surveys— agrees well

with the value computed in this study 2.094 meters (6.87 feet). Comparing mean low

water (MLW) at the same location— -9.7 feet (-2.956 meters) below benchmark *B.M. 1*

(1926) for the 1953/4 USC&GS survey and -3.279 meters (-10.76 feet) computed in the

current study— shows a considerable difference in datum elevation. The difference in

vertical datums— NGVD29 for the 1953/4 USC&GS survey and NAVD88 for the

current study— must be taken into account. Using the NOAA NGS online tool

VERTCON, a datum transformation shift of -0.227 meters (-0.74 feet) is required when

converting NAVD88 elevations to NGVD29 elevations at the Squamscott River station.

Therefore, the MLW value computed in this study, when referenced to NGVD29 is

-3.052 meters (-10.01 feet). An additional factor which must be accounted for is regional

sealevel trending; sealevel for the Portland, ME station has trended up 0.60 feet (0.183

meters) per century. (CO-OPS, 2009) Extrapolating for the time difference between the

110

current study and the 1953/4 USC&GS survey, this upward sealevel trend could account for 0.34 feet (0.104 meters) difference. From these comparisons, the Mn values show equivalence between the current study and historic observation. However the MLW values show a 0.198 meter (0.65 foot) difference between the current study and historic observation. The difference may be due to the observable record length for the earlier record.

A historical comparison of both the high water (HWI) and low water (LWI) lunitidal intervals is also warranted. For the Squamscott River station, the mean high water lunitidal interval (HWI)— 6.37 hours GMT for the 1926 USC&GS survey and 5.90 hours GMT for the current study— shows a difference of nearly a half-hour in the time of high water, while the mean low water lunitidal interval (LWI)— 12.32 hours GMT for the 1926 USC&GS survey and 12.34 hours for the current study— shows an equivalent value. One explanation that may explain both the difference in the HWI and the apparent equivalence in the LWI is the six-day record of the 1926 USC&GS survey; a six-day record is simply not long enough to account for both a full neap-spring tidal cycle or the varying degrees of non-linearity in the estuary.

With the MLLW datum difference from NAVD88 calculated for each subordinate station, the previously orthometric-referenced water level time series for each were re-referenced to MLLW. While only necessary for the model control gauges, the reference process was completed for all subordinate stations.

111

The choice for model control stations took into account the model requirements, geographic extent, and long-term expectations. The TCARI model, as realized in software, requires that two control stations be designated and that one of the model control stations be a NOAA long-term tide gauge. The NOAA secondary tide gauge at Fort Point, NH and the WaterLog MWWL at Squamscott River were chosen for these reasons. For the study area tide stations, the latitude, longitude and elevations (both ellipsoidal and orthometric) for each tide gauge were previously measured in Phase 2 (Table 5.2.2). The latitude, longitude, elevations (ellipsoidal and orthometric) and tidal datums for the tide gauge at Fort Point, NH were obtained from the station information available from the CO-OPS Tides and Currents database.

Position	Shankhassic, Great Bay, NH	Winnicut River, Great Bay, NH	Adam's Point, Great Bay, NH	Squamscott River, Great Bay, NH
Latitude (N)	43.08246980	43.04957120	43.09212219	43.05264471
Longitude (W)	70.88430316	70.84480492	70.86468119	70.91224518
Ellipsoid Height (m)	-28.187	-28.477	-28.357	-24.628
Orthometric Height (m)	-1.409	-1.718	-1.601	2.199

Table 5.2.2: Measured latitude, longitude, ellipsoidal and orthometric height for Phase 2 stations. Latitude, longitude and ellipsoidal height referenced to the North American Datum of 1983 (NAD83) reference frame (CORS96/ Epoch: 2002). Orthometric height referenced to the North American Vertical Datum of 1988 (NAVD88) using Geoid09.

The final piece of the puzzle before TCARI grid generation could begin was providing a shapefile of the shoreline boundary. Shoreline, as defined by the NOAA and as per the requirements of TCARI as implemented, represents the boundary between the water and land at the MHW datum level. (Hicks *et. al.*, 2000) The boundary shapefile representing the shoreline was gathered from the NOAA NOS Shoreline Data Explorer and the NOS NGS Shoreline Data Rescue Project of Portsmouth, New Hampshire, NH2C01 (Fig. 5.2.1). (NGS, 2009) The boundary file was modified to limit the seaward and landward

extent of the estuary. In order to better represent the apparent width of the Squamscott River at the Boston and Maine railroad trestle, the channel was widened in the boundary file. Due to the presence of large mudflats in the Great Bay, the use of another shoreline based upon a different datum level (*e.g.* MLW, MTL, etc.) would have an unknown effect on the model. This aspect is not explored further in the current study.

5.3 TCARI. Due to the specific software required to accomplish the task, the generation of the TCARI *.tc grid file was accomplished by NOAA CO-OPS. While tidal harmonics for each subordinate station had previously been computed in Phase 2, in order for NOAA CO-OPS to generate the spatial grid the tidal harmonics had to match up with a standard list (Table 5.3.1). If this list is compared to the thirty-five tidal harmonic frequencies that could possibly be resolved by t_tide in Phase 2 (Table 5.3.2), there are twelve that do not appear in the NOAA CO-OPS standard list. However minor, the discrepancy results in both a loss of energy in the model and an alteration of the slope of the tide curve in the modeled tides.

Figure 5.2.1: Shoreline boundary for the lower Piscataqua River, the Great Bay and its tributaries. Modified from the NOAA NGS Shoreline Data Rescue Project of Portsmouth, New Hampshire, NH2C01. (NGS, 2009) Processed using GRASS v.6.4. (GRASS Development Team, 2010)

Further compounding this issue, the lunar monthly, *Mm*, and lunisolar synodic fortnightly, *MSf*, tidal constituents were excluded whether or not each was resolved by `t_tide`. The reason for their exclusion lies in the fact that the record lengths in Phase 2 of the study were not long enough to accord accurate and precise resolution of these tidal constituents from the background noise caused primarily by meteorological forcings; a minimum record length of one year is required, while three years is truly recommended. In the region of the United States in which the Great Bay resides, a fortnightly weather force affects the tides and cannot be resolved with a short record length.

114

Names	Frequency (cph)	Shallow-water equivalent
M2	0.080511400	
S2	0.083333330	
N2	0.078999250	
K1	0.041780750	
M4	0.161022800	
O1	0.038730650	
M6	0.241534200	
MK3	0.122292150	
S4	0.166666670	
MN4	0.159510650	
NU2	0.079201647	
S6	0.250000000	
MU2	0.077689470	
2N2	0.077486943	
OO1	0.044830840	
LAM2	0.081821008	
S1	0.041666667	
M1	0.040268590	NO1
J1	0.043292900	
MM	0.001512150	
SSA	0.000228159	
SA	0.000114079	
MSF	0.002821930	
MF	0.003050092	
RHO	0.037420808	
Q1	0.037218500	
T2	0.083219600	
R2	0.083447378	
2Q1	0.035706350	
P1	0.041552570	
2SM2	0.086154907	
M3	0.120767100	
L2	0.082023550	
2MK3	0.119242060	MO3
K2	0.083561735	
M8	0.322045600	
MS4	0.163844730	

Table 5.3.1: NOAA CO-OPS standard list of tidal harmonic frequencies required for TCARI grid generation. Shallow-water equivalent names added for reference. Harmonics in red are not included in the set possibly resolved by t_tide for Phase 2 water level time series.

A grid file, with the weighting functions and boundary included, was processed by NOAA CO-OPS using the data provided. With this TCARI grid, the final step in the model creation process was undertaken. Using the software Pydro, developed by the NOAA HSTP, the TCARI grid file was loaded (Fig. 5.3.1). For visual reference, raster navigational charts (RNC) 13283 and 13285 from NOAA's Office of Coast Survey (OCS) were loaded into the project base layer. (OCS, 2005; 2011)

Names	Frequency (cph)
MM	0.001512152
MSF	0.002821933
ALP1	0.034396570
2Q1	0.035706351
Q1	0.037218502
O1	0.038730654
NO1	0.040268594
K1	0.041780746
J1	0.043292898
OO1	0.044830838
UPS1	0.046342990
EPS2	0.076177316
MU2	0.077689468
N2	0.078999249
M2	0.080511401
L2	0.082023553
S2	0.083333333
ETA2	0.085073644
MO3	0.119242055
M3	0.120767101
MK3	0.122292147
SK3	0.125114080
MN4	0.159510649
M4	0.161022801
SN4	0.162332582
MS4	0.163844734
S4	0.166666667
2MK5	0.202803548
2SK5	0.208447413
2MN6	0.240022050
M6	0.241534202
2MS6	0.244356135
2SM6	0.247178067
3MK7	0.283314948
M8	0.322045603

Table 5.3.2: Tidal harmonic frequencies possibly resolved by t_tide for Phase 2 water level time series. Harmonics in red are not included in the NOAA CO-OPS standard list of tidal harmonic frequencies required for TCARI grid generation.

The next step in the process was to load the MLLW referenced time series from the WaterLog MWWL at Squamscott River, Great Bay, NH and the NOAA Aquatrak at Fort Point, NH, the previously chosen model control stations. A six-minute record from December 01, 2010 at 00:00 to December 31, 2010 at 23:54 was used. Once the data was loaded, a water level surface solution was generated (Fig. 5.3.2). This surface solution represents the MLLW datum spatially interpolated over the model area utilizing the

elevation values from Table 5.2.1. Datum elevation values, in meters referenced to mean sea level (MSL), are depicted by color; brighter red represents larger elevation values while black represents smaller elevation values.

5.4 TCARI Analysis. It is important to note that while the model covers the Great Bay as well as the lower Piscataqua River to the mouth of the estuary, the focus of the model and subsequent analysis is restricted to the Bay. While much of the TCARI model as realized in Pydro is undocumented, dialogue with Barry Gallagher from the NOAA HSTP has provided the necessary information for further analysis (See Appendix G: Personal Communiqués).

Once the TCARI model had been implemented within the Pydro software, a series of analytical figures was generated. Figures 5.4.1-4 show the harmonic constituent weighting function spatially interpolated across the model area for each tide station, respectively (not shown are the analytical figures associated with the Fort Point, NH tide station). Areas filled with cornflower blue represent regions that are not influenced by the weighting functions. The summation of the weights in each of these images equals one across the model area. A visual inspection shows no aberrations in the weighting function of each tide station for the study area.

Figure 5.4.5-7 show the MLLW, MLW, and MHW datum, respectively, interpolated across the model area. The datum elevations are in reference to MSL (as opposed to

NAVD88). Areas filled with cornflower blue represent regions where the datums are not spatially interpolated.

Figure 5.4.8 shows the residual water level weighting function spatially interpolated across the model area for the Squamscott River tide station. Areas filled with cornflower blue represent regions that are not influenced by the weighting function. A visual inspection shows no aberrations in the weighting function of the residual water level weighting function for the study area.

The last analytical figure, Figure 5.4.9, shows the TCARI error surface. The error surface represents the standard deviation, in meters, spatially interpolated over the model area. Each tide station exerts influence on the model a set radius, with control stations exerting influence a greater distance than subordinate stations. The model error is highest at the tide stations (±0.036 m) and gradually decreases farther from each gauge until the radius of influence is reached at which point the error increases. In areas where multiple tide stations' influence intersects, the decrease in error away from each tide station is more rapid. The lowest error in the model will then occur at those points with the greatest confluence of influence. Areas filled with cornflower blue, in this case, represent regions with the lowest error in the model (±0.023 m).
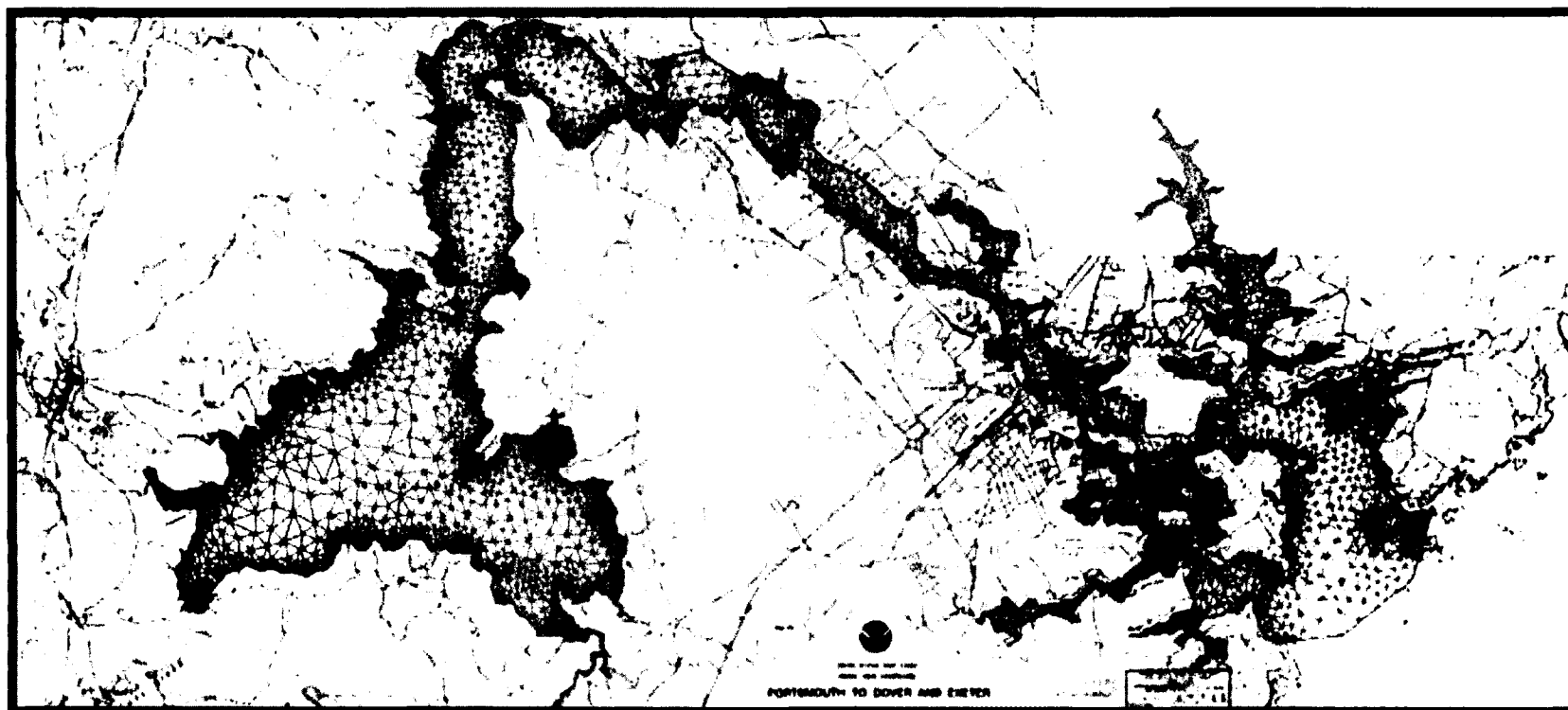
Figure 5.3.1: TCARI grid loaded in Pydro. Note the grid spacing decreases closer to the shoreline boundary. Raster navigational chart (RNC) 13283 and 13285 base layers shown for geographic reference. (OCS, 2005; 2011)
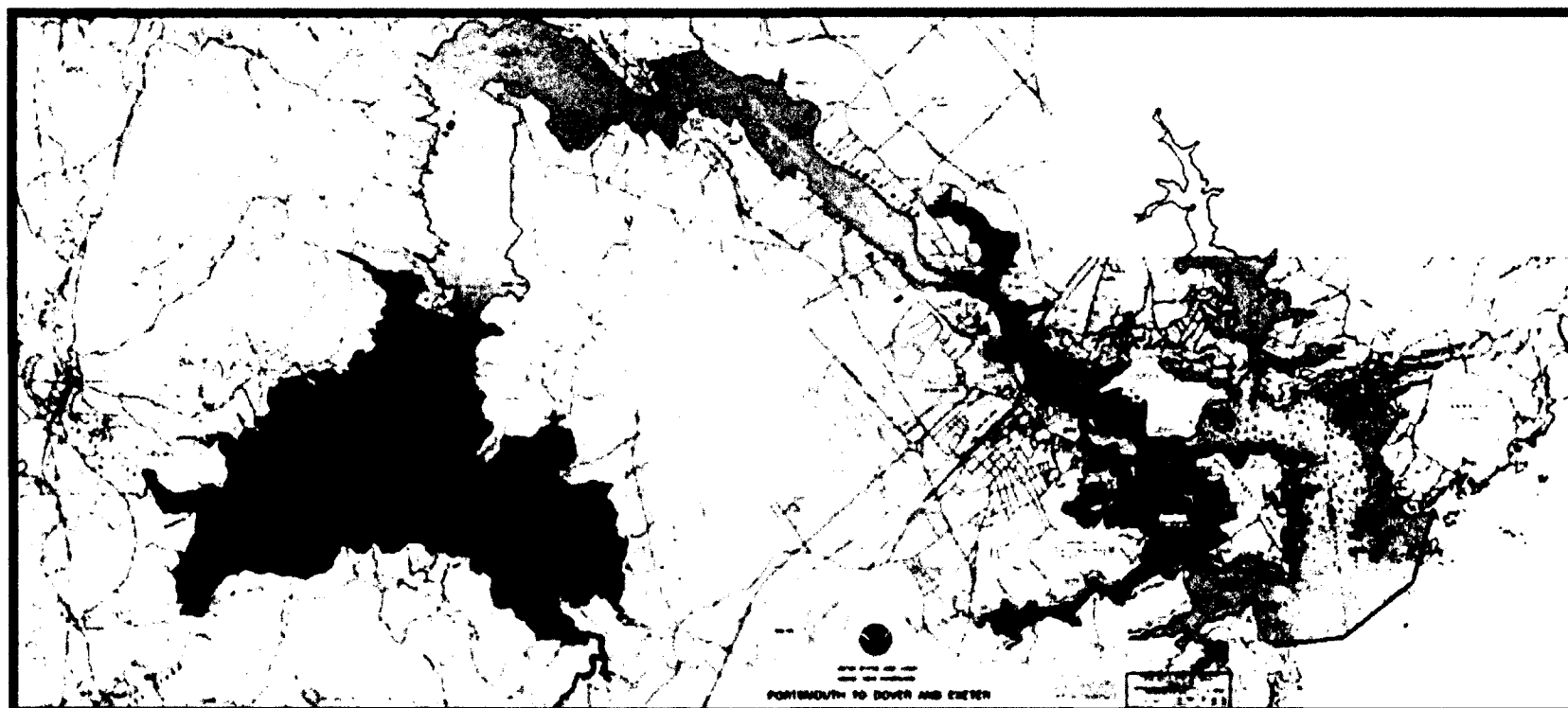
Figure 5.3.2: TCARI solution surface after loading MLLW referenced water level records from the model control gauges. Note the different boundary conditions for open-ocean, upriver, islands, and mainland. See Figure 5.4.8 for more information. Raster navigational chart (RNC) 13283 and 13285 base layers shown for geographic reference. (OCS, 2005; 2011)
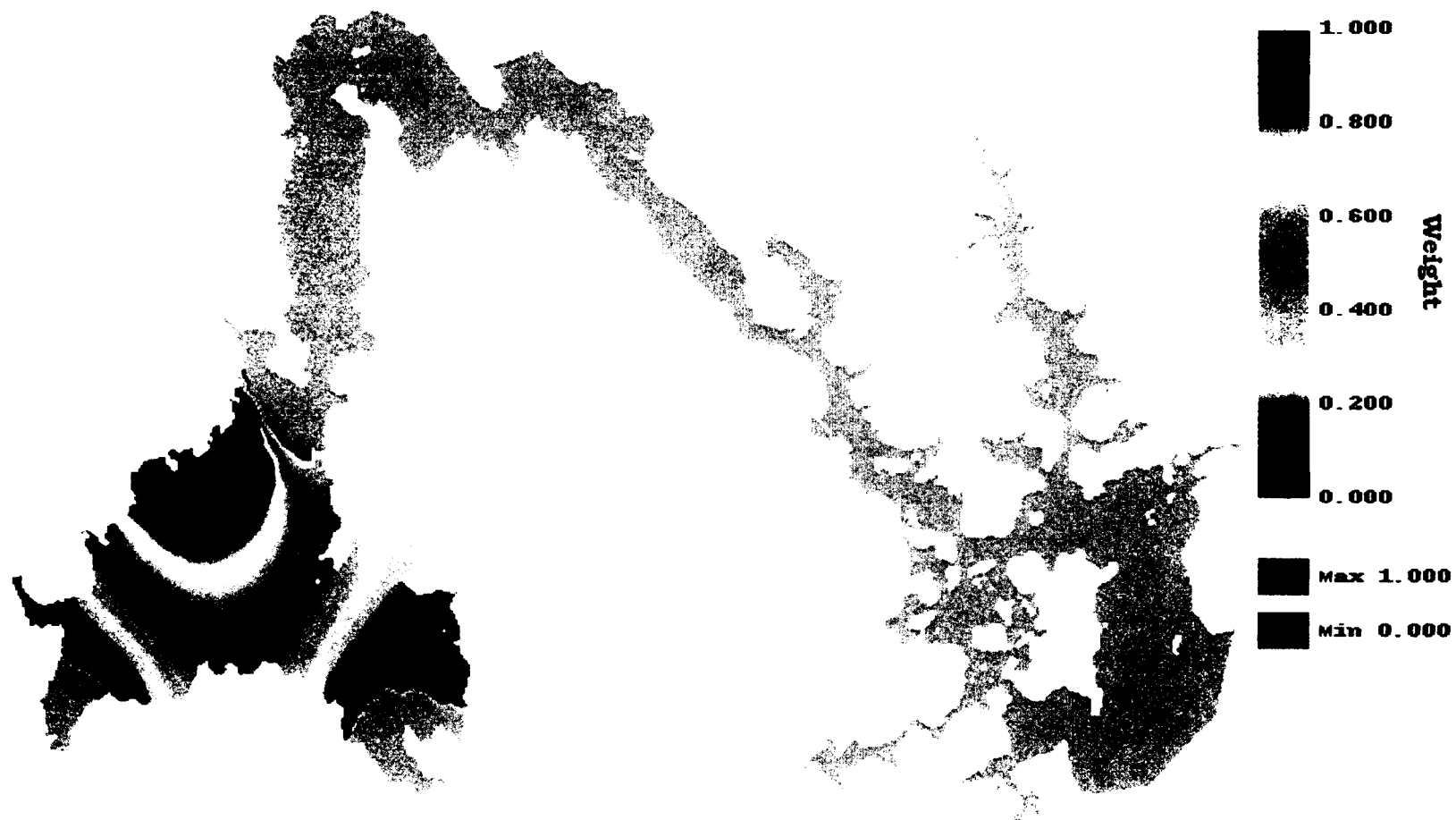
Figure 5.4.1: Harmonic constituent weighting function for Shankhassic, Great Bay, NH spatially interpolated across the TCARI model. Cornflower blue color represents regions that are not influenced by the weighting function.

Figure 5.4.2: Harmonic constituent weighting function for Winnicut River, Great Bay, NH spatially interpolated across the TCARI model. Cornflower blue color represents regions that are not influenced by the weighting function.
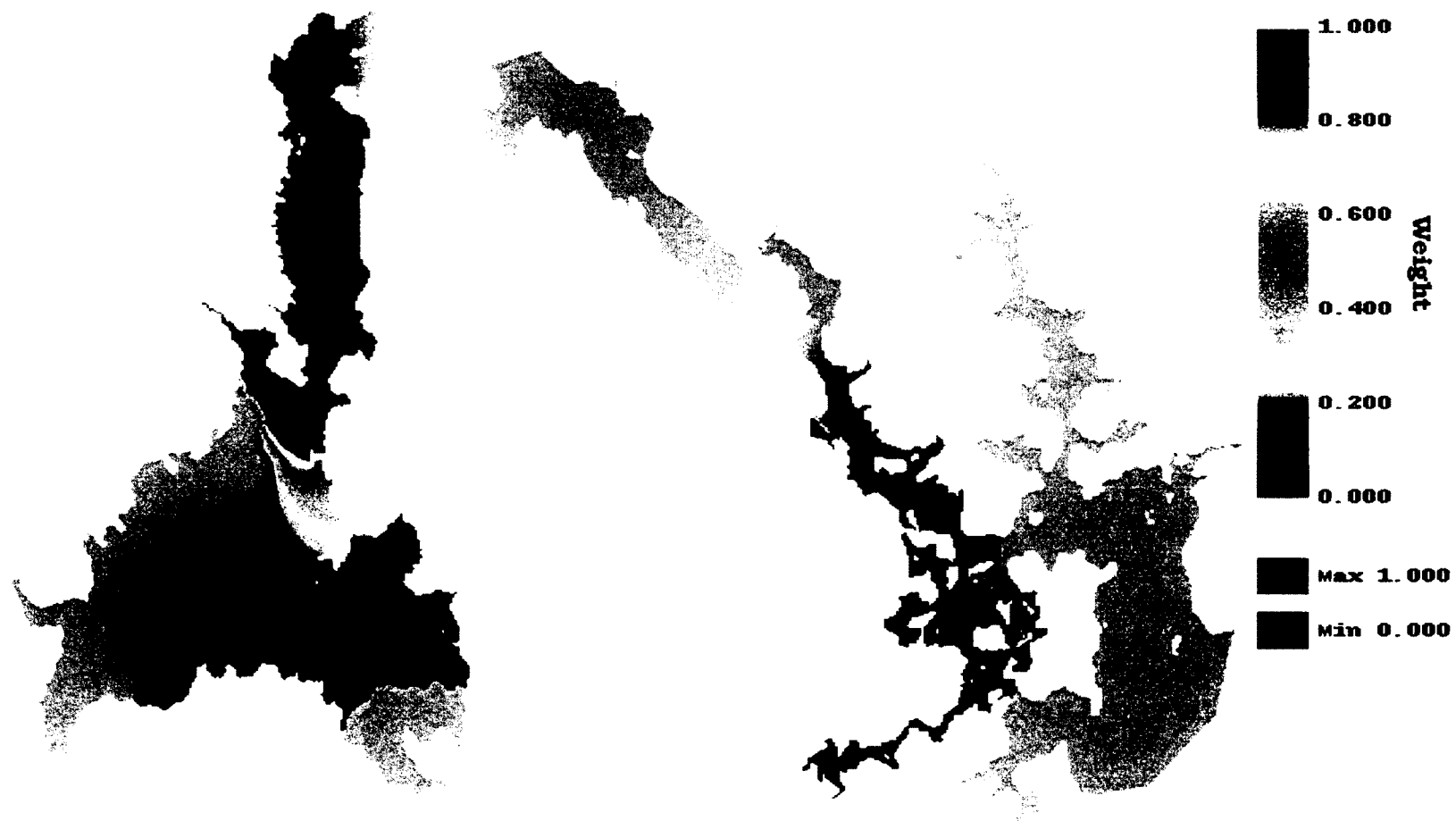
Figure 5.4.3: Harmonic constituent weighting function for Adam's Point, Great Bay, NH spatially interpolated across the TCARI model. Cornflower blue color represents regions that are not influenced by the weighting function.
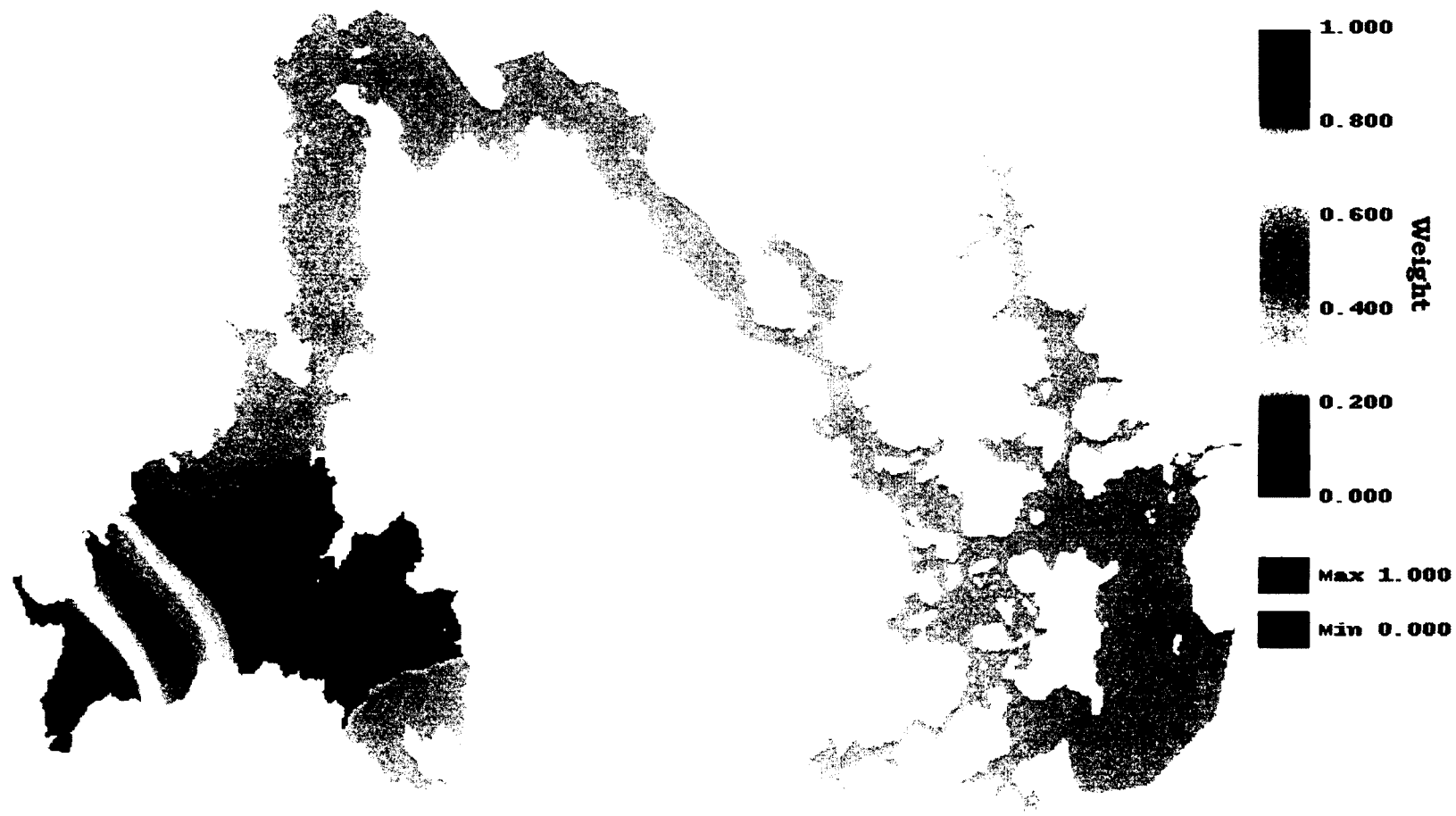
Figure 5.4.4: Harmonic constituent weighting function for Squamscott River, Great Bay, NH spatially interpolated across the TCARI model. Cornflower blue color represents regions that are not influenced by the weighting function.

Figure 5.4.5: Mean lower-low water (MLLW) datum elevations interpolated across the TCARI model. Datum elevations referenced to Mean Sea Level (MSL). Cornflower blue color represents regions where the datum is not spatially interpolated.
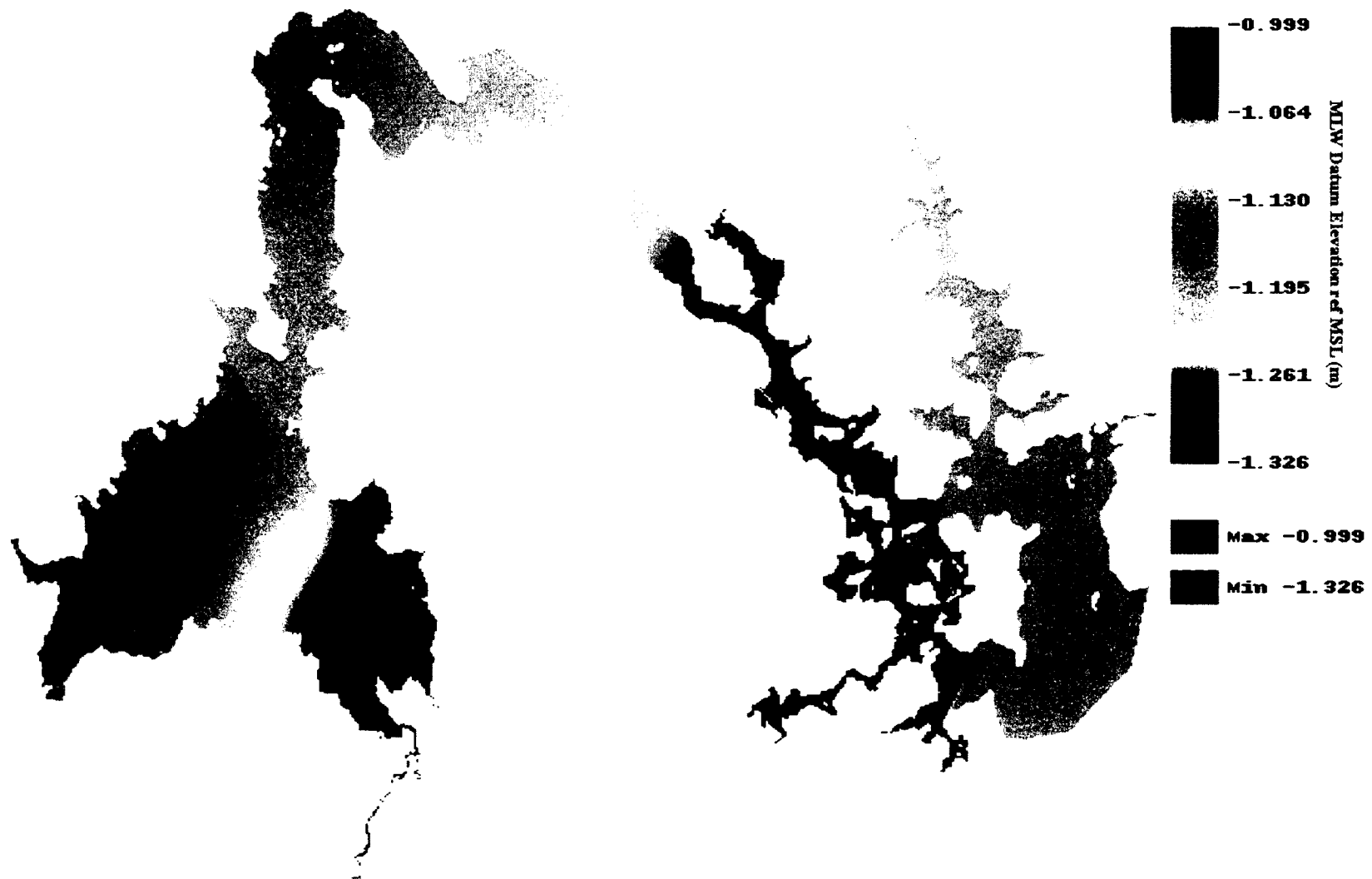
Figure 5.4.6: Mean low water (MLW) datum elevations interpolated across the TCARI model. Datum elevations referenced to Mean Sea Level (MSL). Cornflower blue color represents regions where the datum is not spatially interpolated.

Figure 5.4.7: Mean high water (MHW) datum elevations interpolated across the TCARI model. Datum elevations referenced to Mean Sea Level (MSL). Cornflower blue color represents regions where the datum is not spatially interpolated.
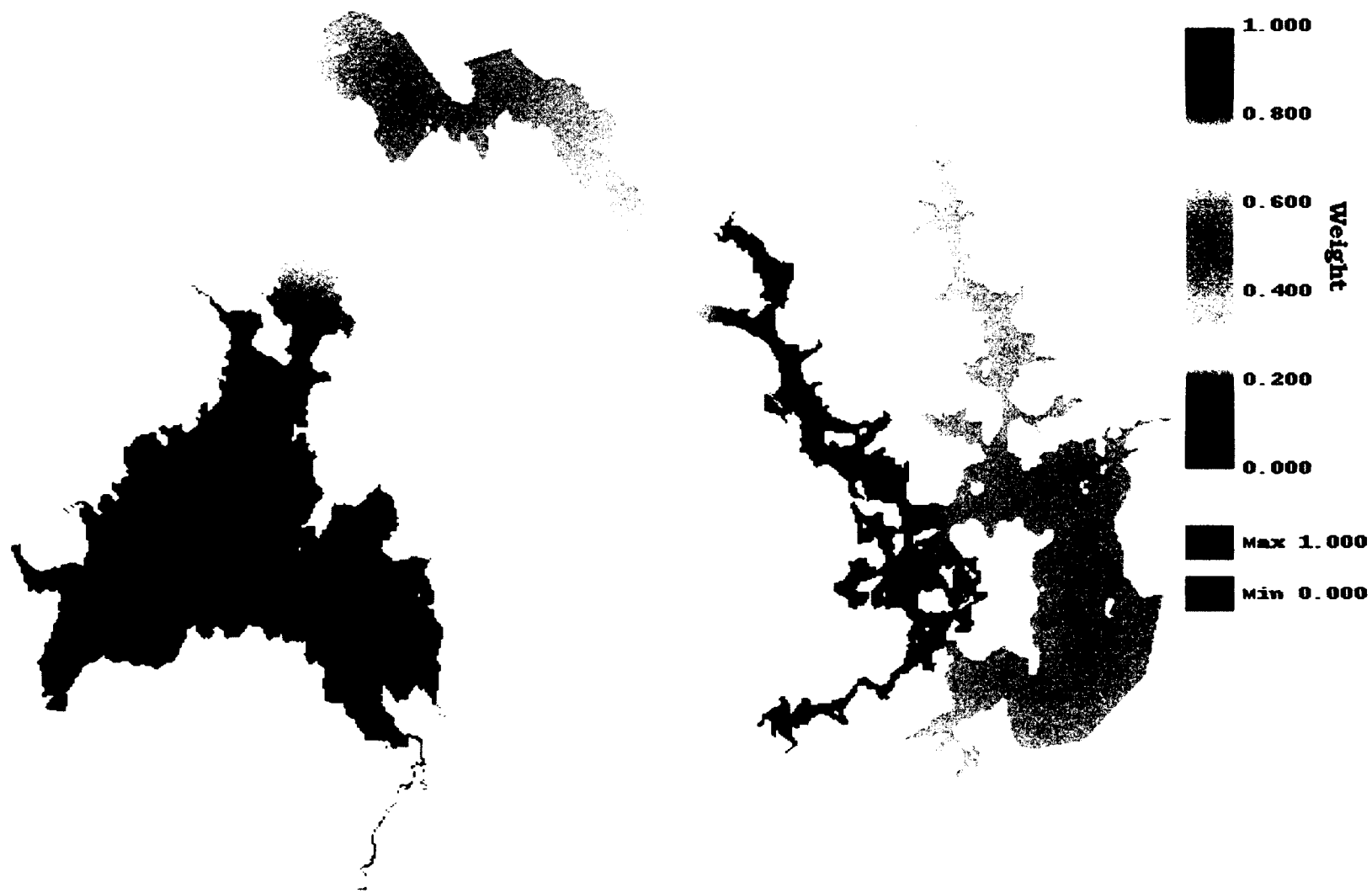
Figure 5.4.8: Residual water level weighting function for Squamscott River, Great Bay, NH spatially interpolated across the TCARI model. Cornflower blue color represents regions that are not influenced by the weighting function.

Figure 5.4.9: TCARI model error surface. Standard deviation, in meters, spatially interpolated across the model area. Note the lower error levels at the confluence of multiple tide stations (black). Red represents the highest error in the model; cornflower blue color represents the lowest error in the model.

VI. PHASE 4: MODEL VERIFICATION

Having developed a TCARI model of the Great Bay, the only remaining aspect of the project was to groundtruth the model against real-world observations. Groundtruthing of the model must consist not only of various locations within the model area, but also of different *epochs*, both past and future. Epochs are relative to the dates and times of the MLLW referenced data used to generate the TCARI solution surface of the model; December 01, 2010 00:00 to December 31, 2010 23:54 in this case. The objective of groundtruthing is to determine the accuracy, or predictive capability, of the model.

6.1 Methods. While the same combination of site availability, pre-existing infrastructure and geographical importance as in Phase 2 were considered, other factors were just as important. For reference, Figure 6.1.1 shows the approximate locations of all the gauges in Phase 4 by location ID (Table 6.1.1).
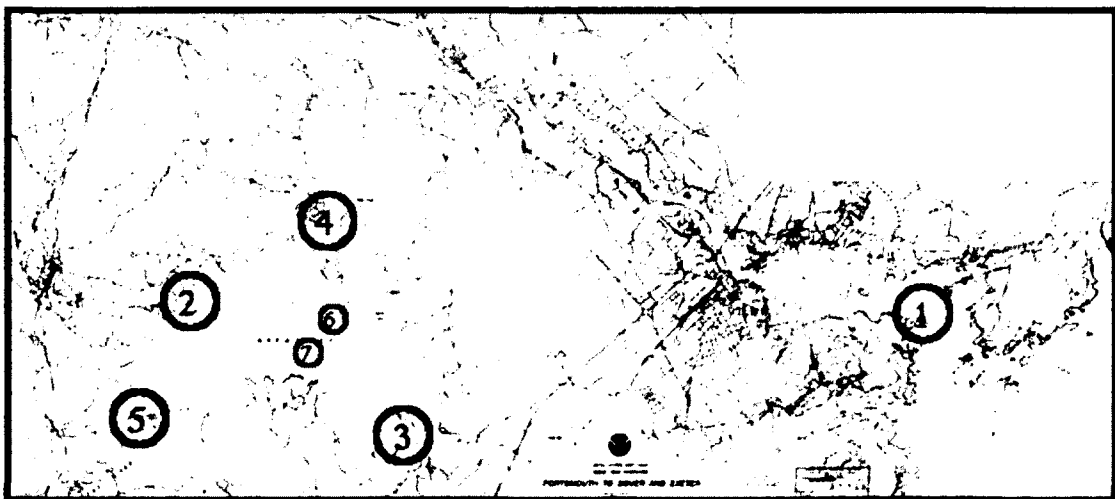
Figure 6.1.1: Phase 4 tide gauge locations. Current areas of study are highlighted in red, while previous areas of interest are muted in grey. (OCS, 2005; 2011)

130

ID	Location Name	Gauge Name	Latitude (N)	Longitude (W)
5	Squamscott River, Great Bay, NH	WaterLog MWWL	43.05264471°	70.91224518°
6	Nannie Island, Great Bay, NH	SeaBird SeaCAT	43.069186°	70.862867°
7	Mooring in Great Bay, NH	SeaBird SeaCAT	43.06560638°	70.86864132°

Table 6.1.1: Phase 4 tide gauge identification, location ID, name, latitude and longitude.

The first location chosen for model verification was Squamscott River, which is one of the model control stations (Table 6.1.1). The WaterLog MWWL had remained in place from its use in Phase 2, thus no additional positioning or leveling work was required. The data collected from this station was performed in a future epoch (Table 6.1.2). As this station is one of the model control stations, the assumed outcome of a comparison between observed and modeled water level should express larger error (relative to the other two model verification stations).

Sensor Name	Location ID	Sample Interval	Start Date (*yyyymmdd*)	Record Length
WaterLog MWWL	5	1 second	20110515	31 days
SeaBird SeaCAT	6	30 seconds	20090827	31 days
SeaBird SeaCAT	7	60 seconds	20110712	20 days

Table 6.1.2: Tidal instrumentation, location ID, sample interval, start date and record length.

The next location chosen for model verification was Nannie Island, a site chosen not for its location but rather the availability of data collected in the past (Table 6.1.1). The same SeaBird SeaCAT used in previous phases of this project was used in the data collection at Nannie Island. The data collected at this location was performed in a past epoch for an ongoing research project in Great Bay, NH by the Center for Coastal and Ocean Mapping – Joint Hydrographic Center (CCOM-JHC) at the UNH (Table 6.1.2). As this site is at another location within the study area and over one year in the past, the

expected outcome of a comparison between observed and modeled water level should show low error based upon the TCARI error surface (Fig. 5.4.9; 6.1.2).

The final location chosen for model verification was derived from the TCARI error surface (Table 6.1.1). The final location was chosen near the center of the blackish area in the TCARI error surface (Fig. 6.1.2). As there was no landmass or pre-existing infrastructure at this site, and without the availability of a GPS buoy for long-term observation, the SeaBird SeaCAT was mounted to a 200-lbs. mushroom anchor and moored at this position. For referencing to the ellipsoid and geoid, GPS observations were taken from the deck of the boat (R/V Cocheco) and tape measurements taken to the water surface. The data collected from this station was collected in a future epoch (Table 6.1.2). As this site is at the confluence of multiple tide station influence in the model, the expected outcome of a comparison between observed and modeled water level is expected to express the lowest error.

Figure 6.1.2: TCARI model error surface. See Figure 5.4.9 for more information. Raster navigational chart (RNC) base layer shown for visual reference to Great Bay, NH. (OCS, 2005)

6.2 Data Processing. In order to analyze and compare time series, the time records must exist on the same time reference, be continuous and have equivalent sample intervals. While no date or time offsets or truncations were applied, a linear interpolation for the SeaBird SeaCAT time series at both Nannie Island and the mooring site were computed. This linear interpolation was needed in order to attain an on-the-thirty-second and on-the-sixty-second time series, respectively. While a cubic spline interpolation is preferable, the short sample intervals between data points allows for a linear interpolation in this case.

For the SeaBird SeaCAT at both Nannie Island and the mooring site, in order to fill in the unknown in Equation 2.4.2, the NCDC atmospheric pressure record from Pease International Tradeport, Portsmouth, NH was used. As in Phases 1 and 2, a similar erratic sample interval was observed in the on-the-hour pressure record. A linear interpolation was used to obtain a true on-the-hour time series. Further linear interpolation was applied in order to achieve a time series with a six-minute sample interval. Duplicates and gaps were solved for and block-averaging was applied to all time series (Table 6.2.1-3). At this point, all time series are both continuous and have six-minute sample intervals. With the necessary time series assembled, computation of water level for the pressure-based tide gauges was performed.

Time Series	Raw Data Size	Duplicates	Gaps (Longest Gap)	Processed Size, N
WaterLog MWWL	2678572	0	0 (0)	7440
Modeled Observations	7440	0	0 (0)	7440
NOAA Aquatrak at Portland, ME	125	0	0 (0)	125

Table 6.2.1: Duplicates and gaps in the time series referenced to Squamscott River, Great Bay, NH.

Time Series	Raw Data Size	Duplicates	Gaps (Longest Gap)	Processed Size, N
SeaBird SeaCAT	89173	0	9 (9)	7440
NCDC Weather Station	741	0	0 (0)	7440
Modeled Observations	7440	0	0 (0)	7440
NOAA Aquatrak at Portland, ME	79	0	0 (0)	79

Table 6.2.2: Duplicates and gaps in the time series referenced to Nannie Island, Great Bay, NH.

Time Series	Raw Data Size	Duplicates	Gaps (Longest Gap)	Processed Size, N
SeaBird SeaCAT	28800	0	0 (0)	4800
NCDC Weather Station	481	0	0 (0)	4800
Modeled Observations	4800	0	0 (0)	4800

Table 6.2.3: Duplicates and gaps in the time series referenced to the mooring site in Great Bay, NH.

For similar purposes detailed in Phase 3, for both Nannie Island and the mooring site, the verified high-low water level from the NOAA primary tide station at Portland, ME was processed. As the modeled observations output by TCARI are referenced to MLLW, in order for a comparison to be made the water level from observations must also be referenced to MLLW. The appropriate datums and translations at Squamscott River had previously been accomplished in Phase 3, thus referencing the water level observations at this station could be made without further complication. For water level at the mooring station, a TBYT, modified range ratio for semidiurnal tides computation was performed. With the relevant orthometric elevations for both stations— Portland, ME and the mooring site,— the translation to an equivalent 19-year MLLW datum was easily computed. This translation was then applied to the computed water level for the mooring site.

Unfortunately, due to a blunder in GPS observations during post-processing at Nannie Island, the elevation data was lost. While a complete observed versus modeled analysis

cannot be completed for this station, a partial analysis in the time domain and full analysis in the spectral domain can still be performed.

6.3 Analysis. The primary objective of the model verification phase of the project was to determine the accuracy, and hence predictive capability of the newly implemented tide model of Great Bay, NH. Both time domain analysis and spectral domain analysis were performed on the processed data. The first aspect of time domain analysis performed was to look at the sample means of each time series and the maximum, mean and standard deviation of the residuals for both the computed water level observations as well as the t_tide generated water levels from the model comparison stations versus the modeled water level at those same locations (Table 6.3.1-6). At the same time, the modeled versus computed water level and t_tide generated water level records were plotted, including the plotted residuals (Fig. 6.3.1-6). For the computed water level observation comparison at Nannie Island, the mean for both the observed and modeled water levels were removed prior to making an analysis of the comparison (Table 6.3.2; Fig. 6.3.2). The sample mean listed is the unadjusted mean value. Visual inspection of these analyses, especially of Figures 6.3.1-6, show large maximum residuals, notably at times of slack tide.

| Time Series | Squamscott River, Great Bay, NH | | | |
	μ (m)	Maximum Residual (m)	Residual Mean (m)	Residual Std. Dev. (m)
Observed Water Level	1.2905	--	--	--
Modeled Water Level	1.2289	0.3210	0.0616	± 0.0910

Table 6.3.1: Maximum, mean, and standard deviation for the computed v. modeled water level residuals at Squamscott River, Great Bay, NH. Sample mean for both time series are given.

135

Time Series	Nannie Island, Great Bay, NH			
	μ (m)	Approximate Maximum Residual (m)	Approximate Residual Mean (m)	Approximate Residual Std. Dev. (m)
Observed Water Level	1.3677	--	--	--
Modeled Water Level	1.1516	0.3319	0.0000	± 0.1196

Table 6.3.2: Approximate maximum, mean, and standard deviation for the computed v. modeled water level residuals at Nannie Island, Great Bay, NH. Sample mean for both time series are given.

Time Series	Mooring Site in Great Bay, NH			
	μ (m)	Maximum Residual (m)	Residual Mean (m)	Residual Std. Dev. (m)
Observed Water Level	1.1330	--	--	--
Modeled Water Level	1.1537	-0.2150	-0.0208	± 0.0804

Table 6.3.3: Maximum, mean, and standard deviation for the computed v. modeled water level residuals at the mooring site in Great Bay, NH. Sample mean for both time series are given.

Time Series	Squamscott River, Great Bay, NH			
	μ (m)	Maximum Residual (m)	Residual Mean (m)	Residual Std. Dev. (m)
t_tide Generated WL	0.0006	--	--	--
Modeled Water Level	0.0007	0.1194	-0.0002	± 0.0422

Table 6.3.4: Maximum, mean, and standard deviation for the t_tide generated v. modeled water level (WL) residuals at Squamscott River, Great Bay, NH. Sample mean for both time series are given.

Time Series	Nannie Island, Great Bay, NH			
	μ (m)	Maximum Residual (m)	Residual Mean (m)	Residual Std. Dev. (m)
t_tide Generated WL	-0.0019	--	--	--
Modeled Water Level	-0.0015	-0.2868	-0.0004	± 0.0938

Table 6.3.5: Maximum, mean, and standard deviation for the t_tide generated v. modeled water level (WL) residuals at Nannie Island, Great Bay, NH. Sample mean for both time series are given.

Time Series	Mooring Site in Great Bay, NH			
	μ (m)	Maximum Residual (m)	Residual Mean (m)	Residual Std. Dev. (m)
t_tide Generated WL	0.0055	--	--	--
Modeled Water Level	-0.0009	-0.1583	0.0065	± 0.0596

Table 6.3.6: Maximum, mean, and standard deviation for the t_tide generated v. modeled water level (WL) residuals at the mooring site in Great Bay, NH. Sample mean for both time series are given.

The last facet of the analysis in the time domain was to plot the atmospheric versus water pressure for the pressure-based stations to determine whether any tidal forcing by the atmospheric pressure had occurred (Fig. 6.3.7-8). Visual inspection shows there was very little effect by the atmospheric tide signal.

The first analysis technique performed in the spectral domain was to look at a comparison of the resolved tidal harmonics between the observed and modeled water level at each station (Table 6.3.8-10). For those stations that are pressure-based, the tidal harmonics resolved from the atmospheric pressure time series are also provided. Simultaneously, the power spectrum of each time series was plotted (Fig. 6.3.9-16). A cursory look at the harmonic constituents for each record shows that while many of the constituents show small residuals in amplitude and phase, others show much larger residuals.

Further analysis of the residuals in the spectral domain is warranted. Looking at the power spectra for the residuals for each station— computed vs. modeled water level (Fig. 6.3.17, 6.3.19, 6.3.21) and t_tide generated vs. modeled water level (Fig. 6.3.18, 6.3.20, 6.3.22),— it is clear that there are numerous frequencies that are not characterized by the model. These residual frequencies can be grouped into four categories: non-tidal forcings, long period tides, short period tides, shallow-water tides.

The first category of frequencies that contribute to the residual power spectra are those caused by non-tidal forcings. As mentioned in §5.3, weather forces affect the water level in the Gulf of Maine, and by extension the Great Bay. These weather forced events can be seen in the range of frequencies smaller than the diurnal. The broadband signal of these meteorological forcings is evident in the residual power spectra (Fig. 6.3.17-22). Other non-tidal forces at work in the Bay include internal waves, and freshwater input from tributaries and upland sources. All of these factors contribute to some part of the

residual energy. One effect of these non-tidal components can be seen in the change of phase in the residual time series in Figures 6.3.1-3.

The long period tides— those tidal constituents whose periods are greater than one day (e.g. Sa, Ssa, Msm, Mm, MSf, Mf, etc.)— are difficult to resolve without very long tidal observation records. The reason for this complexity lies in the previously discussed non-tidal weather forced events. In the course of tidal analysis, the frequencies associated with these non-tidal forces are considered background noise. (Crawford, 1982) The variance of this background noise is often equal or greater-than the variance of the long period tides, thus obfuscating the resolution of each during harmonic analysis. (Foreman and Neufeld, 1991) While the energy from these long period tides is present in the residual power spectrum (Fig. 6.3.17-22), they are not separable without much longer records of observation; a minimum of one year for MSf and Mm.

Looking at the short period tides— n-th diurnal, where $1 \leq n \leq 8$,— there are many tidal constituents that are separated by a single cycle per month or year, but which are dominated by a large amplitude tidal constituent. An example of this is the semidiurnal lunar tide, S_2. The semidiurnal tides K_2, R_2, S_2, and T_2 are separated by a single cycle per annum. As can be seen in Figures 6.3.17-22, the residual power spectra have removed the S_2 tidal constituent at the semidiurnal tides. The remainder of the unresolved energy is partly composed of the K_2, R_2, and T_2 tides, as well as non-linear diurnal tidal effects. Other examples of this are visible at the diurnal, terdiurnal, quarter-diurnal, etc. short period tides.

138

The last category of frequencies that contribute to the residual power spectra are the shallow-water tides. As discussed in §5.3, the shallow-water tides that were not included in the model are evident in the residual power spectrum at each tide station (Fig. 6.3.17, 6.3.19, 6.3.21). Notably absent are the SK_3, $2MK_5$, $2MN_6$, $2MS_6$, and $3MK_7$ shallow-water tidal constituents, as well as higher order harmonics ($n \geq 9$) of the primary lunar tide, M. While not a large contribution to the total energy, these constituents do play a role in the steepening of the rise of tide and in the lengthening of the fall of tide.

The last spectral domain analysis performed was to compute and plot the smoothed spectral densities, smoothed squared coherency spectrum, and smoothed phase spectrum. These cross-spectral analyses were computed and plotted for comparison between the observed versus modeled water level at each station (Fig. 6.3.23-25). This analysis shows that the difference in harmonic constituents included in the model and those derived by t_tide is a main contributor to the difference in correlation between the modeled and observed tides.

During the development of the TCARI model by the NOAA Coast Survey Development Laboratory (CSDL), two sites were used in the verification of the model: Galveston Bay, TX and San Francisco Bay, CA. In assessing the maximum and mean residuals obtained from analysis of the current study, comparison is made to the results from Galveston Bay, TX and San Francisco, CA detailed in Hess et. al. (2004). First, for the computed water level observations, the maximum (0.3210 m, 0.3319 m, and -0.2150 m, respectively) and

mean (0.0616 ± 0.0910 m, 0.000 ± 0.1196 m, and -0.0208 ± 0.0804 m, respectively) residuals compare well with values obtained by Hess *et. al.* (2004) (Table 6.3.7).

Location	TCARI w/ 6-minute Water Level Predictions		
	Maximum Error (m)	Mean Error (m)	Std. Dev. (m)
Galveston Bay, TX	0.246	0.016	±0.073
San Francisco Bay, CA	0.415	0.014	±0.086

Table 6.3.7: Maximum, mean, and standard deviation of residuals from Galveston Bay, TX and San Francisco Bay, CA water level observations versus TCARI water level predictions. (Hess et. al., 2004)

While no equivalent comparison exists, for the t_tide generated water level, the maximum (0.1194 m, -0.2868 m, and -0.1593 m, respectively) and mean (-0.0002 ± 0.0422 m, -0.0004 ± 0.0938 m, and 0.0065 ± 0.0596 m, respectively) residuals are well within the accuracy assessment for TCARI with six-minute water level predictions. (Hess *et. al.*, 2004)

Comparing the residual standard deviation values from Table 6.3.1-3 (±0.0910 m, ±0.1196 m, ±0.0804 m, respectively) to the range of standard deviation values in the TCARI error surface from Figure 5.4.9 (±0.036 m to ±0.023 m), the results are much greater than expected. The reason for this discrepancy is largely related to the default error values (k-values) built into the model. There are two k-values, residual and harmonic constituent, with units of centimeters of error per kilometer of distance. By default, these k-values are set to the values established for Galveston Bay, TX. Compared to the Great Bay, NH the *range of tide* is lower in Galveston Bay, consequently the residual k-value at Galveston is lower than the k-value should be for the model of Great Bay. The lower standard deviations reported in the TCARI error surface

(Fig. 5.4.9) are a direct result of these k-values. Due to constraints on time, this k-value was not changed for the current study.

As discussed in §6.1, the mooring site in the Bay was chosen based upon the TCARI error surface (Fig. 5.4.9; 6.1.2). The residual analysis of observed vs. modeled water level shows that areas of darker color show lower error in the model, while areas of brighter red color show larger error in the model (Table 6.3.1-3). However, the residual analysis of the t_tide generated vs. modeled tide level shows that areas of darker color show larger error in the model, while areas of brighter red color show the lowest error in the model (Table 6.3.4-6). The reason for this incongruity in residual tidal signal may lie in the shorter record of observation for the mooring site (compared to the Squamscott River tide station). Recall from §5.4, the darker the coloration, the greater the convergence of multiple gauges on those areas of the model, which lowers the error in the model; vs. vrs. for brighter colors (See Appendix G.1: Barry Gallagher, November 7-15, 2011).

When looking at both the power spectrum and cross-spectral analyses, it is evident that a discrepancy exists in the energy between the observed and modeled water level time series. As previously discussed in Phase 3, the higher-frequency tidal constituents that are not included in the TCARI model can be seen in the smoothed-*spectral density* of the observed water level time series, but are absent in the modeled water level time series. The variance, or energy, loss between observed and modeled tidal frequencies (Table 6.3.8-10) for the three model verification stations was -1.05%, +5.05%, and +1.35%,

respectively. The negative variance for the Squamscott River tide station indicates the model is overestimating the tidal frequencies at this location, while the positive variances at Nannie Island and the mooring site indicate the model is underestimating the tidal frequencies at these locations. These variances are low in comparison to the energy of the observed tides. Even with this loss in energy, the modeled water levels within the Great Bay are statistically equivalent to real-world observations.

Phase IV: Model Verification
Squamscott River, Great Bay, NH
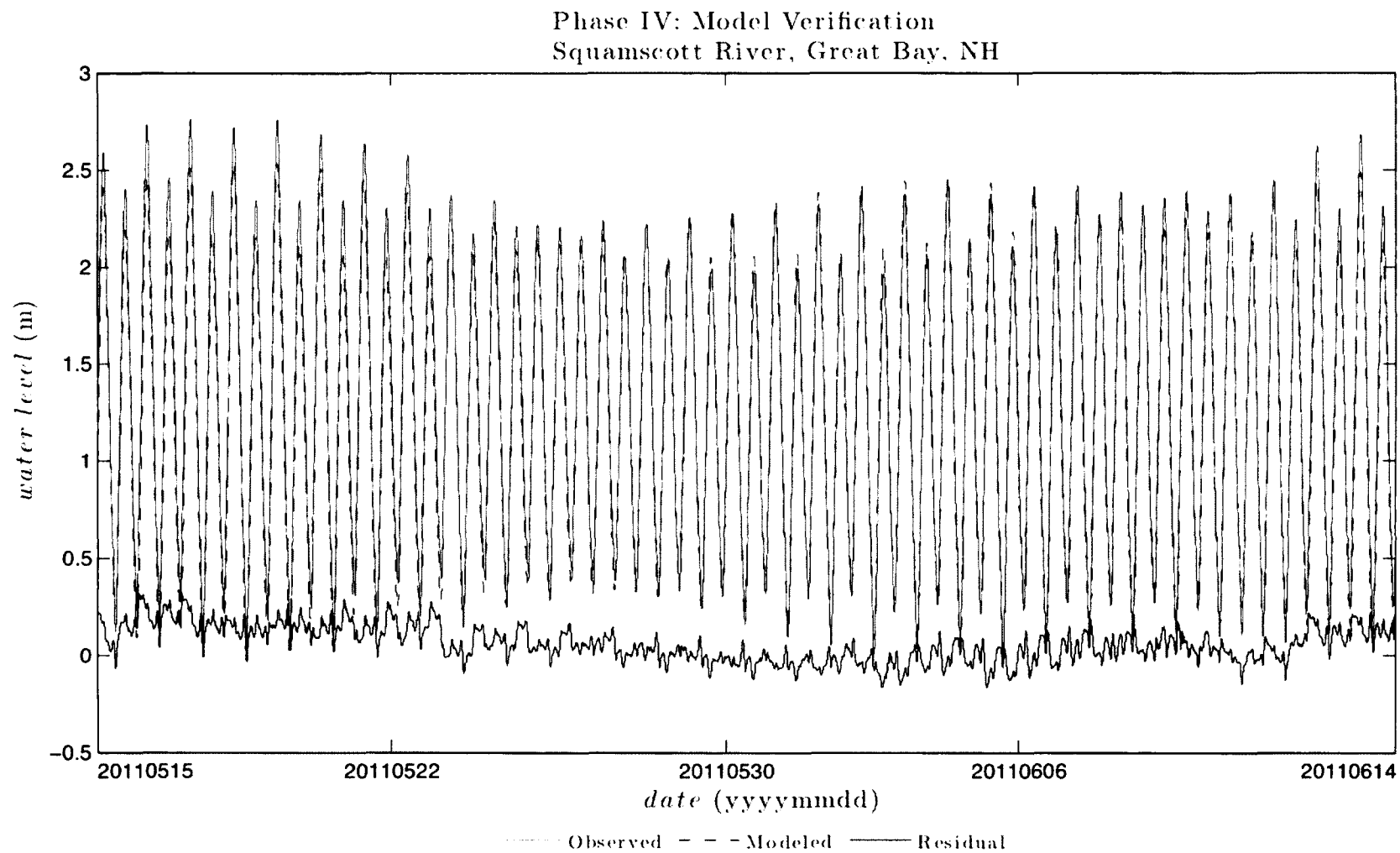
Figure 6.3.1: Modeled v. computed water level at Squamscott River, Great Bay, NH using observations from the WaterLog MWWL and computed residual. N=7440. Representative comparison of tides at a model control gauge in a future epoch. Note the fluctuations in the residual water level. A combination of meteorological and shallow-water tides, and non-tidal forcings (fortnightly weather effect) contribute to the residual water level.

Phase IV: Model Verification
Nannie Island, Great Bay, NH

Observed — — —Modeled ————Residual
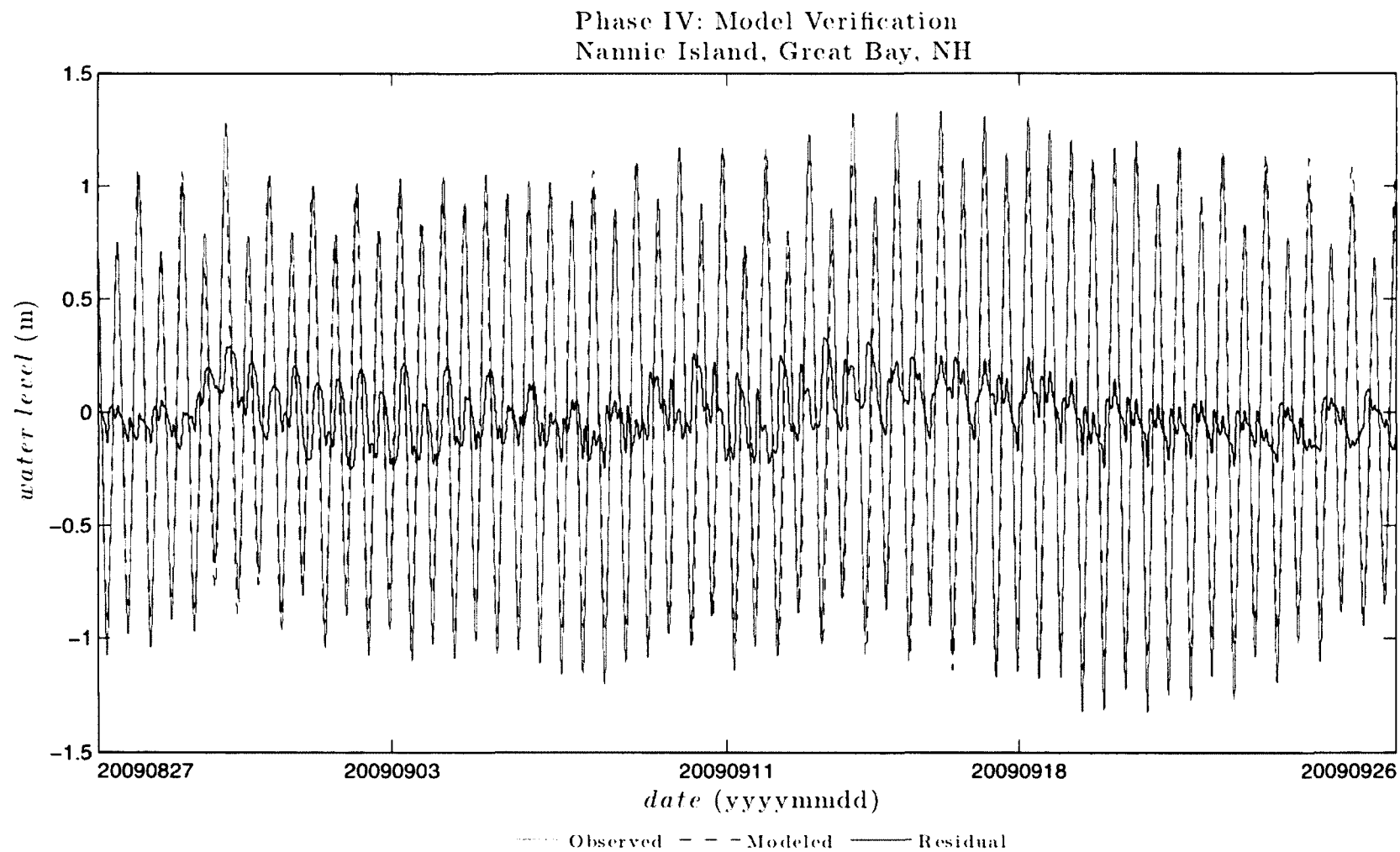
Figure 6.3.2: Modeled v. computed approximate water level at Nannie Island, Great Bay, NH using observations from the SeaBird SeaCAT and computed residual. N=7440. Representative comparison of tides at a random site in a past epoch. Note the fluctuations in the residual water level. A combination of meteorological and shallow-water tides, and non-tidal forcings (fortnightly weather effect) contribute to the residual water level.
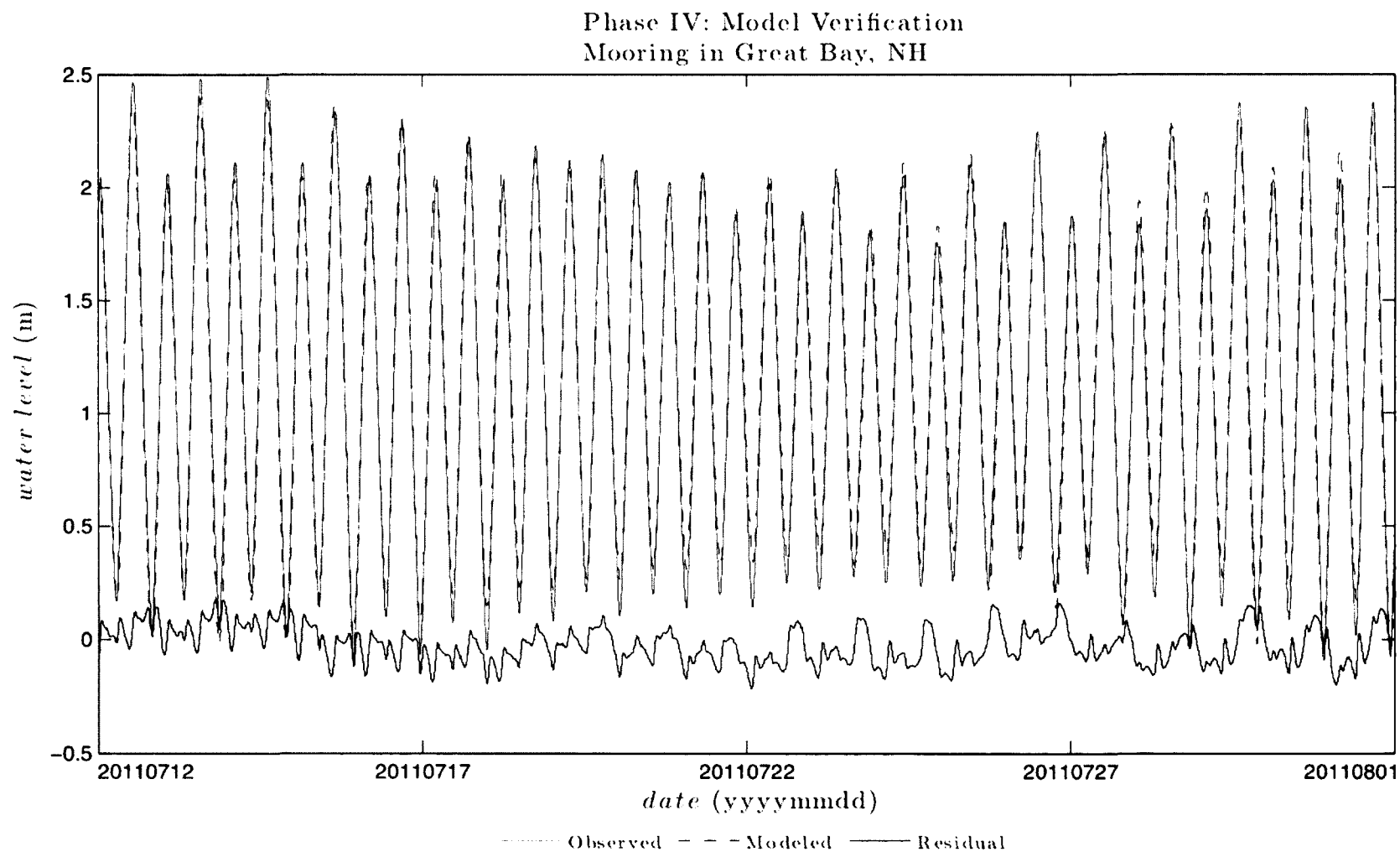
Figure 6.3.3: Modeled v. computed water level at the mooring site in Great Bay, NH using observations from the SeaBird SeaCAT and computed residual. N=4800. Representative comparison of tides at the site of confluence in the TCARI error surface in a future epoch. Note the fluctuations in the residual water level. A combination of meteorological and shallow-water tides, and non-tidal forcings (fortnightly weather effect) contribute to the residual water level.
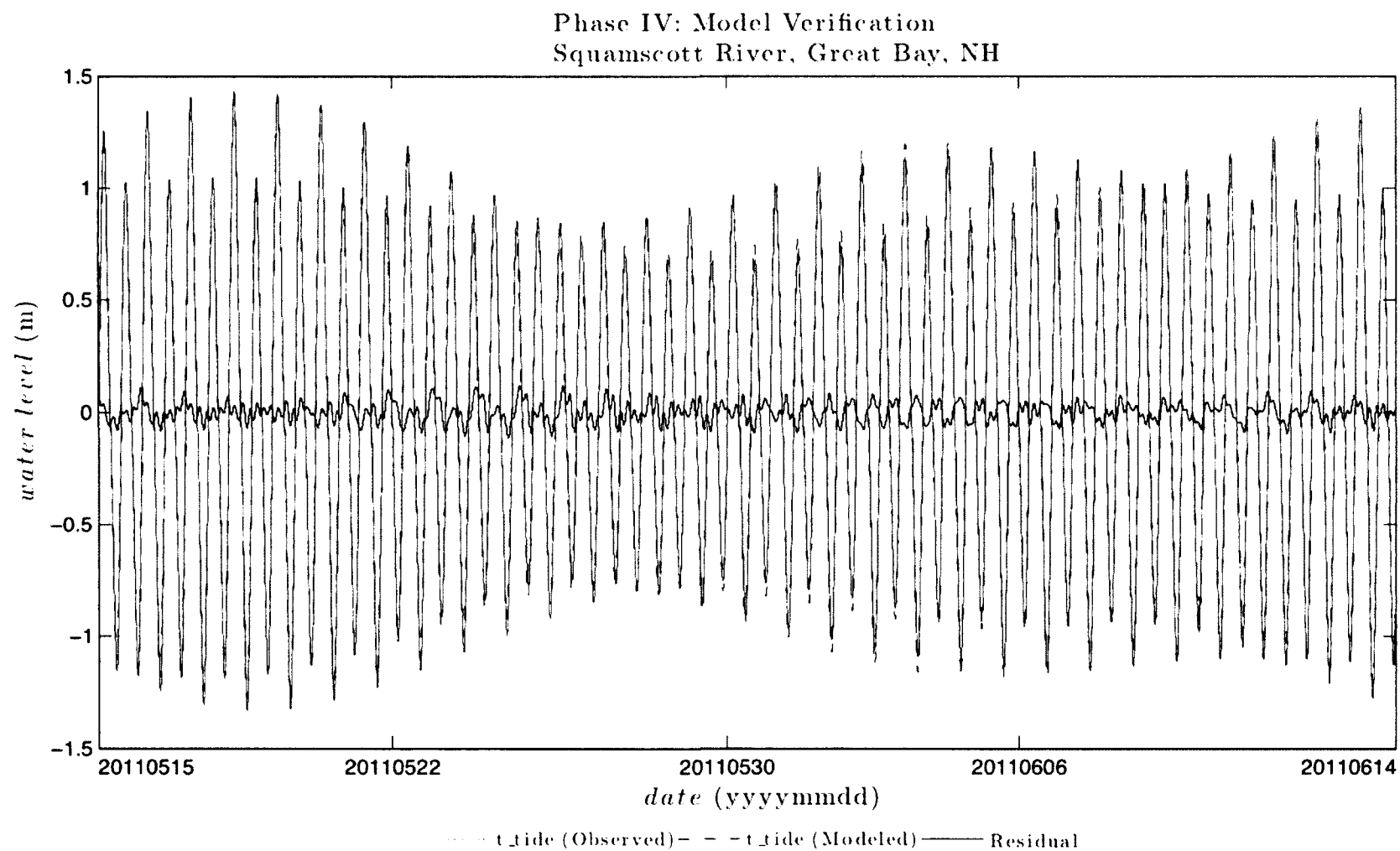
Figure 6.3.4: Modeled v. t_tide generated water level at Squamscott River, Great Bay, NH using observations from the WaterLog MWWL and computed residual. N=7440. Representative comparison of tides at a model control gauge in a future epoch. Note the fluctuations in the residual tide signal. A combination of meteorological and shallow-water tides contributes to the residual tide signal.
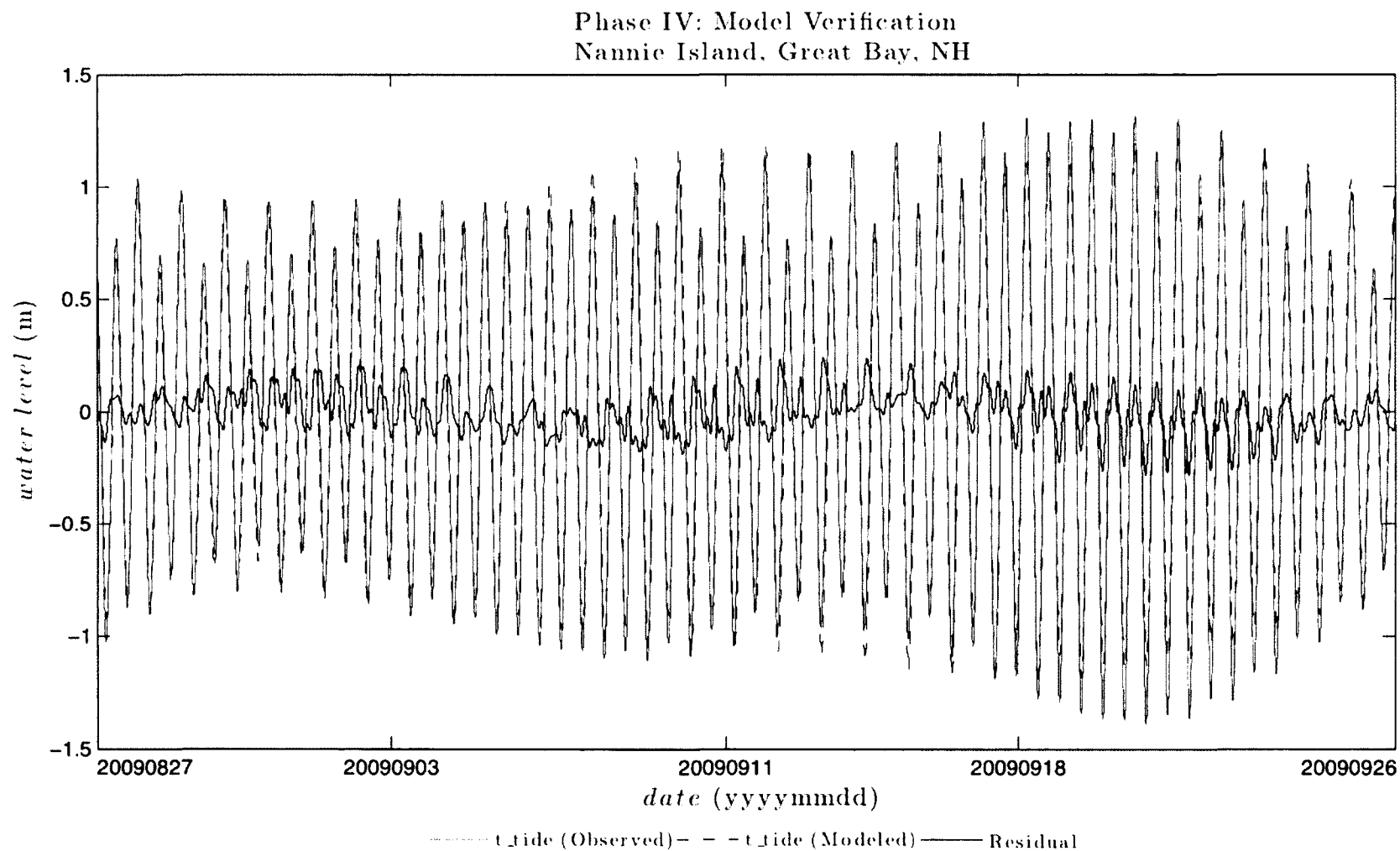
Figure 6.3.5: Modeled v. t_tide generated water level at Nannie Island, Great Bay, NH using observations from the SeaBird SeaCAT and computed residual. N=7440. Representative comparison of tides at a random site in a past epoch. Note the fluctuations in the residual tide signal. A combination of meteorological and shallow-water tides contributes to the residual tide signal.

Phase IV: Model Verification
Mooring in Great Bay, NH
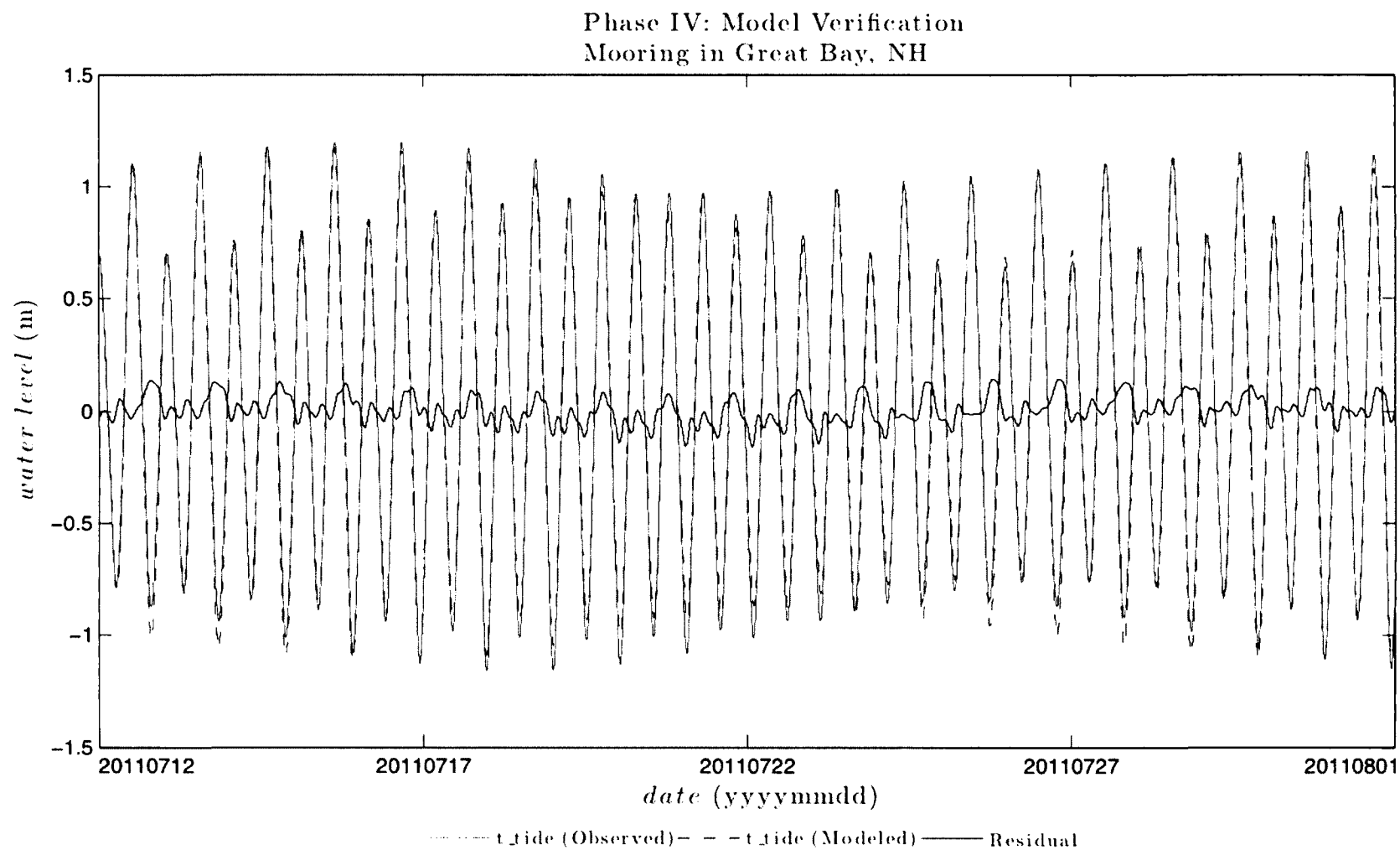
Figure 6.3.6: Modeled v. t_tide generated water level at the mooring site in Great Bay, NH using observations from the SeaBird SeaCAT and computed residual. N=4800. Representative comparison of tides at the site of confluence in the TCARI error surface in a future epoch. Note the fluctuations in the residual tide signal. A combination of meteorological and shallow-water tides contributes to the residual tide signal.

Phase IV: Model Verification
Nannie Island, Great Bay, NH

Atmospheric ———— Water ———— Residual
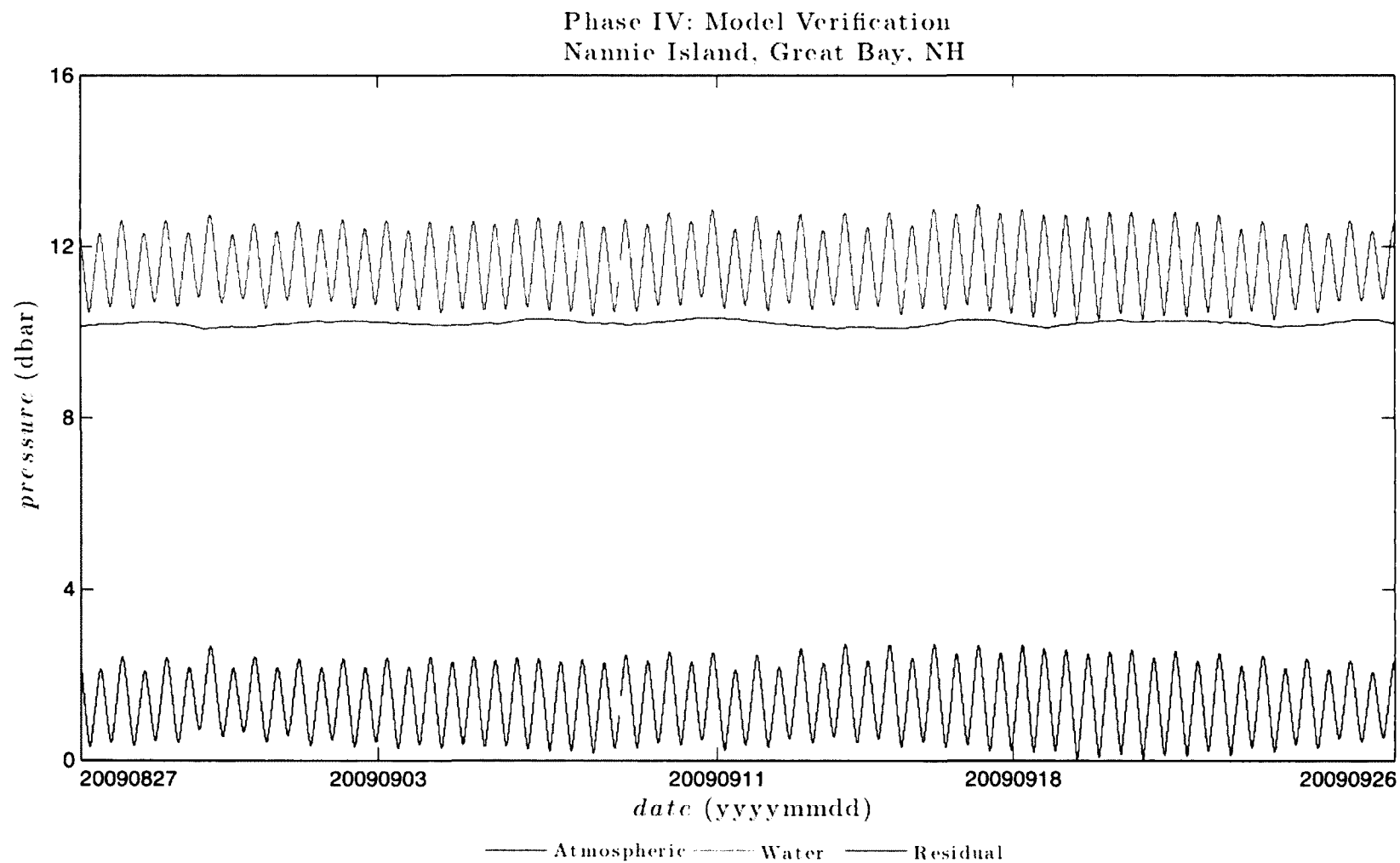
Figure 6.3.7: Observed atmospheric v. water pressure at Nannie Island, Great Bay, NH using observations from the SeaBird SeaCAT and computed residual. N=7440. Representative comparison of tides at a random site in a past epoch. Focus is on atmospheric pressure affect on water level. A gap in the pressure record is evident; no other aberrations are apparent in the residual (differential) pressure in comparison to the water pressure.

Phase IV: Model Verification
Mooring in Great Bay, NH
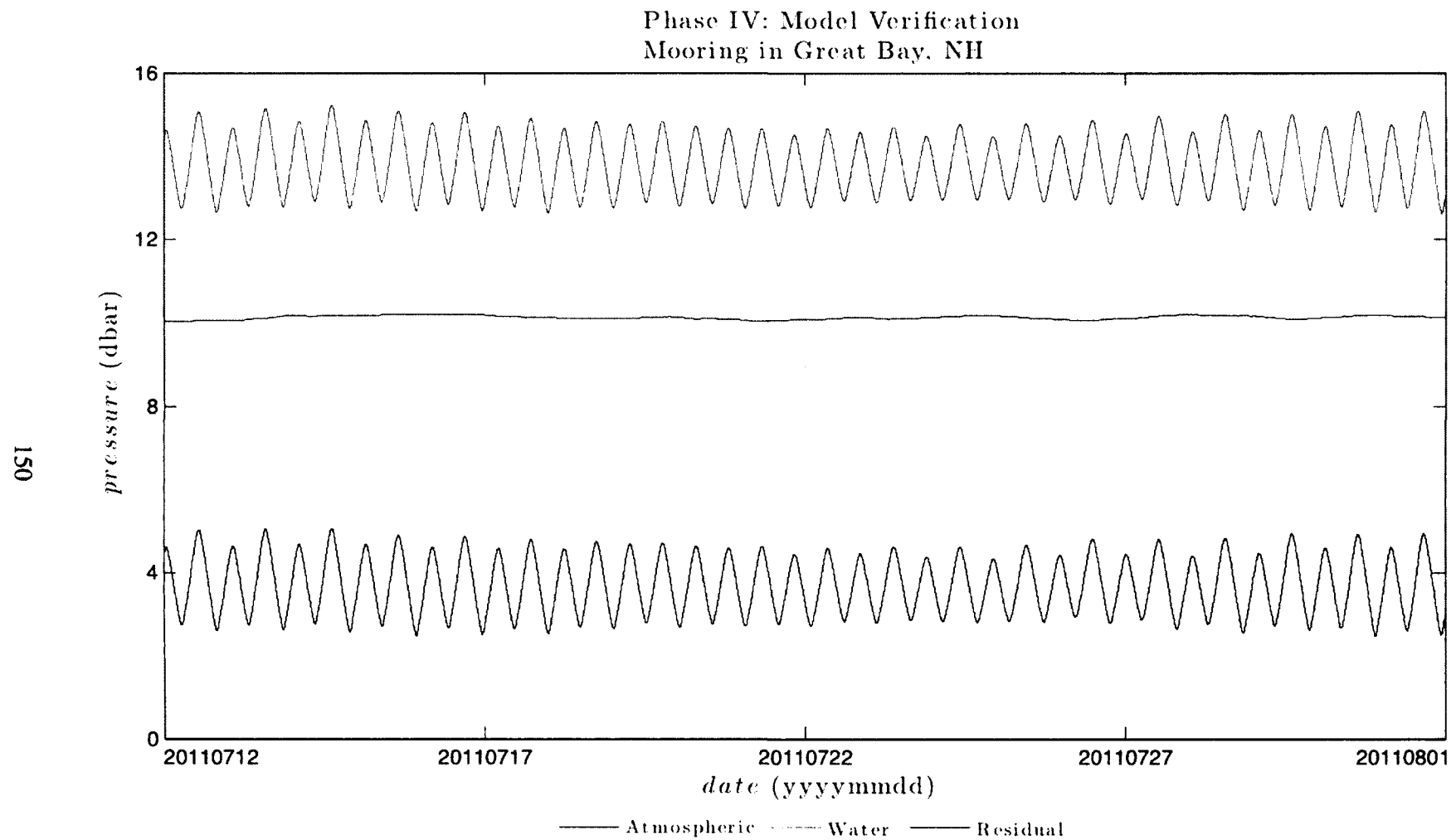
Figure 6.3.8: Observed atmospheric v. water pressure at the mooring site in Great Bay, NH using observations from the SeaBird SeaCAT and computed residual. N=4800. Representative comparison of tides at the site of confluence in the TCARI error surface in a future epoch. Focus is on atmospheric pressure affect on water level. No aberrations are apparent in the residual (differential) pressure in comparison to the water pressure.

Names	Frequency (cpd)	Squamscott River, Great Bay, NH Observations		TCARI Model Predictions		Residuals	
		Amplitude (m)	Phase (°)	Amplitude (m)	Phase (°)	Amplitude (m)	Phase (°)
2Q1	0.856952412	0.0061	151.43	0.0087	52.44	0.0026	-98.99
Q1	0.893244060	0.0112	223.76	0.0076	139.76	-0.0036	-83.99
O1	0.929535707	0.0902	231.75	0.0882	232.04	-0.0020	0.28
NO1	0.966446262	0.0095	293.52	0.0212	264.94	0.0117	-28.58
K1	1.002737909	0.1419	241.82	0.1408	246.62	-0.0011	4.80
J1	1.039029557	0.0062	342.95	0.0006	273.34	-0.0056	-69.61
OO1	1.075940112	0.0069	274.30	0.0007	1.77	-0.0062	87.47
N2	1.895981969	0.1577	135.61	0.1384	144.47	-0.0194	8.86
M2	1.932273616	0.9355	173.26	0.9423	172.19	0.0068	-1.07
S2	2.000000000	0.0777	211.66	0.0987	209.91	0.0210	-1.75
MO3	2.861809323	0.0223	284.61	0.0178	268.64	-0.0045	-15.97
M3	2.898410424	0.0060	209.07	0.0123	217.75	0.0063	8.68
MK3	2.935011525	0.0230	301.43	0.0249	308.20	0.0019	6.78
SK3	3.002737909	0.0025	296.13				
MN4	3.828255585	0.0167	220.62	0.0101	217.34	-0.0066	-3.29
M4	3.864547232	0.0389	257.82	0.0372	254.13	-0.0017	-3.69
MS4	3.932273616	0.0076	291.31	0.0120	283.15	0.0045	-8.16
S4	4.000000000			0.0039	36.80		
2MK5	4.867285141	0.0120	233.39				
2MN6	5.760529201	0.0196	127.59				
M6	5.796820848	0.0446	171.30	0.0491	162.54	0.0045	-8.77
2MS6	5.864547232	0.0101	198.28				
3MK7	6.799558758	0.0082	280.54				
M8	7.729094464	0.0079	233.81	0.0060	202.58	-0.0019	-31.23

Table 6.3.8: t_tide resolved tidal harmonic constituents and residuals with a signal-to-noise ratio (SNR) greater than 2.0 in reference to model verification at Squamscott River, Great Bay, NH. Representative comparison of tides at a model control gauge in a future epoch.

Names	Frequency (cpd)	Nannie Island, Great Bay, NH Observations		TCARI Model Predictions		Residuals		NCDC Atmospheric Pressure	
		Amplitude (m)	Phase (°)	Amplitude (m)	Phase (°)	Amplitude (m)	Phase (°)	Amplitude (m)	Phase (°)
2Q1	0.856952412			0.0089	0.85			0.0031	32.64
Q1	0.893244060	0.0162	215.92	0.0102	202.70	-0.0060	-13.22		
O1	0.929535707	0.0892	226.33	0.0904	231.13	0.0012	4.79	0.0022	212.30
NO1	0.966446262	0.0094	211.79	0.0174	263.08	0.0080	51.29	0.0024	325.92
K1	1.002737909	0.0898	255.64	0.1378	244.89	0.0479	-10.75	0.0061	90.30
J1	1.039029557	0.0038	238.55	0.0088	153.82	0.0050	-84.74	0.0015	268.29
OO1	1.075940112	0.0038	9.38	0.0064	149.06	0.0026	139.67		
N2	1.895981969	0.1884	126.30	0.1512	145.92	-0.0371	19.62	0.0002	97.92
M2	1.932273616	0.9397	169.85	0.9195	169.71	-0.0202	-0.14	0.0007	122.59
S2	2.000000000	0.1557	213.84	0.1030	214.86	-0.0527	1.02	0.0042	70.07
MO3	2.861809323	0.0132	260.69	0.0177	276.34	0.0046	15.66	0.0003	63.46
M3	2.898410424	0.0057	177.44	0.0100	205.85	0.0043	28.41		
MK3	2.935011525	0.0084	286.75	0.0191	296.91	0.0108	10.16	0.0003	2.81
SK3	3.002737909	0.0031	350.84					0.0004	118.75
MN4	3.828255585	0.0046	184.49	0.0150	214.56	0.0104	30.07	0.0004	191.58
M4	3.864547232	0.0093	223.60	0.0331	260.10	0.0237	36.51	0.0002	324.04
MS4	3.932273616	0.0058	231.65	0.0065	291.06	0.0007	59.42	0.0002	54.44
S4	4.000000000			0.0004	337.23				
2MK5	4.867285141	0.0068	211.77					0.0003	208.10
2SK5	5.002737909							0.0001	53.12
2MN6	5.760529201	0.0275	92.88						
M6	5.796820848	0.0441	146.88	0.0336	152.39	-0.0104	5.51	0.0002	132.33
2MS6	5.864547232	0.0243	189.17					0.0002	301.61
2SM6	5.932273616							0.0002	111.50
3MK7	6.799558758	0.0019	242.03					0.0001	325.24
M8	7.729094464	0.0045	156.49	0.0055	199.52	0.0010	43.04	0.0001	8.65

Table 6.3.9: t_tide resolved tidal harmonic constituents and residuals with a signal-to-noise ratio (SNR) greater than 2.0 in reference to model verification at Nannie Island, Great Bay, NH. Representative comparison of tides at a random site in a past epoch.

Names	Frequency (cpd)	Mooring Site in Great Bay, NH Observations		TCARI Model Predictions		Residuals		NCDC Atmospheric Pressure	
		Amplitude (m)	Phase (°)	Amplitude (m)	Phase (°)	Amplitude (m)	Phase (°)	Amplitude (m)	Phase (°)
O1	0.929535707	0.0866	227.88	0.0928	227.11	0.0062	-0.77	0.0037	55.16
K1	1.002737909	0.1262	267.29	0.1345	245.39	0.0083	-21.90	0.0072	15.55
M2	1.932273616	0.8933	170.47	0.8880	171.28	-0.0054	0.81	0.0014	78.86
S2	2.000000000	0.1026	246.26	0.0828	218.19	-0.0199	-28.06	0.0042	51.39
M3	2.898410424	0.0091	195.67	0.0115	233.51	0.0023	37.84	0.0004	301.65
SK3	3.002737909	0.0062	307.47					0.0011	4.92
M4	3.864547232	0.0049	259.87	0.0284	265.60	0.0234	5.73		
MS4	3.932273616	0.0036	272.00	0.0071	287.22	0.0035	15.22	0.0004	159.80
2MK5	4.867285141	0.0121	234.47					0.0003	312.66
M6	5.796820848	0.0435	148.12	0.0344	154.02	-0.0090	5.90	0.0002	85.64
2MS6	5.864547232	0.0148	239.57					0.0004	314.84
2SM6	5.932273616							0.0004	217.46
3MK7	6.799558758	0.0036	287.32					0.0002	82.43
M8	7.729094464	0.0035	144.19	0.0052	200.87	0.0017	56.68	0.0004	195.51

Table 6.3.10: t_tide resolved tidal harmonic constituents and residuals with a signal-to-noise ratio (SNR) greater than 2.0 in reference to model verification at the mooring site in Great Bay, NH. Representative comparison of tides at the site of confluence in the TCARI error surface in a future epoch.

Phase IV: Model Verification
Squamscott River, Great Bay, NH
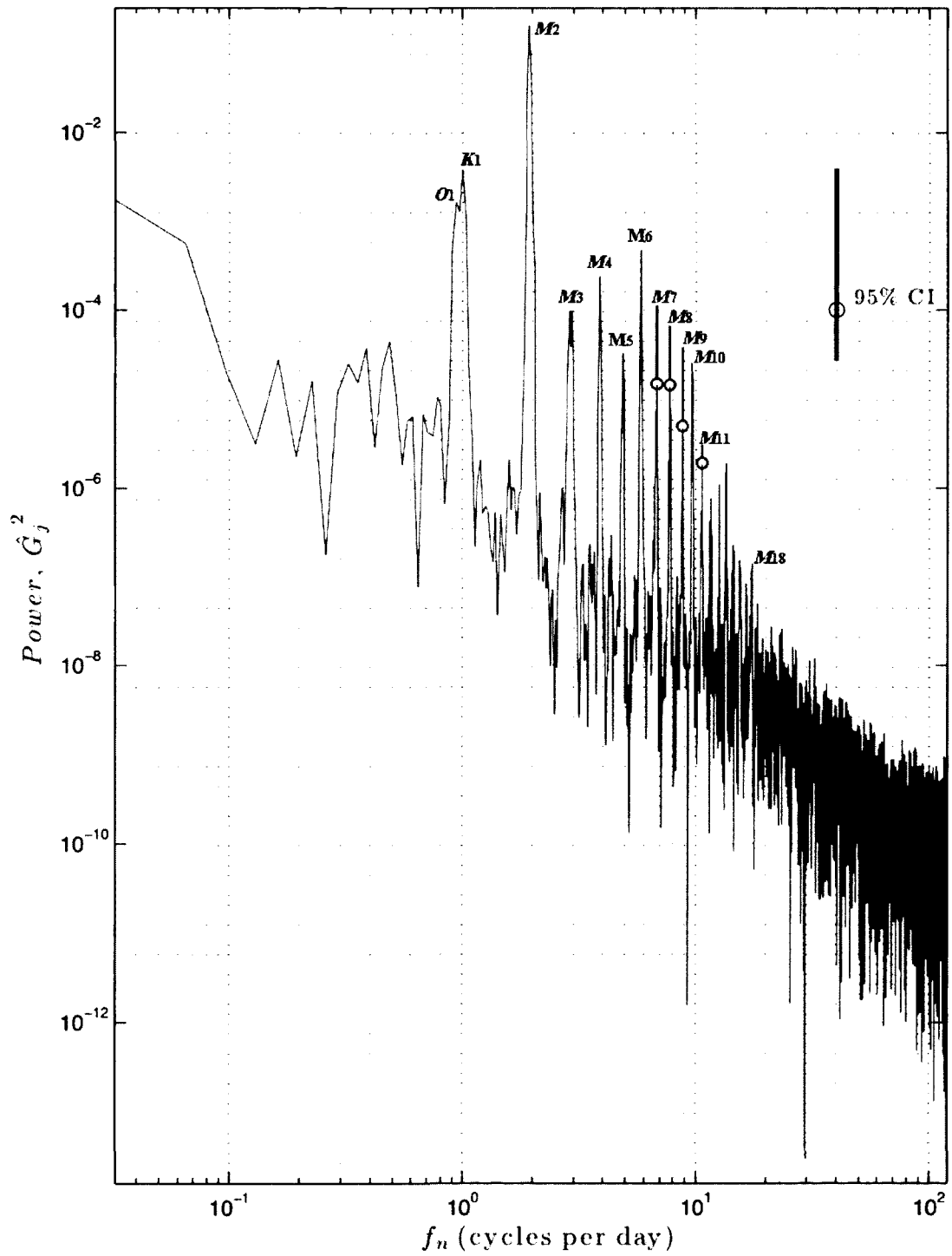
Figure 6.3.9: Water level power spectrum at Squamscott River, Great Bay, NH using observations from the WaterLog MWWL. Hanning window, N=7439. Representative comparison of tides at a model control gauge in a future epoch. Observable n-th order harmonics of the primary lunar tide, M, and the diurnal constituents, O_1 and K_1, are labeled.

Phase IV: Model Verification
Squamscott River, Great Bay, NH
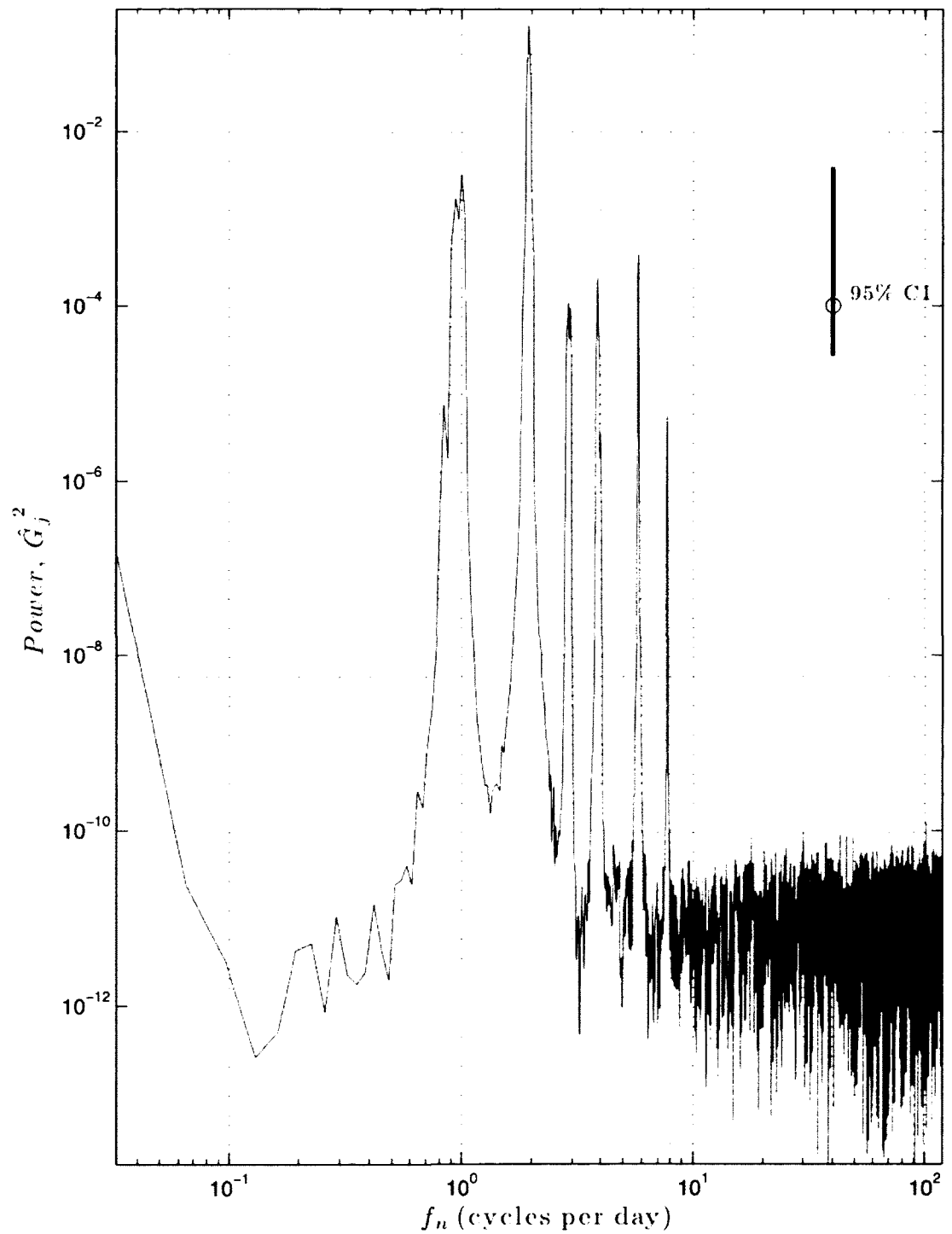
Figure 6.3.10: Water level power spectrum at Squamscott River, Great Bay, NH using TCARI model predictions. Hanning window, N=7439. Representative comparison of tides at a model control gauge in a future epoch. See Figure 6.3.9 for labels of the observable n-th order harmonics of the primary lunar tide, M.

Phase IV: Model Verification
Nannie Island, Great Bay, NH
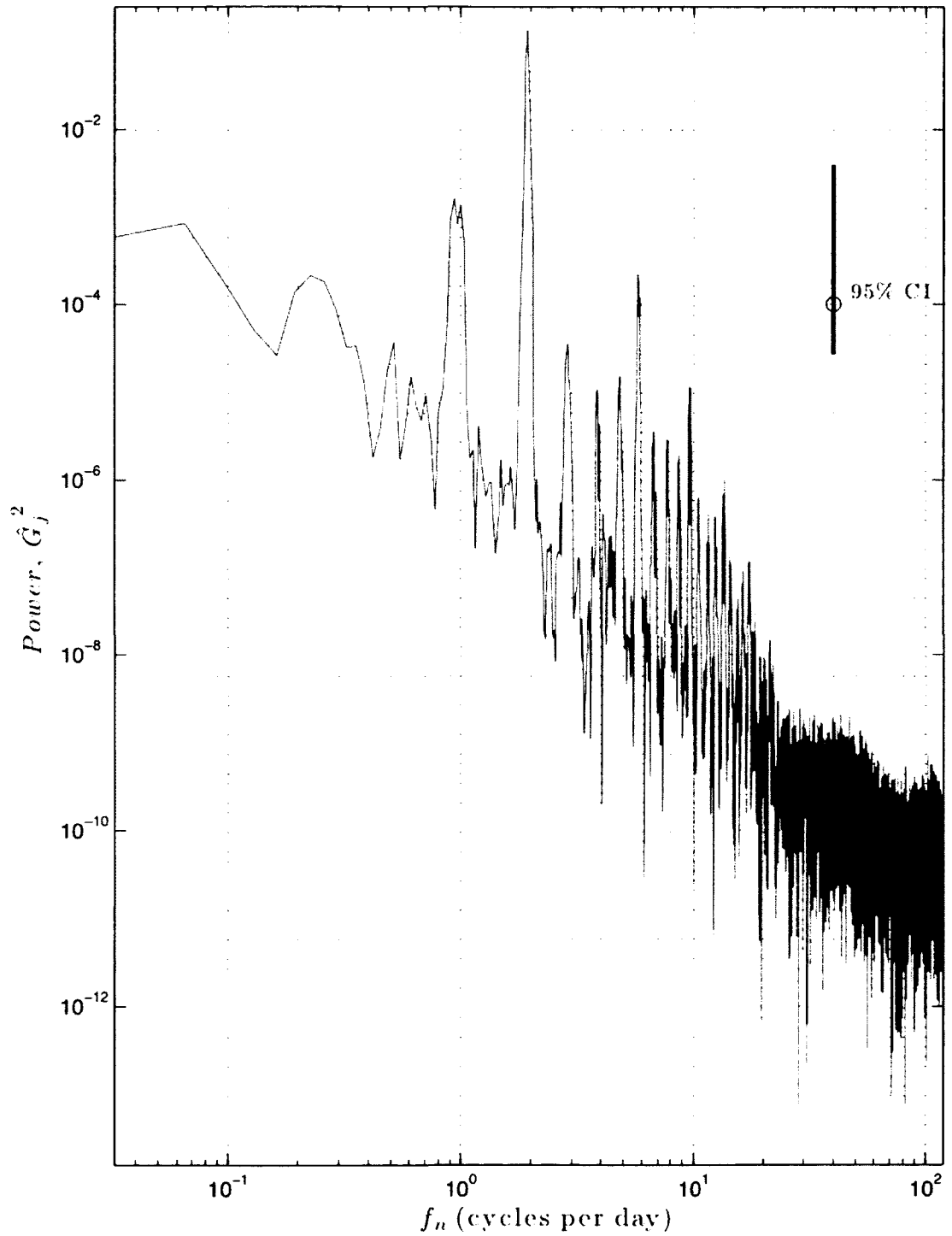
Figure 6.3.11: Water level power spectrum at Nannie Island, Great Bay, NH using observations from the SeaBird SeaCAT. Hanning window, N=7139. Representative comparison of tides at a random site in a past epoch. See Figure 6.3.9 for labels of the observable n-th order harmonics of the primary lunar tide, M.

Phase IV: Model Verification
Nannie Island, Great Bay, NH

Figure 6.3.12: Water level power spectrum at Nannie Island, Great Bay, NH using TCARI model predictions. Hanning window, N=7139. Representative comparison of tides at a random site in a past epoch. See Figure 6.3.9 for labels of the observable n-th order harmonics of the primary lunar tide, M.

Phase IV: Model Verification
Mooring in Great Bay, NH
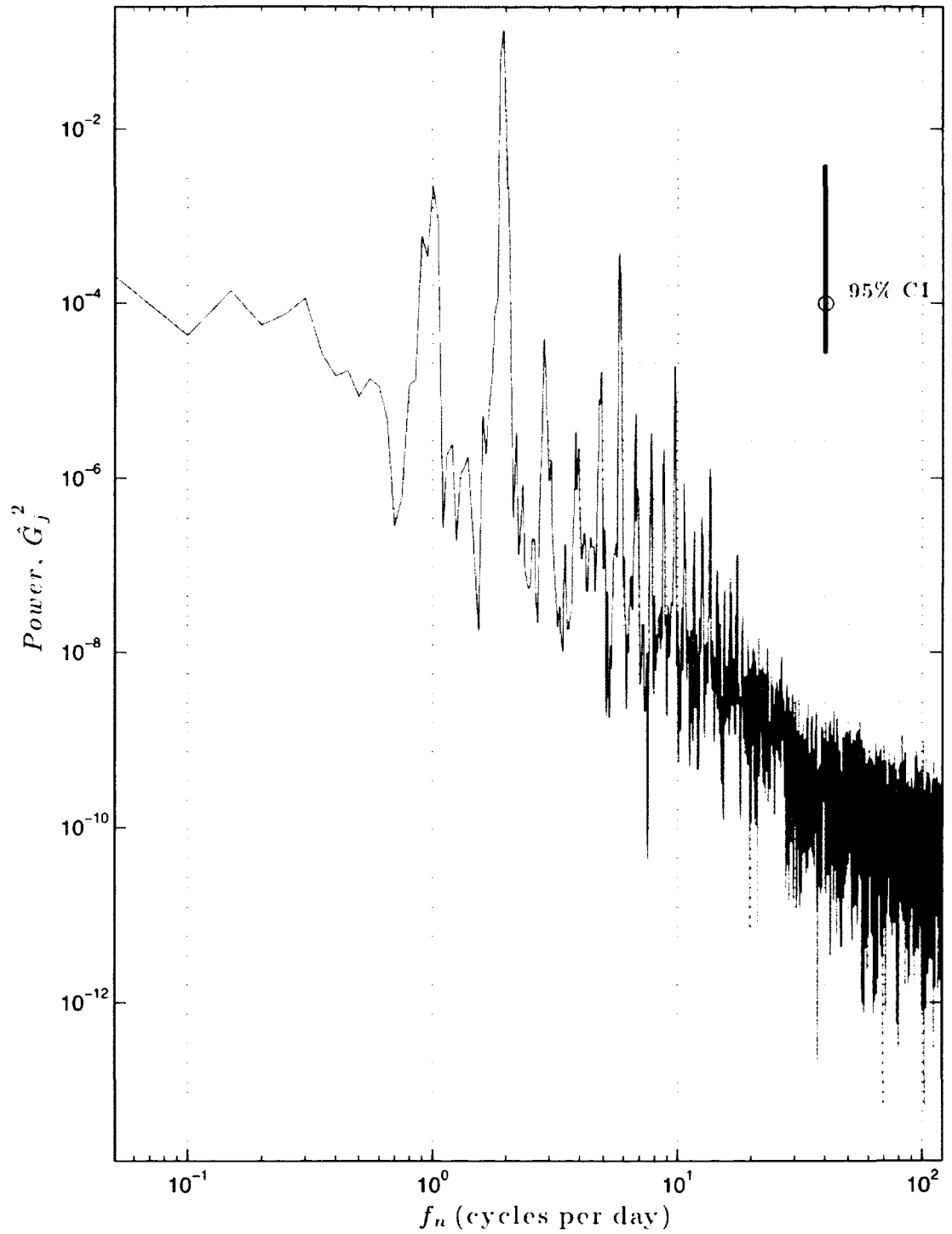
Figure 6.3.13: Water level power spectrum at the mooring site in Great Bay, NH using observations from the SeaBird SeaCAT. Hanning window, N=1799. Representative comparison of tides at the site of confluence in the TCARI error surface in a future epoch. See Figure 6.3.9 for labels of the observable n-th order harmonics of the primary lunar tide, M.

Phase IV: Model Verification
Mooring in Great Bay, NH

Figure 6.3.11: Water level power spectrum at the mooring site in Great Bay, NH using TCARI model predictions. Hanning window, N=4799. Representative comparison of tides at the site of confluence in the TCARI error surface in a future epoch. See Figure 6.3.9 for labels of the observable n-th order harmonics of the primary lunar tide, M.

159
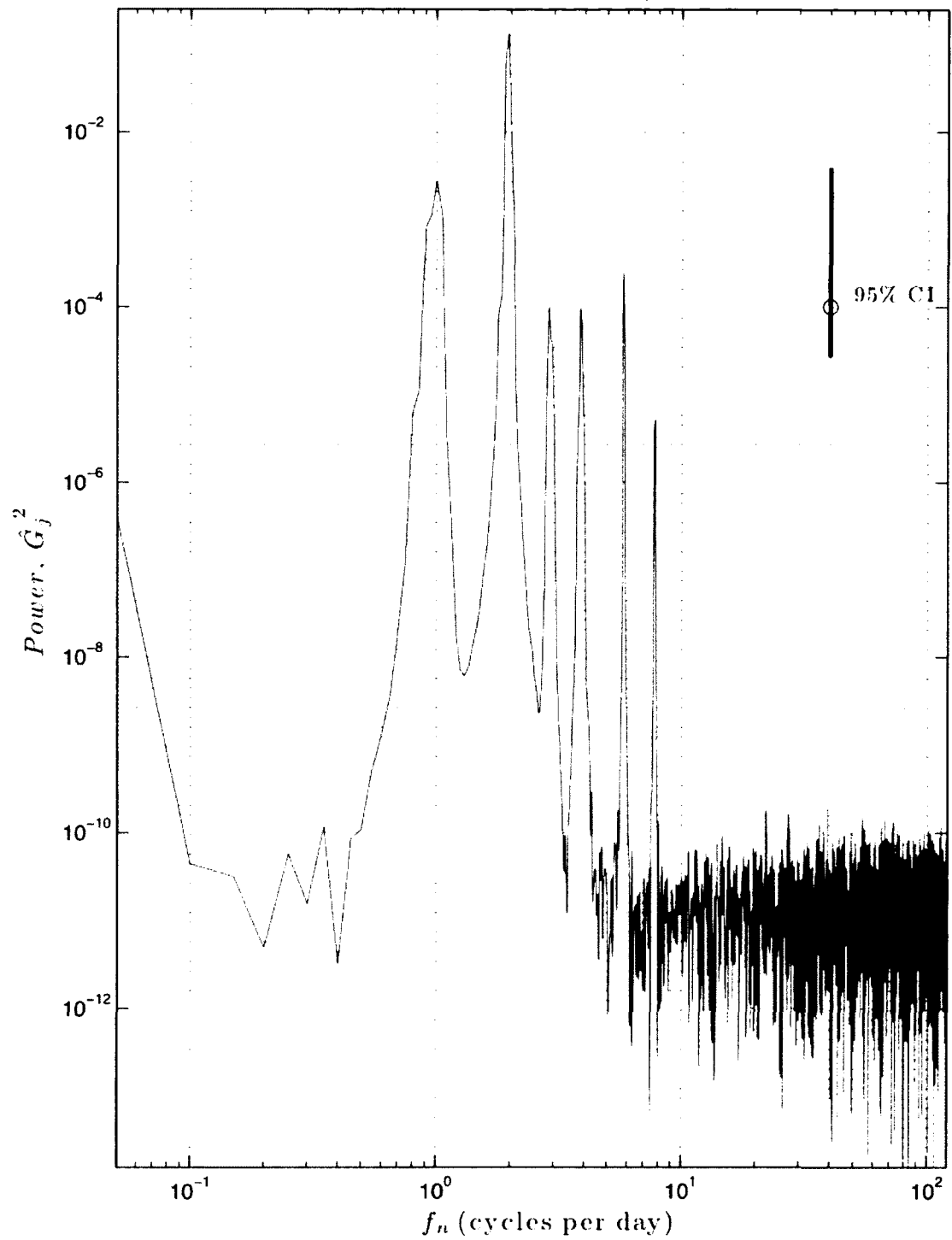
Phase IV: Model Verification
NCDC ref Nannie Island. Great Bay. NH
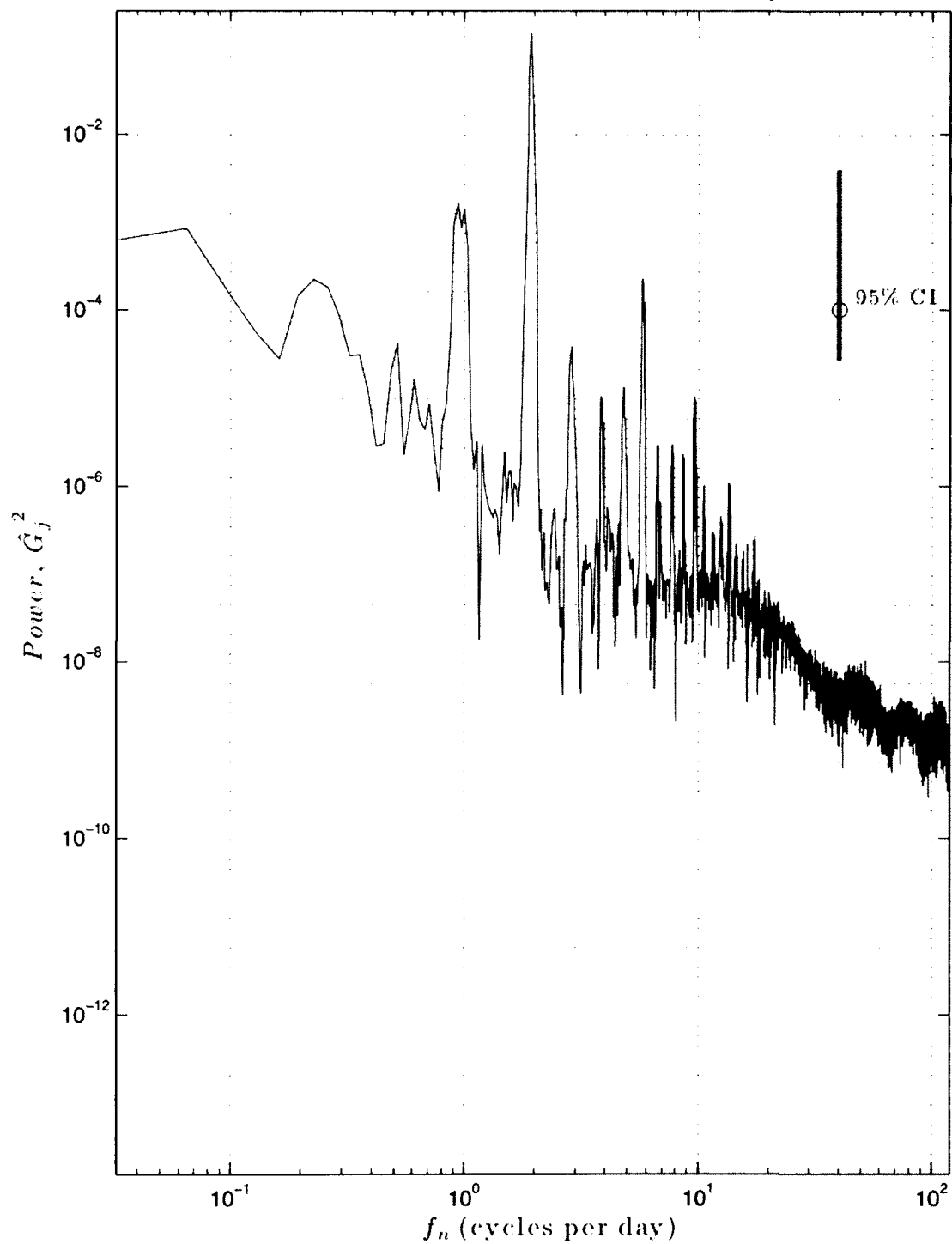
Figure 6.3.15: Atmospheric pressure power spectrum at Nannie Island, Great Bay, NH. Hanning window, N=7139. Representative comparison of tides at a random site in a past epoch. See Figure 6.3.9 for labels of the observable n-th order harmonics of the primary lunar tide, M.

Phase IV: Model Verification
NCDC ref Mooring in Great Bay, NH
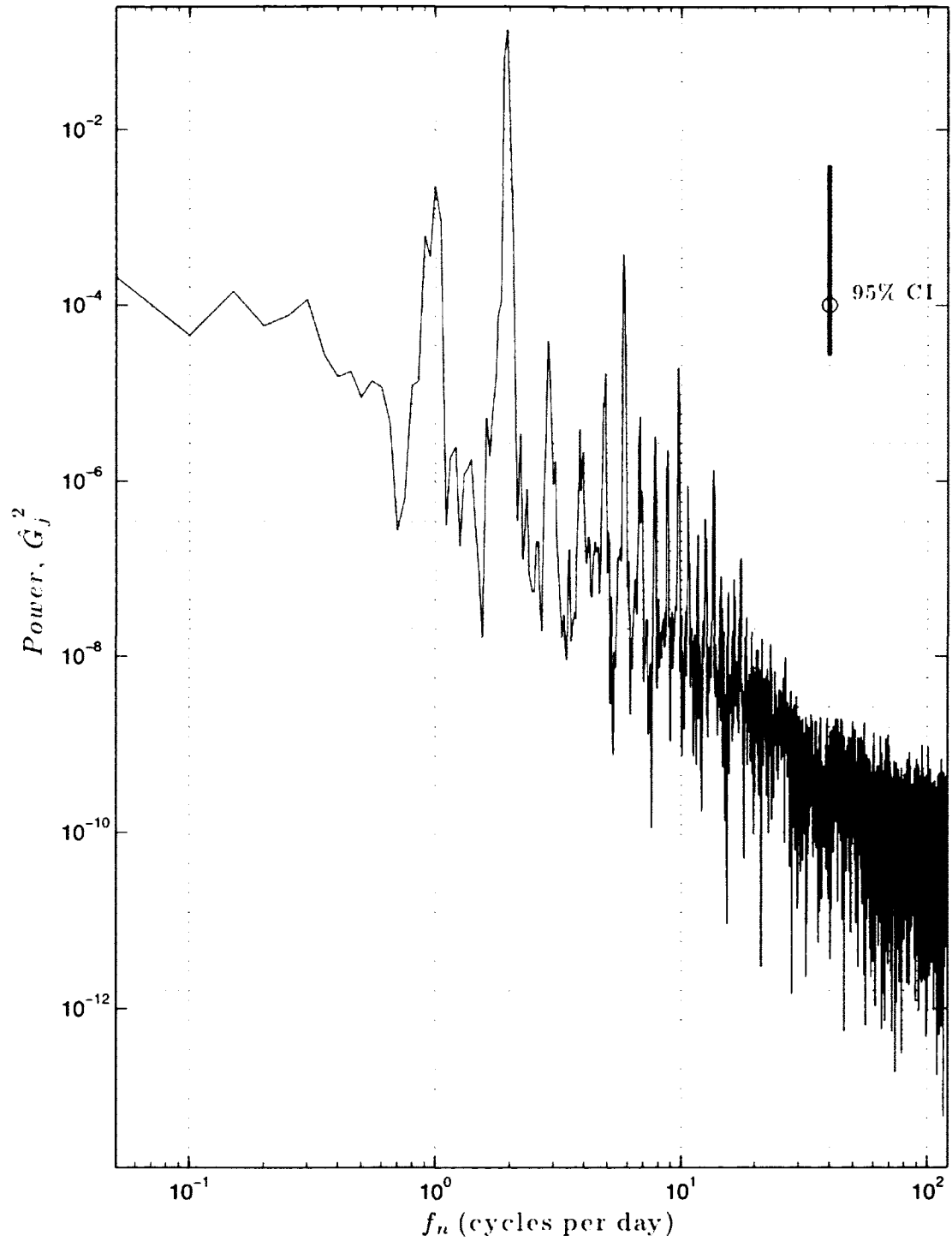
Figure 6.3.16: Atmospheric pressure power spectrum at the mooring site in Great Bay, NH. Hanning window, N=1799. Representative comparison of tides at the site of confluence in the TCARI error surface in a future epoch. See Figure 6.3.9 for labels of the observable n-th order harmonics of the primary lunar tide, M.

Phase IV: Model Verification
Squamscott River, Great Bay, NH
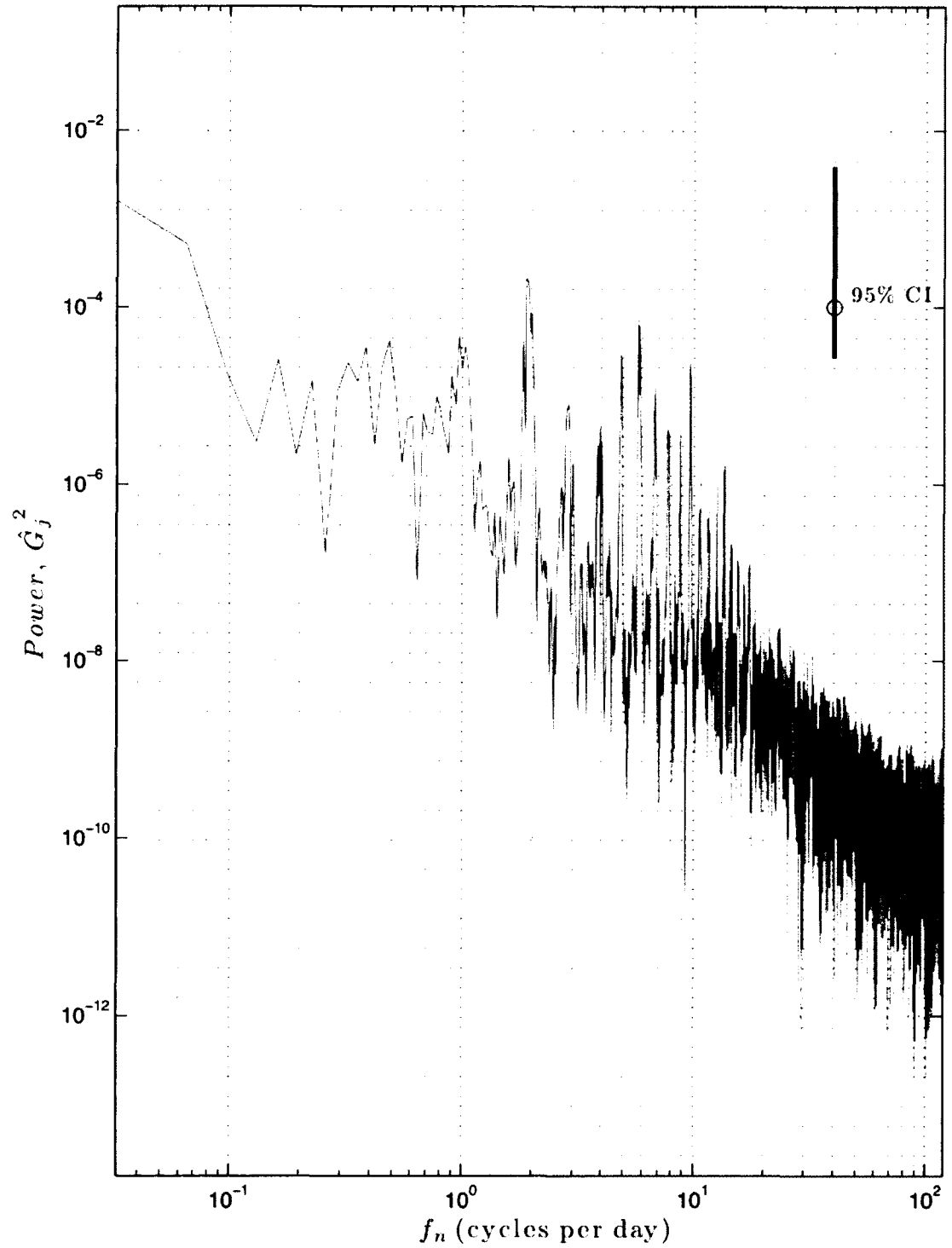
Figure 6.3.17: Residual water level (computed v. modeled) power spectrum at Squamscott River, Great Bay, NH. Hanning window, N=7439. Note the shallow-water constituents in comparison to Figure 6.3.9. See Figure 6.3.9 for labels of the observable n-th order harmonics of the primary lunar tide, M, for $n \geq 9$.

162

Phase IV: Model Verification
Squamscott River, Great Bay, NH

Figure 6.3.18: Residual water level (t_tide generated v. modeled) power spectrum at Squamscott River, Great Bay, NH. Hanning window, N=7439. Note the residual energy is primarily at the n-th diurnal tides, for $1 \le n \le 8$.

Phase IV: Model Verification
Nannie Island, Great Bay, NH
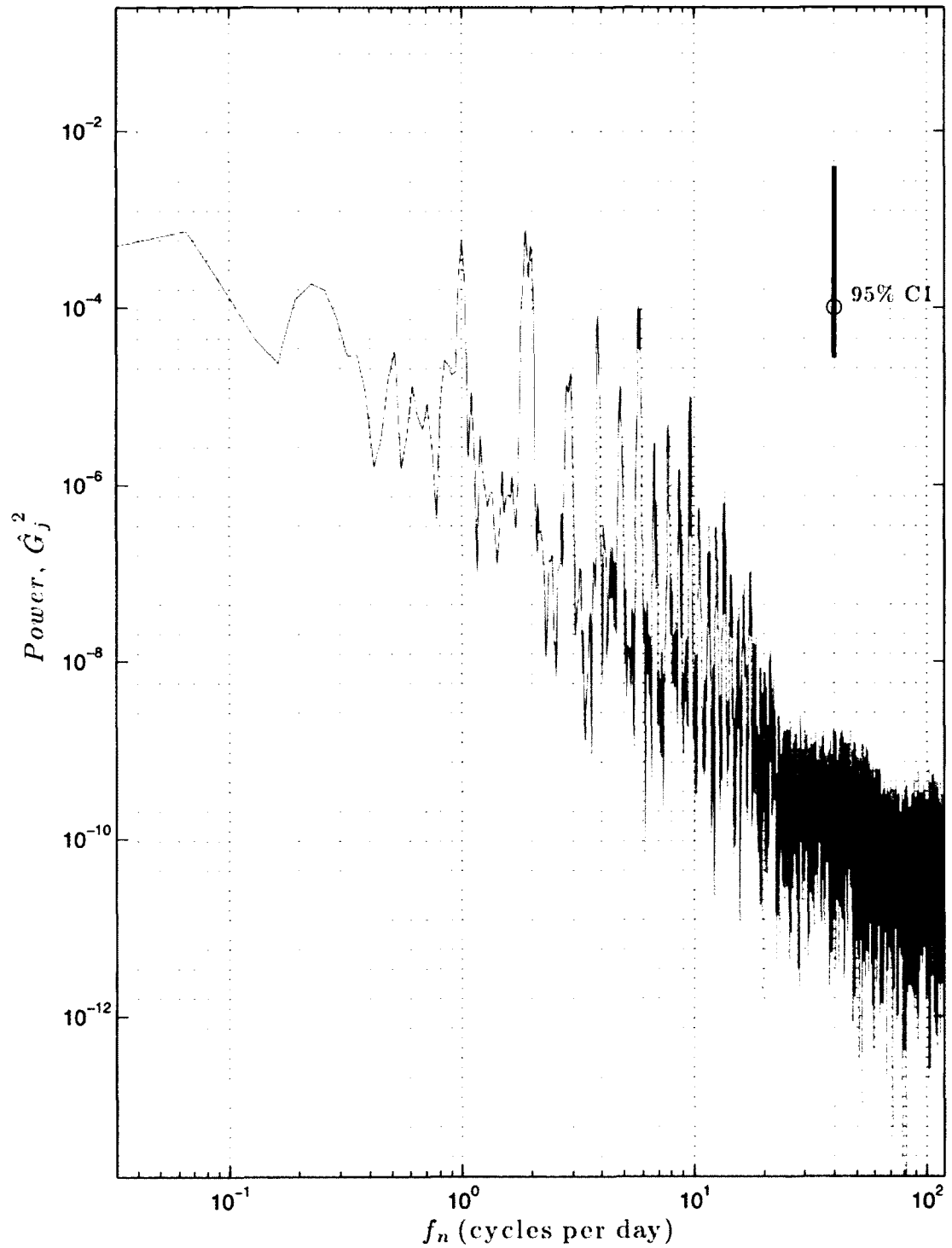
Figure 6.3.19: Residual water level (computed v. modeled) power spectrum at Nannie Island, Great Bay, NH. Hanning window, N=7439. Note the shallow-water constituents in comparison to Figure 6.3.11. See Figure 6.3.9 for labels of the observable n-th order harmonics of the primary lunar tide, M, for $n \geq 9$.

Phase IV: Model Verification
Nannie Island, Great Bay, NH
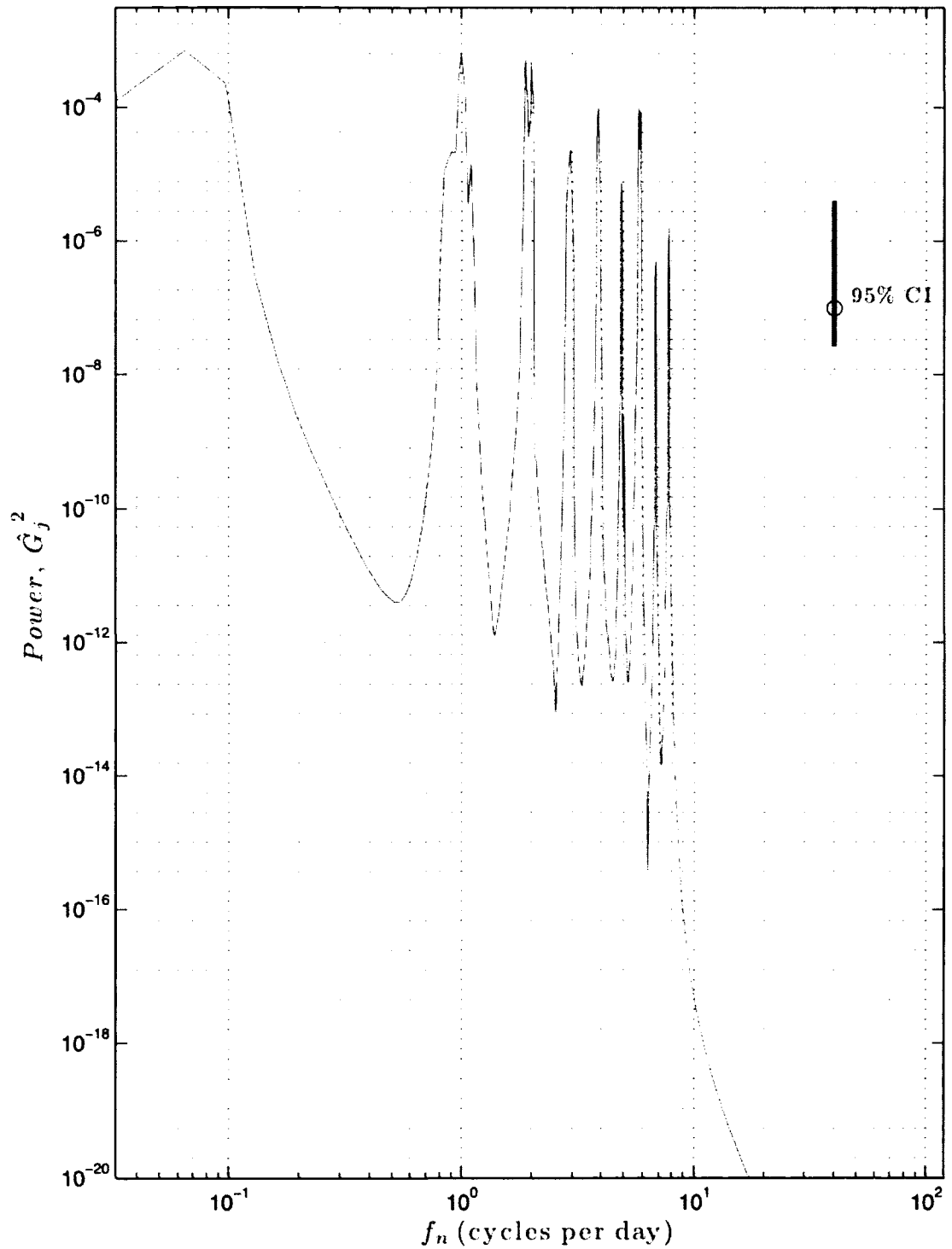
Figure 6.3.20: Residual water level (t_tide generated v. modeled) power spectrum at Nannie Island, Great Bay, NH. Hanning window, N=7139. Note the residual energy is primarily at the n-th diurnal tides, for $1 \le n \le 8$.

Phase IV: Model Verification
Mooring in Great Bay, NH
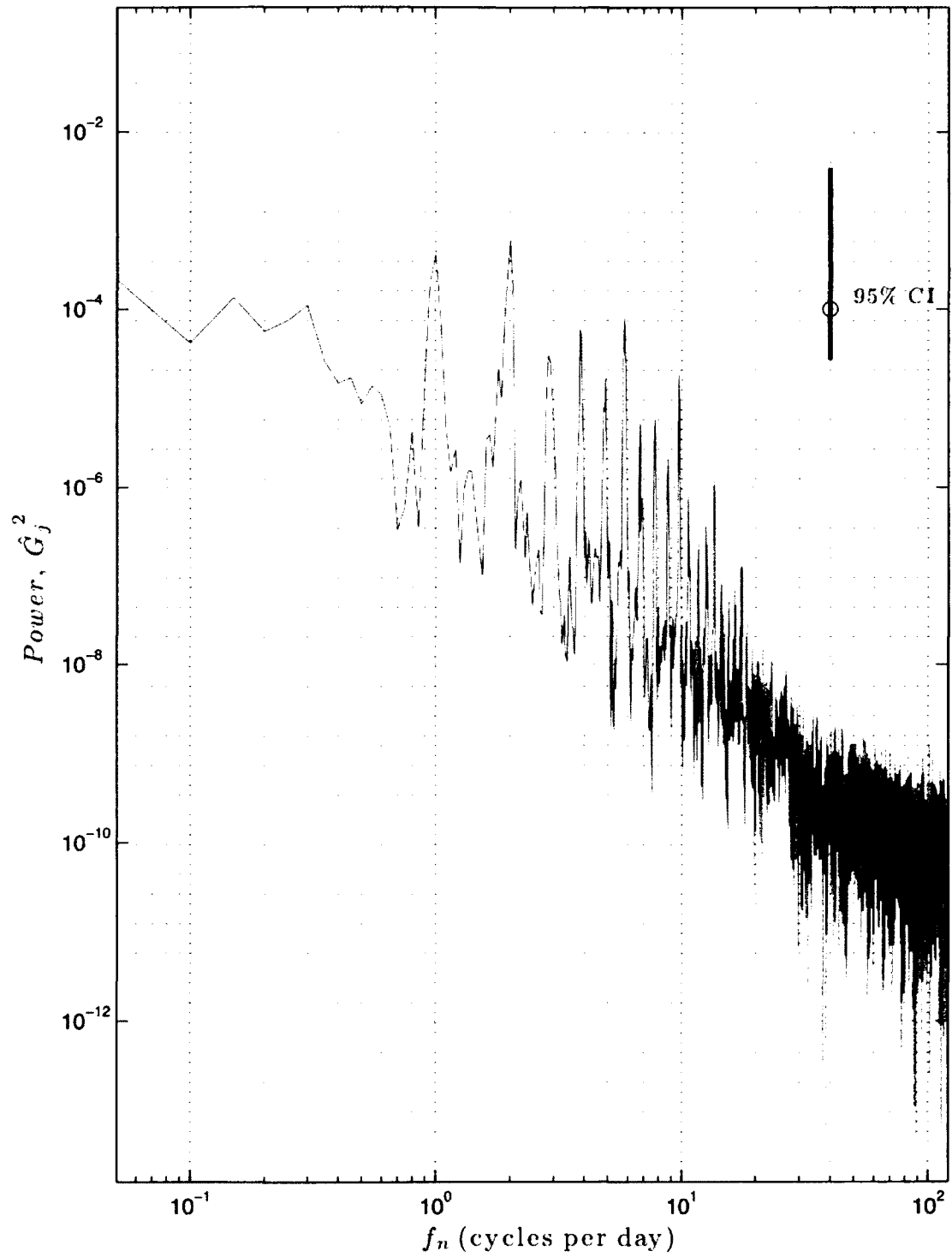
Figure 6.3.21: Residual water level (computed v. modeled) power spectrum at the mooring site in Great Bay, NH. Hanning window, N=4799. Note the shallow-water constituents in comparison to Figure 6.3.13. See Figure 6.3.9 for labels of the observable n-th order harmonics of the primary lunar tide, M, for $n \geq 9$.

Figure 6.3.22: Residual water level (t_tide generated v. modeled) power spectrum at the mooring site in Great Bay, NH. Hanning window, N=4799. Note the residual energy is primarily at the n-th diurnal tides, for $1 \leq n \leq 8$.

Phase IV: Model Verification
Squamscott River, Great Bay, NH
Smoothed Spectral Density
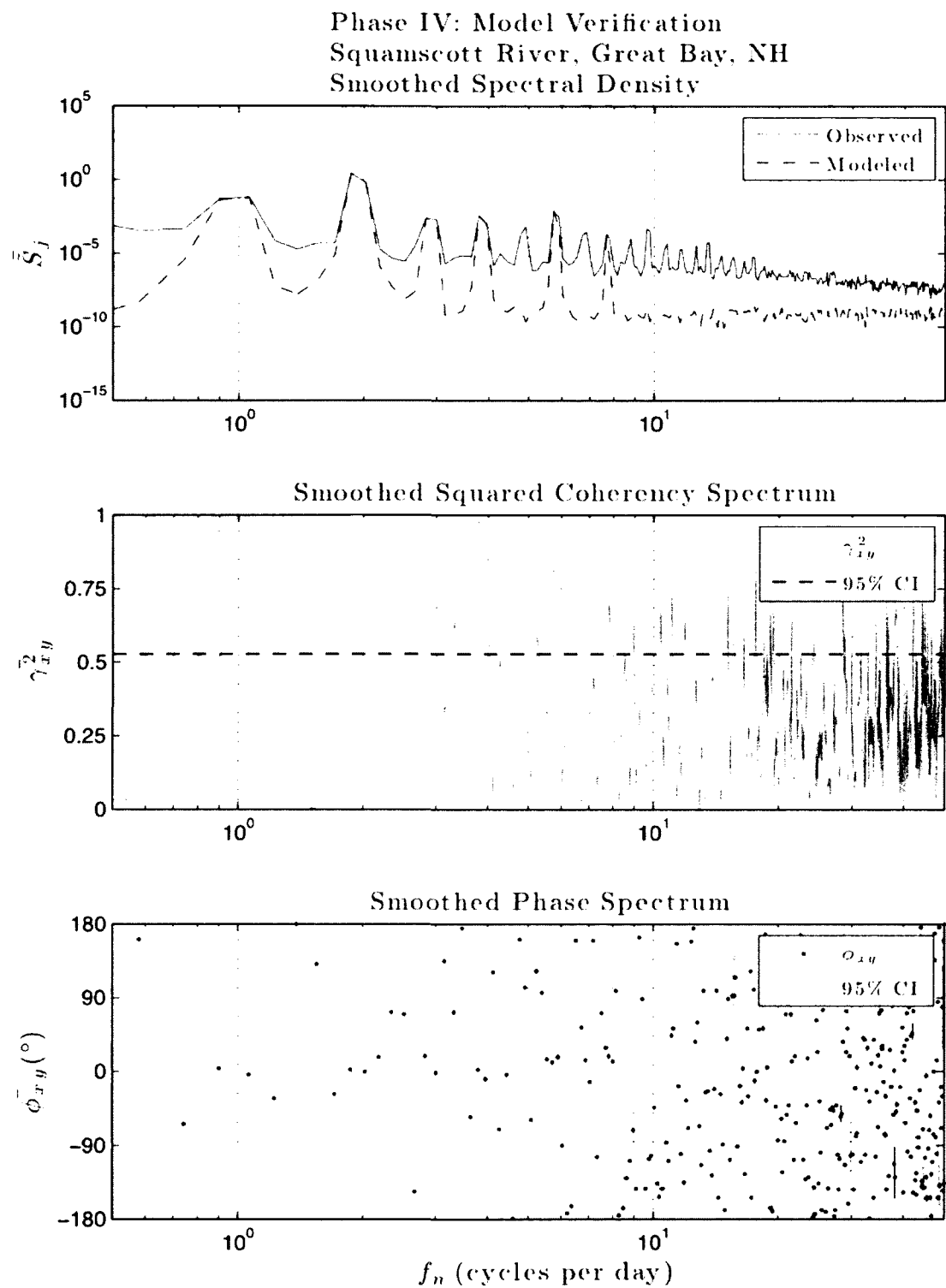
Figure 6.3.23: Smoothed spectral density, smoothed squared coherency spectrum, and smoothed phase spectrum from modeled v. computed water level at Squamscott River, Great Bay, NH using observations from the WaterLog MWWL. Band-averaged, DOF = 10, N=7440. Representative comparison of tides at a model control gauge in a future epoch.

Phase IV: Model Verification
Nannie Island, Great Bay, NH
Smoothed Spectral Density
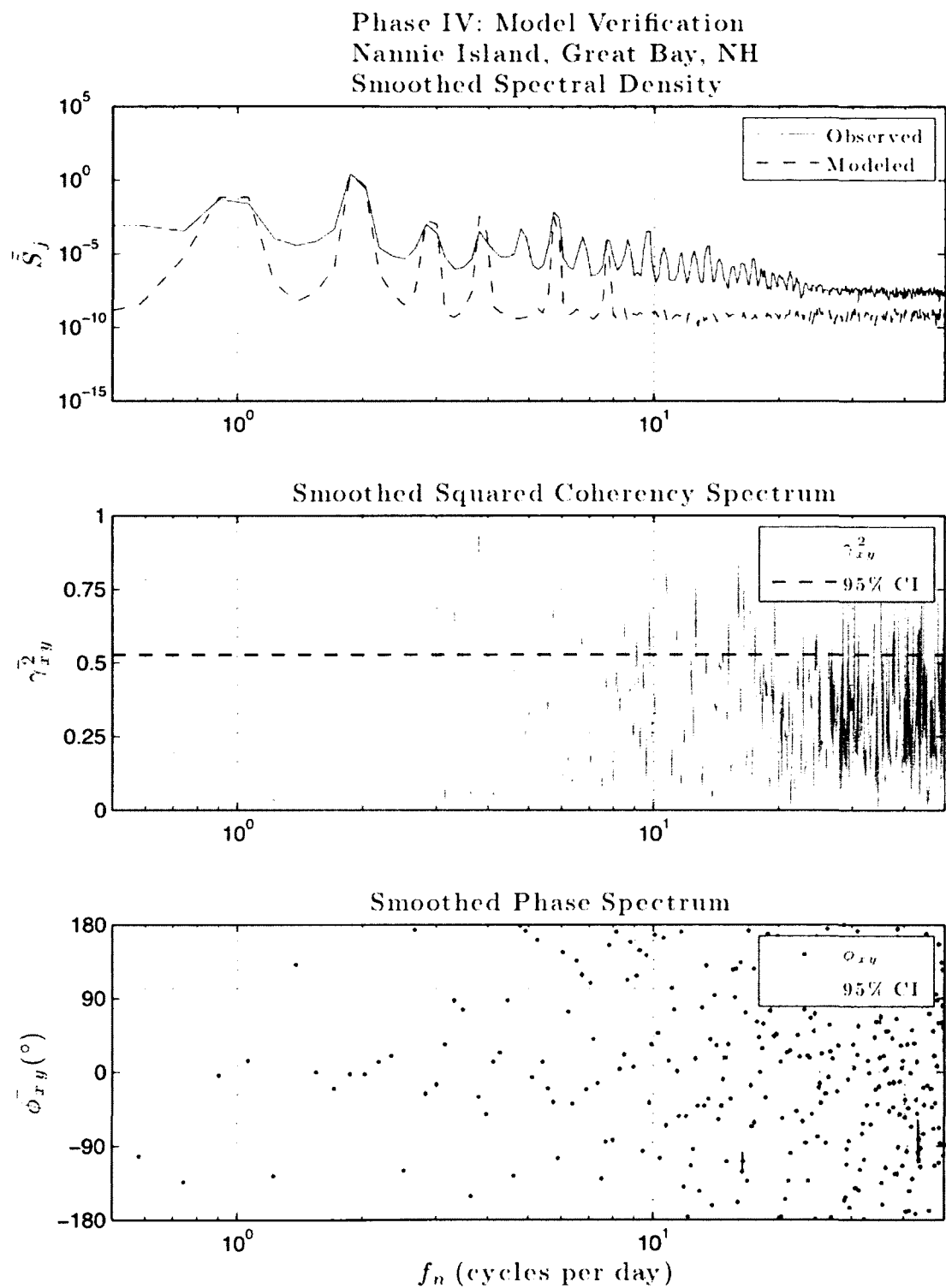
Figure 6.3.24: Smoothed spectral density, smoothed squared coherency spectrum, and smoothed phase spectrum from modeled v. computed water level at Nannie Island, Great Bay, NH using observations from the SeaBird SeaCAT. Band-averaged, DOF = 10, N=7440. Representative comparison of tides at a random site in a past epoch.

Phase IV: Model Verification
Mooring in Great Bay, NH
Smoothed Spectral Density

Smoothed Squared Coherency Spectrum

Smoothed Phase Spectrum
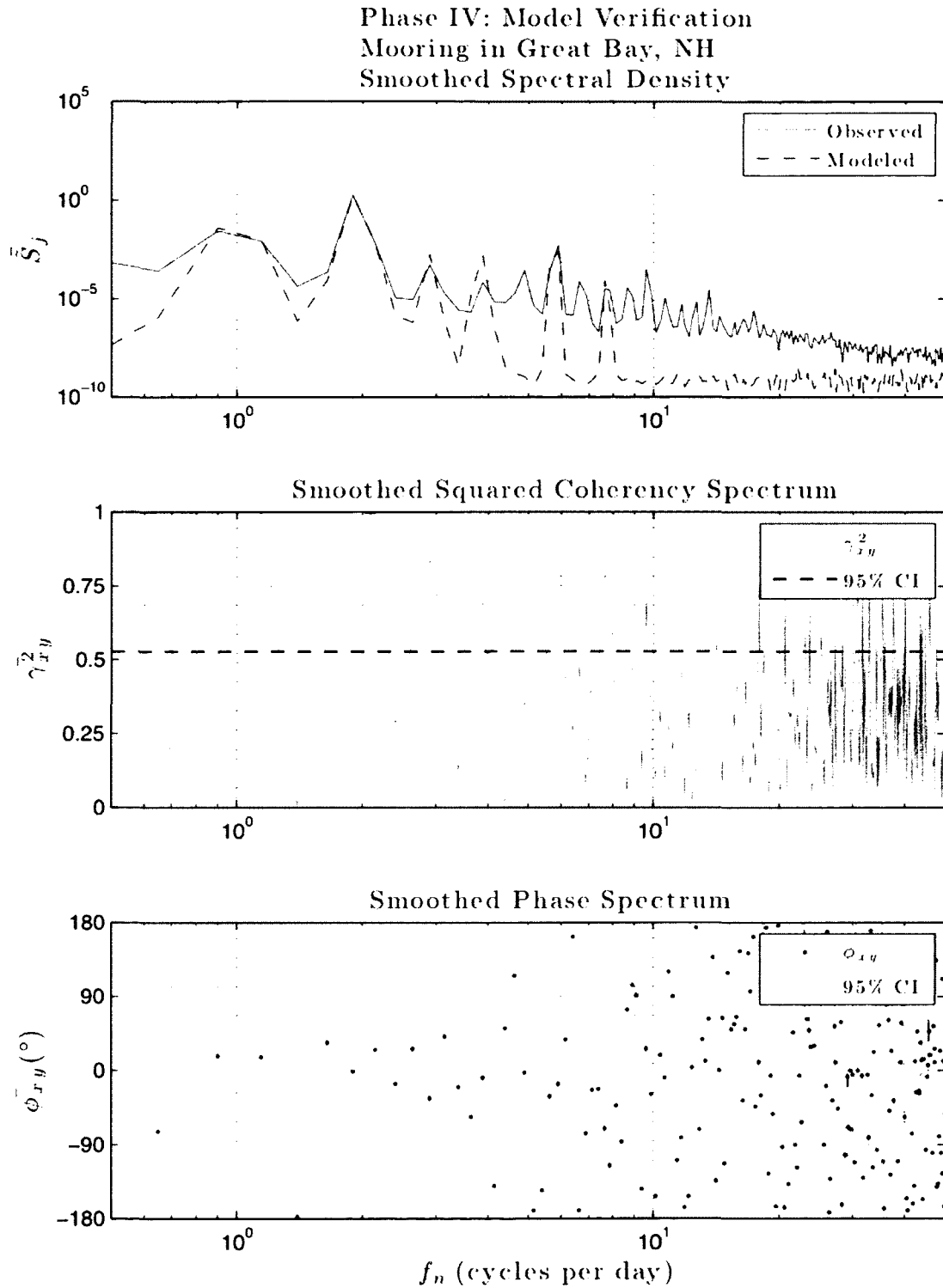
Figure 6.3.25: Smoothed spectral density, smoothed squared coherency spectrum, and smoothed phase spectrum from modeled v. computed water level at the mooring site in Great Bay, NH using observations from the SeaBird SeaCAT. Band-averaged, DOF = 10, N=4800. Representative comparison of tides at the site of confluence in the TCARI error surface in a future epoch.

VII. CONCLUSION

The Great Bay, an estuarine fixture in southern New Hampshire, has been the subject of surveys and research dating back nearly two centuries. The historic accounts— Strough (1913), Hoskinson and Le Lacheur (1929), Reed (1955), and Swenson *et. al.* (1977)— have fallen short of providing complete and comprehensive knowledge of the tides as they relate to the Bay. Past attempts at producing a model representing the tides in the Bay— Swift and Brown (1983), Ip *et. al.* (1998), Ertürk *et. al.* (2002), and McLaughlin *et. al.* (2002)— had met with only modest success. There existed a need for a comprehensive tide model; as an aid to navigation, both commercial and recreational, and to simply further the understanding of the nature of the Great Bay.

This study has produced a satisfactory tide model for the Bay. Prior to data collection in the Bay and with an odd variety of tide gauges, a thorough calibration of each to a control tide gauge was conducted. Through a comprehensive study of the tides at four strategic locations within the Bay, the collected data was processed and tidal datums and ranges, lunitidal intervals, and tidal harmonic constituents were derived. Using a set of pre-existing tools, a TCARI model of the tides in the Bay was developed.

A posteriori model verification was conducted at three locations in the Bay, each with different spatial and temporal characteristics. Maximum, mean, and standard deviation of the residuals between the observed and modeled water levels were computed. Comparisons were then made to existing TCARI model accuracy estimates. (Hess *et. al.*,

2004) The result of all three Phase 4 comparisons confirmed the newly created tide

model as being statistically representative of the tidal regime in the Great Bay.

While it is unlikely further large shipping operations will be commenced through the

Bay, the applications of a completed and verified tidal model are still many. Ongoing

bathymetric re-mapping of the Bay will likely make use of this tidal model to reproject

the data to chart datum (MLLW). Commercial and recreational vessels operating in and

through the Bay can all benefit from both a modern bathymetric chart and more accurate

tidal predictions. Likewise, academic research projects conducted by various groups

within the Bay can make use of more accurate tidal predictions.

In retrospect, particular aspects of the research should have been conducted differently.

On the top of the list would have been changes in the instrumentation. First, only two

types of tide gauges would have been used, dependent upon available infrastructure: 1.

GPS Buoy w/ SeaBird SeaCAT C-T-P Recorder; and 2. WaterLog MWWL. The GPS

Buoy would use *Real-Time Kinematic* (RTK) as opposed to *Post-Processed Kinematic*

(PPK) -GPS and would include a barometric pressure sensor. In addition, a SeaBird

SeaCAT C-T-P Recorder would be bottom mounted on the mooring. An attached

barometric pressure sensor would allow for localized pressure observations with a much

shorter sampling interval (as compared to the records from the NCDC). A tide gauge of

this nature would be capable of recording water level changes in locations without

supporting infrastructure. Water level variations could be observed relative to the

SeaBird SeaCAT and simultaneously referenced to the WGS84 ellipsoid and NAVD88

172

datum. The second type of tide gauge would be the pre-described WaterLog MWWL. So long as the proper infrastructure is available, the WaterLog MWWL requires much less maintenance as no part of the gauge is submerged in water.

The next facet of the study that should have been done differently would be the epochs in which each phase of the study was conducted. As tide gauges became available piecemeal and due to time constraints on the research, the order of the phases of study for each tide gauge and tide station was not always sequential. Ideally, calibration of all the tide gauges during Phase 1 should have been conducted in the same epoch and prior to Phase 2. Also, a comparison not only to the control gauge but also to each other could have been made for further statistical analysis. Likewise, during Phase 2 of the study, all data collection at the four tide stations should have been conducted in the same epoch and after Phase 1. Further, the calibration record length for each tide gauge should have been a minimum of 30 days, while the Phase 2 record lengths should have been no less than one year.

In relation to the TCARI model, the tidal harmonic constituents used should more accurately reflect the environment in which the model represents. The general NOAA CO-OPS set is really not representative of the shallow-water estuarine environment of the Great Bay. The loss of tidal energy in the model is apparent in both the residual power spectra analysis and the cross-spectral analyses during the model verification phase of study. Additionally, the boundary that was submitted to CO-OPS for TCARI grid generation was the shoreline that represents the *interpreted MHW line*. (Hicks *et. al.*,

2000; NGS, 2009) While this may be suitable for coastal or heavily channelized bodies of water, the Great Bay is composed of large mudflats that are flooded and exposed during the tidal cycle. As these mudflats are submerged and uncovered the morphology of the Bay changes, which would alter the tidal amplitude and phase of the tides being modeled. This fact may lead future modeling efforts to using a separate boundary, each representing a different tidal datum line (*e.g.* MLLW, MTL, MHHW, etc).

Modeling tides (or any other natural phenomena) in the Great Bay may be a moving target. Data collection and model implementation may need to be repeated on a periodic basis in order to cope with such a dynamic environment. However, a move to a true hydrodynamic model may be able to better account for this. Taking into account the bathymetry of the water body, especially factors that directly influence the tidal regime in shallow-water environments, the ability to represent what is really happening in the Great Bay might be greatly improved.

LIST OF REFERENCES

Airy, G.B., 1847, Tides and Waves, in Smedley, E., Rose, H.J and Rose, H.J. (eds.), *Encyclopædia Metropolitana*, William Clowes and Sons, London, v. 5, p. 241-396.

The American Heritage Dictionary, 2011, The American Heritage Dictionary of the English Language, 5th Ed., Houghton Mifflin Harcourt Publishing Company, Boston, 2112p. Copyright © 2011 by Houghton Mifflin Harcourt Publishing Company. Reproduced by permission from the American Heritage Dictionary of the English Language, Fifth Edition.

Aquatrak, 2006, Aquatrak Model 4100/ 4110 Series User's Guide, Aquatrak Corporation, Sanford, FL, 53p.

Brown, E.W., 1896, An Introductory Treatise on the Lunar Theory, C.J. Clay and Sons, London, 292p.

Cartwright, D.E., 1999, Tides: A Scientific History, Cambridge University Press, Cambridge, 292p.

Cartwright, D.E. and Edden, A.C., 1973, Corrected tables of tidal harmonics. Geophysical Journal of the Royal Astronomical Society, v. 33, p. 253-264.

Cisternelli, M., Martin, C., Gallagher, B. and Brennan, R., 2007, A comparison of discrete tidal zoning and tidal constituent and residual interpolation (TCARI) methodologies for use in hydrographic sounding reduction, Center for Operational Oceanographic Products and Services (CO-OPS), National Oceanic and Atmospheric Administration (NOAA), Silver Spring, MD, 9p.

Coastal Zone Management Act of 1972, U.S. Code, Title 16: Conservation, Chapter 33: Coastal Zone Management, Sections 1451-1466.

CO-OPS, 2003, NOAA Special Publication 2: Computational Techniques for Tidal Datums Handbook, Center for Operational Oceanographic Products and Services (CO-OPS), National Oceanic and Atmospheric Administration (NOAA), Silver Spring, MD, 113p.

CO-OPS, 2008, Environmental measurement systems sensor specifications and measurement algorithm, Center for Operational Oceanographic Products and Services (CO-OPS), National Oceanic and Atmospheric Administration (NOAA), Silver Spring, MD, 5p.

175

CO-OPS, 2009, NOAA Technical Report NOS CO-OPS 053: Sea Level Variations of the United States, 1854-2006, Center for Operational Oceanographic Products and Services (CO-OPS), National Oceanic and Atmospheric Administration (NOAA), Silver Spring, MD, 194p.

CO-OPS, 2010, Station ID 8422687 tide predictions: Boston and Maine railroad bridge at the Squamscott River, NH, Center for Operational Oceanographic Products and Services (CO-OPS), National Oceanic and Atmospheric Administration (NOAA), Silver Spring, MD.

CO-OPS, 2011, NOAA Technical Report NOS CO-OPS 061: Test and Evaluation Report, Limited Acceptance of the Design Analysis WaterLog H-3611i Microwave Radar Water Level Sensor, Center for Operational Oceanographic Products and Services (CO-OPS), National Oceanic and Atmospheric Administration (NOAA), Silver Spring, MD, 97p.

Crawford, W.R., 1982, Analysis of fortnightly and monthly tides. International Hydrographic Review, v. 59, no. 1, p. 131-141.

Darwin, G.H., 1883, Harmonic analysis of tidal observations. in Report of the 53rd Meeting of the British Association for the Advancement of Science, John Murray, London, p. 49-117.

Darwin, G.H., 1898, The Tides and Kindred Phenomena in the Solar System: The Substance of Lectures Delivered in 1897 at the Lowell Institute, Boston, Massachusetts, The Riverside Press, Cambridge, MA, 379p.

Doodson, A.T., 1921, The harmonic development of the tide-generating potential. Proceedings of the Royal Society of London, Series A, v. 100, no. 704, p. 305-329.

Doodson, A.T., 1924, Perturbations of harmonic tidal constants. Proceedings of the Royal Society of London, Series A, v. 106, no. 739, p. 513-526.

Doodson, A.T., 1928, The analysis of tidal observations. Proceedings of the Royal Society of London, Series A, v. 227, p. 223-279.

Doodson, A.T. and Warburg, H.D., 1941, Admiralty Manual of Tides, His Majesty's Stationary Office, London, 270p.

Druck, 2001, Druck RPT410F Barometric Pressure Sensor User Guide, Campbell Scientific Ltd., 18p.

Ertürk, Ş.N., Bilgili, A., Swift, M.R., Brown, W.S., Çelikkol, B., Ip, J.T.C. and Lynch, D.R., 2002, Simulation of the Great Bay estuarine system: Tides with tidal flats wetting and drying. Journal of Geophysical Research, v. 107, no. c5, p. 6.1-6.9.

Ferrel, W.E., 1874, Tidal Researches, Appendix to Coast Survey Report for 1873, United States Coast Survey, Washington, D.C., 268p.

Ferrel, W.E., 1878, Discussion of Tides in Penobscot Bay, Maine, Appendix to Coast Survey Report of 1878, United States Coast Survey, Washington, D.C., 343p.

Foreman, M.G.G. and Neufeld, E.T., 1991, Harmonic tidal analyses of long time series. International Hydrographic Review, v. 66, no. 1, p. 85-108.

Fourier, J.B.J., 1878, The Analytical Theory of Heat, *trans.* Freeman, A., The University Press, Cambridge, UK, 466p.

Garland, Jeff, 2011, Boost C++ Libraries: Date_Time, v. 1.47.0, CrystalClear Software, Inc., Phoenix, Arizona. http://www.boost.org.

GRASS Development Team, 2010, Geographic Resources Analysis Support System (GRASS) Software, Version 6.4.0, Open Source Geospatial Foundation. http://grass.osgeo.org.

Harris, R.A., 1898, Manual of Tides: Part I, United States Coast and Geodetic Survey (USC&GS), Treasury Department, Washington, D.C., 262p.

Hawking, S. (ed.), 2000, On the Shoulders of Giants: The Great Works of Physics and Astronomy, reprint of Newton, I., 1687, *Philosophiae Naturalis Principia Mathematica*, Running Press, London, p. 733-1160.

Hess, K., Schmalz, R., Zervas, C. and Collier, W., 2004, NOAA Technical Report NOS CS 4: Tidal Constituent and Residual Interpolation (TCARI): A New Method for the Tidal Correction of Bathymetric Data, National Ocean Service (NOS), National Oceanic and Atmospheric Administration (NOAA), Silver Spring, MD, 112p.

Hicks, S.D., Silcox, R.L., Nichols, C.R., Via, B., McCray, E.C. and Zervas, C., 2000, Tide and Current Glossary, Center for Operational Oceanographic Products and Services (CO-OPS), National Oceanic and Atmospheric Administration (NOAA), Silver Spring, MD, 34p.

Hoskinson, A.J. and Le Lacheur, E.A., 1929, Tides and Currents in Portsmouth Harbor: Special Publication No. 150, United States Coast and Geodetic Survey (USC&GS), Department of Commerce, Washington, D.C., 98p.

Ip, J.T.C., Lynch, D.R. and Friedrichs, C.T., 1998, Simulation of estuarine flooding and dewatering with application to Great Bay, New Hampshire. Estuarine, Coastal and Shelf Science, v. 47, p. 119-141.

Lagrange, J.L., 1869, *Mémoire sur la Théorie du mouvement des fluides*, (in French), in *Œvres de Lagrange*, M.J.-A. Serret, Paris, v. 4, p. 695-748.

Legendre, A.M., 1785, *Recherches sur l'Attraction des Spheroides Homogènes*, (in French), in *Mémoires de mathématique et de physique*, l'*Académie des Sciences*, Paris, v. 10, p. 411-434.

McLaughlin, J.W., Bilgili, A. and Lynch, D.R., 2002, Numerical modeling of tides in the Great Bay estuarine system: Dynamical balance and spring-neap residual modulation. Estuarine, Coastal and Shelf Science, v. 57, p. 283-296.

Moritz, H., 1980, Geodetic Reference System 1980. Journal of Geodesy, v. 54, no. 3, p. 395-405.

NGS, 2009, NOAA Shoreline Data Explorer, National Geodetic Survey (NGS), National Oceanic and Atmospheric Administration (NOAA), Silver Spring, MD. http://beta.ngs.noaa.gov/shoreline_raster/.

OCS, 2005, Raster Navigational Chart 13285: Portsmouth to Dover and Exeter, Current Edition: 11, Print Date: 7/1/2005, Office of Coast Survey (OCS), National Oceanic and Atmospheric Administration (NOAA), Silver Spring, MD.

OCS, 2011, Raster Navigational Chart 13283: Portsmouth Harbor: Cape Neddick Harbor to Isles of Shoals, Current Edition: 21, Print Date: 3/1/2011, Office of Coast Survey (OCS), National Oceanic and Atmospheric Administration (NOAA), Silver Spring, MD.

Onset, 2011, HOBO U20 Water Level Data Logger— U20-001-02 Detailed Specifications, Onset Computer Corporation, Cape Cod, MA.

Park, Dave (ed.), 1999, Waves, Tides and Shallow-water Processes, Butterworth-Heinemann, Oxford, 227p.

Parker, B.B., 2007, NOAA Special Publication 3: Tidal Analysis and Prediction, Center for Operational Oceanographic Products and Services (CO-OPS), National Oceanic and Atmospheric Administration (NOAA), Silver Springs, MD, 378p.

Paroscientific, 2005, Intelligent Transmitters: Series 1000, 6000 & 9000 Data Sheet, Paroscientific, Inc., Redmond, WA, 4p.

Pawlowicz, R., Beardsley, B. and Lentz, S., 2002, Classical tidal harmonic analysis including error estimates in MATLAB using T_TIDE. Computers and Geosciences, v. 28, p. 929-937.

Reed, C.R., 1955, Descriptive Report H-8093, United States Coast and Geodetic Survey (USC&GS), Department of Commerce, Washington, D.C., 29p.

SeaBird, 2007, SBE 16plus SEACAT User's Manual, Version #018, SeaBird Electronics, Inc., Bellevue, WA, 89p.

SeaBird, 2010, Application Note No. 27Druck: Minimizing Strain Gauge Pressure Sensor Errors, SeaBird Electronics, Inc., Bellevue, WA, 4p.

SeaBird, 2011, SBE 37-SM MicroCAT User's Manual, Version #034, SeaBird Electronics, Inc., Bellevue, WA, 75p.

Schureman, P., 1924, Special Publication No. 98: A Manual of the Harmonic Analysis and Prediction of Tides, United States Coast and Geodetic Survey (USC&GS), Department of Commerce, Washington, D.C., 431p.

Schureman, P., 1958, Special Publication No. 98: A Manual of the Harmonic Analysis and Prediction of Tides [Revised (1940) Edition; reprinted 1958 with corrections], United States Coast and Geodetic Survey (USC&GS), Department of Commerce, Washington, D.C., 332p.

Simon, P., 1820, Œvres Complétes de Laplace: Théorie Analytique des Probabilités, 3rd Ed., (in French), Mme Ve Courcier, Paris, 643p.

Simon, P., 1829, Mécanique Céleste, trans. Nathaniel Bowditch, Hilliard, Gray, Little and Watkins, Boston, MA, 747p.

Sommers, S. and Wade, T., 2006, A to Z GIS: An Illustrated Dictionary of Geographic Information Systems, ESRI Press, Redlands, CA, 288p.

Strough, R.P., 1913, Descriptive Report H-3524/ H-3525, United States Coast and Geodetic Survey (USC&GS), Department of Commerce, Washington, D.C., 22p.

Sutron, 2006, NOS Tide Station User's Manual, Version 1.2, Sutron Corporation, Sterling, VA.

Swenson, E., Brown, W.S. and Trask, R., 1977, Great Bay Estuarine Field Program, 1975 Data Report, Part 1: Currents and Sea Levels. University of New Hampshire Sea Grant Report UNH-SG-157, 109p.

Swift, M.R. and Brown, W.S., 1983, Distribution of bottom stress and tidal energy dissipation in a well-mixed estuary. Estuarine, Coastal and Shelf Science, v. 17, p. 297-317.

Thomson, W. and Roberts, E., 1872, Report of the committee appointed for the purpose of promoting the extension, improvement, and harmonic analysis of tidal observations, in Report of the 42nd Meeting of the British Association for the Advancement of Science, John Murray, London, p. 355-395.

Thomson, W. and Tait, P.G., 1888, A Treatise on Natural Philosophy: Part I, Cambridge University Press, Cambridge, UK, 508p.

USC&GS, 1913, Smooth Sheet: New Hampshire, Piscataqua River, Great Bay (Register No. 3525), United States Coast and Geodetic Survey (USC&GS), Department of Commerce, Washington, D.C.

USC&GS, 1954, Smooth Sheet: New Hampshire, Portsmouth, Great Bay and Squamscott River (Hydrographic Survey No. 8093), United States Coast and Geodetic Survey (USC&GS), Department of Commerce, Washington, D.C.

WaterLog, 2011, Model H-3611 SDI-12 Radar Water Level Sensor Owner's Manual, Version 1.3, Design Analysis Associates, Inc., Logan, UT, 43p.

Wolf, P.R. and Brinker, R.C., 1994, Elementary Surveying, 9th Ed., Harper Collins College Publishers, New York, 760p.

APPENDICES

APPENDIX A: HISTORIC DATA

Figure A.1: United States Coast and Geodetic Survey (USC&GS) Hydrographic Survey H-3525 Smooth Sheet. Bathymetric sounding map of Great Bay, NH. Note the many channels, especially on the East of Great Bay (right hand side). (USC&GS, 1913)

183

Figure A.2: United States Coast and Geodetic Survey (USC&GS) Hydrographic Survey H-8093 Smooth Sheet. Bathymetric sounding map of Great Bay, NH. Note the loss of channels on the East of Great Bay (right hand side) in comparison to Figure A.1. (USC&GS, 1954)

APPENDIX B: TIDE SENSORS

B.1: Coastal Environmental Systems FMQ-19, Druck Resonant Silicon Pressure Transducer, Model RPT410F-8999.

Coastal Environmental Systems FMQ-19 is a military grade, aviation weather observation system deployed at many United States Air Force air stations. The barometric pressure sensor utilized by the FMQ-19 is the Druck Resonant Silicon Pressure Transducer, Model RPT410F-8999. For redundancy, the FMQ-19 employs three of these units. A specialized algorithm is used to compute and record atmospheric pressure from the three measurements. The Druck RPT410 sensor is designed to measure barometric pressure (mbar). The Model RPT410F-8999 is capable of measurements from 600 – 1100 mbar, with a resolution of 0.01 mbar. From the RPT410F User Manual,

The sensor comprises two elements, one acting as a pressure sensitive diaphragm and the other acting as a resonator. Pressure variations deflect the sensitive diaphragm and change the sensor's resonant frequency. The resonant frequency is measured, corrected for the effects of temperature and non-linearity and then output as a frequency signal. The sensor is characterised over the full temperature and pressure range and the corrections stored in non-volatile memory. (Druck, 2001, p. 7)

Figure B.1: Druck Resonant Silicon Pressure Transducer, Model RPT410F-8999. (Druck, 2001)

186

B.2: Onset HOBO logger, Model U20-001-02.

The Onset HOBO logger sensor is designed to record water temperature (°C) and water pressure (kPa). The Model U20-001-02 is capable of measurements from 0 – 400 kPa and 0 – 40 °C, and is pressure rated to 30.6 meters. The Onset HOBO logger is pre-programmed for a start time and sample interval prior to observations. Data is recorded internally to non-volatile memory for later access. Time synchronization for the Onset HOBO logger sensor is achieved when programming the unit on a personal computer. The date, time, and time zone set in the preferences of the computer are automatically used to set the same on the sensor. For optimal time synchronization, the computer should be set to a reliable network time source. (Onset, 2011)

Figure B.2: Onset HOBO logger, Model U20-001-02.

B.3: Paroscientific Digiquartz Intelligent Transmitter, Model 6000-30G.

The Paroscientific Digiquartz Intelligent Transmitter (Digiquartz) is a specialized pressure transducer, capable of measuring gauge pressure (psig). The Model 6000-30G is capable of measurements from 0 – 30 psig. The Digiquartz has embedded software that can be programmed for various sampling and output options. Data is output through either RS-232 or RS-485 serial protocol to an external data logger. (Paroscientific, 2005)

Figure B.3: Paroscientific Digiquartz Intelligent Transmitter, Model 6000-30G.

B.4: SeaBird MicroCAT C-T Recorder, Model SBE 37-SM.

The SeaBird MicroCAT C-T Recorder (MicroCAT) is designed for long-duration, fixed-position measurement of water conductivity (S/m) and water temperature (°C). The Model SBE 37-SM is capable of measurements from 0 – 7 S/m and -5 – 35 °C, and can withstand depths of 0 – 7000 m. The MicroCAT records data internally to non-volatile memory for later download. Time synchronization for the MicroCAT is performed during programming, manually entering the time from a GPS or GMT referenced timepiece. (SeaBird, 2011)
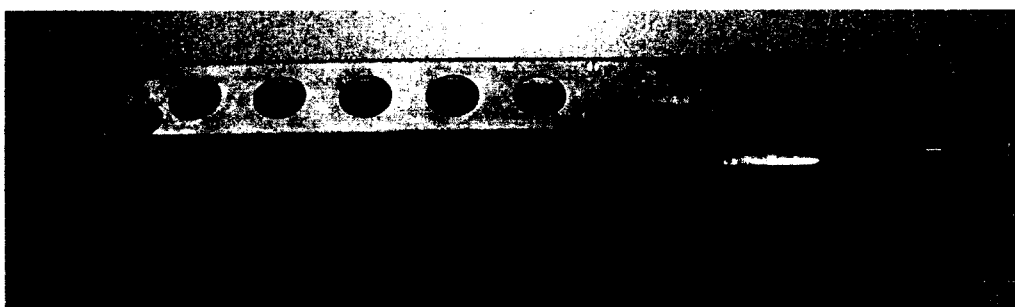
Figure B.4: SeaBird MicroCAT C-T Recorder, Model SBE 37-SM.

B.5 SeaBird SeaCAT C-T-P Recorder, Model SBE 16plus.

Like the MicroCAT, the SeaBird SeaCAT C-T-P Recorder is designed for long-duration, fixed-position measurement of water conductivity (S/m) and water temperature (°C). However, unlike the MicroCAT, the SeaBird SeaCAT C-T-P Recorder includes the ability to measure absolute pressure (psia) via an onboard strain pressure gauge element. The Model SBE 16plus is capable of measurements from 0 – 9 S/m, -5 – 35 °C, and 0 – 100 meter equivalent pressure, in psia. The sensor records data internally to non-volatile memory for later retrieval. Time synchronization for the SeaBird SeaCAT C-T-P Recorder is performed during programming, manually entering the time from a GPS or GMT referenced timepiece. (SeaBird, 2007)
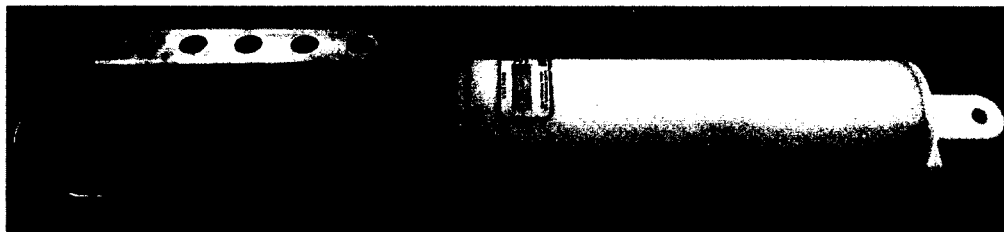
Figure B.5: SeaBird SeaCAT C-T-P Recorder, Model SBE 16plus.

B.6 Aquatrak Absolute Liquid Level Sensor, Model 3000 Series.

The Aquatrak Absolute Liquid Level Sensor is an acoustic water level sensor that measures the differential time of flight, in seconds, between a calibration and a water level pulse return from a single acoustic ping along a fixed tube. The measurement is made for the distance, in air, between the sensor and the water level. (Aquatrak, 2006)
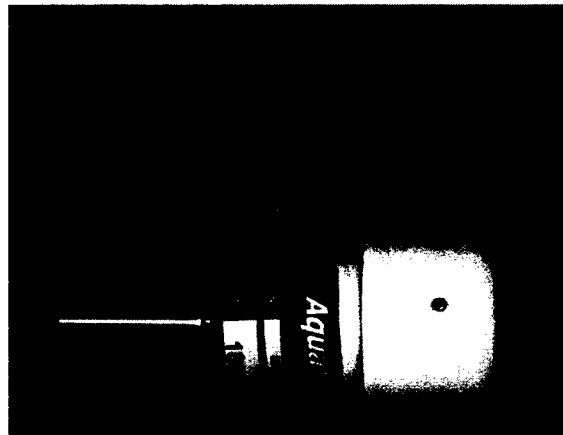
Figure B.6: Aquatrak Absolute Liquid Level Sensor, Model 3000 Series. (Aquatrak, 2006)

B.7 WaterLog Gas Purge Bubbler, Model H-355-30-PM.

The WaterLog Gas Purge Bubbler is a microcontroller-operated air compressor that maintains a constant bubble rate based upon head pressure from a submerged orifice. The Model H-355-30-PM is user programmable to produce between 30 – 120 bubbles per minute, while capable of handling head pressure from 0 – 30 psia. (Sutron, 2006)
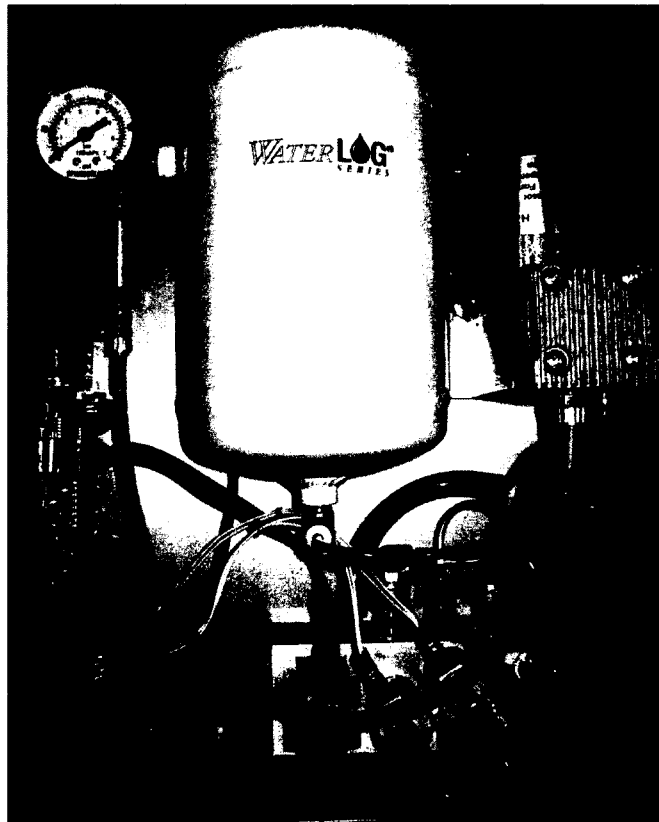
Figure B.7: WaterLog Gas Purge Bubbler, Model H-355-30-PM.

B.8 WaterLog Radar Water Level Sensor, Model H-3611.

The WaterLog Radar Water Level Sensor measures time-of-flight, in seconds, of an emitted pulse in the microwave frequency band, approximately 26 gigaHertz (GHz). Often, especially in the case of fluid measurement, multiple return pulses arrive. An averaging technique is applied to the multiple returned pulses in order to determine the time-of-flight. Data is output using an SDI-12 interface to a data logger. With a known frequency and the averaged time-of-flight, distance above water is then calculated. (WaterLog, 2011)

Figure B.8: WaterLog Radar Water Level Sensor, Model H-3611.

APPENDIX C: FIELD NOTES

ALL-WEATHER WRITING PAPER

ALL-WEATHER
TRANSIT BOOK

Name Sean O. Denney

Address

Phone

Project Master's Research
Great Bay Tidal Datum Study

Certificate of Purchase

Page Pattern			Cover Options	
List age	Page Page		Paper / Cover	General Comment
Customer	Sent / Type		Sent to Stk	Sent to Stk

195

TIDAL GAUGES

GAUGE: 1

MANUFACTURER: Aanderaa
PRODUCT: Pressure/ Temp. Sensor, WLR5
MODEL: 3796A
SERIAL No: 34
INFO: RANGE: 0-50 PSI

COEFF:

	A	B	C
1. PRESSURE (kPa):	-9.893E-01	5.026E-02	7.259E-07
WATER LEVEL (m):	-1.008E-01	5.125E-03	7.402E-08
2. TEMP (°C):	-7.909E+00	4.345E-01	4.796E-04

MANUFACTURER: Aanderaa
PRODUCT: Datalogger
MODEL: 3634
SERIAL No: 223
INFO: CHANNELS: 5   REF No: 636
RS232: 9600 baud, 8 data bits, 2 stop bits
no parity, no handshake

MANUFACTURER: Aanderaa
PRODUCT: Compensating Unit
MODEL: 3848

CTD: 1

MANUFACTURER: SeaBird
PRODUCT: Micro CAT
MODEL: SBE37-SM
SERIAL No: 0739
INFO: VERSION: 1.6
SAMPLE RATE: 120 seconds
REF PRESSURE: 1.0 dB

COEFF:

1. TEMP [23-MAR-10]

$TA0 = -3.932289 E-05$
$TA1 = 2.841157 E-04$
$TA2 = -3.084165 E-06$
$TA3 = 1.710744 E-07$

2. CONDUCTIVITY [23-MAR-10]

$G = -9.988058 E-01$
$H = 1.407917 E-01$
$I = -3.701911 E-04$
$J = 4.830602 E-05$

$CPCOR = -9.570000 E-08$
$CTCOR = 3.250000 E-06$
$WBOTC = -5.578599 E-05$

196

GAUGE: 1

MANUFACTURER   Pandora
PRODUCT: Cobalt
MODEL   3471

GAUGE: 2

MANUFACTURER: Sutron
PRODUCT: 9210 XLite
MODEL   9210-0000-2A
SERIAL No   503193
INFO   MEMORY   2.0GB CompactFlash

PIN-OUT:

No.	To	
8	H-355	Pin 9 (GND)
9	H-355	Pin 7 (+12V)
10	H-355	Pin 8 (Data)
N/C	H-355	Pin 4 (Shield)
	+12V	
	GND	

PORTS: COM 1   LAPTOP
COM 2   SATLINK
COM 3   Barometric Sensor

CTD: 1

3. RTC [23-MAR-10]

$RTCA\phi = 9.999645\ E-01$

$RTCA1 = 1.750101\ E-06$

$RTCA2 = -3.041684\ E-08$

PIN OUT:

PIN		WIRE
2	TX	GREEN
3	RX	
5	GND	WHITE

COMM:

RS232: 9600 baud, 8 databits, 1 stop bit
no parity

: PRESSURE RATING
0-7000m

GAUGE: 2

MANUFACTURER: Paroscientific
PRODUCT: Digiquartz Intelligent Transmitter
MODEL: 6000-30G
SERIAL No.: 97755
INFO: RANGE: 0-30 psig

MANUFACTURER: ProTech
PRODUCT: Solar Panel Voltage Regulator

MANUFACTURER: Sutron
PRODUCT: Industrial Control Panel Enclosure
MODEL: 3102-0000-1
SERIAL No.: 507789

MANUFACTURER: Wilkerson
PRODUCT: Manual Dessicant Dryer
MODEL: X03-02-Q03
INFO: Desiccant: Standard Silica Gel
2- 0.40kg Bags/Charge

GAUGE: 2

MANUFACTURER: Trimble
PRODUCT: Bullet III GPS Antenna
PART No: 57861-00
SERIAL No.: 22b90585
INFO: SOCKET: TNC
VOLTAGE: 3.3V
FREQ: 1575.42 MHz ± 1.023 MHz

MANUFACTURER: NaterLog/Hoffer
PRODUCT: H-355 Gas Purge System
MODEL: H-355-30-PH
SERIAL No: 5861
INFO: REV: L
RANGE: 0-30 psi
OUTPUT: RS-485/SDI-12
INPUT: 10-16V

MANUFACTURER: Sutron
PRODUCT: SatLink 2 Logger/Transmitter
MODEL: SL2-G312-1
SERIAL No.: 5022B3

GAUGE   3

    MANUFACTURER: OHMEX

    PRODUCT: AIS TideMet

    MODEL: TideMet

    SERIAL No: Eval.

    INFO: MMSI: 338040883

            SUPPLY: 12 v

            FREQ: O

    MANUFACTURER: OHMEX

    PRODUCT: AirMar PB100 Marine Weather Transducer

    MODEL: PB100 / 44-801-1-01

    SERIAL No: 1463494

    MANUFACTURER   OHMEX

    PRODUCT: GPS Antenna

    MODEL:

    SERIAL No:

    INFO: VOLTAGE: 3.3 v

    MANUFACTURER: Shakespere

    PRODUCT: VTronix Antenna

    INFO: FREQ RANGE: 161.975 - 162.025 MHz

GAUGE   REFERENCE   MEASUREMENTS

MOUNT:

Location: 1   Foot Point, NH

Gauge: 1
Dist(-): 0.133m, 1.105m
Dist(-): 0.020 m   = 0.020m
Dist(+): 0.252 + 1.371 = 1.623m
TOTAL = 1.603m

Gauge: 2
Dist(-): 0.007
Dist(-): 0.070m
Dist(+): 0.220 + 1.383 = 1.603m
TOTAL = 1.596m

Gauge: 3
Dist(-): 0.109 + 0.020 =   0.129m
Dist(+): 0.333 + 1.405 =   1.738m
TOTAL = 1.609m

Gauge: MonCat

TOTAL =

THREE-WIRE LEVELING
Fort Point, NH

FT. POINT, NH
JULY 23, 2010
(PM) 79°F
OVERCAST
INSTI CARL ZEISS
T-100598
S/N: 362311
CREW: S. DENNETT, N
J. HUNT, R
10

STADIA CONSTANT = 333

STA	B.S.(+)	DIST	F.S.(-)	DIST	ELEV
Portsmouth USCG 1994	0.419	31.302			7.346
	0.407		3.701		
			3.654		
			3.608		
	0.355		3.654	31.635	
	3/1.211		3/10.961		
	+0.404		-3.654		
TP1	0.762	36.630	1.737		4.096
	0.707		1.683		
			1.644		
	0.652		1.627	36.630	
	3/2.121		3/5.047		
	+0.707		-1.682		
TP2	1.705	54.612	0.216		3.121
	1.623		0.129		
	1.541		0.046	54.945	
	3/4.869		3/0.391		
	+1.623		-0.130		
TP3					4.614

A. PORTSMOUTH USCG 1994

B. CONSTITUTION No 1 1941 147

C. 2 1919

D. CONSTITUTION 1941 147

NOTE: PORTSMOUTH USCG 1994 BM

THIS BM IS BOTH A FEDERAL BASE NETWORK
CONTROL STATION AND A TIDAL BENCH MARK

    PID: AB2631

    STABILITY: A

    NAD83 (2007): 42°04'15.17400" N Lat.
            070°42'48.59788" W Lon.

    NAVD88: 7.346 m / 24.10 ft. (ADJUSTED 2002)

    SETTING: SET IN A BOULDER

STADIA CONSTANT = 333

STA	B.S.(+)	DIST	F.S.(-)	DIST	ELEV
TP3					4.614
	1.998		2.140		
	1.954	29.970	2.092	31.635	
	1.908		2.045		
	3√5.860		3√6.277		
	+1.953		-2.092		
CONSTITUTION NO 1 1941					
147	2.386		1.706		
	2.342	29.970	1.662	28.970	
	2.296		1.616		
	3√7.024		3√4.984		
	+2.341		-1.661		4.975
TP 2 1919	3.243		0.723		
	3.220	15.318	0.701	14.985	
	3.197		0.678		
	3√9.660		3√2.102		
	+3.220		-0.701		5.155
TP4					7.674

STADIA CONSTANT: 333

STA	B.S.(+)	DIST	F.S.(-)	DIST	ELEV
TP4	2.403		1.335		7.674
	2.192	7.992	1.322	9.324	
	2.179		1.307		
	3)6.574		3)3.964		
	+2.191		−1.321		
CONSTITUTION 1941 147	0.650		3.187		8.544
	0.636	9.324	3.173	8.991	
	0.622		3.160		
	3)1.908		3)9.520		
	+0.636		−3.173		
TP5	0.193		1.734		6.007
	0.183	6.660	1.724	6.66	
	0.173		1.714		
	3)0.549		3)5.172		
	+0.185		−1.724		
TP6					4.466

NOTE: CONSTITUTION No 1 1941 147

THIS BM IS BOTH A FEDERAL BASE NETWORK
CONTROL STATION AND A TIDAL BENCH MARK

PID: OCD429

STABILITY: A

NAD83 (2007): 43°04' 13.16812" N Lat.
070°42' 39.12781" W Lon.

NAVD88: 4.480 m / 14.70 ft. (ADJUSTED 1991)

SETTING: SET IN ROCK OUTCROP

NOTE: 2 1919

THIS BM IS A TIDAL BENCH MARK

PID: OC0427

STABILITY: C

NAD83 (1986): 43°04'15.0" N Lat

070°42'40.3" W Lon.

NAVD88: 5.160 m / 16.93 ft. (ADJUSTED 1991)

SETTING: SET IN A BOULDER

NOTE: CONSTRUCTION 1941 147

THIS BM IS AN U.S. ARMY MAP-CONTROL DISK

PID: OC0428

STABILITY: C

NAD83 (1986): 43°04'14.58693" N Lat.

070°42'40.61535" W Lon.

NAVD88: 8.555 m / 28.07 ft. (ADJUSTED 1991)

SETTING: SET IN AN 8" SQUARE CONCRETE

MONUMENT FLUSH WITH GROUND

07/23/2010

STADIA CONSTANT = 333

STA	B.S.(+)	DIST	F.S.(-)	DIST	ELEV
TP6					4.466
	0.524	33.966	1.868	33.330	
	0.473		1.818		
	0.422		1.768		
	3)1.419		3)5.454		
	+0.473		-1.818		
TP7					3.121
	1.574	54.945	0.271	50.99	
	1.491		0.195		
	1.409		0.118		
	3)4.474		3)0.584		
	+1.491		-0.195		
TP8					4.417
	3.400	25.508	0.477	27.306	
	3.362		0.436		
	3.324		0.395		
	3)10.086		3)1.308		
	+3.362		-0.436		

PORTSMOUTH USCG 1994

7.343

MISCLOSURE = 0.003

FT. POINT, NH
JULY 27, 2010
(PM) 87°F
MOSTLY CLOUDY
INST: CARL/ZEISS
   T: 100548
   S/N: 362311
CREW: S. DENNEY, N
     J. HUNT, ∅

A. PORTSMOUTH USCG 1994
B. Iron Pin "U.S."
C. 2, 1919
D. CONSTITUTION No 1 1941 147
E. CONSTITUTION No 2 1941 147
F. CONSTITUTION 1941 147

THREE - WIRE LEVELING
FORT POINT, NH

STADIA CONSTANT = 333

STA	B.S.(+)	DIST	F.S.(-)	DIST	ELEV
PORTSMOUTH USCG 1994	0.372		3.420		7.346
	0.326	28.971	3.377	78.205	
	0.285		3.335		
	3/0.985		3/10.152		
	+0.328		-3.377		
TP1	0.448		1.595		4.297
	0.384	42.624	1.530	42.957	
	0.320		1.466		
	3/1.152		3/4.591		
	+0.384		-1.530		
TP2	1.350		3.114		3.151
	1.340	6.327	3.105	5.994	
	1.331		3.096		
	3/4.021		3/9.315		
	+1.340		-3.105		
IRON PIN "U.S."					1.386

STADIA CONSTANT = 333

STA	B.S.(+)	DIST	F.S.(-)	DIST	ELEV
Iron Pin "U.S."					1.386
	3.194		1.430		
	3.179 2.990		1.414 10.656		
	3.164		1.398		
	3)9.557		3)4.242		
	+3.179		-1.414		
TP3					3.151
	1.553		0.988		
	1.514 25.641		0.950 25.308		
	1.476		0.912		
	3)4.543		3)2.850		
	+1.514		-0.950		
TP4					3.715
	1.994		0.547		
	1.979 9.990		0.532 9.990		
	1.964		0.517		
	3)5.937		3)1.596		
	+1.979		-0.532		
2 19/9					5.162

THREE-WIRE LEVELING
FORT POINT, NH

STADIA CONSTANT = 333

FT. POINT, NH
JULY 30. 0102
(AM)
CLEAN SUITES
INST. CAL/ZEISS
T-100598
S/N 362311

CREW: S. BENNETT, N
E. EVANS, B

STA	B.S.(+)	HGT	F.S.(-)	DIST	ELEV
BM 1919	0.231		1.914		5.160
	0.184	31.302	1.866	31.968	
	0.137		1.918		
	3)0.552		3)5.598		
	+ 0.184		- 1.866		
TP1	1.361		1.857		3.478
	1.336	16.317	1.835	14.985	
	1.312		1.812		
	3)4.009		3)5.504		
	+ 1.336		- 1.835		
MOUNT 1 RADAR GAUGE PILING REFERENCE			2.064		2.979
			2.044	13,330	
RADAR GAUGE GPS ANTENNA TOP			2.024		
			3)6.132		2.770
			- 2.044		0.935
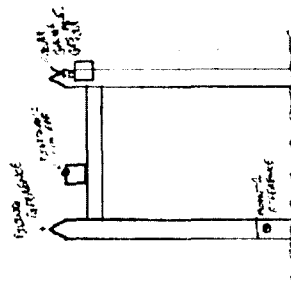
NOTE: PILING REF TO MOUNT 1 REFFERENCE
POINT = 13.14 FT.

NOTE: GPS ANTENNA TOP TO RADAR REFERENCE POINT
= ~2.0 FT
= 2.315 in. + 1.000 in. + 0.615 in. - 0.500 in. + 17.895
= 21.265 in

STADIA CONSTANT = 333

STA	O.S.(+)	INST	F.S.(-)	DIST	ELEV
SYA TP1 DISTANCE AIR REF POINT					3.478
			2.045		
			2.024	13.986	
			2.003		
			3)6.072		
			-2.024		2.790
DITCH QUARTZ ... REF POINT	2.045		1.260		
	2.024	13.986	1.336	16.317	
	2.003		1.311		
	3)6.072		3)4.007		
	+2.024		-1.336		
TP1	1.292 1.267 1.243	16.650	1.841 1.836 1.811	16.650	3.478
	1.242 1.243				
	3)3.801		3)5.508		
	+1.267		-1.836		
NO 1 1919					2.909

NOTE:

NOTE: Box Ref Point To Ditch Quartz Por Tree Ref
Point = ~09 Ft
= 10.625 in

STADIA CONSTANT = 333

STA	B.S.(+)	DIST	F.S.(-)	DIST	ELEV
NO 1 1717	1.861	16.650	1.292	16.317	2.909
	1.836		1.267		
	1.811		1.243		
	3)5.508		3)3.802		
	+1.836		−1.267		
TP1	1.959	31.635	0.177	30.968	3.478
	1.960		0.230		
	1.912		0.184		
	1.864		3)0.691		
	3)5.735		−0.230		
	+1.912				
NO 2 1919					5.160

GAUGE OPERATIONS
Fort Point, NH

GAUGE: 2
START TIME (UTC): 14:18:00
SDI: DT'
DAPH-355 OOLSM00SB61VO10
DC!

GAUGE: 1
START TIME (UTC): 14:26:00
INFO:
STORAGE CAPACITY: 12196 logs (3 ch.)
RECORDING INTERVAL: 2.0 min.
ETA for MEMORY FULL: 08/20/2010
START TIME (UTC): 13:51:00 [2010-08-17]
14:08:00 [2010-08-19]
17:00:00 [2010-08-26]
OFF

DATA COLLECTION

DATE	TIME (UTC)	GAUGE	FILENAME
08/10/2010	14:01:39	2	SSP_20100810.TXT
08/11/2010	13:33:00	1	Andrea_20100811.TXT
09/18/2010	13:39:01	2	SSP_20100918.TXT
	13:44:00	1	Andrea_20100818.TXT
08/26/2010	NA	CTD	NA
	16:23:46	2	SSP_20100826.TXT
	16:32:00	1	Amdrea_20100826.TXT
08/27/2010	14:12:00	CTD	SBE37_20100827.asc
	NA	1	Andrea_20100827.TXT
09/03/2010	13:26:00	CTD	SBE37_20100903.asc
	13:44:00	2	SSP_20100903.TXT
08/16/2010	21:20:00	CTD	SBE37_20100916.asc
	21:53:00	2	SSP_20100916.TXT

Great Bay, NH
Sept. 25, 2010

Gauge Operations
Great Bay, NH

Gauge: 2
Start Time (UTC): 15:00:00
SDI', DC1

Gauge: SBE-37
Start Time (UTC): 15:06:00 (10 Aug 2010)

DATA COLLECTION

DATE	TIME(UTC)	GAUGE	FILENAME
10/05/2010		2	SSP_20101005.txt
		CTD	SBE37_20100005.txt
10/12/2010		2	SSP_20101012.txt
		CTD	SBE37_20101012.txt

THREE-WIRE LEVELING
SQUAMSCOTT R.R. TRESTLE

STADIA CONSTANT = 333

STA	B.S.(+)	DIST	F.S.(-)	DIST	ELEV
A	1.974		2.446		.953
	1.928	30.303	2.436	26.073	
	1.883		2.395		
	3/5.785		3/7.307		
	+1.928		-2.436		
B	2.540		2.875		1.929 (BM95)
	2.487	24.632	2.816	39.461	
	2.436		2.758		
	3/7.463		3/8.448		
	+2.488		-2.816		
C	2.909		1.758		1.608
	2.884	16.65	1.733	16.165	
	2.859		1.707		
	3/8.652		3/5.198		
	+2.884		-1.733		
D					2.759

GREAT BAY, NH
DEC. 02, 2010
(PM) 40°F
CLEAR, WINDY
INST: CARL/ZEISS
T-100548
S/N: 382311
CREW: S. BEAMER, N
  E. TERRY, T
  J. HUNT, J

A. U.S. Coast & Geodetic Survey on "Track3 1926"
B. U.S. Coast & Geodetic Survey on "2 1926"
C. U.S. Coast & Geodetic Survey on "1 1926"
D. Radar Gauge, Top of GPS Antenna
E. U.S. Coast & Geodetic Survey on "BM HON4 1953"

26

STADIA CONSTANT= 333

STA	B.S.(+)	DIST	F.S.(-)	DIST	ELEV
Δ	1.697		2.279		2.752
	1.657	26.307	2.240	25.974	
	1.618		2.201		
	3)4.972		3)6.720		
	+1.657		−2.240		
E	2.330		2.087		2.169
	2.183	96.235	1.115	114.552	
	2.035		.743		
	3)6.548		3)5.745		
	+2.183		−1.915		
A					2.437

GREAT BAY, NH
JAN. 24, 2011
(AM) -6°F
WINDY, LIGHT CLOUDS

FIXED RANGE TEST
SQUAMSCOTT R.R. BRIDGE

DPI   DPT   =   HEIGHT (m)

A
or
B   −   0.046

      +   0.084

C   −   1.418

D   +   0.874   From Four Rover Conf

GPS Antenna to
Rover Reference   =   −0.506
Top
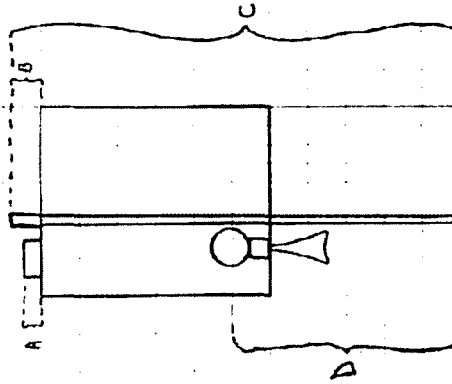
REFERENCE MEASUREMENT
FORT POINT, NH

STA	ELEV (A)
PILING REFERENCE (SEE PG. 18)	2.979

	TO	ES(-)
HODOLOGGER REF PT.	4.101	-1.122
SEACAT REF PT.		
HODOLOGGER REFERENCE	1.688	-7.810

FT. POINT, NH
MAY 10, 2011
(AM)   °F
CLOUDY/WINDY
CREW: S.DENNEY_N
          J. HUNT_J
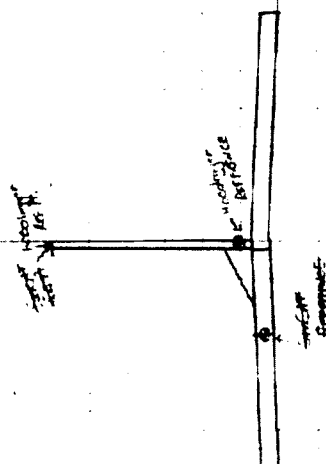
NOTE: DISTANCE FROM HODOLOGGER REF. PT. TO
HODOLOGGER REFERENCE = 5.494, 5.54 ft.

NOTE: DISTANCE FROM SEACAT REF. PT. TO
SEACAT REFERENCE = 07.5"

NOTE: SEACAT DID NOT LOG DATA!

32

FT. POINT, NH
MAY 23, 2011
(AM) 50°F

CREW: S.DENNEY, N
J.HUNT, P

STA	FS(-)	ELEV(m)
PILING REFERENCE (SEE PG 18)		2.979
TO		
SeaCar Ref. Pt.	3.156	-0.177
SeaCar Reference	2.810	-2.987

GPS OBSERVATIONS
Great Bay, NH

STA	DATE	LAT(d)	LON(d)	Ellipsoidal Height(m)	Orthometric Height(m)
Hodologer	12/17/2010	43°04'26.89'08'53'02.19"	-26.261	+0.517	
SDBS-2N5 (SEPRE-26) →RALIK	01/20/2011	43°51'10.03" 070°54'09"	-24.325	+2.412	
SeaCAT	02/24/2011	43°02'58.96" 070°04'41.20°	-25.668	+1.091	
YCH2 (SEP 12-28) →0.266	04/25/2008	43°05'31.64" 070°51'02.85"	-23.543	+3.214	

GREAT BAY, NH

INST:
SOKKIA GSR2300
S/N: SKZ 1232
P/N: 4CC203-017
ASHTECH ANT. L1-L2
S/N: MA 15071
P/N: 700700 (c)

INST:
ASHTEC Goodie IIA
S/N: GC 16702
P/N: 701 0C8-01(d)
ANT. HEIGHT = 2.00 m

REFERENCE MEASUREMENT

ADAMS POINT, NH

STA	ELEV DIFF. (m)	Mean Height (m)	Orthometric Height (m)
TBM 2	-0.609	-23.542	+3.224
TBM 1	-0.572		
STAFF "4"	-1.530		
STAFF MLLW	-0.104	-28.257	-1.601
GAUGE REFERENCE			
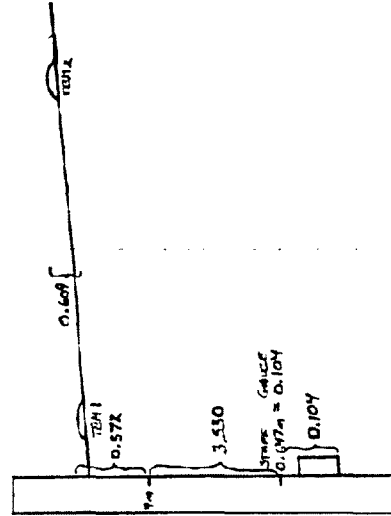
TIDAL GAUGES

GAUGE: 4

MANUFACTURER: Onset
PRODUCT: HOBOlogger
MODEL: U20-001-02
SERIAL No: 9764664
INFO: RANGE: 0 - 30.5 m

GAUGE: 5

MANUFACTURER: Water Log
PRODUCT: Radar Water Level Sensor
MODEL: H-3611
SERIAL No: 1380   REV: F
INFO: RANGE: 0.3 - 22 m
Output: SDI-12, RS-212(&CE)
Power: 9 - 16 V

MANUFACTURER: Sutron
PRODUCT: 8080 XPeer
MODEL: 8080-0000-2B
SERIAL No:

GAUGE: 5

Manufacturer: Garmin
Product: Reclina/Australia, GPS
Model: GPS 17x HVS
Serial No: 10N023172
Part No: 010-00694-00
Info: NMEA 0183 Compatible

GAUGE: 6

Manufacturer: SeaBird
Product: SeaCAT
Model: SBE-16plus
Part No: 70386.128
Serial No: 16P39199-4865
Info: Pressure Rated 0-100 m

JULY 12, 2011
GREAT BAY, NH
(AM) 86°F
PARTLY CLOUDY
INST: Trimble 5700
S/N: 0220363984
(Ruggedized Zephyr Geodetic A.S.)
S/N: 031010061Z
P/N: 65212-00

GPS OBSERVATIONS
GREAT BAY, NH

WATERLINE TO ANTENNA PHASE CENTER

6.35 cm

1.06 m
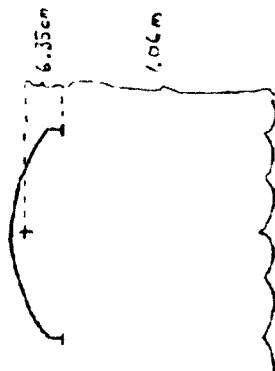
$T_{otal} = 1.1235$ m

SEACAT DEPLOYMENT
START: 1500 UTC 20110712
STOP: 1600 UTC

APPENDIX D: DATA PROCESSING

223

D.1 Raw Data. With such a large assortment of tidal sensors from numerous manufacturers, no universal or industry format was available. A sample of the raw data from each sensor used in the study can be seen in Table D.1.1. While some sensors provide *metadata* or header information to ascertain what each part of the data represents, some do not. Even amongst those data sets that do provide header information, units are nearly never given.

It was then necessary to determine which statistics of the data were needed and which were not (Table D.1.2). For all sensors, date and time information was paramount for time series analysis. The primary computation to be performed was the calculation of water level. For those tide gauges that are based on pressure measurements, a combination of data sets was necessary to calculate water level (Eq. 2.4.2). Gravity is computed as a function of latitude using the *International Gravity Formula of 1980* (Moritz, 1980).

For example, the WaterLog Bubbler computes and records differential pressure (the numerator in Eq. 2.4.2), however water density is an unknown in the computation of water level. The use of a SeaBird MicroCAT allows for the computation of the water density from the temperature and conductivity measurements. Similarly the SeaBird SeaCAT records water pressure, temperature and conductivity, however atmospheric pressure is an unknown. Atmospheric pressure can be interpolated from a nearby NOAA NCDC weather station.

Name
Sample Data

National Climate Data Center (NCDC) Product
PEASE INTL TRADEPOR   ,726055,04743,20090701,0000,4,FM-15,1007.3,1

NOAA Aquatrak @ Fort Point, NH
8423898 20100701 00:00 -1.096 -1.050

NOAA Aquatrak @ Portland, ME
8418150 20090701 05:00 -1.219 LL

Onset HOBOlogger
1,11/24/10 07:00:00 PM,1096.2,6.166,Logged,,,,

Pydro/TCARI Model Predictions
2009-08-27 00:00:00,1.97108729143

SeaBird MicroCAT
13.6663, 3.75983, 06 Jul 2010, 14:05:26

SeaBird SeaCAT (Format 1)
-0.1268, 1.44442,   2.714,   16.3951, 18 Dec 2010, 14:42:01

SeaBird SeaCAT (Format 2)
21.8080   2.509126   1.119   16.3945 208.601979

WaterLog Gas Purge Paroscientific Digiquartz (WaterLog Bubbler)
01/03/2011,17:01:30,PAROS1,2.582, Avg,G

WaterLog Radar Water Level Sensor (WaterLog MWWL)
05/14/2011,23:29:46,h-3611,2.429,M,G

Table D.1.1: Sample raw data from study area instrumentation.

For other sensors, a reference datum is needed in order to translate the measurements to water level (*e.g.* the WaterLog MWWL). Accurate leveling between a reference point on the tide gauge and a series of vertically tied benchmarks is necessary to determine this translation.

D.2 Source Code: C/C++. The bulk of the source code for automating the processing of the raw data and computing water level information is written in C and C++. The functions of the source code can be broken into four categories: file I/O, time series manipulation, statistic computation, and datum referencing.

225

Name
Necessary Statistics (necessary units)
National Climate Data Center (NCDC) Product Date, Time, Atmospheric Pressure (dbar)
NOAA Aquatrak @ Fort Point, NH Date, Time, Observed Water Level (m)
NOAA Aquatrak @ Portland, ME Date, Time, Observed Water Level (m), Water Level Designation (LL, L, H, HH)
Onset HOBOlogger Date, Time, Water Pressure (dbar), Temperature (°C)
Pydro/TCARI Model Predictions Date, Time, Modeled Water Level (m)
SeaBird MicroCAT Date, Time, Water Temperature (°C), Water Conductivity (S/m)
SeaBird SeaCAT (Format 1) Date, Time, Water Pressure (dbar), Water Temperature (°C), Water Conductivity (S/m), Water Salinity(PSU)
WaterLog Gas Purge Paroscientific Digiquartz (WaterLog Bubbler) Date, Time, Differential Pressure (dbar)
WaterLog Radar Water Level Sensor (WaterLog MWWL) Date, Time, Air Gap Distance (m)

Table D.1.2: Statistics needed from study area instrumentation.

The first set of functions in the source code is dedicated to reading data from and writing data to files. The raw data files are all ASCII based, thus no binary decoding is necessary. During the read process for each data source (Table D.1.1) a custom defined typedef struct object is generated to handle the specific statistics required (Table D.1.2). Variables within each object are stored as base data types; station identification is stored as either unsigned int or uint64_t, dependent upon storage requirements; date, time, and water level designation are stored as unsigned int; a variable for whether the data at a particular point in time is good is stored as bool; all other statistics are stored as double. Given both a start and a stop date and time a vector of the custom defined struct objects is used to store the entire time series for each data

226

source and epoch. During the read process, unit conversions may take place in order to comply with the required statistic units.

At various stages in the processing of the raw data, the time series is written to files, both for debugging purposes as well as further processing with MATLAB™ (See Section D.3). The write functions are passed a flag to determine what header information should be written before writing the time series. Date information is written in *yyyymmdd* format, time information is written as seconds since midnight (midnight = 0), water level designation is written as a single digit (*0=HH, 1=H, 2=L, 3=LL*), while all other statistics are written in decimal format.

The second set of functions in the source code is dedicated to the manipulation of date and time series information. In order to perform time series analysis the data must be continuous and have a set sample interval. To those ends, a series of date and time specific functions process the stored **vector**'s of data objects. The first of these functions corrects for date and time blunders. For example, the SeaBird MicroCAT had a forty-four day date offset during data collection. Another function either truncates or linearly interpolates the time series to comply with the per-device sampling interval between a specified start and stop date and time. Another function removes duplicate data entries, averaging the statistic values. Another function fills in gaps in the time series through linear interpolation. The gaps are filled with **NaN** values so as not to unduly influence the data record. The last function in this set applies a block average centered on an output required sampling interval (*e.g.* 359-second average centered on

227

the 6-minute interval). Outside of the custom `struct` objects, all date and time information is handled by the C/ C++ `ctime` library and the C++ Boost `date_time` libraries. (Garland, 2011)

With a continuous time series with a set sampling interval, computations on the statistics can be performed. The next set of functions in the source code is dedicated to performing these calculations. For the WaterLog MWWL, a fixed range test is conducted and a reference distance is computed. This reference distance will be used in the last set of functions. For the pressure-based tide gauges, water level is computed. During the second and fourth phases of the study, regression coefficients are applied to correct for any systematic bias caused by the instrumentation in reference to a control gauge.

The last function in the source code is dedicated to referencing the water level information to a specified datum (WGS84, NAVD88 or MLLW). In the case of the WaterLog MWWL, the fixed range reference calculation and leveling information are combined to reference the air gap distance to a specified water level datum. With the time series referenced to some datum, the information is then written to an output file as previously discussed (Table D.2.1)

D.3 Source Code: MATLAB™. With the required statistics compiled in continuous time series with a common format, analysis and data visualization can be performed. Each phase of the study requires different analysis techniques that produce different results that then contribute to the next phase of the study. The source code used in the time series

```
Name
Header Information
Sample Statistics


National Climate Data Center (NCDC) Product
Date, Time (s), Atm. Pressure (dbar)
20110318, 7200, 10.150
20110318, 7560, 10.149
20110318, 7920, 10.148


NOAA Aquatrak @ Fort Point, NH
Date, Time (s), Water Level (m)
20110318, 7200, 1.368
20110318, 7560, 1.366
20110318, 7920, 1.350


NOAA Aquatrak @ Portland, ME
Date, Time (s), Verified Water Level (m), Designation
20101124, 61920, 1.560, 0
20101124, 85680, -1.872, 3
20101125, 21240, 1.202, 1
20101125, 42840, -1.218, 2


Onset HOBOlogger
Date, Time (s), Water Level (m), Pressure (dbar)
20101125, 0, -0.617, 10.962
20101125, 360, -0.663, 10.917
20101125, 720, -0.704, 10.876


Pydro/TCARI Model Predictions
Date, Time (s), Pred Water Level (m)
20110515, 0, 0.937
20110515, 360, 0.988
20110515, 720, 1.039


SeaBird MicroCAT
Date, Time (s), Temperature (°C), Conductivity (S/m)
20101125, 0, 6.463, 2.259
20101125, 360, 6.471, 2.256
20101125, 720, 6.284, 2.242


SeaBird SeaCAT
Date, Time (s), Water Level (m), Pressure (dbar)
20101119, 0, -0.634, 11.218
20101119, 360, -0.591, 11.261
20101119, 720, -0.545, 11.307


WaterLog Gas Purge Paroscientific Digiquartz (WaterLog Bubbler)
Date, Time (s), Water Level (m), Diff. Pressure (dbar)
20100923, 57600, 0.232, 1.840
20100923, 57960, 0.272, 1.880
20100923, 58320, 0.312, 1.921


WaterLog Radar Water Level Sensor (WaterLog MWWL)
Date, Time (s), Water Level (m)
20101112, 74520, 0.591
20101112, 74880, 0.630
20101112, 75240, 0.666
```

Table D.2.1: Sample output data from C/C++ processing.

analysis and data visualization is written in MathWorks MATLAB™. While slower and more memory intensive— compared to C++,— the visualization capabilities as well as the use of the pre-existing t_tide library and functions (Pawlowicz *et. al.*, 2002) make MATLAB™ the most convenient choice for this part of the data handling.

The functions performed in the analysis of the time series data can be divided into two parts: time domain and spectral domain. Within time domain analysis, there are numerous steps:

    i. Plot water level observations and, if applicable, compute and plot residuals;

    ii. Process the time series observations with t_tide;

    iii. Plot the t_tide generated time series and, if applicable, compute and plot the residuals;

    iv. If applicable, compute the linear regression coefficients and plot the linear regressions; and

    v. Plot the atmospheric and water pressure observations and compute and plot the residual.

Accurate analysis of tidal data is an important aspect of any study of tides. Of the numerous analysis products available, t_tide is one of the most venerable and widely used. (Pawlowicz *et. al.*, 2002) Written in MATLAB™, the t_tide library allows for the tidal harmonic analysis of a time series utilizing a least-squares fitting technique. The time series data must have a specified sampling interval, however there can exist (small) gaps in the data. When processing the time series data with t_tide, the start date and time, the sample interval and the latitude of the observations are given. The latitude of the observations allows t_tide to apply nodal corrections to both amplitude and phase. (Pawlowicz *et. al.*, 2002) The outputs from t_tide include the tidal harmonic names,

230

frequencies (in cycles per hour), amplitudes (in meters), amplitude *confidence intervals* (in ± meters), phases (in decimal degrees referenced to Greenwich Mean Time), phase confidence intervals (in ± decimal degrees), and *signal-to-noise ratio* (SNR) for the given time series. Numerous miscellaneous statistics are output, including variances and linear trend information. t_tide also produces a predicted time series over the same epoch using the resolved harmonic constituents with a SNR greater than 2.0. (Pawlowicz *et. al.*, 2002) This t_tide predicted time series will be noted as the t_tide generated time series throughout this study.

Similarly, within spectral domain analysis, the following steps are taken:

    i. Compute and plot the power spectrum from the water level observations;

    ii. Compute and plot the power spectrum from the atmospheric pressure observations; and

    iii. Compute and plot the smoothed spectral density, smoothed squared coherency spectrum, and smoothed phase spectrum.

Prior to computing the power spectrum the mean of the time series is removed, gaps are filled in using the t_tide generated time series, and a Hanning window is applied to the entire record. In deciding how to fill in the gaps, three options were looked at: the first, replacing the NaN values with a very small, non-zero number (*e.g.* 1E-12); the second, replacing the NaN values with the previously occurring non-NaN value in the time series; and last, replacing the NaN values with the values occurring in the t_tide generated time series at the same time point. As t_tide uses a least-squares fit to fill in gaps in a data series, the third option was chosen over the other two as it had the least amount of influence on the spectral analysis of the data.

As tides are generally regarded as low frequency, the Hanning *data window* was chosen for its inherent ability to attenuate high frequencies. Aside from the boxcar data window, all windowing functions alter the energy, or variance, of the original time series. A correction for the alteration in energy as a result of windowing is computed and applied before the power spectrum is computed. The power spectrum is computed from a simple Fast Fourier Transform (FFT). The ninety-five percent confidence interval is then computed and displayed using two degrees of freedom.

When it is necessary to compare the spectrums from different time series, a common approach is to use a cross-spectral analysis technique. In addition, to help eliminate noise, a *band-averaging* or ensemble-averaging of the time series is often used. In this study, the one-sided, band-averaged sample spectral density of two time series are computed and compared. To account for the fraction of variance that occur between the two time series, the smoothed squared coherency spectrum is also computed. The ninety-five percent confidence interval is then computed. And finally the smoothed phase spectrum is computed. For those frequencies in the squared coherency spectrum whose coherency values are greater than or equal to the ninety-five percent confidence interval, a subsequent confidence interval is computed for the phase spectrum.

In both time domain and spectral domain analysis, the objective is to determine whether the recorded observations are within the parameters of representative data. Outliers, abnormalities, large gaps, spikes, and other artifacts in time series data are visually inspected and numerically analyzed to determine the usefulness of the measurements.

APPENDIX E: t_tide REPORTS

233

E.1.1: Phase 1: NOAA Aquatrak referenced to the Onset HOBOlogger.

```
number of standard constituents used: 35
Points used: 12841 of 12841
percent of var residual after lsqfit/var original:  1.18 %
Greenwich phase computed with nodal corrections applied to amplitude
and phase relative to center time
Using nonlinear bootstrapped error estimates
Generating prediction with nodal corrections, SNR is 2.000000
percent of var residual after synthesis/var original:  1.19 %
---------------------------------
date: 08-Nov-2011
nobs = 12841,  ngood = 12841,  record length (days) = 53.50
start time: 18-Mar-2011 02:00:00
rayleigh criterion = 1.0
Greenwich phase computed with nodal corrections applied to amplitude
and phase relative to center time

x0= -0.00578, x trend= 0

var(x)= 0.97636   var(xp)= 0.96503   var(xres)= 0.011588
percent var predicted/var original= 98.8 %
```

tidal amplitude and phase with 95% CI estimates

tide	freq	amp	amp_err	pha	pha_err	snr
*MM	0.0015122	0.0189	0.012	231.81	38.91	2.4
*MSF	0.0028219	0.0157	0.011	36.43	44.51	2
ALP1	0.0343966	0.0023	0.004	195.94	135.29	0.28
*2Q1	0.0357064	0.0137	0.006	186.58	22.18	6.1
*Q1	0.0372185	0.0245	0.005	155.02	14.34	22
*O1	0.0387307	0.1219	0.007	188.05	2.67	3.2e+02
*NO1	0.0402686	0.0157	0.005	225.96	17.33	12
*K1	0.0417807	0.1083	0.007	188.23	3.14	2.5e+02
J1	0.0432929	0.0049	0.005	210.27	64.53	1
*OO1	0.0448308	0.0124	0.005	246.63	26.82	6
*UPS1	0.0463430	0.0096	0.006	303.22	30.89	2.9
EPS2	0.0761773	0.0033	0.005	284.37	96.57	0.49
*MU2	0.0776895	0.0465	0.006	68.03	7.72	66
*N2	0.0789992	0.3510	0.005	67.54	0.90	6e+03
*M2	0.0805114	1.2908	0.007	104.85	0.27	3.9e+04
*L2	0.0820236	0.0971	0.008	145.18	4.40	1.5e+02
*S2	0.0833333	0.2272	0.006	135.60	1.46	1.7e+03
ETA2	0.0850736	0.0025	0.005	341.82	123.35	0.23
*MO3	0.1192421	0.0066	0.001	231.65	8.43	48
*M3	0.1207671	0.0038	0.001	153.90	15.86	14
*MK3	0.1222921	0.0029	0.001	249.70	20.52	6.9
SK3	0.1251141	0.0011	0.001	210.82	43.47	1.3
*MN4	0.1595106	0.0078	0.001	306.06	7.47	45
*M4	0.1610228	0.0183	0.001	335.35	3.62	3e+02
SN4	0.1623326	0.0013	0.001	87.27	46.15	1.9
*MS4	0.1638447	0.0074	0.001	5.73	7.85	55
*S4	0.1666667	0.0015	0.001	102.76	43.73	2.2
*2MK5	0.2028035	0.0009	0.000	108.94	20.05	6.4
*2SK5	0.2084474	0.0025	0.000	99.14	7.40	63
*2MN6	0.2400221	0.0051	0.001	98.66	6.79	61
*M6	0.2415342	0.0065	0.001	139.72	5.65	1.4e+02
*2MS6	0.2443561	0.0046	0.001	178.09	7.70	50
2SM6	0.2471781	0.0006	0.001	276.63	52.52	0.97
*3MK7	0.2833149	0.0010	0.000	290.18	25.94	5.7
*M8	0.3220456	0.0021	0.000	251.11	11.08	36

E.1.2: Phase 1: Onset HOBOlogger.

```
number of standard constituents used: 35
Points used: 12841 of 12841
percent of var residual after lsqfit/var original:  1.20 %
Greenwich phase computed with nodal corrections applied to amplitude
and phase relative to center time
Using nonlinear bootstrapped error estimates
Generating prediction with nodal corrections, SNR is 2.000000
percent of var residual after synthesis/var original:  1.22 %
----------------------------------
date: 08-Nov-2011
nobs = 12841,  ngood = 12841,  record length (days) = 53.50
start time: 18-Mar-2011 02:00:00
rayleigh criterion = 1.0
Greenwich phase computed with nodal corrections applied to amplitude
and phase relative to center time

x0= -0.033, x trend= 0

var(x)= 0.96052   var(xp)= 0.94909   var(xres)= 0.011705
percent var predicted/var original= 98.8 %

        tidal amplitude and phase with 95% CI estimates
```

tide	freq	amp	amp_err	pha	pha_err	snr
*MM	0.0015122	0.0208	0.014	231.48	35.20	2.1
MSF	0.0028219	0.0154	0.012	41.34	48.51	1.7
ALP1	0.0343966	0.0028	0.005	191.49	116.65	0.37
*2Q1	0.0357064	0.0132	0.005	187.88	26.06	6.1
*Q1	0.0372185	0.0247	0.005	153.99	13.33	22
*O1	0.0387307	0.1213	0.006	187.43	2.73	3.8e+02
*NO1	0.0402686	0.0156	0.004	226.00	16.08	16
*K1	0.0417807	0.1101	0.006	188.35	2.82	2.9e+02
J1	0.0432929	0.0049	0.005	205.91	75.71	0.98
*OO1	0.0448308	0.0124	0.006	248.29	20.81	5.1
*UPS1	0.0463430	0.0096	0.005	300.09	33.63	3.5
EPS2	0.0761773	0.0032	0.005	284.80	103.59	0.44
*MU2	0.0776895	0.0453	0.005	68.03	6.61	75
*N2	0.0789992	0.3469	0.006	67.66	0.88	3.4e+03
*M2	0.0805114	1.2804	0.005	104.86	0.27	6e+04
*L2	0.0820236	0.0987	0.006	145.22	3.98	2.5e+02
*S2	0.0833333	0.2243	0.006	135.53	1.57	1.3e+03
ETA2	0.0850736	0.0023	0.004	343.54	107.97	0.38
*MO3	0.1192421	0.0062	0.001	236.30	8.95	43
*M3	0.1207671	0.0035	0.001	147.52	17.57	12
*MK3	0.1222921	0.0028	0.001	229.37	19.80	8.6
*SK3	0.1251141	0.0019	0.001	207.70	29.86	4
*MN4	0.1595106	0.0073	0.001	302.18	7.41	56
*M4	0.1610228	0.0177	0.001	334.32	3.16	3.6e+02
SN4	0.1623326	0.0009	0.001	91.25	63.51	0.98
*MS4	0.1638447	0.0071	0.001	359.47	7.48	56
S4	0.1666667	0.0009	0.001	71.73	57.91	1.2
*2MK5	0.2028035	0.0010	0.000	104.29	23.89	6.1
*2SK5	0.2084474	0.0024	0.000	98.71	10.80	28
*2MN6	0.2400221	0.0052	0.001	96.40	8.23	56
*M6	0.2415342	0.0061	0.001	137.24	5.54	92
*2MS6	0.2443561	0.0043	0.001	178.01	8.18	34
2SM6	0.2471781	0.0010	0.001	280.27	42.21	1.7
*3MK7	0.2833149	0.0012	0.000	289.70	19.93	7.8
*M8	0.3220456	0.0022	0.000	258.02	11.05	33

E.1.3: Phase 1: NCDC Atmospheric Pressure referenced to the Onset HOBOlogger.

```
number of standard constituents used: 35
Points used: 12841 of 12841
percent of var residual after lsqfit/var original: 91.75 %
Greenwich phase computed with nodal corrections applied to amplitude
and phase relative to center time
Using nonlinear bootstrapped error estimates
Generating prediction with nodal corrections, SNR is 2.000000
percent of var residual after synthesis/var original: 91.80 %
---------------------------------
date: 08-Nov-2011
nobs = 12841,  ngood = 12841,  record length (days) = 53.50
start time: 18-Mar-2011 02:00:00
rayleigh criterion = 1.0
Greenwich phase computed with nodal corrections applied to amplitude
and phase relative to center time

x0= 10.1, x trend= 0

var(x)= 0.0087233   var(xp)= 0.00072071   var(xres)= 0.0080083
percent var predicted/var original= 8.3 %
```

tidal amplitude and phase with 95% CI estimates

tide	freq	amp	amp_err	pha	pha_err	snr
*MM	0.0015122	0.0367	0.013	6.30	25.08	7.5
MSF	0.0028219	0.0012	0.012	327.89	239.50	0.011
*ALP1	0.0343966	0.0027	0.002	339.24	37.21	3
*2Q1	0.0357064	0.0027	0.001	40.55	37.63	3.6
Q1	0.0372185	0.0010	0.001	279.57	102.15	0.56
*O1	0.0387307	0.0032	0.002	271.15	29.40	3.4
*NO1	0.0402686	0.0029	0.001	58.48	23.76	5.6
*K1	0.0417807	0.0050	0.002	252.22	18.93	10
J1	0.0432929	0.0014	0.002	81.23	67.17	0.67
OO1	0.0448308	0.0009	0.001	87.08	89.21	0.71
UPS1	0.0463430	0.0014	0.002	178.99	70.09	0.76
*EPS2	0.0761773	0.0006	0.000	106.93	48.24	2.6
*MU2	0.0776895	0.0007	0.000	116.01	37.32	2.4
N2	0.0789992	0.0003	0.000	145.34	82.20	0.6
M2	0.0805114	0.0002	0.000	238.71	134.46	0.31
L2	0.0820236	0.0006	0.001	5.84	52.26	1.2
*S2	0.0833333	0.0061	0.000	65.31	4.13	2.5e+02
ETA2	0.0850736	0.0005	0.000	219.12	55.46	1.3
MO3	0.1192421	0.0002	0.000	160.95	78.44	0.61
*M3	0.1207671	0.0003	0.000	277.06	37.63	2.9
MK3	0.1222921	0.0001	0.000	227.55	179.41	0.15
SK3	0.1251141	0.0003	0.000	336.45	44.74	1.9
*MN4	0.1595106	0.0003	0.000	85.34	26.02	5.2
M4	0.1610228	0.0002	0.000	133.63	51.45	1.4
*SN4	0.1623326	0.0004	0.000	109.95	19.28	9.2
*MS4	0.1638447	0.0002	0.000	136.16	34.83	2.9
*S4	0.1666667	0.0005	0.000	8.47	17.99	14
2MK5	0.2028035	0.0001	0.000	327.18	59.29	1.6
*2SK5	0.2084474	0.0003	0.000	216.63	21.22	7.2
*2MN6	0.2400221	0.0002	0.000	177.00	19.69	10
M6	0.2415342	0.0001	0.000	191.30	60.28	1
*2MS6	0.2443561	0.0002	0.000	11.09	21.16	6.4
2SM6	0.2471781	0.0001	0.000	272.79	50.94	1.6
*3MK7	0.2833149	0.0002	0.000	42.71	19.09	8.7
M8	0.3220456	0.0000	0.000	256.22	56.65	1.5

E.1.4: Phase 1: NOAA Aquatrak referenced to the SeaBird SeaCAT.

```
number of standard constituents used: 9
Points used: 2363 of 2364
percent of var residual after lsqfit/var original:  2.01 %
Greenwich phase computed with nodal corrections applied to amplitude
and phase relative to center time
Using nonlinear bootstrapped error estimates
Generating prediction with nodal corrections, SNR is 2.000000
percent of var residual after synthesis/var original:  2.01 %
------------------------------------
date: 08-Nov-2011
nobs = 2364,  ngood = 2363,  record length (days) = 9.85
start time: 13-May-2011 18:00:00
rayleigh criterion = 1.0
Greenwich phase computed with nodal corrections applied to amplitude
and phase relative to center time

x0= 0.0896, x trend= 0

var(x)= 1.2769   var(xp)= 1.2512   var(xres)= 0.025667
percent var predicted/var original= 98.0 %

        tidal amplitude and phase with 95% CI estimates
```

tide	freq	amp	amp_err	pha	pha_err	snr
*K1	0.0417807	0.2025	0.039	181.52	13.30	27
*M2	0.0805114	1.5604	0.041	109.17	1.59	1.4e+03
*M3	0.1207671	0.0164	0.002	13.54	9.76	45
*M4	0.1610228	0.0224	0.001	347.23	2.56	5.2e+02
*2MK5	0.2028035	0.0053	0.000	91.51	5.05	1.2e+02
*2SK5	0.2084474	0.0043	0.000	121.57	6.84	79
*M6	0.2415342	0.0134	0.001	140.21	3.65	2.6e+02
*3MK7	0.2833149	0.0024	0.001	347.13	18.42	9.7
*M8	0.3220456	0.0037	0.001	309.14	10.85	28

E.1.5: Phase 1: SeaBird SeaCAT.

```
number of standard constituents used: 9
Points used: 2363 of 2364
percent of var residual after lsqfit/var original:  1.98 %
Greenwich phase computed with nodal corrections applied to amplitude
and phase relative to center time
Using nonlinear bootstrapped error estimates
Generating prediction with nodal corrections, SNR is 2.000000
percent of var residual after synthesis/var original:  1.98 %
---------------------------------
date: 08-Nov-2011
nobs = 2364,  ngood = 2363,  record length (days) = 9.85
start time: 13-May-2011 18:00:00
rayleigh criterion = 1.0
Greenwich phase computed with nodal corrections applied to amplitude
and phase relative to center time

x0= -0.00198, x trend= 0

var(x)= 1.2625   var(xp)= 1.2375   var(xres)= 0.025005
percent var predicted/var original= 98.0 %
```

tidal amplitude and phase with 95% CI estimates

tide	freq	amp	amp_err	pha	pha_err	snr
*K1	0.0417807	0.2012	0.047	181.40	11.37	19
*M2	0.0805114	1.5518	0.040	109.03	1.54	1.5e+03
*M3	0.1207671	0.0163	0.002	12.46	7.96	55
*M4	0.1610228	0.0216	0.001	353.49	2.75	4.2e+02
*2MK5	0.2028035	0.0049	0.001	96.44	6.90	79
*2SK5	0.2084474	0.0038	0.000	120.52	7.73	59
*M6	0.2415342	0.0141	0.001	142.14	3.50	2.4e+02
*3MK7	0.2833149	0.0022	0.001	346.84	19.57	9.6
*M8	0.3220456	0.0038	0.001	307.94	7.91	34

E.1.6: Phase 1: NCDC Atmospheric Pressure referenced to the SeaBird SeaCAT.

```
number of standard constituents used: 9
Points used: 2363 of 2364
percent of var residual after lsqfit/var original: 99.89 %
Greenwich phase computed with nodal corrections applied to amplitude
and phase relative to center time
Using nonlinear bootstrapped error estimates
Generating prediction with nodal corrections, SNR is 2.000000
percent of var residual after synthesis/var original: 99.96 %
-----------------------------------
date: 08-Nov-2011
nobs = 2364,  ngood = 2363,  record length (days) = 9.85
start time: 13-May-2011 18:00:00
rayleigh criterion = 1.0
Greenwich phase computed with nodal corrections applied to amplitude
and phase relative to center time

x0= 10.2, x trend= 0

var(x)= 0.0027673   var(xp)= 1.0124e-06   var(xres)= 0.0027663
percent var predicted/var original= 0.0 %

         tidal amplitude and phase with 95% CI estimates

 tide    freq      amp     amp_err     pha     pha_err    snr
  K1   0.0417807   0.0018    0.002    329.93    71.26     0.7
  M2   0.0805114   0.0011    0.001     91.47    62.77     1.1
 *M3   0.1207671   0.0009    0.000    295.77    14.28      16
 *M4   0.1610228   0.0009    0.000    107.54    12.67      20
 *2MK5 0.2028035   0.0003    0.000    113.65    36.98     2.7
 *2SK5 0.2084474   0.0004    0.000    355.21    24.16     5.7
 *M6   0.2415342   0.0003    0.000    354.14    36.04       3
 *3MK7 0.2833149   0.0003    0.000     51.91    20.86     7.3
 *M8   0.3220456   0.0003    0.000    308.11    13.70      18
```

E.1.7: Phase 1: NOAA Aquatrak referenced to the WaterLog Bubbler.

```
number of standard constituents used: 17
Points used: 5029 of 5030
percent of var residual after lsqfit/var original:  8.50 %
Greenwich phase computed with nodal corrections applied to amplitude
and phase relative to center time
Using nonlinear bootstrapped error estimates
Generating prediction with nodal corrections, SNR is 2.000000
percent of var residual after synthesis/var original:  8.51 %
----------------------------------
date: 08-Nov-2011
nobs = 5030,  ngood = 5029,  record length (days) = 20.96
start time: 19-Aug-2010 14:12:00
rayleigh criterion = 1.0
Greenwich phase computed with nodal corrections applied to amplitude
and phase relative to center time

x0= 0.0166, x trend= 0

var(x)= 0.84349   var(xp)= 0.77177   var(xres)= 0.07179
percent var predicted/var original= 91.5 %

        tidal amplitude and phase with 95% CI estimates
```

tide	freq	amp	amp_err	pha	pha_err	snr
MSF	0.0028219	0.0162	0.022	347.94	96.77	0.54
*O1	0.0387307	0.1032	0.006	174.16	3.43	2.8e+02
*K1	0.0417807	0.1143	0.005	224.23	2.99	5.3e+02
*M2	0.0805114	1.2124	0.042	101.84	1.74	8.4e+02
*S2	0.0833333	0.2742	0.040	144.49	8.46	47
*M3	0.1207671	0.0050	0.001	166.72	11.42	25
*SK3	0.1251141	0.0055	0.001	230.67	10.28	39
*M4	0.1610228	0.0168	0.002	318.85	7.43	66
*MS4	0.1638447	0.0137	0.002	5.49	8.63	41
*S4	0.1666667	0.0029	0.002	152.26	41.73	2.3
*2MK5	0.2028035	0.0026	0.001	125.53	16.21	15
*2SK5	0.2084474	0.0019	0.001	255.64	22.28	6.1
*M6	0.2415342	0.0047	0.001	129.92	16.47	15
*2MS6	0.2443561	0.0059	0.001	194.09	12.46	22
*2SM6	0.2471781	0.0027	0.001	4.00	25.56	4.2
*3MK7	0.2833149	0.0027	0.000	60.43	8.73	30
*M8	0.3220456	0.0013	0.001	268.63	27.09	6

E.1.8: Phase 1: WaterLog Bubbler.

```
number of standard constituents used: 17
Points used: 5028 of 5030
percent of var residual after lsqfit/var original:  8.51 %
Greenwich phase computed with nodal corrections applied to amplitude
and phase relative to center time
Using nonlinear bootstrapped error estimates
Generating prediction with nodal corrections, SNR is 2.000000
percent of var residual after synthesis/var original:  8.53 %
----------------------------------
date: 08-Nov-2011
nobs = 5030,  ngood = 5028,  record length (days) = 20.96
start time: 19-Aug-2010 14:12:00
rayleigh criterion = 1.0
Greenwich phase computed with nodal corrections applied to amplitude
and phase relative to center time

x0= 0.0117, x trend= 0

var(x)= 0.84044   var(xp)= 0.76882   var(xres)= 0.071704
percent var predicted/var original= 91.5 %
```

tidal amplitude and phase with 95% CI estimates

tide	freq	amp	amp_err	pha	pha_err	snr
MSF	0.0028219	0.0184	0.024	351.08	84.15	0.56
*O1	0.0387307	0.1003	0.006	174.57	3.33	3.2e+02
*K1	0.0417807	0.1128	0.006	226.70	2.92	4.1e+02
*M2	0.0805114	1.2107	0.044	101.89	2.01	7.7e+02
*S2	0.0833333	0.2717	0.046	144.49	9.16	36
*M3	0.1207671	0.0053	0.001	178.29	15.28	13
*SK3	0.1251141	0.0051	0.001	242.45	14.66	15
*M4	0.1610228	0.0161	0.002	320.56	7.27	79
*MS4	0.1638447	0.0128	0.002	1.70	9.90	35
S4	0.1666667	0.0012	0.002	138.39	99.43	0.53
*2MK5	0.2028035	0.0026	0.001	130.78	14.82	17
*2SK5	0.2084474	0.0015	0.001	253.41	23.06	6.8
*M6	0.2415342	0.0052	0.001	130.93	14.54	18
*2MS6	0.2443561	0.0061	0.001	195.21	11.79	17
*2SM6	0.2471781	0.0028	0.001	355.44	24.60	5.2
*3MK7	0.2833149	0.0026	0.000	56.32	9.87	55
*M8	0.3220456	0.0012	0.001	272.51	23.46	4.9

E.1.9: Phase 1: NCDC Atmospheric Pressure referenced to the WaterLog Bubbler.

```
number of standard constituents used: 17
Points used: 5029 of 5030
percent of var residual after lsqfit/var original: 91.61 %
Greenwich phase computed with nodal corrections applied to amplitude
and phase relative to center time
Using nonlinear bootstrapped error estimates
Generating prediction with nodal corrections, SNR is 2.000000
percent of var residual after synthesis/var original: 99.15 %
--------------------------------
date: 08-Nov-2011
nobs = 5030, ngood = 5029, record length (days) = 20.96
start time: 19-Aug-2010 14:12:00
rayleigh criterion = 1.0
Greenwich phase computed with nodal corrections applied to amplitude
and phase relative to center time

x0= 10.1, x trend= 0

var(x)= 0.0036815   var(xp)= 3.0994e-05   var(xres)= 0.0036504
percent var predicted/var original= 0.8 %

        tidal amplitude and phase with 95% CI estimates
```

tide	freq	amp	amp_err	pha	pha_err	snr
MSF	0.0028219	0.0241	0.020	86.39	52.10	1.5
*O1	0.0387307	0.0032	0.001	153.03	24.80	4.8
*K1	0.0417807	0.0050	0.001	83.74	15.59	18
*M2	0.0805114	0.0010	0.000	65.03	22.86	6.3
*S2	0.0833333	0.0053	0.000	75.34	4.49	1.7e+02
*M3	0.1207671	0.0006	0.000	119.61	22.20	6.3
SK3	0.1251141	0.0002	0.000	229.17	63.78	0.67
*M4	0.1610228	0.0004	0.000	114.29	16.91	10
*MS4	0.1638447	0.0005	0.000	135.40	16.94	16
*S4	0.1666667	0.0003	0.000	124.14	30.04	4.8
*2MK5	0.2028035	0.0005	0.000	213.51	16.96	17
*2SK5	0.2084474	0.0006	0.000	299.22	12.84	24
*M6	0.2415342	0.0004	0.000	128.33	17.40	13
*2MS6	0.2443561	0.0004	0.000	158.83	18.94	8.9
*2SM6	0.2471781	0.0004	0.000	192.55	16.52	11
*3MK7	0.2833149	0.0002	0.000	220.09	15.17	17
*M8	0.3220456	0.0003	0.000	136.04	8.21	59

E.1.10: Phase 1: NOAA Aquatrak referenced to the WaterLog MWWL.

```
number of standard constituents used: 35
Points used: 8281 of 8291
percent of var residual after lsqfit/var original:  0.17 %
Greenwich phase computed with nodal corrections applied to amplitude
and phase relative to center time
Using nonlinear bootstrapped error estimates
Generating prediction with nodal corrections, SNR is 2.000000
percent of var residual after synthesis/var original:  0.17 %
-----------------------------------
date: 08-Nov-2011
nobs = 8291,  ngood = 8281,  record length (days) = 34.55
start time: 01-Jul-2010
rayleigh criterion = 1.0
Greenwich phase computed with nodal corrections applied to amplitude \n and
phase relative to center time

x0= -0.00848, x trend= 0

var(x)= 0.86204   var(xp)= 0.86056   var(xres)= 0.0014583
percent var predicted/var original= 99.8 %
```

tidal amplitude and phase with 95% CI estimates

tide	freq	amp	amp_err	pha	pha_err	snr
*MM	0.0015122	0.0418	0.005	45.21	7.14	81
MSF	0.0028219	0.0060	0.005	246.19	50.69	1.6
*ALP1	0.0343966	0.0055	0.001	296.50	15.96	14
*2Q1	0.0357064	0.0046	0.002	258.39	20.02	9.4
*Q1	0.0372185	0.0165	0.002	170.27	4.75	1.1e+02
*O1	0.0387307	0.1134	0.002	185.09	0.84	4.9e+03
*NO1	0.0402686	0.0146	0.001	202.80	4.16	1.7e+02
*K1	0.0417807	0.1647	0.002	214.18	0.58	1e+04
*J1	0.0432929	0.0074	0.002	196.91	11.20	19
*OO1	0.0448308	0.0031	0.001	229.20	23.81	5.7
*UPS1	0.0463430	0.0037	0.001	321.05	20.75	9.5
*EPS2	0.0761773	0.0025	0.002	346.22	44.40	2.3
*MU2	0.0776895	0.0268	0.002	350.73	4.11	2.5e+02
*N2	0.0789992	0.3155	0.002	84.69	0.37	3.3e+04
*M2	0.0805114	1.2968	0.002	107.29	0.08	4.4e+05
*L2	0.0820236	0.0956	0.003	147.21	1.64	1.3e+03
*S2	0.0833333	0.1639	0.002	159.71	0.69	7e+03
*ETA2	0.0850736	0.0079	0.002	298.41	12.98	21
*MO3	0.1192421	0.0057	0.001	200.84	6.96	69
*M3	0.1207671	0.0031	0.001	145.73	11.70	21
*MK3	0.1222921	0.0047	0.001	278.11	7.60	43
SK3	0.1251141	0.0007	0.001	161.97	58.33	1.1
*MN4	0.1595106	0.0092	0.001	321.09	3.12	3.3e+02
*M4	0.1610228	0.0208	0.001	329.02	1.51	1.5e+03
*SN4	0.1623326	0.0029	0.001	243.54	9.52	30
*MS4	0.1638447	0.0066	0.001	31.34	4.35	1.6e+02
*S4	0.1666667	0.0020	0.001	137.49	13.47	16
*2MK5	0.2028035	0.0022	0.000	112.08	8.59	40
*2SK5	0.2084474	0.0021	0.000	155.37	10.04	28
*2MN6	0.2400221	0.0041	0.001	140.40	14.27	13
*M6	0.2415342	0.0078	0.001	141.73	7.91	46
*2MS6	0.2443561	0.0027	0.001	209.87	22.67	6.8
2SM6	0.2471781	0.0007	0.001	347.40	84.58	0.63
*3MK7	0.2833149	0.0008	0.000	14.87	18.91	8.9
*M8	0.3220456	0.0018	0.000	324.08	11.07	20

E.1.11: Phase 1: WaterLog MWWL.

```
number of standard constituents used: 35
Points used: 8215 of 8291
percent of var residual after lsqfit/var original:  0.17 %
Greenwich phase computed with nodal corrections applied to amplitude
and phase relative to center time
Using nonlinear bootstrapped error estimates
Generating prediction with nodal corrections, SNR is 2.000000
percent of var residual after synthesis/var original:  0.17 %
----------------------------------
date: 08-Nov-2011
nobs = 8291,  ngood = 8215,  record length (days) = 34.55
start time: 01-Jul-2010
rayleigh criterion = 1.0
Greenwich phase computed with nodal corrections applied to amplitude
and phase relative to center time

x0= -0.00525, x trend= 0

var(x)= 0.86072   var(xp)= 0.8591   var(xres)= 0.0015026
percent var predicted/var original= 99.8 %
```

tidal amplitude and phase with 95% CI estimates

tide	freq	amp	amp_err	pha	pha_err	snr
*MM	0.0015122	0.0425	0.005	46.46	6.31	76
MSF	0.0028219	0.0049	0.005	251.78	56.61	1
*ALP1	0.0343966	0.0055	0.002	303.25	15.65	12
*2Q1	0.0357064	0.0058	0.001	254.19	14.86	17
*Q1	0.0372185	0.0165	0.001	169.24	5.91	1.3e+02
*O1	0.0387307	0.1103	0.002	185.37	0.77	5.1e+03
*NO1	0.0402686	0.0144	0.001	204.27	5.10	1.4e+02
*K1	0.0417807	0.1665	0.001	216.25	0.57	1.3e+04
*J1	0.0432929	0.0078	0.002	191.75	11.13	25
*OO1	0.0448308	0.0034	0.001	234.76	21.44	7.8
*UPS1	0.0463430	0.0036	0.001	322.41	20.53	7.2
EPS2	0.0761773	0.0024	0.002	352.49	45.68	1.8
*MU2	0.0776895	0.0267	0.002	348.78	3.70	2.2e+02
*N2	0.0789992	0.3158	0.002	84.85	0.35	3.1e+04
*M2	0.0805114	1.2951	0.002	107.38	0.08	5e+05
*L2	0.0820236	0.0948	0.002	147.74	1.37	1.8e+03
*S2	0.0833333	0.1628	0.002	160.05	0.65	6.5e+03
*ETA2	0.0850736	0.0080	0.002	299.24	10.57	27
*MO3	0.1192421	0.0062	0.001	211.76	5.43	84
*M3	0.1207671	0.0037	0.001	145.65	9.41	34
*MK3	0.1222921	0.0064	0.001	272.60	6.14	86
*SK3	0.1251141	0.0018	0.001	268.78	19.81	8.5
*MN4	0.1595106	0.0087	0.000	324.85	2.66	3.6e+02
*M4	0.1610228	0.0201	0.000	331.32	1.19	2.6e+03
*SN4	0.1623326	0.0023	0.000	241.41	10.48	33
*MS4	0.1638447	0.0063	0.000	26.42	3.56	3e+02
*S4	0.1666667	0.0009	0.000	137.40	23.17	3.6
*2MK5	0.2028035	0.0016	0.000	118.20	11.83	26
*2SK5	0.2084474	0.0017	0.000	161.68	11.11	23
*2MN6	0.2400221	0.0037	0.001	133.01	14.38	12
*M6	0.2415342	0.0071	0.001	142.89	7.97	47
*2MS6	0.2443561	0.0027	0.001	214.81	20.01	7.7
2SM6	0.2471781	0.0011	0.001	309.64	46.11	1.7
*3MK7	0.2833149	0.0006	0.000	340.55	22.32	4.9
*M8	0.3220456	0.0018	0.000	332.04	11.80	21

E.2.1: Phase 2: Shankhassic, Great Bay, NH.

```
number of standard constituents used: 35
    Points used: 10705 of 10706
    percent of var residual after lsqfit/var original:   4.30 %
    Greenwich phase computed with nodal corrections applied to amplitude
 and phase relative to center time
    Using nonlinear bootstrapped error estimates
    Generating prediction with nodal corrections, SNR is 2.000000
    percent of var residual after synthesis/var original:   4.86 %
----------------------------------
date: 08-Nov-2011
nobs = 10706,  ngood = 10705,  record length (days) = 44.61
start time: 25-Nov-2010
rayleigh criterion = 1.0
Greenwich phase computed with nodal corrections applied to amplitude
and phase relative to center time

x0= 0.0706, x trend= 0

var(x)= 0.51211   var(xp)= 0.48757   var(xres)= 0.024907
percent var predicted/var original= 95.2 %

        tidal amplitude and phase with 95% CI estimates

tide    freq       amp      amp_err     pha    pha_err     snr
 MM    0.0015122  0.0384    0.040     267.34    75.35      0.94
 MSF   0.0028219  0.0702    0.056      23.47    44.00      1.6
*ALP1  0.0343966  0.0096    0.003     211.39    23.87      8
*2Q1   0.0357064  0.0144    0.004     350.94    14.39      15
*Q1    0.0372185  0.0099    0.003     208.10    20.47      8.3
*O1    0.0387307  0.0943    0.004     230.33     2.13    5.2e+02
*NO1   0.0402686  0.0147    0.003     288.58     9.95      30
*K1    0.0417807  0.1426    0.003     242.04     1.59    1.7e+03
*J1    0.0432929  0.0080    0.004     154.11    24.55      5
*OO1   0.0448308  0.0087    0.003     143.68    19.99      8
 UPS1  0.0463430  0.0020    0.003     101.03    86.55      0.51
*EPS2  0.0761773  0.0138    0.003     233.87    12.51      24
*MU2   0.0776895  0.0383    0.003     279.41     4.60    1.6e+02
*N2    0.0789992  0.1470    0.003     145.56     1.12    2.7e+03
*M2    0.0805114  0.9353    0.003     168.50     0.19    8.5e+04
*L2    0.0820236  0.0768    0.004     183.75     3.21    3.6e+02
*S2    0.0833333  0.0907    0.003     218.12     1.82    1e+03
*ETA2  0.0850736  0.0070    0.003     259.93    22.73      6.1
*MO3   0.1192421  0.0182    0.001     271.11     3.61    2.5e+02
*M3    0.1207671  0.0080    0.001     202.69     8.18      43
*MK3   0.1222921  0.0144    0.001     287.63     4.80    1.7e+02
*SK3   0.1251141  0.0023    0.001     307.97    27.15      3
*MN4   0.1595106  0.0051    0.001     184.81    12.42      16
*M4    0.1610228  0.0167    0.001     236.86     4.38    1.4e+02
*SN4   0.1623326  0.0025    0.001     272.15    30.04      4.3
*MS4   0.1638447  0.0051    0.001     282.94    14.75      16
 S4    0.1666667  0.0008    0.001     242.83    91.28      0.52
*2MK5  0.2028035  0.0125    0.001     214.47     6.57      72
 2SK5  0.2084474  0.0011    0.001     343.62    77.68      0.75
*2MN6  0.2400221  0.0204    0.003     113.98     7.77      51
*M6    0.2415342  0.0404    0.003     146.06     3.99    2e+02
*2MS6  0.2443561  0.0116    0.003     202.68    13.33      16
 2SM6  0.2471781  0.0022    0.003     270.24    74.09      0.61
*3MK7  0.2833149  0.0053    0.001     272.43    10.37      41
*M8    0.3220456  0.0043    0.001     177.12     8.46      43
```

E.2.2: Phase 2: NCDC Atmospheric Pressure referenced to Shankhassic, Great Bay, NH.

```
number of standard constituents used: 35
Points used: 10705 of 10706
percent of var residual after lsqfit/var original: 93.60 %
Greenwich phase computed with nodal corrections applied to amplitude
and phase relative to center time
Using nonlinear bootstrapped error estimates
Generating prediction with nodal corrections, SNR is 2.000000
percent of var residual after synthesis/var original: 99.64 %
---------------------------------
date: 08-Nov-2011
nobs = 10706,  ngood = 10705,  record length (days) = 44.61
start time: 25-Nov-2010
rayleigh criterion = 1.0
Greenwich phase computed with nodal corrections applied to amplitude
and phase relative to center time

x0= 10.1, x trend= 0

var(x)= 0.012882   var(xp)= 4.7945e-05   var(xres)= 0.012836
percent var predicted/var original= 0.4 %
```

tidal amplitude and phase with 95% CI estimates

tide	freq	amp	amp_err	pha	pha_err	snr
MM	0.0015122	0.0263	0.029	8.73	75.11	0.82
MSF	0.0028219	0.0249	0.030	232.78	85.99	0.69
*ALP1	0.0343966	0.0049	0.001	13.83	11.63	22
*2Q1	0.0357064	0.0026	0.001	86.66	23.33	6.6
*Q1	0.0372185	0.0025	0.001	298.17	22.86	6.3
*O1	0.0387307	0.0024	0.001	14.69	26.86	5.5
*NO1	0.0402686	0.0024	0.001	114.12	18.54	9.1
K1	0.0417807	0.0011	0.001	112.27	59.61	1.2
*J1	0.0432929	0.0017	0.001	34.57	36.58	2.3
*OO1	0.0448308	0.0022	0.001	321.97	22.66	6.2
UPS1	0.0463430	0.0009	0.001	225.01	55.46	1.2
EPS2	0.0761773	0.0004	0.000	359.08	38.23	1.8
*MU2	0.0776895	0.0008	0.000	324.45	25.17	7.7
N2	0.0789992	0.0001	0.000	217.26	107.66	0.3
*M2	0.0805114	0.0010	0.000	43.58	15.76	14
*L2	0.0820236	0.0010	0.000	101.90	23.52	8.5
*S2	0.0833333	0.0052	0.000	40.24	3.05	3.1e+02
ETA2	0.0850736	0.0002	0.000	254.23	98.88	0.36
*MO3	0.1192421	0.0004	0.000	274.13	27.21	5.2
*M3	0.1207671	0.0004	0.000	312.24	25.58	5
*MK3	0.1222921	0.0003	0.000	331.80	29.95	4.4
*SK3	0.1251141	0.0022	0.000	316.38	4.79	1.6e+02
*MN4	0.1595106	0.0003	0.000	264.02	27.14	4.4
*M4	0.1610228	0.0003	0.000	357.75	26.58	2.7
*SN4	0.1623326	0.0004	0.000	16.57	22.86	7.4
*MS4	0.1638447	0.0003	0.000	258.25	23.80	5.8
*S4	0.1666667	0.0011	0.000	161.88	8.74	45
*2MK5	0.2028035	0.0003	0.000	217.73	18.12	13
*2SK5	0.2084474	0.0004	0.000	100.35	13.52	15
2MN6	0.2400221	0.0001	0.000	254.35	62.37	0.96
M6	0.2415342	0.0002	0.000	170.47	38.94	1.9
2MS6	0.2443561	0.0001	0.000	254.84	67.15	1.4
2SM6	0.2471781	0.0001	0.000	342.06	92.03	0.41
*3MK7	0.2833149	0.0001	0.000	221.57	43.11	2.1
*M8	0.3220456	0.0001	0.000	32.11	18.00	7.7

E.2.3: Phase 2: Winnicut River, Great Bay, NH.

```
number of standard constituents used: 35
Points used: 13681 of 13681
percent of var residual after lsqfit/var original:  4.88 %
Greenwich phase computed with nodal corrections applied to amplitude
and phase relative to center time
Using nonlinear bootstrapped error estimates
Generating prediction with nodal corrections, SNR is 2.000000
percent of var residual after synthesis/var original:  5.04 %
---------------------------------
date: 08-Nov-2011
nobs = 13681,  ngood = 13681,  record length (days) = 57.00
start time: 19-Nov-2010
rayleigh criterion = 1.0
Greenwich phase computed with nodal corrections applied to amplitude
and phase relative to center time

x0= 0.052, x trend= 0

var(x)= 0.45166   var(xp)= 0.42944   var(xres)= 0.022752
percent var predicted/var original= 95.1 %

        tidal amplitude and phase with 95% CI estimates

tide    freq       amp     amp_err    pha     pha_err    snr
*MM    0.0015122  0.0648    0.025    27.42     23.19     6.8
 MSF   0.0028219  0.0336    0.030    79.20     48.05     1.3
 ALP1  0.0343966  0.0039    0.005    38.21     72.75     0.68
 2Q1   0.0357064  0.0064    0.005    11.70     44.12     1.9
*Q1    0.0372185  0.0108    0.005   211.84     25.56     5.3
*O1    0.0387307  0.0858    0.005   234.93      3.11   2.7e+02
*NO1   0.0402686  0.0087    0.003   255.52     23.35     7.1
*K1    0.0417807  0.1373    0.005   250.88      2.05   7.4e+02
*J1    0.0432929  0.0133    0.004   133.50     17.58     9
*OO1   0.0448308  0.0060    0.004   157.02     40.64     2.6
*UPS1  0.0463430  0.0077    0.004   186.11     31.05     3.1
 EPS2  0.0761773  0.0095    0.009    33.19     57.18     1.2
*MU2   0.0776895  0.0256    0.010   275.75     22.36     6.1
*N2    0.0789992  0.1366    0.010   160.28      3.88   2e+02
*M2    0.0805114  0.8836    0.011   171.58      0.65   6.6e+03
*L2    0.0820236  0.1084    0.013   186.68      6.70     66
*S2    0.0833333  0.1064    0.009   218.09      4.88   1.3e+02
 ETA2  0.0850736  0.0105    0.009    15.23     45.03     1.4
*MO3   0.1192421  0.0213    0.002   293.90      6.32     80
*M3    0.1207671  0.0138    0.002   221.78      9.55     40
*MK3   0.1222921  0.0285    0.003   334.62      5.41   1.2e+02
*SK3   0.1251141  0.0034    0.002   286.33     37.88      2
*MN4   0.1595106  0.0360    0.007   267.87     10.44     28
*M4    0.1610228  0.0664    0.006   292.92      5.08   1.1e+02
*SN4   0.1623326  0.0163    0.006   209.15     20.59     6.6
*MS4   0.1638447  0.0103    0.007   302.76     43.17     2.4
 S4    0.1666667  0.0019    0.005    96.93    156.14     0.17
 2MK5  0.2028035  0.0028    0.002   336.04     42.20     1.9
 2SK5  0.2084474  0.0004    0.001   300.38    173.28     0.083
 2MN6  0.2400221  0.0036    0.003   197.56     38.22     1.7
*M6    0.2415342  0.0209    0.003   166.10      7.92     52
*2MS6  0.2443561  0.0074    0.003   259.37     21.72     6.6
 2SM6  0.2471781  0.0027    0.002   143.34     68.86     1.2
*3MK7  0.2833149  0.0056    0.001   334.97     17.47     14
*M8    0.3220456  0.0092    0.001   266.38      5.44   1.1e+02
```

E.2.4: Phase 2: NCDC Atmospheric Pressure referenced to Winnicut River, Great Bay, NH.

```
number of standard constituents used: 35
Points used: 13681 of 13681
percent of var residual after lsqfit/var original: 93.53 %
Greenwich phase computed with nodal corrections applied to amplitude
and phase relative to center time
Using nonlinear bootstrapped error estimates
Generating prediction with nodal corrections, SNR is 2.000000
percent of var residual after synthesis/var original: 99.81 %
-----------------------------------
date: 08-Nov-2011
nobs = 13681,  ngood = 13681,  record length (days) = 57.00
start time: 19-Nov-2010
rayleigh criterion = 1.0
Greenwich phase computed with nodal corrections applied to amplitude
and phase relative to center time

x0= 10.1, x trend= 0

var(x)= 0.013156   var(xp)= 2.5434e-05   var(xres)= 0.01313
percent var predicted/var original= 0.2 %
```

```
        tidal amplitude and phase with 95% CI estimates

   tide   freq       amp     amp_err    pha     pha_err    snr
    MM   0.0015122  0.0325   0.026    303.91    55.17     1.5
   MSF   0.0028219  0.0267   0.030    276.61    65.04     0.81
   ALP1  0.0343966  0.0002   0.001    215.41   203.36     0.056
    2Q1  0.0357064  0.0009   0.001    128.94    83.12     0.55
   *Q1   0.0372185  0.0029   0.001    292.26    31.12     4
    O1   0.0387307  0.0006   0.001      6.34   121.70     0.22
    NO1  0.0402686  0.0010   0.001    143.71    61.04     0.95
   *K1   0.0417807  0.0027   0.001    126.21    35.73     3.6
    J1   0.0432929  0.0021   0.001      3.99    45.18     1.9
    OO1  0.0448308  0.0007   0.001    317.03    97.55     0.42
   UPS1  0.0463430  0.0010   0.001    346.77    81.96     0.63
  *EPS2  0.0761773  0.0003   0.000    353.03    31.79     2.7
    MU2  0.0776895  0.0002   0.000     18.72    56.15     1.2
    N2   0.0789992  0.0003   0.000    193.01    44.61     1.6
   *M2   0.0805114  0.0006   0.000     62.14    20.49     8.4
   *L2   0.0820236  0.0006   0.000    144.11    29.34     3.9
   *S2   0.0833333  0.0051   0.000     34.77     2.61   5.1e+02
  *ETA2  0.0850736  0.0004   0.000     25.12    23.44     5.8
    MO3  0.1192421  0.0001   0.000    235.31    61.09     0.86
   *M3   0.1207671  0.0002   0.000    239.12    31.83     2.6
    MK3  0.1222921  0.0002   0.000    114.71    53.61     1.6
   *SK3  0.1251141  0.0025   0.000    307.90     3.20   3.5e+02
   *MN4  0.1595106  0.0003   0.000    245.34    31.73     4.1
    M4   0.1610228  0.0001   0.000    112.68    94.61     0.59
    SN4  0.1623326  0.0001   0.000    114.00    82.91     0.65
   *MS4  0.1638447  0.0004   0.000    292.82    23.22     5.6
   *S4   0.1666667  0.0011   0.000    167.51     8.06    51
  *2MK5  0.2028035  0.0004   0.000    181.89    12.72    23
   2SK5  0.2084474  0.0001   0.000     60.92    76.48     1.1
   2MN6  0.2400221  0.0001   0.000     59.66    64.30     1.1
    M6   0.2415342  0.0001   0.000    222.05    38.98     1.9
   2MS6  0.2443561  0.0001   0.000    234.61   114.57     0.33
   2SM6  0.2471781  0.0001   0.000     53.33    44.18     1.9
  *3MK7  0.2833149  0.0001   0.000    279.17    34.80     3.9
   *M8   0.3220456  0.0001   0.000     12.07    24.64     6.9
```

E.2.5: Phase 2: Adam's Point, Great Bay, NH.

```
number of standard constituents used: 35
Points used: 24456 of 24481
percent of var residual after lsqfit/var original:  4.04 %
Greenwich phase computed with nodal corrections applied to amplitude
and phase relative to center time
Using nonlinear bootstrapped error estimates
Generating prediction with nodal corrections, SNR is 2.000000
percent of var residual after synthesis/var original:  4.10 %
-----------------------------------
date: 08-Nov-2011
nobs = 24481,  ngood = 24456,  record length (days) = 102.00
start time: 23-Sep-2010 16:00:00
rayleigh criterion = 1.0
Greenwich phase computed with nodal corrections applied to amplitude
and phase relative to center time

x0= -0.101, x trend= 0

var(x)= 0.4798   var(xp)= 0.46012   var(xres)= 0.019694
percent var predicted/var original= 95.9 %
```

tidal amplitude and phase with 95% CI estimates

tide	freq	amp	amp_err	pha	pha_err	snr
*MM	0.0015122	0.0386	0.021	90.38	33.01	3.5
MSF	0.0028219	0.0242	0.020	90.26	52.07	1.5
ALP1	0.0343966	0.0005	0.002	79.17	208.21	0.047
2Q1	0.0357064	0.0023	0.003	79.90	74.65	0.6
*Q1	0.0372185	0.0102	0.003	201.39	17.45	8.8
*O1	0.0387307	0.0846	0.003	224.76	2.43	6e+02
*NO1	0.0402686	0.0105	0.002	277.54	13.92	24
*K1	0.0417807	0.1182	0.004	236.79	1.61	1.1e+03
*J1	0.0432929	0.0085	0.003	294.88	22.08	6.7
OO1	0.0448308	0.0020	0.003	41.86	78.22	0.63
*UPS1	0.0463430	0.0056	0.003	141.68	30.68	3.8
*EPS2	0.0761773	0.0125	0.004	226.28	18.76	9.2
*MU2	0.0776895	0.0389	0.005	269.69	5.88	71
*N2	0.0789992	0.1714	0.004	131.58	1.34	1.6e+03
*M2	0.0805114	0.9199	0.004	165.82	0.27	5.7e+04
*L2	0.0820236	0.1007	0.006	196.92	3.30	3.2e+02
*S2	0.0833333	0.1039	0.004	199.25	2.34	6.2e+02
ETA2	0.0850736	0.0040	0.004	173.28	53.25	0.93
*MO3	0.1192421	0.0128	0.001	270.14	3.18	2.3e+02
*M3	0.1207671	0.0058	0.001	188.46	6.33	62
*MK3	0.1222921	0.0117	0.001	278.67	2.82	2.9e+02
*SK3	0.1251141	0.0020	0.001	339.72	21.78	7.6
*MN4	0.1595106	0.0045	0.001	202.74	8.39	43
*M4	0.1610228	0.0087	0.001	263.03	4.54	1.8e+02
*SN4	0.1623326	0.0017	0.001	297.80	24.94	8.9
*MS4	0.1638447	0.0022	0.001	284.59	15.96	13
*S4	0.1666667	0.0011	0.001	212.99	37.54	3.2
*2MK5	0.2028035	0.0107	0.001	185.68	5.56	1.9e+02
2SK5	0.2084474	0.0002	0.001	161.23	171.53	0.14
*2MN6	0.2400221	0.0204	0.002	97.60	4.31	1.7e+02
*M6	0.2415342	0.0372	0.002	136.82	2.52	5.2e+02
*2MS6	0.2443561	0.0127	0.002	164.21	6.22	66
2SM6	0.2471781	0.0017	0.002	187.32	51.82	1.3
*3MK7	0.2833149	0.0031	0.000	213.25	7.55	62
*M8	0.3220456	0.0021	0.000	130.87	9.74	38

E.2.6: Phase 2: NCDC Atmospheric Pressure referenced to Adam's Point, Great Bay, NH.

```
number of standard constituents used: 35
Points used: 24481 of 24481
percent of var residual after lsqfit/var original: 98.75 %
Greenwich phase computed with nodal corrections applied to amplitude
and phase relative to center time
Using nonlinear bootstrapped error estimates
Generating prediction with nodal corrections, SNR is 2.000000
percent of var residual after synthesis/var original: 99.77 %
-----------------------------------
date: 08-Nov-2011
nobs = 24481, ngood = 24481, record length (days) = 102.00
start time: 23-Sep-2010 16:00:00
rayleigh criterion = 1.0
Greenwich phase computed with nodal corrections applied to amplitude
and phase relative to center time

x0= 10.1, x trend= 0

var(x)= 0.010756   var(xp)= 2.3922e-05   var(xres)= 0.010731
percent var predicted/var original= 0.2 %
```

tidal amplitude and phase with 95% CI estimates

tide	freq	amp	amp_err	pha	pha_err	snr
MM	0.0015122	0.0138	0.017	290.17	74.37	0.64
MSF	0.0028219	0.0055	0.013	233.53	179.46	0.19
ALP1	0.0343966	0.0008	0.001	321.34	88.49	0.53
*2Q1	0.0357064	0.0020	0.001	57.33	34.10	2.3
*Q1	0.0372185	0.0019	0.001	246.31	36.09	3.1
O1	0.0387307	0.0008	0.001	322.42	90.84	0.59
NO1	0.0402686	0.0010	0.001	172.27	52.32	1.5
*K1	0.0417807	0.0033	0.001	77.59	20.82	6.5
J1	0.0432929	0.0011	0.001	63.53	56.43	1.1
OO1	0.0448308	0.0004	0.001	356.59	131.73	0.31
UPS1	0.0463430	0.0008	0.001	258.76	73.98	0.91
*EPS2	0.0761773	0.0007	0.000	355.77	19.81	7.2
MU2	0.0776895	0.0002	0.000	224.50	76.03	0.69
N2	0.0789992	0.0002	0.000	213.45	73.65	0.89
*M2	0.0805114	0.0006	0.000	68.00	26.46	5
L2	0.0820236	0.0003	0.000	318.28	78.11	0.76
*S2	0.0833333	0.0049	0.000	50.74	3.15	3.5e+02
*ETA2	0.0850736	0.0004	0.000	18.01	44.45	2.1
MO3	0.1192421	0.0002	0.000	186.54	45.89	1.9
M3	0.1207671	0.0002	0.000	121.88	48.12	1.9
MK3	0.1222921	0.0002	0.000	318.90	55.73	1.6
*SK3	0.1251141	0.0017	0.000	284.95	5.04	1.5e+02
MN4	0.1595106	0.0001	0.000	157.32	44.78	1.6
M4	0.1610228	0.0001	0.000	329.34	47.41	1.5
*SN4	0.1623326	0.0001	0.000	49.95	32.96	3
*MS4	0.1638447	0.0002	0.000	270.61	20.12	9
*S4	0.1666667	0.0005	0.000	169.40	10.11	48
*2MK5	0.2028035	0.0002	0.000	137.63	16.50	11
*2SK5	0.2084474	0.0002	0.000	85.99	13.69	14
*2MN6	0.2400221	0.0001	0.000	255.27	21.29	7.1
*M6	0.2415342	0.0001	0.000	76.08	26.02	5.7
*2MS6	0.2443561	0.0001	0.000	45.48	22.00	6.8
*2SM6	0.2471781	0.0001	0.000	29.59	23.25	4.5
*3MK7	0.2833149	0.0001	0.000	236.87	17.94	9.5
*M8	0.3220456	0.0001	0.000	169.00	20.61	6.4

E.2.7: Phase 2: Squamscott River, Great Bay, NH.

```
number of standard constituents used: 35
Points used: 13853 of 13854
percent of var residual after lsqfit/var original:  4.95 %
Greenwich phase computed with nodal corrections applied to amplitude
and phase relative to center time
Using nonlinear bootstrapped error estimates
Generating prediction with nodal corrections, SNR is 2.000000
percent of var residual after synthesis/var original:  5.11 %
---------------------------------
date: 08-Nov-2011
nobs = 13854,  ngood = 13853,  record length (days) = 57.73
start time: 12-Nov-2010 20:42:00
rayleigh criterion = 1.0
Greenwich phase computed with nodal corrections applied to amplitude
and phase relative to center time

x0= 0.128, x trend= 0

var(x)= 0.50939   var(xp)= 0.48329   var(xres)= 0.026022
percent var predicted/var original= 94.9 %
```

tidal amplitude and phase with 95% CI estimates

tide	freq	amp	amp_err	pha	pha_err	snr
MM	0.0015122	0.0229	0.034	328.46	84.96	0.44
MSF	0.0028219	0.0291	0.037	96.36	75.41	0.6
ALP1	0.0343966	0.0058	0.005	277.41	46.00	1.6
*2Q1	0.0357064	0.0079	0.005	51.01	30.35	3
*Q1	0.0372185	0.0065	0.004	146.08	48.50	2.5
*O1	0.0387307	0.0879	0.005	233.05	3.06	2.9e+02
*NO1	0.0402686	0.0152	0.003	276.54	14.43	20
*K1	0.0417807	0.1407	0.005	246.63	2.04	7.3e+02
J1	0.0432929	0.0026	0.005	26.54	115.69	0.31
OO1	0.0448308	0.0038	0.003	209.69	55.88	1.3
UPS1	0.0463430	0.0002	0.003	256.85	256.23	0.0057
*EPS2	0.0761773	0.0159	0.004	222.04	17.94	17
*MU2	0.0776895	0.0437	0.005	293.78	6.70	84
*N2	0.0789992	0.1459	0.004	145.13	1.47	1.3e+03
*M2	0.0805114	0.9482	0.004	172.08	0.28	5.3e+04
*L2	0.0820236	0.0911	0.006	196.93	3.60	2.3e+02
*S2	0.0833333	0.0965	0.004	213.10	2.81	4.7e+02
ETA2	0.0850736	0.0016	0.003	200.37	153.00	0.29
*MO3	0.1192421	0.0190	0.002	272.37	5.93	1.3e+02
*M3	0.1207671	0.0110	0.002	218.07	9.92	35
*MK3	0.1222921	0.0241	0.002	307.45	4.20	1.6e+02
*SK3	0.1251141	0.0026	0.002	71.02	43.95	2.2
*MN4	0.1595106	0.0108	0.002	218.46	9.63	30
*M4	0.1610228	0.0369	0.002	253.88	2.84	4.9e+02
*SN4	0.1623326	0.0065	0.002	258.64	15.00	14
*MS4	0.1638447	0.0114	0.002	285.44	8.28	42
*S4	0.1666667	0.0038	0.002	35.25	26.83	4.7
*2MK5	0.2028035	0.0088	0.002	250.35	10.49	25
2SK5	0.2084474	0.0024	0.002	327.68	39.82	1.9
*2MN6	0.2400221	0.0198	0.003	126.50	8.15	52
*M6	0.2415342	0.0485	0.003	162.78	3.27	2.6e+02
*2MS6	0.2443561	0.0118	0.003	215.36	15.88	20
2SM6	0.2471781	0.0014	0.002	47.31	117.96	0.33
*3MK7	0.2833149	0.0060	0.001	299.94	11.23	23
*M8	0.3220456	0.0066	0.001	206.31	8.59	35

E.3.1: Phase 4: Water level observations at Squamscott River, Great Bay, NH.

```
number of standard constituents used: 29
Points used: 7439 of 7440
percent of var residual after lsqfit/var original:  1.76 %
Greenwich phase computed with nodal corrections applied to amplitude
and phase relative to center time
Using nonlinear bootstrapped error estimates
Generating prediction with nodal corrections, SNR is 2.000000
percent of var residual after synthesis/var original:  1.78 %
-----------------------------------
date: 08-Nov-2011
nobs = 7440,  ngood = 7439,  record length (days) = 31.00
start time: 15-May-2011
rayleigh criterion = 1.0
Greenwich phase computed with nodal corrections applied to amplitude
and phase relative to center time

x0= 1.29, x trend= 0

var(x)= 0.49882   var(xp)= 0.49069   var(xres)= 0.0088841
percent var predicted/var original= 98.4 %

         tidal amplitude and phase with 95% CI estimates
```

tide	freq	amp	amp_err	pha	pha_err	snr
MSF	0.0028219	0.0125	0.029	33.42	144.06	0.18
*2Q1	0.0357064	0.0061	0.003	151.43	22.83	4.4
*Q1	0.0372185	0.0112	0.003	223.76	14.99	17
*O1	0.0387307	0.0902	0.003	231.75	1.73	1.1e+03
*NO1	0.0402686	0.0095	0.002	293.52	11.22	20
*K1	0.0417807	0.1419	0.003	241.82	1.23	2.1e+03
*J1	0.0432929	0.0062	0.003	342.95	27.63	5.1
*OO1	0.0448308	0.0069	0.002	274.30	18.34	7.8
UPS1	0.0463430	0.0019	0.002	319.71	88.07	0.62
*N2	0.0789992	0.1577	0.013	135.61	4.83	1.4e+02
*M2	0.0805114	0.9355	0.014	173.26	0.88	4.3e+03
*S2	0.0833333	0.0777	0.016	211.66	9.03	24
ETA2	0.0850736	0.0082	0.013	176.07	97.69	0.41
*MO3	0.1192421	0.0223	0.001	284.61	4.14	2.4e+02
*M3	0.1207671	0.0060	0.001	209.07	14.28	19
*MK3	0.1222921	0.0230	0.001	301.43	3.53	2.4e+02
*SK3	0.1251141	0.0025	0.001	296.13	34.60	3
*MN4	0.1595106	0.0167	0.001	220.62	3.82	2.3e+02
*M4	0.1610228	0.0389	0.001	257.82	1.85	1.1e+03
*MS4	0.1638447	0.0076	0.001	291.31	8.45	50
S4	0.1666667	0.0009	0.001	298.30	76.80	0.93
*2MK5	0.2028035	0.0120	0.001	233.39	7.16	77
2SK5	0.2084474	0.0001	0.001	83.91	214.83	0.021
*2MN6	0.2400221	0.0196	0.003	127.59	8.48	38
*M6	0.2415342	0.0446	0.003	171.30	3.85	1.7e+02
*2MS6	0.2443561	0.0101	0.003	198.28	17.72	11
2SM6	0.2471781	0.0014	0.002	192.15	134.30	0.31
*3MK7	0.2833149	0.0082	0.001	280.54	8.06	63
*M8	0.3220456	0.0079	0.001	233.81	6.48	63

E.3.2: Phase 4: TCARI model predictions at Squamscott River, Great Bay, NH.

```
number of standard constituents used: 29
Points used: 7439 of 7440
percent of var residual after lsqfit/var original:  0.77 %
Greenwich phase computed with nodal corrections applied to amplitude
and phase relative to center time
Using nonlinear bootstrapped error estimates
Generating prediction with nodal corrections, SNR is 2.000000
percent of var residual after synthesis/var original:  0.77 %
-----------------------------------
date: 08-Nov-2011
nobs = 7440,  ngood = 7439,  record length (days) = 31.00
start time: 15-May-2011
rayleigh criterion = 1.0
Greenwich phase computed with nodal corrections applied to amplitude
and phase relative to center time

x0= 1.23, x trend= 0

var(x)= 0.4963   var(xp)= 0.4931   var(xres)= 0.0038264
percent var predicted/var original= 99.4 %
```

tidal amplitude and phase with 95% CI estimates

tide	freq	amp	amp_err	pha	pha_err	snr
*MSF	0.0028219	0.0004	0.000	349.10	23.02	8.3
*2Q1	0.0357064	0.0087	0.000	52.44	1.38	1.8e+03
*Q1	0.0372185	0.0076	0.000	139.76	1.46	1.6e+03
*O1	0.0387307	0.0882	0.000	232.04	0.12	1.5e+05
*NO1	0.0402686	0.0212	0.000	264.94	0.43	2.1e+04
*K1	0.0417807	0.1408	0.000	246.62	0.08	5.3e+05
*J1	0.0432929	0.0006	0.000	273.34	21.61	8
*OO1	0.0448308	0.0007	0.000	1.77	16.74	16
*UPS1	0.0463430	0.0009	0.000	53.83	12.33	20
*N2	0.0789992	0.1384	0.017	144.47	7.19	63
*M2	0.0805114	0.9423	0.016	172.19	0.92	3.3e+03
*S2	0.0833333	0.0987	0.017	209.91	9.75	33
ETA2	0.0850736	0.0076	0.012	134.25	121.01	0.38
*MO3	0.1192421	0.0178	0.000	268.64	0.23	5.4e+04
*M3	0.1207671	0.0123	0.000	217.75	0.36	2.8e+04
*MK3	0.1222921	0.0249	0.000	308.20	0.18	1.1e+05
*SK3	0.1251141	0.0002	0.000	34.73	17.23	11
*MN4	0.1595106	0.0101	0.000	217.34	0.19	6.8e+04
*M4	0.1610228	0.0372	0.000	254.13	0.05	1.1e+06
*MS4	0.1638447	0.0120	0.000	283.15	0.17	1.2e+05
*S4	0.1666667	0.0039	0.000	36.80	0.57	1.2e+04
*2MK5	0.2028035	0.0001	0.000	53.07	8.03	64
*2SK5	0.2084474	0.0001	0.000	30.70	10.88	26
*2MN6	0.2400221	0.0001	0.000	210.20	10.27	28
*M6	0.2415342	0.0491	0.000	162.54	0.02	1.1e+07
*2MS6	0.2443561	0.0000	0.000	242.18	19.47	8.5
*2SM6	0.2471781	0.0000	0.000	195.56	23.96	5.8
*3MK7	0.2833149	0.0001	0.000	79.23	6.07	1.1e+02
*M8	0.3220456	0.0060	0.000	202.58	0.04	2e+06

E.3.3: Phase 4: Residual water level (computed v. modeled) at Squamscott River, Great Bay, NH.

```
number of standard constituents used: 29
Points used: 7439 of 7440
percent of var residual after lsqfit/var original: 77.10 %
Greenwich phase computed with nodal corrections applied to amplitude
and phase relative to center time
Using nonlinear bootstrapped error estimates
Generating prediction with nodal corrections, SNR is 2.000000
percent of var residual after synthesis/var original: 78.22 %
-----------------------------------
date: 15-Apr-2012
nobs = 7440,  ngood = 7439,  record length (days) = 31.00
start time: 15-May-2011
rayleigh criterion = 1.0
Greenwich phase computed with nodal corrections applied to amplitude
and phase relative to center time

x0= 0.0616, x trend= 0

var(x)= 0.0082904   var(xp)= 0.0017711   var(xres)= 0.0064845
percent var predicted/var original= 21.4 %
```

```
        tidal amplitude and phase with 95% CI estimates

tide    freq       amp      amp_err    pha     pha_err     snr
 MSF  0.0028219   0.0122    0.025     34.61   155.06      0.24
*2Q1  0.0357064   0.0114    0.003    200.52    15.00      16
 *Q1  0.0372185   0.0129    0.003    259.88    12.22      23
  O1  0.0387307   0.0020    0.003    219.36    77.83      0.63
*NO1  0.0402686   0.0137    0.002     65.59     8.32      37
 *K1  0.0417807   0.0119    0.003    159.68    12.70      22
 *J1  0.0432929   0.0060    0.002    348.30    26.52      6.6
*OO1  0.0448308   0.0069    0.003    268.45    19.34      7.4
 UPS1 0.0463430   0.0021    0.002    296.05    73.34      0.82
 *N2  0.0789992   0.0300    0.005     90.23     8.79      33
 *M2  0.0805114   0.0188    0.005    283.97    15.46      13
 *S2  0.0833333   0.0212    0.005     23.49    13.63      19
 ETA2 0.0850736   0.0057    0.006    238.98    54.63      1.1
*MO3  0.1192421   0.0071    0.002    328.13    10.68      20
 *M3  0.1207671   0.0064    0.002     45.83    11.65      17
*MK3  0.1222921   0.0034    0.001    181.55    23.84      6.6
*SK3  0.1251141   0.0025    0.001    290.92    31.90      3
*MN4  0.1595106   0.0066    0.001    225.65    10.56      37
 *M4  0.1610228   0.0030    0.001    311.40    20.19      7.1
*MS4  0.1638447   0.0047    0.001     89.91    15.34      19
 *S4  0.1666667   0.0042    0.001    229.79    14.71      11
*2MK5 0.2028035   0.0120    0.001    233.38     7.03      80
 2SK5 0.2084474   0.0001    0.001    111.50   254.57      0.012
*2MN6 0.2400221   0.0196    0.003    127.32     9.27      36
 *M6  0.2415342   0.0085    0.003    289.22    21.04      8.7
*2MS6 0.2443561   0.0101    0.003    198.09    20.55      11
 2SM6 0.2471781   0.0013    0.002    192.05   138.77      0.31
*3MK7 0.2833149   0.0083    0.001    280.40     6.61      59
 *M8  0.3220456   0.0041    0.001    282.53    14.64      18
```

255

E.3.4: Phase 4: Residual water level (t tide generated v. modeled) at Squamscott River, Great Bay, NH.

```
number of standard constituents used: 29
Points used: 7439 of 7440
percent of var residual after lsqfit/var original:  0.00 %
Greenwich phase computed with nodal corrections applied to amplitude
and phase relative to center time
Using nonlinear bootstrapped error estimates
Generating prediction with nodal corrections, SNR is 2.000000
percent of var residual after synthesis/var original:  0.00 %
-----------------------------------
date: 15-Apr-2012
nobs = 7440, ngood = 7439,  record length (days) = 31.00
start time: 15-May-2011
rayleigh criterion = 1.0
Greenwich phase computed with nodal corrections applied to amplitude
and phase relative to center time

x0= 1.62e-15, x trend= 0

var(x)= 0.0017814   var(xp)= 0.0017814   var(xres)= 1.7072e-22
percent var predicted/var original= 100.0 %
```

tidal amplitude and phase with 95% CI estimates

tide	freq	amp	amp_err	pha	pha_err	snr
*MSF	0.0028219	0.0004	0.000	169.10	0.00	7.1e+22
*2Q1	0.0357064	0.0114	0.000	200.52	0.00	2.6e+27
*Q1	0.0372185	0.0129	0.000	259.88	0.00	2.7e+27
*O1	0.0387307	0.0020	0.000	219.36	0.00	7.5e+25
*NO1	0.0402686	0.0137	0.000	65.59	0.00	8.4e+27
*K1	0.0417807	0.0119	0.000	159.68	0.00	3.1e+27
*J1	0.0432929	0.0060	0.000	348.30	0.00	7e+26
*OO1	0.0448308	0.0069	0.000	268.45	0.00	1.3e+27
*UPS1	0.0463430	0.0009	0.000	233.83	0.00	1.9e+25
*N2	0.0789992	0.0300	0.000	90.23	0.00	2.9e+27
*M2	0.0805114	0.0188	0.000	283.97	0.00	1.2e+27
*S2	0.0833333	0.0212	0.000	23.49	0.00	1.3e+27
*ETA2	0.0850736	0.0000	0.000	186.27	29.64	3.9
*MO3	0.1192421	0.0071	0.000	328.13	0.00	1.7e+26
*M3	0.1207671	0.0064	0.000	45.83	0.00	1.1e+26
*MK3	0.1222921	0.0034	0.000	181.55	0.00	2.9e+25
*SK3	0.1251141	0.0025	0.000	290.92	0.00	1.8e+25
*MN4	0.1595106	0.0066	0.000	225.65	0.00	9e+25
*M4	0.1610228	0.0030	0.000	311.40	0.00	1.6e+25
*MS4	0.1638447	0.0047	0.000	89.91	0.00	4.2e+25
*S4	0.1666667	0.0039	0.000	216.80	0.00	2.7e+25
*2MK5	0.2028035	0.0120	0.000	233.38	0.00	6.7e+26
*2SK5	0.2084474	0.0001	0.000	210.70	0.00	1.7e+22
*2MN6	0.2400221	0.0196	0.000	127.32	0.00	3.7e+26
*M6	0.2415342	0.0085	0.000	289.22	0.00	7.2e+25
*2MS6	0.2443561	0.0101	0.000	198.09	0.00	8.8e+25
*2SM6	0.2471781	0.0000	0.000	15.56	0.00	1.3e+21
*3MK7	0.2833149	0.0083	0.000	280.40	0.00	1.5e+26
*M8	0.3220456	0.0041	0.000	282.53	0.00	3.2e+20

E.3.5: Phase 4: Water level observations at Nannie Island, Great Bay, NH.

```
number of standard constituents used: 29
Points used: 7430 of 7440
percent of var residual after lsqfit/var original:  1.79 %
Greenwich phase computed with nodal corrections applied to amplitude
and phase relative to center time
Using nonlinear bootstrapped error estimates
Generating prediction with nodal corrections, SNR is 2.000000
percent of var residual after synthesis/var original:  1.80 %
-----------------------------------
date: 08-Nov-2011
nobs = 7440,  ngood = 7430,  record length (days) = 31.00
start time: 27-Aug-2009
rayleigh criterion = 1.0
Greenwich phase computed with nodal corrections applied to amplitude
and phase relative to center time


x0= 1.37, x trend= 0

var(x)= 0.47209   var(xp)= 0.463   var(xres)= 0.0084903
percent var predicted/var original= 98.1 %
```

tidal amplitude and phase with 95% CI estimates

tide	freq	amp	amp_err	pha	pha_err	snr
*MSF	0.0028219	0.0658	0.018	263.02	14.96	13
2Q1	0.0357064	0.0017	0.002	242.73	60.52	0.93
*Q1	0.0372185	0.0162	0.002	215.92	7.07	85
*O1	0.0387307	0.0892	0.002	226.33	1.26	1.7e+03
*NO1	0.0402686	0.0094	0.002	211.79	14.98	17
*K1	0.0417807	0.0898	0.002	255.64	1.27	1.9e+03
*J1	0.0432929	0.0038	0.002	238.55	29.94	5.7
*OO1	0.0448308	0.0038	0.002	9.38	25.58	6.5
UPS1	0.0463430	0.0006	0.001	137.37	121.72	0.24
*N2	0.0789992	0.1884	0.019	126.30	7.09	97
*M2	0.0805114	0.9397	0.018	169.85	1.22	2.7e+03
*S2	0.0833333	0.1557	0.018	213.84	6.80	77
ETA2	0.0850736	0.0065	0.012	125.69	126.52	0.29
*MO3	0.1192421	0.0132	0.001	260.69	6.84	90
*M3	0.1207671	0.0057	0.002	177.44	17.48	11
*MK3	0.1222921	0.0084	0.002	286.75	10.69	28
*SK3	0.1251141	0.0031	0.001	350.84	22.60	4.7
*MN4	0.1595106	0.0046	0.001	184.49	7.91	44
*M4	0.1610228	0.0093	0.001	223.60	4.57	2.2e+02
*MS4	0.1638447	0.0058	0.001	231.65	7.28	60
S4	0.1666667	0.0004	0.001	41.40	91.36	0.56
*2MK5	0.2028035	0.0068	0.003	211.77	22.17	5.5
2SK5	0.2084474	0.0014	0.002	339.96	91.66	0.39
*2MN6	0.2400221	0.0275	0.004	92.88	7.69	57
*M6	0.2415342	0.0441	0.004	146.88	4.14	1.4e+02
*2MS6	0.2443561	0.0243	0.003	189.17	8.38	54
2SM6	0.2471781	0.0036	0.004	211.15	50.52	1.1
*3MK7	0.2833149	0.0019	0.001	242.03	31.02	2.7
*M8	0.3220456	0.0045	0.001	156.49	12.44	18

E.3.6: Phase 4: TCARI model predictions at Nannie Island, Great Bay, NH.

```
number of standard constituents used: 29
Points used: 7439 of 7440
percent of var residual after lsqfit/var original:  0.67 %
Greenwich phase computed with nodal corrections applied to amplitude
and phase relative to center time
Using nonlinear bootstrapped error estimates
Generating prediction with nodal corrections, SNR is 2.000000
percent of var residual after synthesis/var original:  0.68 %
----------------------------------
date: 08-Nov-2011
nobs = 7440,  ngood = 7439,  record length (days) = 31.00
start time: 27-Aug-2009
rayleigh criterion = 1.0
Greenwich phase computed with nodal corrections applied to amplitude
and phase relative to center time

x0= 1.15, x trend= 0

var(x)= 0.43723   var(xp)= 0.43392   var(xres)= 0.002971
percent var predicted/var original= 99.2 %
```

tidal amplitude and phase with 95% CI estimates

tide	freq	amp	amp_err	pha	pha_err	snr
*MSF	0.0028219	0.0001	0.000	173.45	25.23	5.6
*2Q1	0.0357064	0.0089	0.000	0.85	0.48	1.5e+04
*Q1	0.0372185	0.0102	0.000	202.70	0.46	1.7e+04
*O1	0.0387307	0.0904	0.000	231.13	0.05	1.5e+06
*NO1	0.0402686	0.0174	0.000	263.08	0.30	5.5e+04
*K1	0.0417807	0.1378	0.000	244.89	0.03	3.5e+06
*J1	0.0432929	0.0088	0.000	153.82	0.49	1.7e+04
*OO1	0.0448308	0.0064	0.000	149.06	0.55	1.1e+04
*UPS1	0.0463430	0.0003	0.000	47.64	12.57	24
*N2	0.0789992	0.1512	0.017	145.92	6.51	76
*M2	0.0805114	0.9195	0.013	169.71	0.93	5.1e+03
*S2	0.0833333	0.1030	0.014	214.86	7.99	54
ETA2	0.0850736	0.0046	0.008	156.72	114.33	0.33
*MO3	0.1192421	0.0177	0.000	276.34	0.24	7.6e+04
*M3	0.1207671	0.0100	0.000	205.85	0.45	1.3e+04
*MK3	0.1222921	0.0191	0.000	296.91	0.23	5.6e+04
*SK3	0.1251141	0.0002	0.000	206.13	16.68	10
*MN4	0.1595106	0.0150	0.000	214.56	0.23	6.3e+04
*M4	0.1610228	0.0331	0.000	260.10	0.10	3.2e+05
*MS4	0.1638447	0.0065	0.000	291.06	0.54	1.2e+04
*S4	0.1666667	0.0004	0.000	337.23	8.73	70
*2MK5	0.2028035	0.0002	0.000	144.90	8.91	50
*2SK5	0.2084474	0.0001	0.000	191.71	12.04	24
*2MN6	0.2400221	0.0002	0.000	253.52	12.08	20
*M6	0.2415342	0.0336	0.000	152.39	0.07	6.8e+05
*2MS6	0.2443561	0.0001	0.000	225.31	19.06	8.2
*2SM6	0.2471781	0.0001	0.000	53.70	24.39	5.9
*3MK7	0.2833149	0.0001	0.000	318.39	5.59	1.2e+02
*M8	0.3220456	0.0055	0.000	199.52	0.08	5e+05

E.3.7: Phase 4: NCDC Atmospheric Pressure referenced to Nannie Island, Great Bay, NH.

```
number of standard constituents used: 29
Points used: 7439 of 7440
percent of var residual after lsqfit/var original: 83.70 %
Greenwich phase computed with nodal corrections applied to amplitude
and phase relative to center time
Using nonlinear bootstrapped error estimates
Generating prediction with nodal corrections, SNR is 2.000000
percent of var residual after synthesis/var original: 83.73 %
------------------------------------
date: 08-Nov-2011
nobs = 7440,  ngood = 7439,   record length (days) = 31.00
start time: 27-Aug-2009
rayleigh criterion = 1.0
Greenwich phase computed with nodal corrections applied to amplitude
and phase relative to center time

x0= 10.2, x trend= 0

var(x)= 0.0037916    var(xp)= 0.00061637    var(xres)= 0.0031746
percent var predicted/var original= 16.3 %
```

```
        tidal amplitude and phase with 95% CI estimates

tide    freq       amp      amp_err   pha     pha_err   snr
*MSF  0.0028219  0.0346    0.011     72.77    21.73      9.3
*2Q1  0.0357064  0.0031    0.001     32.64    15.49      11
 Q1   0.0372185  0.0009    0.001    184.60    56.84      1.3
*O1   0.0387307  0.0022    0.001    212.30    24.59      6.3
*NO1  0.0402686  0.0024    0.001    325.92    21.47      5.6
*K1   0.0417807  0.0061    0.001     90.30     7.99      36
*J1   0.0432929  0.0015    0.001    268.29    31.87      3
 OO1  0.0448308  0.0003    0.001    258.51   111.33      0.37
 UPS1 0.0463430  0.0006    0.001    121.49    70.35      1.3
*N2   0.0789992  0.0002    0.000     97.92    41.31      2.4
*M2   0.0805114  0.0007    0.000    122.59    14.15      15
*S2   0.0833333  0.0042    0.000     70.07     1.84    5.9e+02
 ETA2 0.0850736  0.0000    0.000    189.96   264.81      0.0072
*MO3  0.1192421  0.0003    0.000     63.46    17.49      11
 M3   0.1207671  0.0001    0.000    208.37    50.79      1.5
*MK3  0.1222921  0.0003    0.000      2.81    17.24      13
*SK3  0.1251141  0.0004    0.000    118.75    15.98      12
*MN4  0.1595106  0.0004    0.000    191.58    19.99      8.8
*M4   0.1610228  0.0002    0.000    324.04    30.51      3.5
*MS4  0.1638447  0.0002    0.000     54.44    37.58      2
*S4   0.1666667  0.0002    0.000      4.22    42.61      2.3
*2MK5 0.2028035  0.0003    0.000    208.10    14.27      22
*2SK5 0.2084474  0.0001    0.000     53.12    27.33      3
 2MN6 0.2400221  0.0001    0.000    250.22    79.60      0.69
*M6   0.2415342  0.0002    0.000    132.33    26.73      4
*2MS6 0.2443561  0.0002    0.000    301.61    30.04      5.2
*2SM6 0.2471781  0.0002    0.000    111.50    21.45      5.8
*3MK7 0.2833149  0.0001    0.000    325.24    42.01      2.7
*M8   0.3220456  0.0001    0.000      8.65    12.38      18
```

E.3.8: Phase 4: Residual water level (computed v. modeled) at Nannie Island, Great Bay, NH.

```
number of standard constituents used: 29
Points used: 7439 of 7440
percent of var residual after lsqfit/var original: 38.15 %
Greenwich phase computed with nodal corrections applied to amplitude
and phase relative to center time
Using nonlinear bootstrapped error estimates
Generating prediction with nodal corrections, SNR is 2.000000
percent of var residual after synthesis/var original: 38.29 %
----------------------------------
date: 15-Apr-2012
nobs = 7440,  ngood = 7439,  record length (days) = 31.00
start time: 27-Aug-2009
rayleigh criterion = 1.0
Greenwich phase computed with nodal corrections applied to amplitude
and phase relative to center time

x0= 0.00039, x trend= 0

var(x)= 0.014296   var(xp)= 0.0088124   var(xres)= 0.0054743
percent var predicted/var original= 61.6 %
```

tidal amplitude and phase with 95% CI estimates

tide	freq	amp	amp_err	pha	pha_err	snr
*MSF	0.0028219	0.0658	0.017	263.09	14.71	16
*2Q1	0.0357064	0.0098	0.002	189.70	10.95	30
*Q1	0.0372185	0.0067	0.002	236.39	14.60	14
*O1	0.0387307	0.0076	0.002	129.44	13.99	15
*NO1	0.0402686	0.0137	0.002	115.50	9.47	50
*K1	0.0417807	0.0523	0.002	46.18	2.37	7.9e+02
*J1	0.0432929	0.0093	0.002	309.50	11.37	26
*OO1	0.0448308	0.0096	0.002	343.97	10.89	38
UPS1	0.0463430	0.0006	0.001	162.63	121.89	0.34
*N2	0.0789992	0.0684	0.014	78.42	10.55	25
*M2	0.0805114	0.0203	0.014	176.27	40.80	2.2
*S2	0.0833333	0.0528	0.015	211.86	16.09	13
ETA2	0.0850736	0.0035	0.007	83.10	123.83	0.22
*MO3	0.1192421	0.0062	0.002	131.36	12.68	17
*M3	0.1207671	0.0057	0.002	54.64	17.60	13
*MK3	0.1222921	0.0110	0.002	124.60	8.68	49
*SK3	0.1251141	0.0033	0.002	353.31	23.98	4.6
*MN4	0.1595106	0.0112	0.001	46.49	3.62	2.4e+02
*M4	0.1610228	0.0262	0.001	92.33	1.55	1.5e+03
*MS4	0.1638447	0.0061	0.001	165.72	6.24	68
S4	0.1666667	0.0004	0.001	100.30	85.64	0.48
*2MK5	0.2028035	0.0067	0.003	212.94	25.19	5.9
2SK5	0.2084474	0.0015	0.002	341.80	91.19	0.56
*2MN6	0.2400221	0.0276	0.004	92.74	6.94	61
*M6	0.2415342	0.0111	0.003	129.89	16.66	10
*2MS6	0.2443561	0.0242	0.004	188.98	9.18	44
2SM6	0.2471781	0.0037	0.003	211.64	55.07	1.3
*3MK7	0.2833149	0.0019	0.001	237.92	29.01	3.6
*M8	0.3220456	0.0038	0.001	73.66	14.11	14

E.3.9: Phase 4: Residual water level (t_tide generated v. modeled) at Nannie Island, Great Bay, NH.

```
number of standard constituents used: 29
Points used: 7439 of 7440
percent of var residual after lsqfit/var original:  0.00 %
Greenwich phase computed with nodal corrections applied to amplitude
and phase relative to center time
Using nonlinear bootstrapped error estimates
Generating prediction with nodal corrections, SNR is 2.000000
percent of var residual after synthesis/var original:  0.00 %
-----------------------------------
date: 15-Apr-2012
nobs = 7440,  ngood = 7439,  record length (days) = 31.00
start time: 27-Aug-2009
rayleigh criterion = 1.0
Greenwich phase computed with nodal corrections applied to amplitude
and phase relative to center time

x0= 2.66e-15, x trend= 0

var(x)= 0.0087988   var(xp)= 0.0087988   var(xres)= 4.2533e-22
percent var predicted/var original= 100.0 %
```

```
        tidal amplitude and phase with 95% CI estimates

    tide   freq      amp     amp_err    pha    pha_err    snr
   *MSF  0.0028219  0.0658   0.000    263.09    0.00   1.1e+27
   *2Q1  0.0357064  0.0089   0.000    180.85    0.00   1.5e+27
   *Q1   0.0372185  0.0067   0.000    236.45    0.00   5.8e+26
   *O1   0.0387307  0.0076   0.000    129.49    0.00     9e+26
   *NO1  0.0402686  0.0137   0.000    115.51    0.00   1.6e+27
   *K1   0.0417807  0.0523   0.000     46.19    0.00   2.7e+28
   *J1   0.0432929  0.0093   0.000    309.53    0.00   1.5e+27
   *OO1  0.0448308  0.0096   0.000    343.94    0.00   2.1e+27
   *UPS1 0.0463430  0.0003   0.000    227.64    0.00   2.2e+24
   *N2   0.0789992  0.0685   0.000     78.42    0.00   5.3e+27
   *M2   0.0805114  0.0203   0.000    176.25    0.00     4e+26
   *S2   0.0833333  0.0528   0.000    211.85    0.00   2.8e+27
   *ETA2 0.0850736  0.0000   0.000    129.03   54.64       2
   *MO3  0.1192421  0.0062   0.000    131.38    0.00   5.5e+25
   *M3   0.1207671  0.0057   0.000     54.62    0.00   3.1e+25
   *MK3  0.1222921  0.0110   0.000    124.63    0.00   1.6e+26
   *SK3  0.1251141  0.0033   0.000    353.23    0.00   1.4e+25
   *MN4  0.1595106  0.0112   0.000     46.52    0.00     8e+25
   *M4   0.1610228  0.0262   0.000     92.33    0.00   4.4e+26
   *MS4  0.1638447  0.0061   0.000    165.75    0.00   2.4e+25
   *S4   0.1666667  0.0004   0.000    157.23    0.00   9.7e+22
   *2MK5 0.2028035  0.0068   0.000    212.97    0.00   1.3e+26
   *2SK5 0.2084474  0.0001   0.000     11.71    0.00   3.2e+22
   *2MN6 0.2400221  0.0276   0.000     92.75    0.00   4.5e+26
   *M6   0.2415342  0.0111   0.000    129.90    0.00   7.5e+25
   *2MS6 0.2443561  0.0242   0.000    189.00    0.00   4.4e+26
   *2SM6 0.2471781  0.0001   0.000    233.70    0.00   6.1e+21
   *3MK7 0.2833149  0.0019   0.000    238.09    0.00   1.6e+25
   *M8   0.3220456  0.0038   0.000     73.73    0.00   1.6e+20
```

E.3.10: Phase 4: Water level observations at the mooring site in Great Bay, NH.

```
number of standard constituents used: 17
Points used: 4799 of 4800
percent of var residual after lsqfit/var original:  3.71 %
Greenwich phase computed with nodal corrections applied to amplitude
and phase relative to center time
Using nonlinear bootstrapped error estimates
Generating prediction with nodal corrections, SNR is 2.000000
percent of var residual after synthesis/var original:  3.71 %
---------------------------------
date: 08-Nov-2011
nobs = 4800,  ngood = 4799,  record length (days) = 20.00
start time: 12-Jul-2011 14:48:00
rayleigh criterion = 1.0
Greenwich phase computed with nodal corrections applied to amplitude
and phase relative to center time

x0= 1.13, x trend= 0

var(x)= 0.44305   var(xp)= 0.42661   var(xres)= 0.016425
percent var predicted/var original= 96.3 %
```

tidal amplitude and phase with 95% CI estimates

tide	freq	amp	amp_err	pha	pha_err	snr
*MSF	0.0028219	0.0356	0.010	320.30	17.41	13
*O1	0.0387307	0.0866	0.004	227.88	3.69	4.1e+02
*K1	0.0417807	0.1262	0.005	267.29	2.30	6.1e+02
*M2	0.0805114	0.8933	0.030	170.47	2.09	9.1e+02
*S2	0.0833333	0.1026	0.032	246.26	17.87	10
*M3	0.1207671	0.0091	0.003	195.67	23.47	7.9
*SK3	0.1251141	0.0062	0.003	307.47	31.86	3.9
*M4	0.1610228	0.0049	0.001	259.87	7.53	44
*MS4	0.1638447	0.0036	0.001	272.00	12.42	25
S4	0.1666667	0.0010	0.001	230.74	40.91	1.9
*2MK5	0.2028035	0.0121	0.002	234.47	11.35	33
2SK5	0.2084474	0.0015	0.002	310.89	82.52	0.73
*M6	0.2415342	0.0435	0.003	148.12	4.23	1.6e+02
*2MS6	0.2443561	0.0148	0.004	239.57	12.49	18
2SM6	0.2471781	0.0036	0.004	85.43	60.66	1
*3MK7	0.2833149	0.0036	0.001	287.32	20.34	9.5
*M8	0.3220456	0.0035	0.001	144.19	11.89	19

E.3.11: Phase 4: TCARI model predictions at the mooring site in Great Bay, NH.

```
number of standard constituents used: 17
Points used: 4799 of 4800
percent of var residual after lsqfit/var original:  3.05 %
Greenwich phase computed with nodal corrections applied to amplitude
and phase relative to center time
Using nonlinear bootstrapped error estimates
Generating prediction with nodal corrections, SNR is 2.000000
percent of var residual after synthesis/var original:  3.06 %
---------------------------------
date: 08-Nov-2011
nobs = 4800,  ngood = 4799,  record length (days) = 20.00
start time: 12-Jul-2011 14:48:00
rayleigh criterion = 1.0
Greenwich phase computed with nodal corrections applied to amplitude
and phase relative to center time

x0= 1.15, x trend= 0

var(x)= 0.44056   var(xp)= 0.42702   var(xres)= 0.01347
percent var predicted/var original= 96.9 %

        tidal amplitude and phase with 95% CI estimates
```

tide	freq	amp	amp_err	pha	pha_err	snr
*MSF	0.0028219	0.0029	0.001	252.79	22.92	6.4
*O1	0.0387307	0.0928	0.005	227.11	3.69	3.5e+02
*K1	0.0417807	0.1345	0.005	245.39	2.24	8e+02
*M2	0.0805114	0.8880	0.027	171.28	1.72	1.1e+03
*S2	0.0833333	0.0828	0.029	218.19	19.73	8.3
*M3	0.1207671	0.0115	0.005	233.51	31.63	4.5
SK3	0.1251141	0.0052	0.005	287.91	61.88	0.89
*M4	0.1610228	0.0284	0.003	265.60	5.27	1.2e+02
*MS4	0.1638447	0.0071	0.003	287.22	20.60	7.1
S4	0.1666667	0.0017	0.002	219.61	94.41	0.59
*2MK5	0.2028035	0.0010	0.000	136.61	10.02	24
*2SK5	0.2084474	0.0006	0.000	304.13	16.08	13
*M6	0.2415342	0.0344	0.000	154.02	0.09	2.9e+05
*2MS6	0.2443561	0.0006	0.000	137.06	6.15	93
*2SM6	0.2471781	0.0004	0.000	87.92	8.68	34
*3MK7	0.2833149	0.0002	0.000	270.40	5.35	1.4e+02
*M8	0.3220456	0.0052	0.000	200.87	0.21	9.5e+04

E.3.12: Phase 4: NCDC Atmospheric Pressure referenced to the mooring site in Great Bay, NH.

```
number of standard constituents used: 17
Points used: 4799 of 4800
percent of var residual after lsqfit/var original: 75.02 %
Greenwich phase computed with nodal corrections applied to amplitude
and phase relative to center time
Using nonlinear bootstrapped error estimates
Generating prediction with nodal corrections, SNR is 2.000000
percent of var residual after synthesis/var original: 75.02 %
----------------------------------------
date: 08-Nov-2011
nobs = 4800,  ngood = 4799,  record length (days) = 20.00
start time: 12-Jul-2011 14:48:00
rayleigh criterion = 1.0
Greenwich phase computed with nodal corrections applied to amplitude
and phase relative to center time

x0= 10.1, x trend= 0

var(x)= 0.0021299   var(xp)= 0.0005321   var(xres)= 0.0015978
percent var predicted/var original= 25.0 %
```

tidal amplitude and phase with 95% CI estimates

tide	freq	amp	amp_err	pha	pha_err	snr
*MSF	0.0028219	0.0315	0.014	15.67	26.89	5.1
*O1	0.0387307	0.0037	0.001	55.16	19.79	7.5
*K1	0.0417807	0.0072	0.001	15.55	10.01	26
*M2	0.0805114	0.0014	0.000	78.86	20.32	12
*S2	0.0833333	0.0042	0.000	51.39	5.89	87
*M3	0.1207671	0.0004	0.000	301.65	31.13	3.9
*SK3	0.1251141	0.0011	0.000	4.92	11.40	26
M4	0.1610228	0.0001	0.000	154.07	82.23	0.68
*MS4	0.1638447	0.0004	0.000	159.80	23.54	5.9
*S4	0.1666667	0.0002	0.000	37.12	45.40	2.2
*2MK5	0.2028035	0.0003	0.000	312.66	15.70	14
2SK5	0.2084474	0.0001	0.000	325.31	112.92	0.49
*M6	0.2415342	0.0002	0.000	85.64	21.56	5.2
*2MS6	0.2443561	0.0004	0.000	314.84	12.67	21
*2SM6	0.2471781	0.0004	0.000	217.46	13.65	12
*3MK7	0.2833149	0.0002	0.000	82.43	19.55	9
*M8	0.3220456	0.0004	0.000	195.51	5.84	90

E.3.13: Phase 4: Residual water level (computed v. modeled) at the mooring site in Great Bay, NH.

```
number of standard constituents used: 17
Points used: 4799 of 4800
percent of var residual after lsqfit/var original: 45.30 %
Greenwich phase computed with nodal corrections applied to amplitude
and phase relative to center time
Using nonlinear bootstrapped error estimates
Generating prediction with nodal corrections, SNR is 2.000000
percent of var residual after synthesis/var original: 45.42 %
----------------------------------
date: 15-Apr-2012
nobs = 4800,  ngood = 4799,  record length (days) = 20.00
start time: 12-Jul-2011 14:48:00
rayleigh criterion = 1.0
Greenwich phase computed with nodal corrections applied to amplitude
and phase relative to center time

x0= -0.0273, x trend= 0

var(x)= 0.0064709   var(xp)= 0.0035371   var(xres)= 0.0029394
percent var predicted/var original= 54.7 %

        tidal amplitude and phase with 95% CI estimates
```

tide	freq	amp	amp_err	pha	pha_err	snr
*MSF	0.0028219	0.0346	0.009	324.73	16.06	13
*O1	0.0387307	0.0063	0.003	36.55	25.90	6.4
*K1	0.0417807	0.0502	0.003	355.67	3.02	3.4e+02
*M2	0.0805114	0.0137	0.004	104.07	16.30	12
*S2	0.0833333	0.0489	0.004	299.00	4.74	1.6e+02
*M3	0.1207671	0.0070	0.003	106.40	26.15	7.5
SK3	0.1251141	0.0022	0.002	359.51	81.61	0.79
*M4	0.1610228	0.0235	0.002	86.80	5.45	1e+02
*MS4	0.1638447	0.0038	0.002	121.60	35.18	3.6
S4	0.1666667	0.0007	0.001	24.12	147.52	0.3
*2MK5	0.2028035	0.0123	0.002	239.15	9.54	28
2SK5	0.2084474	0.0008	0.002	316.08	144.01	0.28
*M6	0.2415342	0.0099	0.004	127.11	19.59	6.7
*2MS6	0.2443561	0.0149	0.004	241.77	12.57	18
2SM6	0.2471781	0.0032	0.003	85.13	72.05	0.96
*3MK7	0.2833149	0.0034	0.001	288.48	20.89	8.1
*M8	0.3220456	0.0044	0.001	62.87	10.73	31

E.3.14: Phase 4: Residual water level (t_tide generated v. modeled) at the mooring site in Great Bay, NH.

```
number of standard constituents used: 17
Points used: 4799 of 4800
percent of var residual after lsqfit/var original:  0.00 %
Greenwich phase computed with nodal corrections applied to amplitude
and phase relative to center time
Using nonlinear bootstrapped error estimates
Generating prediction with nodal corrections, SNR is 2.000000
percent of var residual after synthesis/var original:  0.00 %
------------------------------------
date: 15-Apr-2012
nobs = 4800,  ngood = 4799,  record length (days) = 20.00
start time: 12-Jul-2011 14:48:00
rayleigh criterion = 1.0
Greenwich phase computed with nodal corrections applied to amplitude
and phase relative to center time

x0= 1.63e-15, x trend= 0

var(x)= 0.0035575   var(xp)= 0.0035575   var(xres)= 1.775e-22
percent var predicted/var original= 100.0 %
```

tidal amplitude and phase with 95% CI estimates

tide	freq	amp	amp_err	pha	pha_err	snr
*MSF	0.0028219	0.0346	0.000	324.73	0.00	2.4e+27
*O1	0.0387307	0.0063	0.000	36.55	0.00	1.3e+26
*K1	0.0417807	0.0502	0.000	355.67	0.00	1e+28
*M2	0.0805114	0.0137	0.000	104.07	0.00	8.8e+26
*S2	0.0833333	0.0489	0.000	299.00	0.00	8.4e+27
*M3	0.1207671	0.0070	0.000	106.40	0.00	7.2e+25
*SK3	0.1251141	0.0062	0.000	307.47	0.00	4.7e+25
*M4	0.1610228	0.0235	0.000	86.80	0.00	7.1e+26
*MS4	0.1638447	0.0038	0.000	121.60	0.00	2.1e+25
*S4	0.1666667	0.0010	0.000	230.74	0.00	1.1e+24
*2MK5	0.2028035	0.0123	0.000	239.15	0.00	2.8e+26
*2SK5	0.2084474	0.0006	0.000	124.13	0.00	6.7e+23
*M6	0.2415342	0.0099	0.000	127.11	0.00	7.6e+25
*2MS6	0.2443561	0.0149	0.000	241.77	0.00	1.9e+26
*2SM6	0.2471781	0.0004	0.000	267.92	0.00	1.1e+23
*3MK7	0.2833149	0.0034	0.000	288.48	0.00	1.6e+25
*M8	0.3220456	0.0044	0.000	62.87	0.00	4.7e+20

APPENDIX F: OPUS REPORTS

F.1: Shankhassic, Great Bay, NH.

ILE: BrovrA10.obs 000253865

```
1008    NOTE: Antenna offsets supplied by the user were zero.  Coordinates
1008    returned will be for the antenna reference point (ARP).
1008
                        NGS OPUS-RS SOLUTION REPORT
                        ===========================
```

```
           USER:                           DATE: May 16, 2011
    RINEX FILE: brov351t.10o                TIME: 15:54:52 UTC

      SOFTWARE: rsgps  1.35.1 RS10.prl 1.70   START: 2010/12/17 19:45:01
     EPHEMERIS: igs16145.eph [precise]        STOP: 2010/12/17 21:18:20
      NAV FILE: brdc3510.10n              OBS USED: 7056 / 8505   : 83%
      ANT NAME: ASH700700.C             QUALITY IND.  43.62/ 75.41
    ARP HEIGHT: 0.0                      NORMALIZED RMS:       0.339
```

```
    REF FRAME: NAD_83(CORS96)(EPOCH:2002.0000)      ITRF00 (EPOCH:2010.96125)

          X:     1527902.105(m)   0.007(m)      1527901.327(m)   0.007(m)
          Y:    -4408411.703(m)   0.011(m)     -4408410.279(m)   0.011(m)
          Z:     4334179.884(m)   0.018(m)      4334179.828(m)   0.018(m)

        LAT:  43  4 56.89128      0.011(m)    43  4 56.92537      0.011(m)
      E LON: 289  6 56.50861      0.007(m)   289  6 56.49672      0.007(m)
      W LON:  70 53  3.49139      0.007(m)    70 53  3.50328      0.007(m)
     EL HGT:        -26.261(m)    0.018(m)           -27.468(m)   0.018(m)
   ORTHO HGT:         0.517(m)    0.020(m)  [NAVD88 (Computed using GEOID09)]
```

```
                    UTM COORDINATES     STATE PLANE COORDINATES
                    UTM (Zone 19)         SPC (2800 NH  )
   Northing (Y) [meters]   4771696.087        65000.745
   Easting (X)  [meters]    346617.226       363707.303
   Convergence  [degrees]   -1.28732416        0.53441157
   Point Scale              0.99988942         1.00001658
   Combined Factor          0.99989354         1.00002069
```

US NATIONAL GRID DESIGNATOR: 19TCH4661771696(NAD 83)

```
                    BASE STATIONS USED
   PID      DESIGNATION                    LATITUDE     LONGITUDE  DISTANCE(m)
   DI1075 NHUN U NEW HAMPSHIRE CORS ARP    N430833.179 W0705706.863   8650.3
   DL7764 P776 GUNSTOCKMRNH2008 CORS ARP   N433235.721 W0712242.789  65030.1
   AF9520 WES2 WESTFORD CORS ARP           N423647.975 W0712935.968  72072.4
   AJ2693 YMTS MTS YARMOUTH COOP CORS ARP  N434754.610 W0701120.298  97452.0
   AJ1830 BARN BARTLETT CORS ARP           N440556.684 W0710934.400 115115.4
   DJ8961 VTSP SPRINGFIELD VT CORS ARP     N431653.241 W0722839.238 131402.1
   DJ8953 VTD2 DUMMERSTON CORS ARP         N425506.108 W0723206.441 135833.4
   DJ8957 VTOX BRADFORD CORS ARP           N440028.165 W0720651.610 143003.9
   DI0876 ACU5 ACUSHNET 5 CORS ARP         N414436.796 W0705313.027 148725.0
```

```
                 NEAREST NGS PUBLISHED CONTROL POINT
   OC2494      DURHAM 1851                 N430519.201 W0705336.992   1023.9
```

This position and the above vector components were computed without any
knowledge by the National Geodetic Survey regarding the equipment or
field operating procedures used.

F.2: Winnicut River, Great Bay, NH.

FILE: BrovrB11055.obs 000253860

```
1008    NOTE: Antenna offsets supplied by the user were zero.  Coordinates
1008    returned will be for the antenna reference point (ARP).
1008
                          NGS OPUS-RS SOLUTION REPORT
                          ===========================

         USER:                               DATE: May 16, 2011
   RINEX FILE: brov055r.11o                  TIME: 15:40:19 UTC

     SOFTWARE: rsgps  1.35.1 RS41.prl 1.70   START: 2011/02/24 17:44:32
    EPHEMERIS: igs16244.eph [precise]         STOP: 2011/02/24 18:17:05
     NAV FILE: brdc0550.11n              OBS USED: 3159 / 3447   :  92%
     ANT NAME: ASH700700.C            QUALITY IND.  20.13/ 27.07
   ARP HEIGHT: 0.0                  NORMALIZED RMS:        0.326

    REF FRAME: NAD_83(CORS96)(EPOCH:2002.0000)      ITRF00 (EPOCH:2011.15000)

          X:      1531759.827(m)   0.006(m)     1531759.046(m)   0.006(m)
          Y:     -4409715.253(m)   0.014(m)    -4409713.828(m)   0.014(m)
          Z:      4331510.195(m)   0.012(m)     4331510.140(m)   0.012(m)

        LAT:   43  2 58.45632      0.007(m)   43  2 58.49047     0.007(m)
      E LON:  289  9 18.70230      0.008(m)  289  9 18.69036     0.008(m)
      W LON:   70 50 41.29770      0.008(m)   70 50 41.30964     0.008(m)
     EL HGT:         -25.668(m)    0.017(m)          -26.876(m)  0.017(m)
  ORTHO HGT:           1.091(m)    0.019(m)  [NAVD88 (Computed using GEOID09)]
```

```
                     UTM COORDINATES    STATE PLANE COORDINATES
                     UTM (Zone 19)         SPC (2800 NH  )
Northing (Y) [meters]    4767971.086           61376.761
Easting (X)  [meters]     349752.117          366959.432
Convergence  [degrees]    -1.25955570           0.56104896
Point Scale               0.99987771           1.00002180
Combined Factor           0.99988174           1.00002583
```

US NATIONAL GRID DESIGNATOR: 19TCH4975267971(NAD 83)

```
                      BASE STATIONS USED
PID        DESIGNATION                    LATITUDE     LONGITUDE DISTANCE(m)
DI1075 NHUN U NEW HAMPSHIRE CORS ARP      N430833.179 W0705706.863   13517.7
DL7764 P776 GUNSTOCKMRNH2008 CORS ARP     N433235.721 W0712242.789   69890.9
DI0964 FMTS MTS FRAM COOP CORS ARP        N421800.171 W0712630.865   96580.6
DI0966 XMTS MTS FOX COOP CORS ARP         N420350.018 W0711501.669  114447.5
DJ7833 BRU6 BRUNSWICK 6 CORS ARP          N435322.916 W0695647.885  118294.0
DJ8961 VTSP SPRINGFIELD VT CORS ARP       N431653.241 W0722839.238  135251.7
DJ8953 VTD2 DUMMERSTON CORS ARP           N425506.108 W0723206.441  138630.1
DI0876 ACU5 ACUSHNET 5 CORS ARP           N414436.796 W0705313.027  145111.7
DH5837 CTPU PUTNAM CORS ARP               N415358.888 W0715320.889  153910.1

             NEAREST NGS PUBLISHED CONTROL POINT
OC0405      R 28                          N430231.    W0705033.      869.5
```

This position and the above vector components were computed without any
knowledge by the National Geodetic Survey regarding the equipment or
field operating procedures used.

F.3: Adam's Point, Great Bay, NH.

```
FILE: bbasea09_1sec.176o 000231149

                        NGS OPUS SOLUTION REPORT
                        ========================

All computed coordinate accuracies are listed as peak-to-peak values.
For additional information: http://www.ngs.noaa.gov/OPUS/about.html#accuracy

       USER:                            DATE: May 18, 2011
RINEX FILE: bbas176p.09o                TIME: 15:36:04 UTC


 SOFTWARE: page5  1009.28 master11.pl 051211   START: 2009/06/25  15:33:00
EPHEMERIS: igs15374.eph [precise]              STOP: 2009/06/25  18:40:30
 NAV FILE: brdc1760.09n                    OBS USED: 6475 / 6774   :  96%
 ANT NAME: ASH701008.01B   NONE         # FIXED AMB:   38 /   38   : 100%
ARP HEIGHT: 2.0                         OVERALL RMS: 0.013(m)


REF FRAME: NAD_83(CORS96)(EPOCH:2002.0000)      ITRF00 (EPOCH:2009.4814)

        X:      1529172.287(m)   0.026(m)      1529171.532(m)   0.026(m)
        Y:     -4407198.020(m)   0.052(m)     -4407196.594(m)   0.052(m)
        Z:      4334964.874(m)   0.038(m)      4334964.814(m)   0.038(m)

      LAT:   43  5 31.63990      0.025(m)    43  5 31.67379      0.025(m)
    E LON:  289  8  7.14770      0.031(m)   289  8  7.13683      0.031(m)
    W LON:   70 51 52.85230      0.031(m)    70 51 52.86317      0.031(m)
   EL HGT:         -23.542(m)    0.051(m)          -24.747(m)    0.051(m)
ORTHO HGT:           3.214(m)    0.087(m)  [NAVD88 (Computed using GEOID09)]

                    UTM COORDINATES    STATE PLANE COORDINATES
                    UTM (Zone 19)        SPC (2800 NH  )
Northing (Y) [meters]    4772732.317         66088.135
Easting (X)  [meters]     348238.338        365294.860
Convergence  [degrees]    -1.27414301         0.54791441
Point Scale               0.99988333         1.00001909
Combined Factor           0.99988703         1.00002279

US NATIONAL GRID DESIGNATOR: 19TCH4823872732(NAD 83)

                   BASE STATIONS USED
PID        DESIGNATION                LATITUDE     LONGITUDE  DISTANCE(m)
DE6240 NHDT CONCORD COOP CORS ARP     N431246.196 W0713111.474  54952.6
DF9215 ZBW1 BOSTON WAAS 1 CORS ARP    N424408.559 W0712849.518  63996.3
DI1075 NHUN U NEW HAMPSHIRE CORS ARP  N430833.179 W0705706.863   9043.3

               NEAREST NGS PUBLISHED CONTROL POINT
OC2451      BOATHOUSE SOUTHWEST GABLE  N430452.969 W0705151.291   1196.3

This position and the above vector components were computed without any
knowledge by the National Geodetic Survey regarding the equipment or
field operating procedures used.
```

F.4: Squamscott River, Great Bay, NH: Elevation Only.

```
FILE: B____All.obs 000253858

1008    NOTE:  Antenna offsets supplied by the user were zero.  Coordinates
1008    returned will be for the antenna reference point (ARP).
1008
                          NGS OPUS-RS SOLUTION REPORT
                          ===========================

      USER:                              DATE: May 16, 2011
RINEX FILE: b___020p.11o                 TIME: 15:37:22 UTC

 SOFTWARE: rsgps  1.35.1 RS40.prl 1.70   START: 2011/01/20 15:20:01
EPHEMERIS: igs16194.eph [precise]         STOP: 2011/01/20 16:20:05
 NAV FILE: brdc0200.11n               OBS USED: 5130 / 5553   :  92%
 ANT NAME: ASH700700.C              QUALITY IND. 30.88/ 64.21
ARP HEIGHT: 0.0                     NORMALIZED RMS:      0.309

REF FRAME: NAD_83(CORS96)(EPOCH:2002.0000)      ITRF00 (EPOCH:2011.05386)

      X:      1526587.976(m)  0.006(m)      1526587.197(m)  0.006(m)
      Y:     -4411251.364(m)  0.028(m)     -4411249.939(m)  0.028(m)
      Z:      4331772.113(m)  0.032(m)      4331772.057(m)  0.032(m)

     LAT:  43  3 10.03086     0.014(m)    43  3 10.06496    0.014(m)
   E LON: 289  5 20.55126     0.009(m)   289  5 20.53932    0.009(m)
   W LON:  70 54 39.44874     0.009(m)    70 54 39.46068    0.009(m)
  EL HGT:        -24.335(m)   0.040(m)           -25.543(m)  0.040(m)
ORTHO HGT:         2.492(m)   0.041(m)  [NAVD88 (Computed using GEOID09)]

                  UTM COORDINATES    STATE PLANE COORDINATES
                  UTM (Zone 19)        SPC (2800 NH  )
Northing (Y) [meters]    4768448.728      61683.280
Easting (X)  [meters]     344372.357     361566.513
Convergence  [degrees]     -1.30481837     0.51591720
Point Scale                0.99989796     1.00001328
Combined Factor            0.99990177     1.00001709

US NATIONAL GRID DESIGNATOR: 19TCH4437268448(NAD 83)

                     BASE STATIONS USED
PID        DESIGNATION                    LATITUDE     LONGITUDE DISTANCE(m)
DI1075 NHUN U NEW HAMPSHIRE CORS ARP      N430833.179 W0705706.863   10514.8
DL7764 P776 GUNSTOCKMRNH2008 CORS ARP     N433235.721 W0712242.789   66403.3
DI0964 FMTS MTS FRAM COOP CORS ARP        N421800.171 W0712630.865   94265.3
AJ2693 YMTS MTS YARMOUTH COOP CORS ARP    N434754.610 W0701120.298  101398.4
DI0966 XMTS MTS FOX COOP CORS ARP         N420350.018 W0711501.669  113331.9
AJ1830 BARN BARTLETT CORS ARP             N440556.684 W0710934.400  117968.2
DJ7833 BRU6 BRUNSWICK 6 CORS ARP          N435322.916 W0695647.885  121380.4
DJ8961 VTSP SPRINGFIELD VT CORS ARP       N431653.241 W0722839.238  129901.4
DJ8953 VTD2 DUMMERSTON CORS ARP           N425506.108 W0723206.441  133302.3

              NEAREST NGS PUBLISHED CONTROL POINT
OC0399        TIDAL 2 STA 2             N430310.    W0705438.      32.7

This position and the above vector components were computed without any
knowledge by the National Geodetic Survey regarding the equipment or
field operating procedures used.
```

F.5: Squamscott River, Great Bay, NH: Latitude and Longitude Only.

```
FILE: B____A11.158.obs 000265812

1008    NOTE:  Antenna offsets supplied by the user were zero.  Coordinates
1008    returned will be for the antenna reference point (ARP).
1008
                            NGS OPUS-RS SOLUTION REPORT
                            ===========================

       USER:                              DATE: June 13, 2011
  RINEX FILE: b___158s.11o                TIME: 17:13:38 UTC


   SOFTWARE: rsgps  1.35.1 RS5.prl 1.70      START: 2011/06/07 18:28:31
  EPHEMERIS: igr16392.eph [rapid]            STOP:  2011/06/07 19:32:55
   NAV FILE: brdc1580.11n              OBS USED:  6426 /  7236   :  89%
   ANT NAME: ASH700700.C               QUALITY IND.   4.18/ 15.87
  ARP HEIGHT: 0.0                      NORMALIZED RMS:      0.369

  REF FRAME: NAD_83(CORS96)(EPOCH:2002.0000)      ITRF00 (EPOCH:2011.43231)


        X:       1526492.547(m)  0.008(m)       1526491.762(m)  0.008(m)
        Y:      -4411296.275(m)  0.011(m)      -4411294.851(m)  0.011(m)
        Z:       4331761.075(m)  0.023(m)       4331761.020(m)  0.023(m)


      LAT:   43  3  9.52097    0.013(m)      43  3  9.55512    0.013(m)
    E LON:  289  5 15.91736    0.009(m)     289  5 15.90515    0.009(m)
    W LON:   70 54 44.08264    0.009(m)      70 54 44.09485    0.009(m)
    EL HGT:          -23.661(m)  0.021(m)             -24.870(m)  0.021(m)
  ORTHO HGT:           3.167(m)  0.023(m) [NAVD88 (Computed using GEOID09)]

                      UTM COORDINATES    STATE PLANE COORDINATES
                      UTM (Zone 19)         SPC (2800 NH  )
  Northing (Y) [meters]    4768435.388         61666.602
  Easting  (X) [meters]     344267.167        361461.788
  Convergence [degrees]    -1.30569417          0.51503703
  Point Scale               0.99989836         1.00001312
  Combined Factor           0.99990207         1.00001683

  US NATIONAL GRID DESIGNATOR: 19TCH4426768435(NAD 83)


                       BASE STATIONS USED
  PID          DESIGNATION                     LATITUDE    LONGITUDE  DISTANCE(m)
  DI1075 NHUN U NEW HAMPSHIRE CORS ARP       N430833.179 W0705706.863   10497.0
  DL7764 P776 GUNSTOCKMRNH2008 CORS ARP      N433235.721 W0712242.789   66356.6
  DI0964 FMTS MTS FRAM COOP CORS ARP         N421800.171 W0712630.865   94202.8
  AJ2693 YMTS MTS YARMOUTH COOP CORS ARP     N434754.610 W0701120.298  101471.5
  DI0966 XMTS MTS FOX COOP CORS ARP          N420350.018 W0711501.669  113290.7
  DJ8961 VTSP SPRINGFIELD VT CORS ARP        N431653.241 W0722839.238  129802.0
  DJ8953 VTD2 DUMMERSTON CORS ARP            N425506.108 W0723206.441  133196.4
  DJ8957 VTOX BRADFORD CORS ARP              N440028.165 W0720651.610  143886.0
  DH5837 CTPU PUTNAM CORS ARP                N415358.888 W0715320.889  151174.8

                NEAREST NGS PUBLISHED CONTROL POINT
  OC0399      TIDAL 2 STA 2                   N430310.    W0705438.      138.2
```

This position and the above vector components were computed without any
knowledge by the National Geodetic Survey regarding the equipment or
field operating procedures used.

APPENDIX G: PERSONAL COMMUNIQUÉS

Re: Pydro/TCARI license update
From: Barry Gallagher <██████████████████>
To: Sean Denney <███████████>
Date: November 15, 2011 12:53:54 PM

On 11/15/2011 11:21 AM, Sean Denney wrote:

> Barry,
>
> Thanks for the reply. I have a few follow-up questions for you.
>
> On Nov 15, 2011, at 10:21 AM, Barry Gallagher <████████████████████████> wrote:
>
>> On 11/7/2011 4:34 PM, Sean Denney wrote:
>>
>>> Here are a few questions that I've been guessing at:
>>>
>>> 1. When generating the TCARI grid, what level of tide should the boundary represent? From the COOPS glossary "shoreline" is defined as MHW. Is this the case for then for TCARI?
>>
>> Really, it doesn't matter. The shoreline used isn't reliable at that level anyway. We use charted shoreline currently that was hand digitized by NGDC and has outright errors that get corrected when going through CO-OPS in making operational TCARI products.
>
> Wouldn't changes to the level the boundary represents alter the dimensions of whatever bay, etc. that is being modeled? The consequence would alter the tidal amplitude and phase of the modeled predictions, wouldn't it?

Yes, but not meaningfully in general.

>>> 2. When generating the TCARI grid, is it possible to use a different set of harmonic constituents from the general NOAA set of 37? In my situation I am dealing with many shallow-water constituents that are being lost because the NOAA set doesn't include them.
>>
>> You can use other values -- TCARI only computes a weighting factor and then rebuilds the time series using harmonics. It would take a quick change in the code as I think the harmonics are set to be the standard 37 that CO-OPS publishes, as opposed to read from the input file.
>
> While I don't have the time to do this for my thesis, I think this may become important in the current re-mapping of the Great Bay that CCOM is engaged in.

It would interesting to see how this changes the modeled tides using the resolved HC's from t_tide analysis.

Like I said, changing the code is easy -- but actually running it and analyzing it is a different story. Maybe in the future...

> 3. What exactly does the solution surface represent?

> It's either the weighting percentage used for residual/harmonic portions or it's an actual datum level in whatever units were passed in with the station data (MLLW in meters for example).

> As a follow up to this. I noticed a menu option for "Show next solution set." What does this do? Does it change the datum from MLLW to another datum?

There is a "solutions" dialog where you can choose which solution set is displayed. Yes, that Show Next item cycles through from one gauge to the next for HCs/Residuals or from datum to datum. I think I'm the only one that uses it :)

> > 4. When generating and viewing the error surface, what do the colors and numbers represent in the legend? I assumed that black meant more error, but the numbers in the legend seem to contradict my assumption if the numbers represent std. dev.

> My machine is refusing to boot so I'm on an alternate machine currently -- and don't have an error image to look at. The values are standard dev in meters as I recall and should be higher around the gauges and lower in between gauges when multiple gauges are being used. The exception would be if the gauges are so far apart that the K distance term is too high and it'd be higher in between gauges.

Attached is the error surface image that was generated from the TCARI solution in my case. What you say makes sense and is backed up in my final analysis. I compared observed v. modeled tides at three locations (and epochs). one at a model control gauge and one in the blackish area of the error surface. The maximum. mean and standard deviation for the residuals at the latter location were better than the former.

275

5. Similarly, the analysis images that are generated: I think I understand the weights_HC... images (they are the influence per tide station if only that station's harmonic constants were weighted to 1). Can you explain what the weights_(MHW, MLLW, MLW, MSL)... and weights_Residual... images represent?

Same as above, datums are actual values (assuming the datum values passed into TCARI were correct). Residual is a weighting percentage that is analogous to the HC percentages but has a different set of gauges that it's generated from. If all stations with HCs are residual (operating) gauges then the two images will be identical.

I'll take a look at this.

6. I've read the paper by Hess et. al. (2004) regarding TCARI. Comparing TCARI in that paper to how TCARI is treated now, are LTE still used in the spatial interpolation computations or is a more complex set of equations being used? If LTE is still used, how did the grid generation change from square cells (in Hess) to triangles now?

LTE... drawing blank on acronym. Shewchucks' Triangle code is used to generate a mesh from shoreline. A finite element solver, SUPERLU, is used to compute values for the laplacian and modified neumann boundary conditions are iteratively applied in python/C. Gareth Elston, Alex Pletzer and I put this into place a while back. MMAP (here in silver spring) did an equivalent conversion using matlab that you could get a hold of. Lei Shi in MMAP has been improving the Matlab version recently.

This is the missing piece of the puzzle I just couldn't get my head around. I'll be doing some reading on this. LTE stands for Laplace's Tidal Equations. I noticed in Hess et. al. (2004) that one of the future enhancements to TCARI would be to use the "complex version of the shallow-water, uniform-depth, single-constituent tide wave equation" rather than LTE. Are there any plans to implement this?

No plan for me to do it. That may be where Lei Shi is heading but I've got other fish to fry and am not actively improving the fundamental TCARI code.

Cheers,
bg

Thanks again for the help
--- Sean

I appreciate your help on this.

Thanks
--- Sean

GLOSSARY

Band-average – a technique for smoothing the *spectral density* of a *time series* by averaging an arbitrary number of adjacent bands (or frequency indices).

Bay – a body of water partly enclosed by land, but having a wide outlet to the sea.

Benchmark (BM) – "a fixed physical object or mark used as reference for a horizontal or vertical datum. A *tidal benchmark* (TBM) is a benchmark near a tide station to which tidal datums are referred. A *geodetic benchmark* identifies a surveyed point in the National Spatial Reference System." (Hicks *et. al.*, 2000)

Blunder – mistakes in measurements or observations "usually caused by a misunderstanding of the problem, carelessness, fatigue, missed communication, or poor judgement." (Wolf and Brinker, 1994)

bool – C/ C++ boolean data type.

Coherency spectrum – a technique employed in cross-spectral analysis that quantifies the coherence as a function of frequency between two *time series*.

Confidence interval – "a range of values that contains with a specified probability the true value of a given parameter." (The American Heritage Dictionary, 2011)

Data window – a technique employed in *time series* analysis that is used to systematically filter the *frequency domain* of a *time series*.

Datum – "a base elevation used as a reference from which to reckon heights or depths. It is called a tidal datum when defined in terms of a certain phase of the tide." (Hicks *et. al.*, 2000)

Diurnal Tide Level (DTL) – "a tidal datum equivalent to the average of Mean Higher-High Water and Mean Lower-Low Water." (NOS, 2003)

double – C/ C++ floating-point data type with 15-digit precision.

Ellipsoid – "a mathematical surface obtained by revolving an ellipse about the earth's polar axis. The ellipse dimensions are selected to give a good fit of the ellipsoid to the geoid over a large area." (Wolf and Brinker, 1994)

Ellipsoidal height – "the vertical distance from the ellipsoid to ground." (Wolf and Brinker, 1994)

278

Epoch[1] – a specified or particular period of time (*e.g.* one month, ten years, etc.)

Epoch[2] – a specified or particular time reference (*e.g.* local, Greenwich, etc.)

Estuary[1] – "that part of a river or stream or other body of water having unimpaired connection with the open sea, where the sea-water is measurably diluted with freshwater derived from land drainage." (Coastal Zone Management Act of 1972)

Estuary[2] – "an embayment of the coast in which fresh river water entering at its head mixes with the relatively saline ocean water. When tidal action is the dominant mixing agent it is usually termed a *tidal estuary*. Also, the lower reaches and mouth of a river emptying directly into the sea where tidal mixing takes place. The latter is sometime called a *river estuary*." (Hicks *et. al.*, 2000)

First point of Aries – "the point where the apparent path of the sun crosses the equator from south to north." (Doodson and Warburg, 1941)

Fourier series – "an infinite series whose terms are constants multiplied by sine and cosine functions and that can, if uniformly convergent, approximate a wide variety of functions." (The American Heritage Dictionary, 2011)

Fourier transform – "an operation that maps a function to its corresponding Fourier series or to an analogous continuous frequency distribution." (The American Heritage Dictionary, 2011)

Frequency domain – the set of spectral values, indexed by frequency.

Geoid – "the earth's mean sea level surface, ... everywhere perpendicular to the direction of gravity." (Wolf and Brinker, 1994)

Geoidal height – "the vertical distance between [an] ellipsoid and geoid." (Wolf and Brinker, 1994)

Great Tropic Range (Gt) – "a tidal range computed from the difference between Mean Higher-High Water and Mean Lower-Low Water." (NOS, 2003)

Harmonic analysis – "the mathematical process by which the observed tide or tidal current at any place is separated into basic harmonic constituents." (Hicks *et. al.*, 2000)

Harmonic constituents – "one of the harmonic elements in a mathematical expression for the tide-producing force and in corresponding formulas for the tide. Each constituent represents a periodic change or variation in the relative positions of the Earth, Moon, and Sun." (Hicks *et. al.*, 2000)

`int` – C/ C++ integer data type.

Least-squares method – "a method of determining the curve that best describes the relationship between expected and observed sets of data by minimizing the sums of the squares of deviation between observed and expected values." (The American Heritage Dictionary, 2011)

Latitude – "the angular distance between a terrestrial position and the equator measured northward or southward from the equator along a meridian of longitude." (Hicks *et. al.*, 2000)

Legendre differential equation – The second-order, ordinary differential equation. The solution to this equation is the *Legendre polynomial*, often represented as an approximation to some arbitrary *n*-th order.

Legendre polynomial – The solution to the *Legendre differential equation* using a contour integrals. A method of approximation to some arbitrary *n*-th order is often used.

Level – an apparatus used in the process of *leveling*.

Leveling – "the process of finding elevations of points, or their difference in elevation." (Wolf and Brinker, 1994)

Longitude – "the angular distance along the equator to a terrestrial position measured east or west of the meridian of Greenwich." (Hicks *et. al.*, 2000)

Lunitidal interval – "the interval between the Moon's transit (upper or lower) over the local or Greenwich meridian and the following high or low water." (Hicks *et. al.*, 2000)

Metadata – "data that describes other data," (*i.e.* "the origin, structure, or characteristics of" data). (The American Heritage Dictionary, 2011)

Mean Diurnal High Water Inequality (DHQ) – "a tidal range computed from the difference between Mean Higher-High Water and Mean High Water." (NOS, 2003)

Mean Diurnal Low Water Inequality (DLQ) – "a tidal range computed from the difference between Mean Low Water and Mean Lower-Low Water." (NOS, 2003)

Mean Higher-High Water (MHHW) – "a tidal datum computed from the arithmetic mean of the higher-high water heights of the tide observed over a specific 19-year Metonic cycle. Only the higher high water of each pair of high waters of a tidal day is included in the mean." (NOS, 2003)

Mean High Water (MHW) – a tidal datum computed from "the arithmetic mean of all of the high water heights observed over a specific 19-year Metonic cycle." (NOS, 2003)

Mean Lower-Low Water (MLLW) – a tidal datum computed from "the arithmetic mean of the lower low water heights of the tide observed over a specific 19-year Metonic cycle. Only the lower low water of each pair of low waters of a tidal day is included in the mean." (NOS, 2003)

Mean Low Water (MLW) – a tidal datum computed from "the arithmetic mean of all of the low water heights observed over a specific 19-year Metonic cycle." (NOS, 2003)

Mean Range of Tide (Mn) – "a tidal range computed from the difference between Mean High Water and Mean Low Water." (NOS, 2003)

Mean Sea Level (MSL) – a tidal datum computed from "the arithmetic mean of hourly heights observed over a specific 19-year Metonic cycle." (NOS, 2003)

Mean Tide Level (MTL) – "a tidal datum equivalent to the average of Mean High Water and Mean Low Water." (NOS, 2003)

Metonic cycle – "a period of almost 19 years (6939.75 days) or 235 lunations (6939.69 days)." (Hicks *et. al.*, 2000)

NaN or nan – C/ C++ and MATLAB™ data object representing "not a number."

Orthometric height – "elevation given with respect to the geoid." (Wolf and Brinker, 1994)

Phase spectrum – a technique employed in cross-spectral analysis that quantifies the phase relationship as a function of frequency between two *time series*.

Post-processed kinematic – non-stationary positioning information (*i.e.* GNSS) that is corrected after the data is collected.

Power spectrum – a technique employed in spectral analysis of a *time series* denoting the power (or variance) of the *time series* as a function of frequency.

Range of tide – "the difference in height between consecutive high and low waters." (Hicks *et. al.*, 2000)

Real-time kinematic – non-stationary positioning information (*i.e.* GNSS) that is corrected during data collection. Often the data is re-processed using the *post-processed kinematic* technique to attain greater positioning accuracy.

Sample interval – an arbitrary interval value in the domain of the parameter to be measured or observed (*e.g.* 6-minutes in the *time domain*).

Shapefile – "a vector data storage format for storing the location, shape, and attributes of geographic features." (Sommers and Wade, 2006)

Shoreline – "the intersection of the land with the water surface. The shoreline shown on charts represents the line of contact between the land and a selected water elevation. In areas affected by tidal fluctuations, this line of contact is the mean high water line." (Hicks *et. al.*, 2000)

Signal-to-noise ratio (SNR) – "the ratio of the power of an electrical, electromagnetic, or optical signal to the power of background noise accompanying the signal." (The American Heritage Dictionary, 2011)

Spectral density – a technique employed in spectral analysis that quantifies the power (or variance) associated with any particular frequency band of the power spectrum.

Spectral domain – the set of spectral values, often indexed by frequency. (See *frequency domain*).

`struct` – C/ C++ user-defined data structure.

Three-wire level – a *leveling* technique which "consists in making [level] rod readings on the upper, middle, and lower cross hairs" of a *level*. (Wolf and Brinker, 1994)

Tidal benchmark – See *Benchmark*.

Tide-by-tide (TBYT), *modified range ratio for semi-diurnal tides* – "a method used to compute equivalent 19-year tidal datums, tidal ranges, and lunitidal intervals for short-term tide stations." (NOS, 2003)

Time domain – the set of spatial values, indexed by time.

Time series – a set of values measured or observed in the *time domain* at a certain *sample interval*.

`typedef` – C/ C++ user-defined type definition.

`uint64_t` – C/ C++ 64-bit, unsigned integer data type.

`unsigned` – C/ C++ designation for integer data types unable to store negative values.

`vector` – C/ C++ sequential data objects container that can change in size dynamically.